GEOCHEMICAL APPROACHES TO THE STUDY OF LIFE AND DEATH OF DINOSAURS FROM THE EARLY CRETACEOUS CEDAR MOUNTAIN FORMATION, UTAH

By

© 2010
Celina Angelica Suarez
B.S., Trinity University, 2003
M.S., Temple University, 2005

Submitted to the Department of Geology and the Faculty of the Graduate School of The University of Kansas in partial fulfillment of the requirements for the degree of Doctor of Philosophy

Advisory Committee:

_____
Luis A González, Chair

_____
David A. Fowle

_____
Bruce S. Lieberman

_____
Gregory A. Ludvigson

_____
G.L. Macpherson

_____
Larry D. Martin

Date defended:_____

The dissertation committee for Celina Angelica Suarez certifies
that this is the approved version of the following dissertation:

GEOCHEMICAL APPROACHES TO THE STUDY OF LIFE AND DEATH OF DINOSAURS FROM THE EARLY CRETACEOUS CEDAR MOUNTAIN FORMATION, UTAH

Advisory Committee:

_____
Luis A González, Chair

_____
David A. Fowle

_____
Bruce S. Lieberman

_____
Gregory A. Ludvigson

_____
G.L. Macpherson

_____
Larry D. Martin

Date defended:_____

ABSTRACT

Celina A. Suarez, Ph.D.
Department of Geology, April 2010
University of Kansas

In this dissertation, geochemical analysis of fossil vertebrate remains are carried out to elucidate fossil diagenesis and for paleoenvironmental reconstructions. Rare earth elements (REE) are analyzed via laser ablation inductively coupled plasma mass spectrometry (ICP-MS) in order to determine REE distribution within a bone. Analysis indicates REE can vary significantly within a single bone and that thin-walled bones fossilized in vadose settings should not be analyzed via solution ICP-MS. Stable isotopic analysis of oxygen preserved in tooth enamel and scale ganoine is used to discriminate water reservoirs used by the taxa making up several faunal assemblages from the Cedar Mountain Formation. Based on the isotopic composition of calculated ingested/living water of theses taxa, it can be determined that the proximity of the Western Interior Seaway and the rise of the Sevier Mountains were the cause of isotopic variability and dominant control on regional climate during the Cedar Mountain Formation time.

ACKNOWLEDGMENTS

First, I must thank my family for all their support, encouragement, and understand during the process of my graduate career. I especially thank my parents: Arturo and Sylvia Suarez, my grandparents: Samuel and Aurora Suarez, and José and Susie Sanchez, my sisters: Bettina Suarez-Cromley, Marina Suarez, and Elisa Suarez, and my brother-in-law Samuel Cromley, and all of my aunts, uncles and cousins. It has not been easy to be away from home missing the many trials and triumphs our family has encountered throughout the last several years. They have been very patient and understanding, and for that, I thank you and hope that you all realize that pursuit of this research has always been with you in mind.

I also thank the amazing mentors I have encountered throughout my undergraduate and graduate career: Drs. Edward C. Roy Jr., David E. Grandstaff, Dennis O. Terry, Luis A. González, Gregory A. Ludvigson, and Gwen L. Macpherson. Their support, advice, encouragement, guidance, and patience have been invaluable Thanks to Greg for finding me (and Marina) in the desert, and introducing us to Luis. To my dissertation advisor, Luis González thank you for being patient, emphasizing attention to details, putting up with my "obtuseness" and for the endless scientific, career, and personal advice you have given me. Words cannot express the gratitude I have to you for your mentorship throughout these five years, thank you.

Completing this dissertation would not have been possible without the company and support of a great group of fellow graduate students, aka: lab mates and aka: intramural-sport team mates. Thanks to Marina Suarez, Julie Retrum, Aisha Al-Suwadii, Alvin Bonilla, Becky Totten, Emily Tremain, Stacey Rosner, Paul Kenward, Ezra Kulczycki, Pete Schillig, Arne Sturm, Karla Leslie, Brian Platt, Jeffery Schroeder, Eugene Szymanski, Christian Hager, Dr. Jon Smith and the many I probably forgot to mention. I especially thank Marina for everything, seriously, everything. There is nothing like mulling over ideas, decisions, interpretations, frustrations, and triumphs with your identical twin. No one will ever understand the bond we have, so thank you. Many people besides my advisor have helped muddle through my writing; so for all their time and advice I thank Dr. Jon Smith, Dr. Marina Suarez, Aisha Al-Suwaidi, and Julie Retrum. I also thank my writing buddies, Paul Kenward and Natalie Ciaccio for just being there for me and each other while going through the "exciting" writing process. I could not have completed my dissertation research without the dedicated staff in the department and in our lab. For that I express my sincere gratitude to Yolanda Davis, Gwethalyn Williams, Jenna Coker, Liz Gravatt, Terri Herberger, Ann Smith, Carla Ramirez, and our incredibly dedicated lab manager Greg Cane, who has done an amazing job keeping the lab running. For assistance and advice on the silver phosphate method, I'd like to thank Dr. Damon Bassett for taking the time to come to Lawrence to go through the method with me. It was incredibly helpful. Thank you also to Dr. Hans-Peter Schultze who offered his expertise on fish fossil identification and ecology. Without access to fossil materials,

this research would not be possible and so, for access to fossil materials, I would like to thank Dr. James Kirkland (Utah Geological Survey), Dr. Reese Barrick (The Sternberg Museum), John Bird (College of Eastern Utah), Dr. Brooks Britt (Brigham Young University), Dr. Richard Cifelli (Sam Noble Oklahoma Museum of Natural History), Dr. Randall Irmus (Utah Museum of Natural History), Dr. Kenneth Carpenter (Denver Museum of Nature and Science, and Dr. Scott Foss (Bureau of Land Management). For the company, help, and housing while in the field in Utah I especially thank my "triplet brother" Don DeBlieux, Scott Madsen, Gary Hunt, and Jennifer Cavin. Finally, I would never have been put in the situation to meet Greg and come to Kansas if it were not for the opportunity given to me by Dr. James Kirkland, and so I owe him an extra bit of gratitude. Jim, your endless passion and enthusiasm for paleontology and geology is amazing and addicting, never change.

Funding for this study was provided by NSF grant EAR-0325072 to Luis. González and Greg Ludvigson. Additional funding was provided by the GSA Graduate Student Research Grant, the Paleontological Society's Stephen J. Gould Student Research Award, Sigma Xi Grant-in-Aid of Research Program, the Department of Geology's Geology Associates Board and Patterson Scholarships, and the Utah Friends of Paleontology. Funding by the American Geological Institute's Minority Participation Program has been provided throughout my graduate career, and I sincerely thank them for their support in promoting geosciences to minority students. I would also like to thank the University of Kansas Graduate School for a four-year Fellowship and a research assistantship provided by Dr. Greg Ludvigson.

Finally, this work is especially dedicated to the memories of Dr. Edward C. Roy Jr., Master Staff Sergeant Samuel Suarez Sr., and Elisa Suarez. Dr. Roy was my "geology grandpa" and first geology mentor. He was instrumental in my decision to come to the University of Kansas. Recalling his support and enthusiasm for paleontology and geology was a source of inspiration during the tough times. Growing up, my grandfather Samuel Suarez always emphasized the need for education and was always supportive of my research endeavors; this work is especially dedicated to you. Lastly, to my little sister Elisa Suarez whose hard work and achievements despite the many set-backs she had was an inspiration. I miss you every day but know that you are sharing in the many endeavors I embark on.

TABLE OF CONTENTS

CHAPTER 1. INTRODUCTION

Paleobiologic, paleoenvironmental, and paleoclimatic information derived from the morphology, distribution, and physical taphonomy of fossils, can offer a glimpse into past ecosystems and by inference climates. The geochemical composition of fossils holds a wealth of paleobiologic, paleoecologic, and paleoclimatic information unobtainable from the physical analysis of fossils. An understanding of ancient ecosystems and climates is of extreme importance when evaluating the trajectory of future climate and its effect on modern ecosystems. For geologists and paleontologists, the rock record allows us to observe climate change and its effect on ecosystems. The geochemical information preserved in fossils provides an empirical means for which these changes and their effects can be observed and quantified.

In this dissertation, I use the continental vertebrate fauna preserved in the Cretaceous Cedar Mountain Formation (CMF) of Utah to explore the utility of geochemical data from fossil vertebrates. The title of this dissertation "Geochemical Approaches to the Study of Life and Death of Dinosaurs of the early Cretaceous Cedar Mountain Formation, Utah" represents the two main geochemical approaches used in this study and their objectives: 1) rare earth element concentrations and patterns in bone to decipher fossilization history and 2) oxygen isotopic composition of tooth enamel to interpret water utilization strategies of vertebrate taxa which are then used to infer changes in paleohydrology caused by local and regional changes in climate, and to hypothesize on possible causes of these changes.

Post-mortem, the vertebrate body undergoes a variety of physical and chemical changes resulting from the necrosis of the body tissues and its incorporation into the rock record. Rare earth elements (REE) have been used as a proxy for understanding bone: 1) fossilization rates

(Kohn, 2008; Trueman et al., 2008), 2) burial environments and chemistry (Grandjean-Lecúyer et al., 1993; Trueman et al., 2003), 3) taphonomic history (time and spatial averaging) (C. Suarez et al., 2007), and 4) provenance, (MacFadden et al., 2007). Recently it has been suggested that bone REE chemistry can be used as forensic tools (Lukens et al., 2009; Terry et al., 2009; C. Suarez et al., 2009) and there have been renewed attempts to use the decay of REE (i.e. Lu to Hf) to date fossil bone (Kocsis et al., 2009). If REE are to be accurately used for such endeavors, then a detailed understanding of REE incorporation and distribution within the bone is important. Chapter 2, (C. Suarez et al, 2010), explains and discusses the utilization of laser ablation inductively coupled plasma mass spectrometry (ICP-MS) to address this issue of REE incorporation and distribution and finds that significant REE heterogeneity can exist in fossil bones. Such heterogeneity can significantly alter the interpretation of reworking in taphonomic studies, alter dating-techniques (i.e. Lu-Hf geochronology), and obscure provenance or forensic interpretation. In this study it is suggested that thin-walled (< 1 cm) bones are not suitable for broad-scale taphonomic analysis using solution ICP-MS. Thin-walled bone can preserve a range of geochemical conditions experienced during the fossilization process. Bone encrusted by nodules (such as pedogenic carbonate) can isolate and potentially preserve the earliest geochemical conditions.

Although the biogenic integrity of fossil bone has been questioned (Kolodny et al., 1996; Trueman et al., 2008) fossil teeth and scales contain a much more diagenetically resistant form of bioapatite: enamel and ganoine (Kolodny et al., 1996; Fricke et al., 2008). Analysis of the oxygen isotopic composition of enamel and ganoine can be used to understand water utilization habits of different continental vertebrate taxa. Differences in water utilization are directly

influenced by the regional and local hydrologic cycle. Chapter 3 concentrates on the life habits of vertebrates by using one of the most diverse vertebrate faunas from the early Cretaceous, the Mussentuchit Member fauna from the CMF (Cifelli et al., 1999). The $\delta^{18}O$ of phosphate ($\delta^{18}O_p$) was analyzed from a large sample set of fish, turtles, crocodiles, mammals, and dinosaurs. The results of the robust data set suggest that dinosaurs obtain their water predominantly from rivers. Turtle $\delta^{18}O_p$ compositions best record average local meteoric water, whereas co-existing pedogenic calcite preserves an isotopically enriched end-member of meteoric water since they form during evaporative conditions. Crocodiles represent local meteoric water that is evaporatively enriched compared to the river-water in which turtles live and their $\delta^{18}O$ tend to be equal to the enriched meteoric water preserved by pedogenic calcite.

The $\delta^{18}O_p$ from co-existing mammals and aquatic/semi-aquatic taxa can be used as a measure of humidity. Based on the $\delta^{18}O$ of mammal phosphate and calculated ingested/living water from aquatic taxa, the average relative humidity from the Mussentuchit Member was ~68%.

Fish remains of *Lepidotes*-like teeth document water temperatures that are consistent with mean annual temperature (MAT) derived from leaf physiognomy (Spicer and Corfield 1992). Actinopterygian scales do not accurately document water temperatures because their $\delta^{18}O_p$ is enriched due to either habitat in evaporatively enriched pools or migration to the estuaries of the Western Interior Seaway (WIS).

The isotopic composition of the different water reservoirs of the Mussentuchit Member as documented by the vertebrate fauna suggests that moisture was primarily derived from the WIS which provided high relative humidity (compared to the rest of the CMF). The Sevier Mountains

contributed isotopically light run-off to rivers sourced from high-altitude melt waters as recorded by dinosaurs, but was otherwise not a significant factor in the hydrologic cycle of the Mussentuchit Member. The Sevier Mountain rainshadow prevented moisture contribution from the Pacific Ocean to the lower elevations where deposition of the Mussentuchit Member took place.

By constraining the ecological partitioning of water sources recorded by the different taxa, inferences are made about paleoclimatic conditions that resulted in changes to water reservoirs (local versus regional rivers and meteoric water). In chapter 4, I incorporate vertebrate fauna from two other members of the CMF (Yellow Cat Member and Ruby Ranch Member) to the Mussentuchit Member fauna to elucidate climatic changes that occur during the deposition of the CMF. Based on changes to oxygen isotopic composition of vertebrate taxa, we can infer that one of the driving forces for regional and local climate perturbations was the rise of the Sevier Mountains and the proximity of the WIS.

The aridity that is evidenced by the formation of pedogenic calcite in the upper part of the Yellow Cat Member is most likely a result of moisture delivery limitations caused by the distance of the Yellow Cat Member sites from the WIS, as well as blockage of most paleo-westerly-transported Pacific moisture by the Sevier Mountains. By the end of the deposition of the Ruby Ranch Member, blockage of nearly all Pacific-derived moisture (by the Sevier Orogen) occurs. During Ruby Ranch Member-time, the mountains reached sufficient height for seasonal snow-fall in the high-elevations. Rivers draining the Sevier Mountains to the west were isotopically depleted due to seasonal snow-melt. Towards the end of Ruby Ranch Member-

deposition and during the deposition of the Mussentuchit Member, the encroaching WIS dominated regional and local climate and provided significant moisture to the area

The over-arching theme of this work, "geochemical approaches" to studying fossil vertebrates, has provided a wealth of information to which future research can be built upon. The REE distribution within bone may document the various geochemical changes bone encounters during its fossilization process and therefore, we may be able to identify bones that preserve very early diagenetic conditions. We can then use REE to not only determine the taphonomic history of bone, but we may also be able to use it to identify bone that is suitable for paleoecologic/paleoclimatic studies. The successful identification of water reservoirs recorded by the $\delta^{18}O_p$ of various taxa suggests that vertebrate fossils, when combined with other paleoclimatic proxies (such as isotopic composition of pedogenic carbonate), can be used to tease out the relative contributions and impacts of sea level oscillations and orogeny on regional climate. This may be an important tool to differentiating between global changes to paleohydrology (i.e. intensification of the global hydrologic cycle) and regionally induced changes to the paleohydrology (i.e. orogeny). Results of the oxygen isotopic analysis of fossil vertebrates may be used to construct boundary conditions for global circulation models (GCMs) and interpretation of GCM results. This in turn is important to modeling of future changes to the hydrologic cycle and its impact on climate change.

REFERENCES

Cifelli, R. L., Nydam, R. L., Gardner, J. D., Weil, A., Eaton, J. G., Kirkland, J. I., and Madsen, S. K. (1999) Medial Cretaceous Vertebrates from the Cedar Mountain Formation, Emery

County, Utah: The Mussentuchit Local Fauna. In: Gillette, D. D. (Ed.), *Vertebrate Paleontology in Utah*, **Misc. Publications 99-1**, Utah Geological Survey, Salt Lake City. 219-242.

Fricke, H.C., Rogers, R.R., Backlund, R., Dwyer, C.N., and Echt, S. (2008) Preservation of primary stable isotope signals in dinosaur remains, and environmental gradients of the Late Cretaceous of Montana and Alberta. *Palaeogeog. Palaeoclimatol. Palaeoecol*. **266**, 13-27.

Grandjean-Lecúyer, P., Feist, R., and Albarede, F. (1993) Rare earth elements in old biogenic apatites. *Geochim. et Cosmochim. Acta* 57, 2507-2514.

Kocsis, L., Trueman, C.N., and Palmer, M.R. (2009) Dating of fossils with Lu-Hf isotopic system: revisiting an old idea with new approaches. In: Tutken, T. and Pjor, N. (Eds.), 6th International Bone Diagenesis Meeting, September 18-21, Bonn, Germany, p. 29.

Kohn, M. J. (2008) Model of diffusion-limited uptake of trace elements in fossils and rates of fossilization. *Geochim. et Cosmochim. Acta* **72**, 3758-3770.

Kolodny, Y., Luz, B., Sander, M., and Clemens, W.A. (1996) Dinosaur bones: fossils or pseudomorphs? The pitfalls of physiology reconstruction from apatitic fossils. Palaeogeogr. Palaeoclimatol. Palaeoecol. 126, 161-171.

Lukens, W. E., Grandstaff, D. E., and Terry Jr., D. O. (2009) Rare earth element signatures in fossil bones: a tool for mitigating fossil poaching on federal lands. In: Foss, S., Cavin, J., Brown, T., Kirkland, J., and Stantucci, V. (Eds.), Proceedings of the 8th Conference on Fossil Resources, May, 19-21, St. George, UT, 10-13

MacFadden, B. J., Labs-Hochstein, J., Hulbert, R.C. Jr., and Baskin, J.A. (2007) Revised age of the late Neogene terror bird (Titanis) in North America during the Great American Interchange. Geol. 35, 123-126.

Spicer, R.A. Corfield, R.M., 1992. A review of terrestrial and marine climates in the Cretaceous with implications for modeling the "Greenhouse Earth". Geological Magazine. 2, 169-180.

Suarez, C. A., Suarez, M.B., Terry Jr., D.O., and Grandstaff, D.E. (2007) Rare earth element geochemistry and taphonomy of the Early Cretaceous Crystal Geyser Dinosaur Quarry, east-central Utah. PALAIOS 22, 500-512.

Suarez, C. A., Macpherson, G. L., and Grandstaff, D. E. (2009) Rare earth element geochemistry of fossil bone: using geochemical patterns to trace illegally excavated fossils. In: Foss, S., Cavin, J., Brown, T., Kirkland, J., and Stantucci, V. (Eds.), Proceedings of the 8th Conference on Fossil Resources, May 19-21, St. George, UT. 4-6.

Suarez, C.A., Macpherson, G.L., González, L.A., and Grandstaff, D.E. (2010) Heterogeneous rare earth element (REE) patterns and concentrations in a fossil bone: Implications for the use of REE in vertebrate taphonomy and fossilization history. *Geochim. Cosmochim. Acta*, doi:10.1016/j.gca.2010.02.023.

Terry Jr., D. O., Grandstaff, D. E., Lukens, W. E., and Beasley, B. A. (2009) The use of rare earth element signatures in vertebrate fossils as a tool to investigate fossil poaching: A cooperative effort between Nebraska Forest and Temple University. In: Foss, S., Cavin, J., Brown, T., Kirkland, J., and Stantucci, V. (Eds.), Proceedings of the 8th Conference on Fossil Resources, May 19-21, St. George, UT. 7-9.

Trueman, C. N., Benton, M.J., and Palmer, M.R. (2003) Geochemical taphonomy and shallow marine vertebrate assemblages. *Palaeogeog., Palaeoecol., Palaeoclimatol.* 197, 151-169.

Trueman, C. N., Palmer, M. R., Field, J., Privat, K., Ludgate, N., Chavagnac, V., Eberth, D. A., Cifelli, R., and Rogers, R. R. (2008) Comparing rates of recrystallisation and the potential of preservation of biomolecules from the distribution of trace elements in fossil bones. *Comptes Rendus Palevol* **7**, 145 - 158.

CHAPTER 2. HETEROGENEOUS RARE EARTH ELEMENT (REE) PATTERNS AND CONCENTRATIONS IN A FOSSIL BONE: IMPLICATIONS FOR THE USE OF REE IN VERTEBRATE TAPHONOMY AND FOSSILIZATION HISTORY

ABSTRACT

A bone fragment (CGDQ-3) of *Falcarius utahensis,* a therizinosaur from the Early Cretaceous Cedar Mountain Formation, Utah, contained within a carbonate nodule, was analyzed by laser ablation inductively coupled plasma mass spectrometry (LA-ICP-MS) in order to investigate REE variability within a thin-walled phalanx. Previous studies have found depth-related REE pattern variations; however, in CGDQ-3 variation occurs along the circumference of the bone. NASC-normalized REE patterns and concentrations vary between two apparent end members. A light-REE enriched (LREE) pattern, similar to solution ICP-MS analysis of this bone, characterizes approximately two-thirds of the bone fragment. Total REE concentrations are high and do not vary significantly from the periosteal surface to the medullar surface. Conversely, the remaining one-third of the bone has REE patterns that are MREE-depleted and low in total REE concentrations. REE concentrations in this part of the bone do not vary significantly from the periosteal to the medullar surface. A positive Ce anomaly is found throughout the entire bone, and is greatest within the LREE-enriched portion of the bone. This, in combination with the LREE-enrichment, suggests that the bone fossilized under reducing conditions. The distance between the LREE-enriched and MREE-depleted regions is less than 1 mm. Isotopic and petrographic analyses of the bone and surrounding carbonate matrix suggest

the REE patterns in the bone were the result of partial fossilization/incomplete filling of micro-pore spaces around bone crystallites in an environment with changing redox conditions. The lower, MREE-depleted part of the bone fossilized contemporaneously with a pendant cement that formed on the underside of the bone in the vadose zone. Formation of the pendant cement restricted water flow through the bone, isolating the lower portion, which incorporated a MREE-depleted pattern. The upper part of the bone (LREE-enriched side) fossilized under more reducing conditions than the lower part. This resulted in reductive dissolution of minerals (such as hydrous ferric oxides and manganese oxides) which were LREE-enriched with positive Ce anomalies. These REE were then incorporated into the upper part of the bone. This likely occurred after the bone entered the saturated zone (below the water table). The thinness of the bone and presence of a pendant cement helped facilitate partial fossilization of the bone, preserving the REE signature of an earlier fluid. As demonstrated by this case study, differences in REE patterns within a fossil may record changes in geochemical conditions during fossilization, particularly, when bones are encased in a material that reduces fluid permeability, such as micritic vadose calcite. Analysis of such bones may offer the opportunity to decipher complex fluid histories that occur during fossilization. LA-ICP-MS should be utilized to confirm solution ICP-MS analysis if it yields high REE variability, prior to an interpretation of reworking or time-averaging.

INTRODUCTION

The mineral component of bone in living terrestrial vertebrates is a poorly crystalline and non-stochiometric form of carbonate hydroxyapatite (Lowenstam and Weiner, 1989; Berna et al., 2004). Such phosphate minerals have a strong affinity for the actinide and lanthanide or rare earth elements (REE) (Koeppenkastrop and De Carlo, 1992; Fleet and Pan, 1995; Fleet et al., 2000; Trueman and Tuross, 2002; Trueman et al., 2008) which are incorporated into vertebrate remains during fossilization. Because REE concentrations in these remains are affected by fluid chemistry and mineral reactions specific to the depositional environment where fossilization takes place, researchers have used REE in vertebrate bones for various purposes such as paleoenvironmental reconstruction and taphonomic studies (Trueman, 1999; Picard et al., 2002; Trueman et al., 2003; Metzger et al., 2004; Anderson, et al., 2007; C. Suarez et al., 2007), stratigraphic association of taxa, or provenance studies (Staron et al., 2001; Patrick et al., 2004, 2007; Martin et al., 2005; Trueman et al., 2005, 2006; MacFadden et al., 2007) and paleoredox studies (Elderfield and Pagett, 1986; German and Elderfield, 1990, Grandjean-Lecúyer et al., 1993). In most previous studies, REE have been analyzed in solutions prepared by dissolving 0.01 to 0.2 g of fossil bone obtained through drilling or crushing. It is assumed that the REE pattern (i.e. normalized concentration versus atomic number) generated from solution analysis characterizes the entire bone. Such bulk techniques cannot generally reveal intra-bone REE variability. A few studies, however, (e.g., Henderson et al., 1983; Trueman and Tuross, 2002; Trueman et al., 2008; Koenig et al., 2009) have revealed that REE may vary within individual bones, with REE concentrations often decreasing with depth in the bone. Such differences may

be crucial to fossilization history and taphonomic interpretations. This study demonstrates the extent of extreme within-bone variability using laser ablation ICP-MS (LA-ICP-MS).

Bones from different units in the Crystal Geyser Dinosaur Quarry (CGDQ), east-central Utah (Kirkland et al., 2005) have different REE patterns (C. Suarez et al., 2007), making CGDQ samples ideal for this study. In one of the specimens analyzed from this site, REE differ along the bone circumference. Such variation has not been recognized by previous researchers for this or any other fossil-bearing locality. The REE heterogeneity within this CGDQ specimen has important implications for the use of whole bone chemistry and reveals the complexity of bone fossilization (Koenig et al., 2009). Other provenance studies indicate that REE could potentially be used as a forensic tool for identifying material illegally removed from public lands (Lukens et al., 2009; Terry et al., 2009; C. Suarez et al., 2009). Issues, such as intra-bone variability, however, must be resolved before such applications are utilized unambiguously.

BACKGROUND

In-vivo bone REE concentrations are generally low, typically 0.001-1 ppm (Trueman and Tuross, 2002). Bone crystallites become extremely reactive upon death and decomposition of the surrounding organic matrix due to their large surface area to volume ratio (Chinsamy-Turan, 2005). This promotes authigenic growth of a more stable form of apatite during the fossilization process (Berna et al., 2004) and creates an opportunity for REE substitution for Ca (Trueman and Tuross, 2002). Apatite crystal surfaces are negatively charged at pH > 4 (Chaïrat et al., 2007) allowing REE and other positively charged ions to be sorbed from pore-waters. These elements are incorporated into the apatite and retained, unless the apatite is dissolved or metamorphosed

(Trueman, 1999; Armstrong et al., 2001). Fossilization rate and REE incorporation in bone are controlled by growth of authigenic mineral phases and the resulting reduction of bone porosity (Millard and Hedges, 1996; Trueman and Tuross, 2002; Trueman et al., 2006, 2008). Diffusion-based rate models suggest fossilization may occur in as little as 10^3 to as much as 10^6 years depending on the thickness of the bone and burial environment (Millard and Hedges, 1996; Kohn, 2008; Koenig et al., 2009). Fossil bone typically has REE concentrations between 1 ppm and 10,000 ppm (Trueman and Tuross, 2002), depending on pore-water chemistries during fossilization (Koeppenkastrop and De Carlo, 1992; Trueman and Benton, 1997; Trueman and Tuross, 2002; Lécuyer et al., 2004; Martin et al., 2005). REE pore-water chemistry is influenced by environmental factors including fluid pH, redox, concentrations of complexing inorganic and organic ligands, and reactions with colloids (Erel and Stolper, 1993; Johannesson and Zhou, 1997; Dia et al., 2000; Johannesson et al., 2000; Gruau et al., 2004). These geochemical conditions generate characteristic REE patterns that are light REE (LREE), middle REE (MREE), or heavy REE (HREE) enriched (Trueman and Tuross, 2002). Additionally, Ce anomalies in these patterns (negative or positive deviations in Ce relative to normalized values of neighboring REE) have allowed marine bioapatites to be used as paleoredox indicators in paleooceanographic studies (German and Elderfield, 1990, Grandjean-Lecúyer et al., 1993). Fossil bone REE concentrations and patterns, thus, reflect pore-water chemistries specific to different depositional and burial environments.

GEOLOGIC SETTING

Bone for this study was collected from the Crystal Geyser Dinosaur Quarry (CGDQ), a bone-bed in the early Cretaceous (Barremian) Cedar Mountain Formation, located ~16 km south of Green River, Utah (Fig. 1), as part of a taphonomic study by C. Suarez et al. (2007). This site has a monospecific accumulation of bones of the basal therizinosaur, *Falcarius utahensis* (Kirkland et al., 2005). Bone is preserved in a ~1m thick interval composed of three units (Fig. 1) with distinct lithologic, taphonomic, and geochemical (REE chemistry) characteristics (C. Suarez et al., 2007; M. Suarez et al., 2007). Unit 1 is a 10 cm carbonate-cemented accumulation of mudstone rip-up clasts from the underlying Jurassic Morrison Formation, chert pebbles, pisolitic nodules, and bone and travertine fragments (M. Suarez et al., 2007). This unit was interpreted as calcrete developed in overbank floodplain deposits. All bones from unit 1 are characterized by MREE-enriched patterns with positive Ce anomalies. Unit 1 bones were interpreted as an autochthonous bone accumulation due to the low variability of REE patterns from bone to bone (C. Suarez et al., 2007; M. Suarez et al., 2007). Units 2 and 3 are separated by a discontinuous carbonate layer and are composed of poorly sorted green and purple silty-mudstone with floating chert pebbles and granules, rip-up mud clasts, pisolitic and pedogenic carbonate nodules, and travertine fragments. Based on the abundance of pisoliths and travertine fragments, these units were interpreted as spring-influenced proximal-floodplain deposits (M. Suarez et al., 2007). Unit 2 contains fragmentary bones that are both carbonate-free and encased in carbonate nodules. REE patterns vary from LREE-enriched to MREE-depleted (described as HREE-enriched in C. Suarez et al., 2007) with a positive Ce anomaly and the unit was

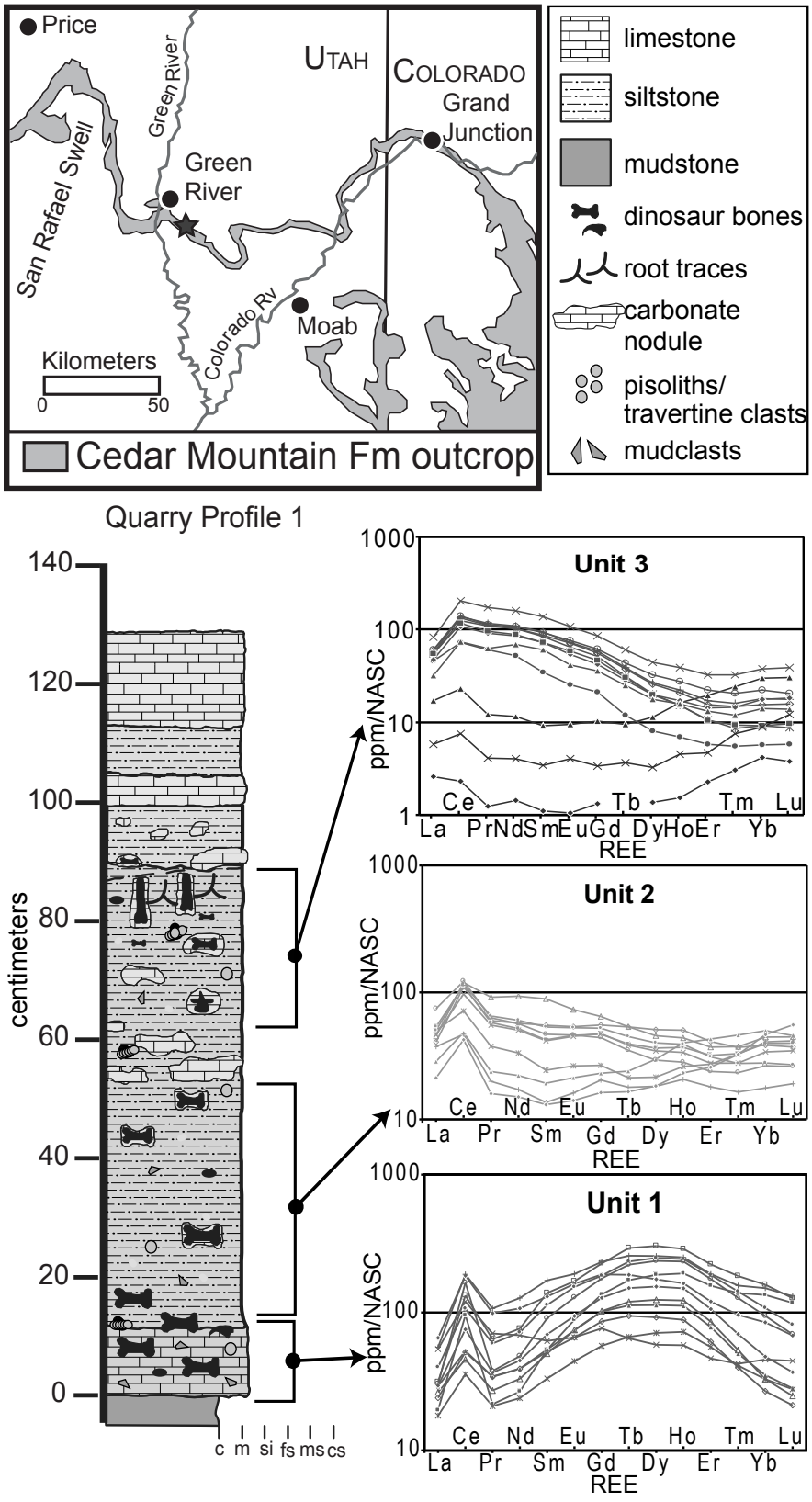

Fig. 1. Inset map of the Cedar Mountain Formation outcrop and location of the Crystal Geyser Dinosaur Quarry (filled star) with a representative stratigraphic section of the quarry. The three spider diagrams show representative REE patterns characteristic of the three bone units at the quarry site (C. Suarez et al., 2007). The three MREE-depleted patterns in unit 3 are from the three vertically-oriented limb bones (see text for details).

interpreted as a reworked accumulation due to the high REE variability from bone to bone. Unit 3 bones are LREE-enriched with a positive Ce anomaly and slightly higher La concentration. As with unit 1 bone, unit 3 was interpreted as an autochthonous fossil deposit due to its consistent LREE-enriched patterns (C. Suarez et al., 2007). However, three vertically oriented bones from unit 3 (Fig. 1), filled and encrusted with micritic calcite, differ in that they have low ΣREE concentrations and are MREE-depleted. These oriented bones may represent different fossilization conditions from the surrounding un-oriented bones of unit 3.

METHODS

The specimen for this study (CGDQ-3) was selected from the taphonomic study of the CGDQ (C. Suarez et al., 2007). CGDQ-3, collected from unit 2 (Fig. 1), is a partial phalanx covered in part with pedogenic or vadose-zone carbonate. The bone is broken into eight main closely-associated fragments, likely the result of fracturing during formation of the surrounding carbonate nodule. This specimen is an almost complete bone, allowing full characterization of the REE throughout the bone cortex. Many of the small bones (<3 cm in diameter) from unit 2 and 3 are contained within carbonate nodules. Both HREE-enriched (MREE-depleted) patterns (indicative of high pH and conducive to carbonate formation) and (LREE-enriched patterns indicative of low pH and/or low redox and not conducive to carbonate formation) are preserved in bone from unit 2 and 3. CGDQ-3 is an ideal bone to analyze as it is both contained in a carbonate nodule and has a LREE-enriched pattern. Since bones in pedogenic nodules are common throughout the terrestrial rock record (Bao et al., 1998; Gates, 2005, Kohn and Law, 2006; C. Suarez et al., 2007) and are often geochemically sampled because they are not

morphologically distinct, it is important to elucidate any taphonomic biases that occur during preservation under pedogenic conditions.

Thin (~30 μm) and thick (~100 μm) sections were prepared for petrography and LA-ICP-MS analysis, respectively. The sections were cut back-to-back, so they were approximate mirror images of each other. Both sections were rinsed in distilled water, polished with diamond paste, and then sonicated in deionized water for 2 minutes. Prior to LA-ICP-MS analysis, the thick section was briefly rinsed in 2% (v/v) distilled nitric acid, 18 MΩ water, HPLC-grade isopropanol, and then dried with a small amount of dust-free compressed air.

Petrographic Analysis

Petrographic analysis of thin and thick sections under transmitted plane polarized, reflected, and cross polarized light reveal the paragenesis of carbonate surrounding and infilling the bone, as well as any post-fossilization diagenetic alteration of bone material. Analysis was carried out using a Nikon SMZ1500 microscope fitted with an Optronics Magnafire SP digital camera and an Olympus BX51 microscope fitted with a Diagnostic Instruments SPOT Insight 4 digital camera. Cathodoluminescent (CL) analysis of CGDQ-3 thin sections was conducted using a Reliotron III CL cathodoluminoscope attached to an Olympus BX41 research microscope with Diagnostic Instruments SPOT RT3 camera at the Kansas Geological Survey.

Laser Ablation ICP-MS Analysis

Traces and spot chemical analyses were made using a New Wave Research-Merchantek EO LUV266X Nd:YAG laser attached to a PlasmaQuadII+XS ICP-MS in the Department of Geology, Plasma Analytical Laboratory at the University of Kansas. Use of 266 nm wavelength

is suggested for colorless minerals that are weakly absorbent (Jackson, 2001) and other authors have successfully used 266nm wavelength for apatite (Sha and Chappell, 1999). NIST 610 trace elements in glass standard was the external calibration standard. Glass reference standards such as NIST 610 and NIST 612, though not matrix matched, have been shown to be an appropriate standard for analysis of REE in apatite by several authors (Norman et al., 1996; Eggins, 1998; Sha and Chappell, 1999; Gunther et al., 2000; Koenig et al., 2009). The internal standard used to calculate concentrations in bone apatite was 55.601 wt. % CaO in francolite.

Traces consisted of continuous firing of the laser at 10Hz while the sample chamber moved along a computer-programmed path. The chamber moved at a speed of ~27 μm/s and created a 45 to 50 μm wide line of ablation. Background signal noise was collected for one minute prior to each acquisition. Replicates were performed by lasing three times over the exact same path, with background signal collected each time; concentration differences were insignificant among the three traces. For this study, concentrations from the second pass are reported, because that pass has the least chance of being affected by surface contamination or depth-dependent fractionation. Data were collected along two traces on the bone (Fig. 2). Trace 1 was a total of 3.706 mm and analyzed 3 mm of bone and 0.706 mm of carbonate. Trace 2 was a total of 2.878 mm and analyzed 2.781 mm of bone and 0.097 mm of carbonate.

Spot analysis consisted of firing of the laser at 10Hz, for one minute of background signal acquisition and then an additional 30-60 seconds of firing with the laser focused on the sample. The result was a cylindrical pit about 40-60 μm in diameter (Fig 2b). Element concentrations were calculated by the computer program LAMTRACE® using the algorithm of Longerich et al. (1996). Per cent relative standard deviation (%RSD) for all REE in NIST 610 was <5%.

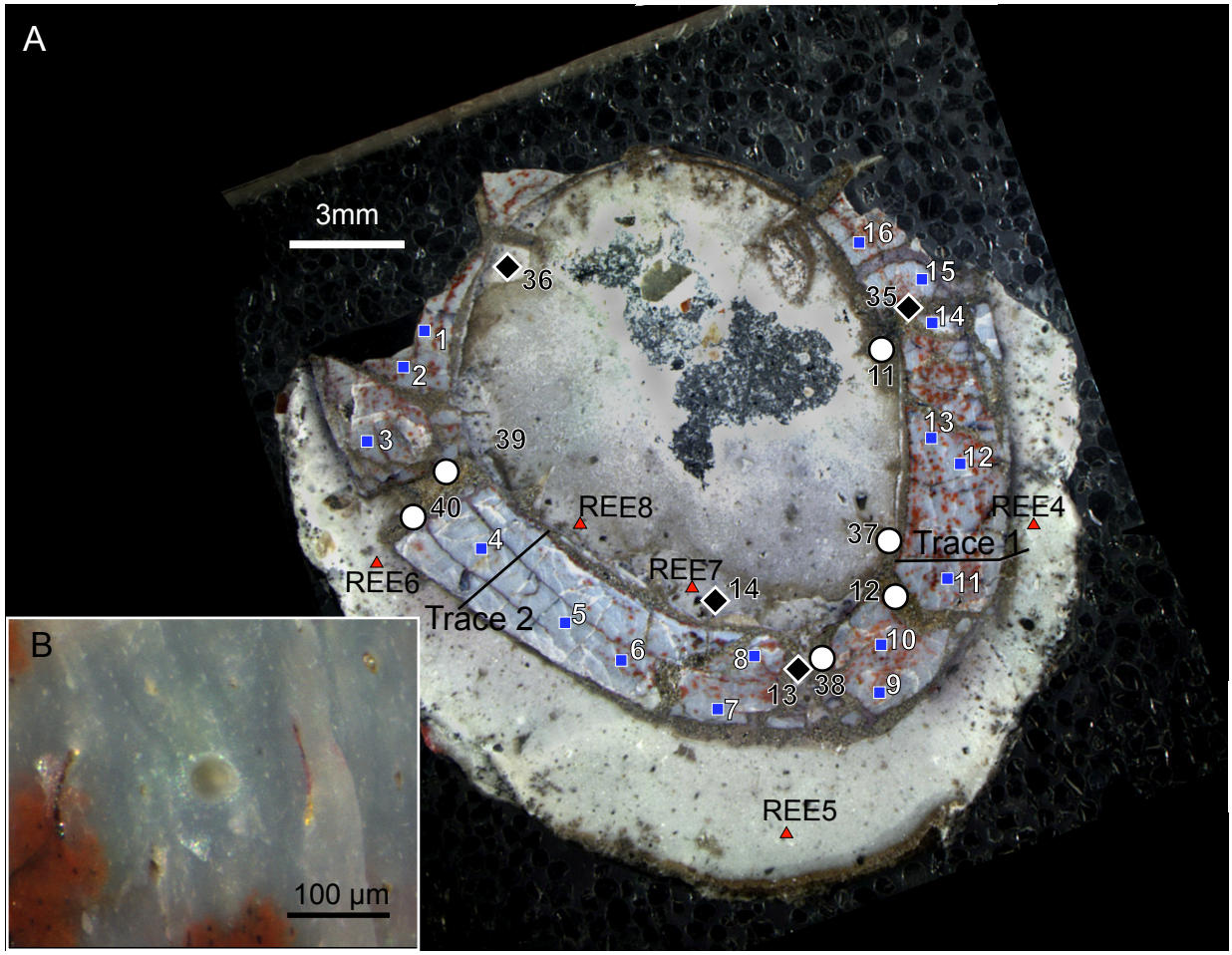

Fig. 2. (A) Locations of LA-ICP-MS analyses for CGDQ-3, the specimen used in this study. Locations of spot bone analyses are represented by squares. Locations of continuous transects are given by solid lines (Traces 1 and 2). Locations of carbonate spot analyses are represented by triangles and labeled "REE#." Locations sampled for isotopic analyses in the carbonates are labeled in white outlined black numbers and correspond to sample numbers in Table 3. Mn-rich Sparry Calcite: white circles. Inner Micrite: black diamonds. Symbols correspond to data plotted in Fig. 8. (B) Example of a laser pit in bone.

Sixteen spots (Fig. 2, Spots 1-16; Table 2, CGDQ-3-1 to CGDQ-3-16) along the circumference of the bone were analyzed. In addition, five spots were analyzed in the infilling and surrounding carbonate (Fig. 2, REE-4 to REE-8; Table 2, CGDQ-3-REE-4 to CGDQ-3-REE-8). Two of these were of the in-filling carbonate and three were of the surrounding carbonate.

For traces and spots, major oxides (MgO, CaO, ΣFeO, ΣMnO, SiO_2, and P_2O_5) are reported as weight per cent, transition elements, alkaline earth elements (including Ba and Sr), and trace elements (including REE and U) are reported in parts per million (ppm). Precision expressed as per cent relative standard deviation for most elements was better than 5%; for P_2O_5 was about 10% and FeO was about 20% if concentrations were less than about 1 weight%. REE concentrations were normalized using the North American Shale Composite (NASC) (Gromet et al., 1984). Cerium anomalies (redox proxy) were calculated and are presented in Table 2.

The time required for REE-apatite equilibrium was calculated based on the diffusion-adsorption model of uranium uptake by Millard and Hedges (1996). An exponential curve fitted to the uranium profile data was used to calculate the reduced dimensionless concentration parameter, Z' (Millard and Hedges, 1996; equation 4 and Figure 1) at the bone center (where $x' = 0$ is the center of the bone and $x' = 1$ and -1 are the outer and inner surfaces respectively). For the high ∑REE side of the bone the equation is:

$$Z' = 0.8856e^{-0.124x'} \quad (1)$$

For the low ∑REE side of the bone the equation is:

$$Z' = 0.6206e^{-0.115x'} \quad (2)$$

The reduced time (t') was then calculated from Z' (at $x' = 0$). The equilibrium time (t) was then calculated using the parameter values of Millard and Hedges (1996) with the exception

of temperature. We used a temperature of 22.7ºC, the mean annual temperature (MAT) for the middle Cretaceous of continental North American estimated by Ufnar et al. (2002). This also alters the viscosity of water to 0.0094 g/cm/s and, using the Stokes-Einstein equation, increases the diffusion coefficient for uranium (D_o) to ca. 2.88 x 10^{-6} cm^2 s^{-1} (Millard and Hedges, 1996).

Stable Isotopic Analysis

Approximately 250 to 400 µg of bone powder and 60 to 100 µg of carbonate phases were milled from the thick section analyzed by LA-ICP-MS and the billet used to make the thick section CGDQ-3 (Fig 3, Table 3) for stable isotopic analysis. Samples were roasted at 200ºC for 1 hour to remove volatile components. To determine if diagenetic calcite was present and to assess its possible effects on stable isotope results, a sample subset of bone powder ranging from 1 to 2 mg of bone powder was cleaned in acetic acid-Ca acetate solution buffered to pH ~ 4.5, rinsed with ultrapure water, dried, and roasted at 200ºC following procedures outlined in Koch et al. (1997). Samples were analyzed at the W. M. Keck Paleoenvironmental and Environmental Stable Isotope Laboratory at the University of Kansas by reaction with 100% H_3PO_4 at 75°C using a Kiel III carbonate reaction device interfaced to the inlet of a ThermoFinnigan MAT 253 Dual Inlet mass spectrometer. All data are reported in part per thousand (‰) relative to VPDB, using standard δ-notation. Precision was monitored through the daily analysis of NBS-18 and NBS-19 and is better than 0.10‰ for both $\delta^{13}C$ and $\delta^{18}O$. Stable isotopic sampling was performed prior to CL-imaging and therefore, sampling was conducted strictly on transmitted and cross-polarized light observations.

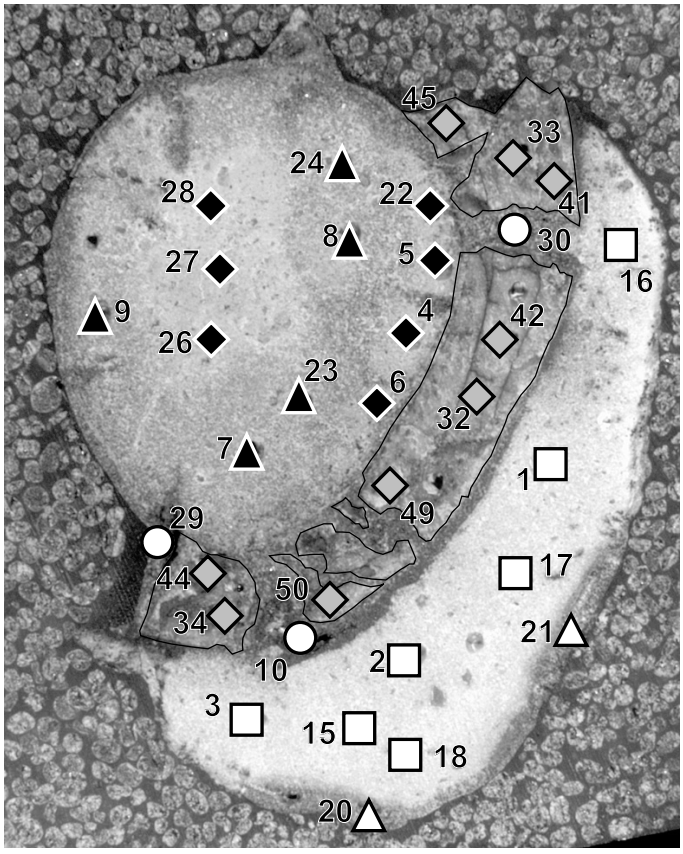

Fig. 3. Carbonate isotope sampling locations on sample billet. A polished thick section for carbonate isotope analyses was made from the billet facing that used for LA-ICP-MS analyses. Thus, this image is a mirror image of Fig. 2A. Labeled sample numbers correspond to Table 3. Bone: grey diamonds. Mn-rich Sparry Calcite: white circles. Inner Micrite: black diamonds. Microsparry Calcite: black triangles. Outer Micrite: white squares. Mn-stained outer edge of Outer Micrite: white triangles. Bone fragments are outlined in black. Additional samples were taken from the thick section used to sample REE (see Fig. 2). Symbols correspond to plotted data in Fig. 8.

RESULTS

Petrographic and Cathodoluminescence Analysis

Five calcite zones infill and surround the bone (Fig. 4); their characteristics are summarized in Table 1. The zones are: (1) a light gray Inner Micrite lining the inside surface of the bone and filling the center portion of the carbonate that fills the medullary cavity. This micrite grades into (2) a gray Microsparry Calcite that surrounds the center portion of Inner Micrite and fills the rest of the inside of the bone. Surrounding part of the bone exterior is (3) a lighter gray Outer Micrite. An Fe-rich Sparry Calcite (4) is present mostly along bone fractures and in contact with both the Inner and Outer Micrite. A Mn-rich Sparry Calcite covers some bones surfaces, fills some fractures, and overgrows the Fe-rich Sparry Calcite. Minor amounts of silt to fine sand-sized grains that include quartz, iron oxides, and other silicates are present in both Outer and Inner Micrite.

Although the specimen is fragmented and surrounded by carbonate, the bone micromorphology is well preserved. Thin and thick sections (Fig. 2 and 4) of CGDQ-3 reveal that *Falcarius* has fibrolamellar bone and structures such as original osteons, secondary osteons from bone remodeling, some original endosteal bone and osteocyte

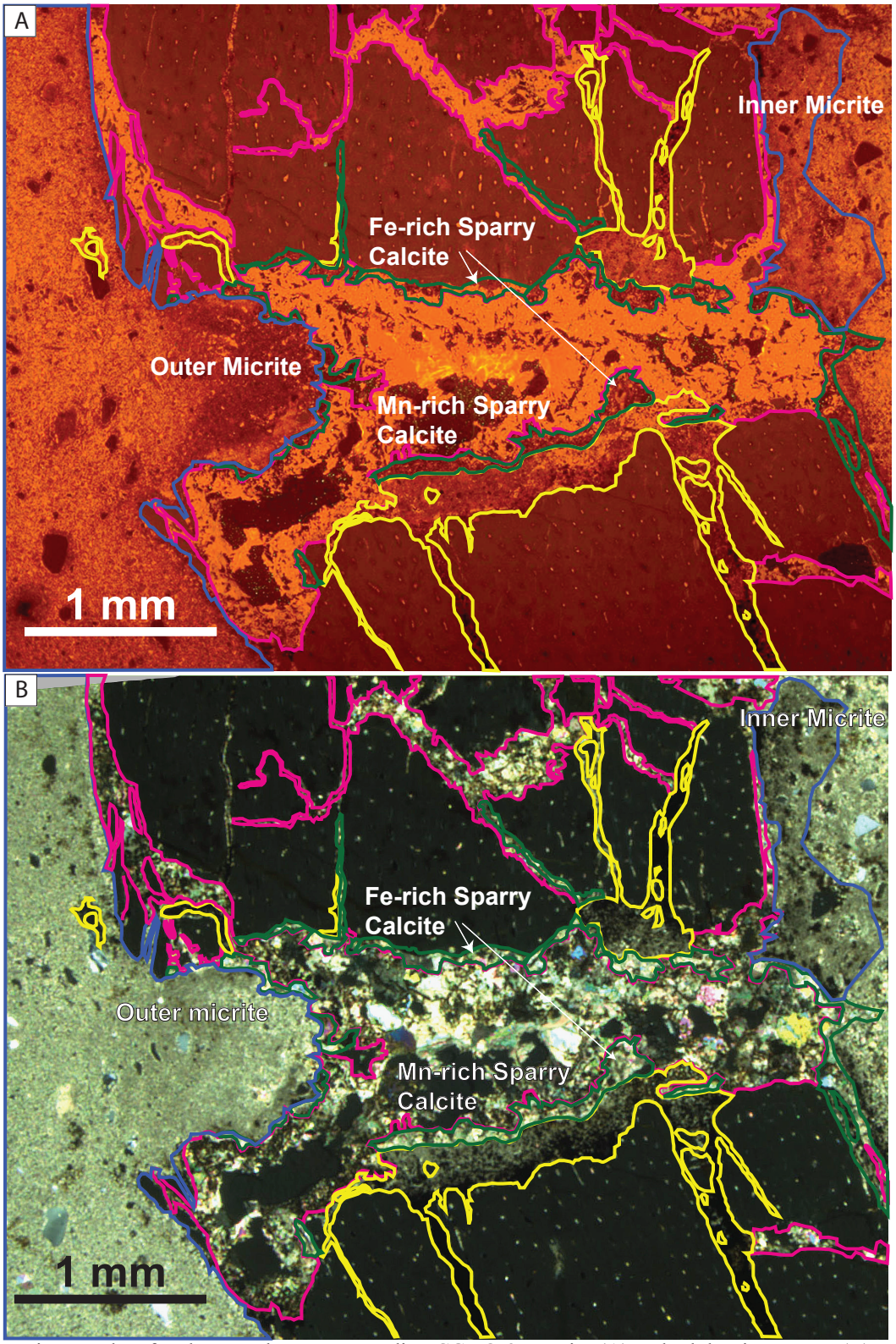

Fig. 4. Photomicrographs of carbonate phases surrounding CGDQ-3 seen in: (A) cathodoluminescence. (B) cross-polarized light. Blue = surrounds the Outer and Inner Micrite. Yellow = micrite with local abundant Fe-oxide grains (opaque patches). Magenta = luminescent sparry calcite (Mn-rich Sparry Calcite). Green = non-luminescent sparry calcite (Fe-rich Sparry Calcite).

TABLE 1. Carbonate Phases

Carbonate Phase	Transmitted light	Cross-polarized light	Reflected light	CL imaging
Inner Micrite	Light grey; contains opaque Fe-oxide particles that accumulate along the bone surfaces and cracks	Moderate-weak first-order interference colors	Light grey-white, contains red Fe-oxide particles that accumulate along the bone surfaces and cracks	Moderate orange luminescence
Microsparry Calcite	grey; contains pieces of inner micritic	Moderate-weak first-order interference colors	Grey	Moderate-strong orange luminescence
Outer Micrite	Light grey (lighter than Inner Micrite)	Moderate-weak first-order interference colors	Light grey-white	Moderate orange luminescence
Fe-rich Sparry Calcite	translucent	Strong first-order interference colors; smaller cleavage faces than Mn-rich Sparry Calcite	translucent	Low luminescence
Mn-rich Sparry Calcite	Dark brown	Strong first-order interference colors	Dark brown	Very strong orange luminescence; larger euhedral crystals have alternating luminescent and non-luminescent growth terminations

lacunae. Fe-oxides fill and stain the centers of osteons and radiate from the osteons to the osteocytes through the canuliculi canals, resulting in a distinct pattern of Fe-oxide-filled osteocytes. We call these "red mineral accumulations" (RMA). Extinction patterns suggest apatite crystals are still aligned as they were *in-vivo*, parallel to collagen fibers. Overall, the microstructures throughout the bone preserve the fine structures of typical dinosaur bone micromorphology (e.g., Chinsamy-Turan, 2005).

Geochemical Analyses

Trace Element Analysis

REE data are presented in Table 2 and concentrations of representative light (Nd), middle (Gd), heavy (Yb) REE; the redox-sensitive REE Ce, the redox-sensitive actinide U, and weight % for ΣFeO and ΣMnO are presented from the traces as a function of bone depth (defined as exterior to interior of bone) in Fig. 5. For Trace 2 (Fig. 5B), there is a slight and gradual decrease in REE and U concentrations from the outer periosteal surface into the center of the bone cortex and inner medullar surface. The concentration gradients are slightly steeper in the first few microns than in the rest of the bone. The gradient flattens as concentrations gradually decrease throughout the rest of the bone. In Trace 1, REE concentrations decrease only very slightly through the depth of the bone and are much more variable than in Trace 2. REE concentration gradients are shallower than those found by Trueman et al. (2006) and are typical of "flat" profiles described by Millard and Hedges (1996) and

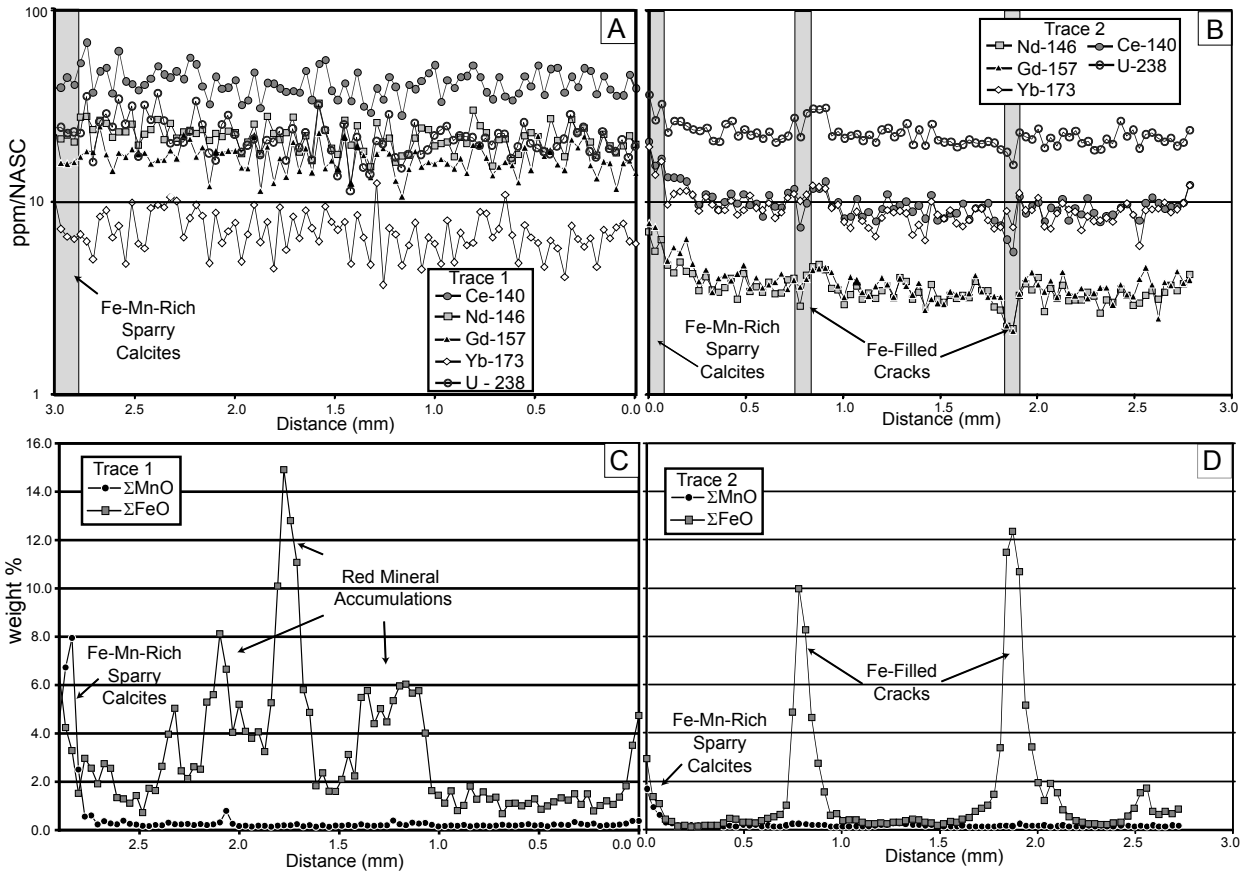

Fig. 5. CGDQ-3 concentration profiles on a log scale of: (A) selected REE (normalized) and U concentrations along Trace 1. Grey bars are locations where the laser ablated Mn-rich and Fe-rich Sparry Calcites surrounding the bone (see Fig. 4). (B) Selected REE (normalized) and U concentrations through Trace 2. The first few µm ablated (represented by the grey bar) were of Mn-rich and Fe-rich Sparry Calcites surrounding the bone. (C) Weight percent ∑FeO (total Fe calculated as FeO) and ∑MnO (total Mn calculated as MnO) in Trace 1. The first few µm are high in both ∑MnO and ∑FeO and correspond to the Fe- and Mn-rich Sparry Calcites. Red spots visible in Fig. 2 have high ΣFeO content. (D) Weight percent ∑FeO and ∑MnO in Trace 2. The first few µm and fracture-fills have high weight percent ∑MnO and ∑FeO.

TABLE 2. Elemental Concentrations of Spot Analyses†

Spot:	Sr	Ba	Y	La	Ce	Pr	Nd	Sm	Eu	Gd	Tb	Dy	Ho	Er	Tm	Yb	Lu	ΣREE	Ce*
CGDQ-3-#																			
1	3640	462	535	799	3750	284	926	162	33.7	123	16.5	83.9	14.8	33.4	4.3	28.8	4.1	6260	0.82
2	3750	461	524	824	3670	291	986	172	34.4	136	18.1	92.2	16.2	33.1	4.0	25.4	3.6	6300	0.74
3	3890	476	621	916	3860	275	941	159	33.4	136	18.0	95.9	17.1	39.8	4.9	33.7	4.6	6530	0.80
4	3620	471	266	391	887	43.6	134	20.8	4.4	26.1	3.0	19.9	5.2	18.0	3.9	37.4	7.0	1600	0.47
5	3560	471	263	383	808	39.3	122	16.4	4.0	23.8	2.8	19.0	4.8	18.8	3.9	40.0	7.4	1490	0.40
6	3650	456	288	394	749	37.5	116	16.8	3.9	23.6	2.8	19.8	5.5	20.7	4.3	42.4	8.0	1440	0.29
7	3690	517	189	161	259	10.1	30.1	4.4	1.2	12.9	1.1	11.1	3.9	19.2	4.5	44.6	8.3	572	0.20
8	3700	491	184	155	207	8.2	23.6	3.6	1.0	10.2	0.9	9.2	3.5	17.9	4.3	44.9	8.1	497	0.03
9	3600	470	339	306	756	36.0	115	16.4	4.2	26.3	3.5	27.2	7.9	31.1	5.9	51.4	8.2	1400	0.58
10	3550	454	323	302	755	35.7	109	17.7	3.8	24.3	3.3	26.4	7.7	28.4	5.5	50.3	7.9	1380	0.59
11	3650	455	547	782	3470	246	805	137	28.8	116	15.2	82.1	14.7	34.0	4.3	28.8	4.1	5770	0.85
12	3620	482	550	809	3520	251	802	135	29.1	114	15.1	78.9	14.2	33.0	4.2	27.8	4.0	5840	0.83
13	3780	520	555	776	3530	245	781	129	27.2	112	15.0	76.4	14.0	32.8	4.3	29.1	4.30	5780	0.89
14	3380	419	552	836	2790	173	547	85.2	18.9	84.5	11.0	63.8	13.4	36.4	5.1	36.2	5.4	4700	0.71
15	3620	489	514	818	2930	182	571	89.1	19.5	82.3	10.9	62.3	12.7	33.4	4.5	34.1	4.7	4860	0.78
16	3480	469	506	813	2690	162	503	78.4	17.5	78.3	10.4	60.7	12.6	34.5	4.8	34.3	4.9	4500	0.73
CGDQ3-$CaCO_3$-REE-#																			
4	465	16.8	8.8	7.4	17.1	1.1	3.6	0.84	0.14	1.5	0.12	1.2	0.30	1.3	0.27	2.3	0.43	37.6	0.35
5	840	14.8	4.8	6.8	9.8	0.76	3.2	0.53	n.d.	0.51	n.d.	0.48	0.08	0.50	0.12	0.74	n.d.	23.5	-0.06
6	900	46.4	8.1	10.9	30.1	1.5	5.5	0.86	0.21	0.97	0.24	1.6	0.34	0.90	0.19	1.6	0.25	55.2	0.67
7	314	36.9	8.5	7.2	21.2	1.0	4.4	n.d.	0.22	n.d.	n.d.	1.1	0.23	1.2	0.21	3.6	0.61	41.0	0.78
8	579	83.7	3.8	5.6	9.6	1.0	3.2	n.d.	n.d	n.d.	n.d.	n.d.	0.17	0.43	0.12	n.d.	0.19	20.3	-0.06

†concentration in ppm; $Ce^* = [2Ce_N/(La_N + Pr_N)] - 1$ (subscript N = NASC normalized values (Gromet et al., 1984).

Trueman et al. (2008). Ratios of the various REE for both traces also do not significantly change with depth in the bone.

The iron and manganese-oxide profiles (Fig. 5) corroborate the presence of Mn-rich Sparry Calcite revealed by CL imaging (orange luminescent calcite). Profiles across the RMA that line and infill vascular canals are rich in iron, as are the two distinct iron-oxide filled cracks along Trace 2. REE concentrations and signatures in the RMAs and crusts do not seem to differ significantly from those of surrounding bone apatite.

Results of previously reported (C. Suarez et al., 2007) solution analysis and subsequent re-analysis of CGDQ-3 and surrounding carbonates by LA-ICP-MS are shown in Fig. 6. Solution analysis of the bone (C. Suarez et al., 2007) produced a high ΣREE concentration, LREE-enriched pattern similar to LA-ICP-MS results from Spots 1-3 and 11-16 and Trace 1. However, LA-ICP-MS analyses for Spots 4-10 and Trace 2 produced patterns greatly different from the solution ICP-MS results. The ΣREE concentrations of Spots 4-10 are low in ΣREE, with pronounced W-type tetrad effects (positive Gd anomaly; e.g., Grandstaff and Terry, 2009), and have MREE-depleted (i.e. relative enrichment in LREE and HREE) patterns, rather than the LREE-enriched pattern of the solution analysis (Figs. 6 and 7). Carbonate REE concentrations are lower than bone REE patterns in most cases. Mn-rich Sparry Calcite is higher in REE concentration than the Outer Micrite and Inner Micrite. The REE pattern is in general MREE-depleted (Fig. 6).

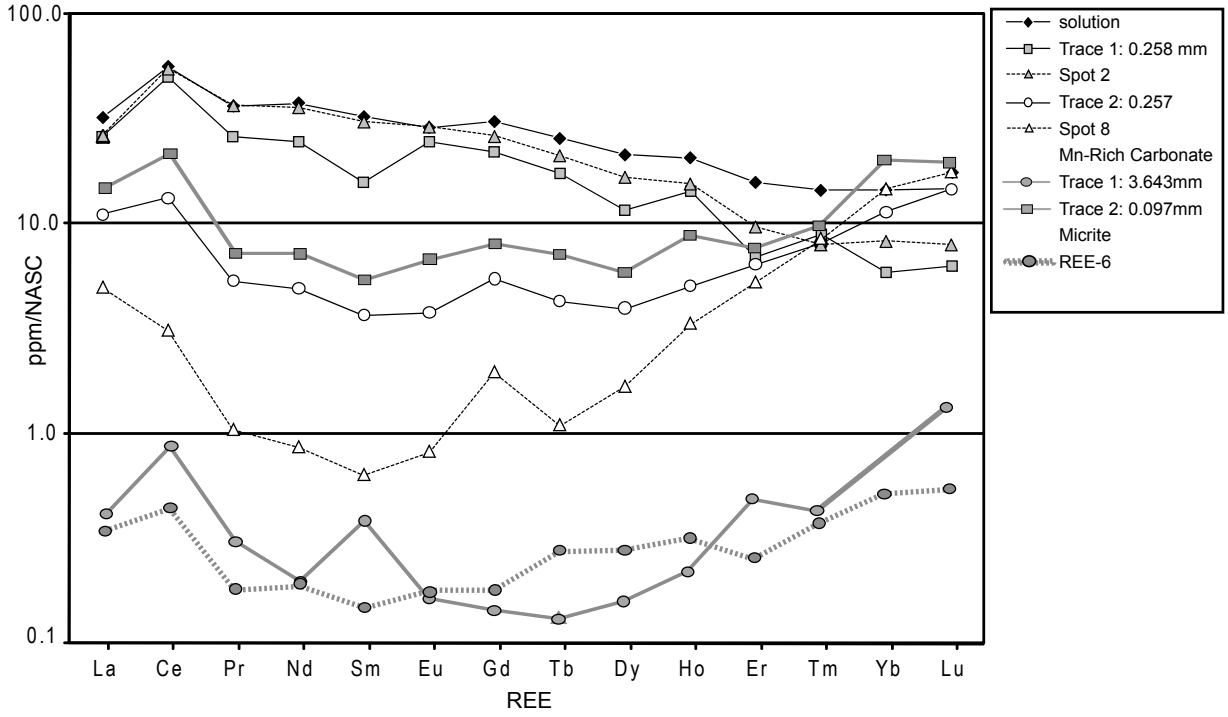

Fig. 6. Selected REE patterns from the solution analysis, along traces, and for spot analyses for the bone and carbonate specimen. Trace 1 is LREE-enriched. Trace 2 is MREE-depleted. The REE pattern determined by solution ICP-MS (black diamond, solid line) has the highest concentration and is similar to the Trace 1 patterns. The lowest bone concentration is represented by Spot 8 (white triangle, dotted line) which has a pattern similar to Trace 2. REE concentrations for the Mn-rich Sparry Calcite along Trace 1 and 2 (gray lines and symbols) and the Outer Micrite (dotted grey lines and symbols) are MREE-depleted and generally lower in REE concentration than bone.

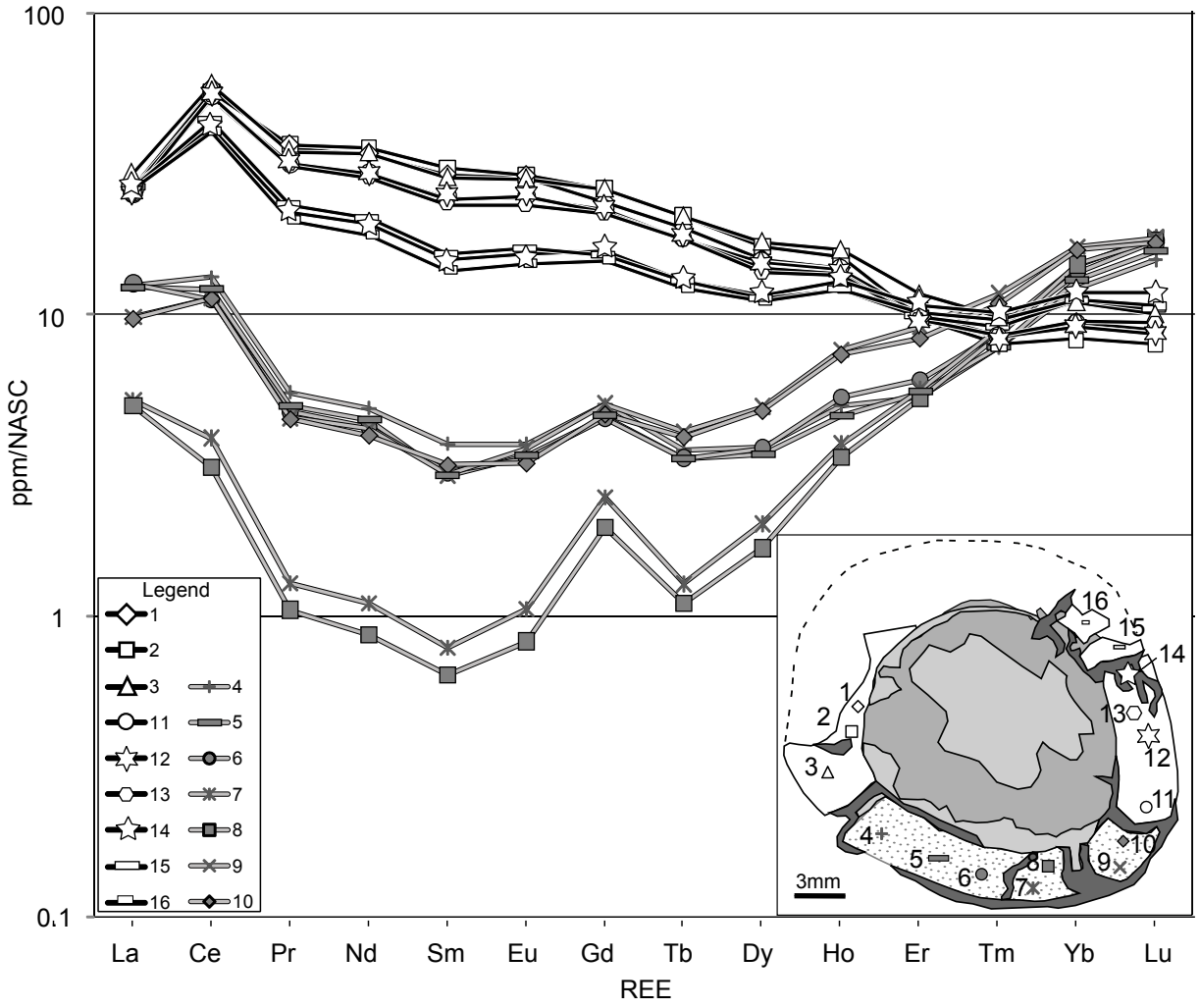

Fig. 7. Distribution of REE patterns along bone specimen. LREE-enriched patterns (black line/ open symbols) occur in Spots 1-3 and 11-16. MREE-depleted patterns characterize Spots 4-10 (grey lines/ closed dark grey symbols). The inset figure depicts the position and symbol of each spot on the bone. The stippled part of the bone contains the MREE-depleted spot analyses, whereas the un-stippled part of the bone contains the LREE-enriched spot analyses.

Stable Isotopic Analysis

The various calcite phases have $\delta^{18}O$ values that range from -10.05 to -6.59‰ and $\delta^{13}C$ from -4.14 to -0.70‰ (Table 3). Mn-rich carbonate (which probably includes both the Mn-rich Sparry Calcite and Fe-rich Sparry Calcite) are somewhat lighter in $\delta^{18}O$ (-8.45 to -10.05‰) and more variable in $\delta^{13}C$ (-0.70 to -4.14‰) than the Inner Micrite (average $\delta^{18}O$ = -7.28‰ ±0.31, $\delta^{13}C$ = -3.02‰ ±0.17), Microsparry Calcite (average $\delta^{18}O$ = -7.05‰ ±0.05, $\delta^{13}C$ = -1.90‰±0.34), and Outer Micrite (average $\delta^{18}O$= -6.91‰ ± 0.05, $\delta^{13}C$ = -1.93‰ ± 0.17). Stable isotopic values for the structural carbonate of apatite are extremely variable in $\delta^{18}O$ ranging from -1.27 to 11.31‰ and are less variable for $\delta^{13}C$ ranging from -5.42 to -2.48‰ (Fig 8).

Equilibrium Rate Calculations

Uranium concentration profiles generated in Traces 1 and 2 were used to calculate the time for U to equilibrate with bone apatite (an approximation of fossilization time, assuming no post-fossilization recrystallization has occurred, which is suggested by the well preserved micromorphology). The exponential curve fitted to the data for the high ∑REE, LREE-enriched area generated $Z'(x' = 0) = 0.89$, yielding a reduced time, t' value of 0.98. In contrast, the low ∑REE, MREE-depleted area exponential generates a Z' ($x' = 0$) = 0.60, which yields $t' = 0.49$. Based on these values, a U equilibrium time of ~12,300 years was calculated for the LREE-enriched area and ~5,600 years for the MREE-depleted area.

TABLE 3. Stable Isotopes

Sample	Description	$\delta^{18}O_{VPDB}$	$\delta^{13}C_{VPDB}$
CGDQ-3-14	Inner Micrite	-6.59	-3.06
CGDQ-3-4	Inner Micrite	-7.54	-2.83
CGDQ-3-5	Inner Micrite	-7.48	-2.94
CGDQ-3-6	Inner Micrite	-7.43	-2.92
CGDQ-3-22	Inner Micrite	-7.42	-2.89
CGDQ-3-36	Inner Micrite	-7.47	-3.35
CGDQ-3-26	Inner Micrite	-6.97	-2.97
CGDQ-3-27	Inner Micrite	-7.38	-2.77
CGDQ-3-28	Inner Micrite	-7.16	-3.09
CGDQ-3-13	Inner Micrite	-7.28	-3.11
CGDQ-3-35	Inner Micrite	-7.368	-3.26
CGDQ-3-3	Outer Micrite	-7.00	-2.18
CGDQ-3-1	Outer Micrite	-6.92	-1.83
CGDQ-3-15	Outer Micrite	-6.86	-1.80
CGDQ-3-16	Outer Micrite	-6.93	-2.04
CGDQ-3-17	Outer Micrite	-6.89	-1.73
CGDQ-3-18	Outer Micrite	-6.86	-2.01
CGDQ-3-20	Mn-rich edge of Outer Micrite	-8.21	-2.50
CGDQ-3-21	Mn-rich edge of Outer Micrite	-8.18	-2.25
CGDQ-3-7	Microsparry Calcite	-7.06	-1.63
CGDQ-3-8	Microsparry Calcite	-6.97	-1.56
CGDQ-3-9	Microsparry Calcite	-7.09	-1.79
CGDQ-3-23	Microsparry Calcite	-7.04	-2.30
CGDQ-3-24	Microsparry Calcite	-7.09	-2.22
CGDQ-3-10	Mn-rich Sparry Calcite - outer bone	-9.58	-3.52
CGDQ-3-11	Mn-rich Sparry Calcite - inner bone	-8.59	-3.73
CGDQ-3-37	Mn-rich Sparry Calcite - inner bone	-10.05	-4.14
CGDQ-3-12	Mn-rich Sparry Calcite - between bone	-9.04	-1.77
CGDQ-3-29	Mn-rich Sparry Calcite - between bone	-8.69	-1.53
CGDQ-3-30	Mn-rich Sparry Calcite - between bone	-8.72	-1.76
CGDQ-3-38	Mn-rich Sparry Calcite - between bone	-9.95	-3.94
CGDQ-3-40	Mn-rich Sparry Calcite - between bone	-9.72	-3.94
CGDQ-3-39	Mn-rich Sparry Calcite - between bone	-8.45	-0.70
CGDQ-3-32	bone - HREE side	8.64	-2.81
CGDQ-3-42	bone - HREE side	1.68	-3.99
CGDQ-3-33	bone - LREE side	5.68	-3.17
CGDQ-3-34	bone - HREE side	11.31	-2.48
CGDQ-3-41	bone - LREE side	-1.27	-3.59
CGDQ-3-44	bone - HREE side	0.35	-4.57
CGDQ-3-45	bone - LREE side	7.80	-3.59
CGDQ-3-49	bone - HREE side	0.19	-5.42
CGDQ-3-50	bone - HREE side	-0.22	-4.49

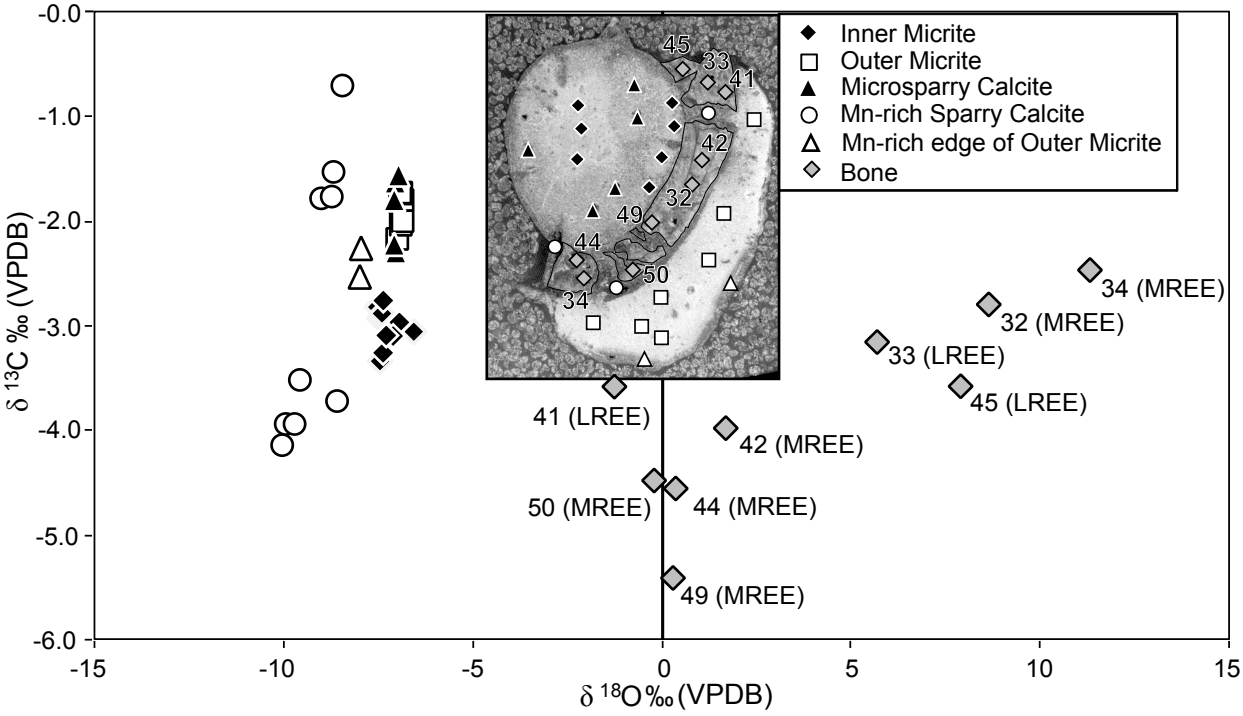

Fig. 8. Cross-plot of carbon and oxygen stable isotopic values of the various carbonate phases and bone structural carbonate. Bone samples are labeled in the inset picture and their representative REE patterns are presented in parentheses. The Outer Micrite (white squares), Inner Micrite (black diamonds), and Microsparry Calcite (black triangles), all fall along a meteoric calcite line. Mn-rich Sparry Calcite (white circles) also falls along a meteoric calcite line that is shifted toward a slightly lighter composition. The Mn-stained outer edge of the Outer Micrite (open triangles) seems to be a mixture of the Mn-rich Sparry Calcite and the Outer Micrite. Bone structural carbonate (grey diamonds) is highly enriched in 18O. Diagenetic fluids that precipitated the carbonate phases do not correlate isotopically to the fluids that precipitated the bone carbonate. Note: during sampling, it was nearly impossible to distinguish between the Mn-rich and Fe-rich Sparry Calcite, and therefore, the Mn-rich Sparry Calcite composition includes values of both Fe- and Mn-rich phases.

INTERPRETATION AND DISCUSSION

Stable Isotope Geochemistry

Similar $\delta^{13}C$ and $\delta^{18}O$ isotopic values in fossil-bone structural carbonate and the surrounding carbonate would suggest concurrent carbonate precipitation and likely post-fossilization alteration by the same diagenetic fluids. However, the isotopic trends and values are very different (Fig. 8). In general, the relatively invariant $\delta^{18}O$ and highly variable $\delta^{13}C$ in the diagenetic calcite define meteoric calcite lines (Fig. 8) (*sensu* Lohmann, 1988). The bone carbonate $\delta^{18}O$ is significantly heavier than any calcite (Fig. 8) and positively co-varies with $\delta^{13}C$.

The $\delta^{18}O$ of the precipitating fluids for calcite and structural carbonate of apatite were calculated assuming an abiotic origin for all phases in order to compare the isotopic values of the precipitating fluids. Carbonate $\delta^{18}O_{VPDB}$ values were converted to $\delta^{18}O_{SMOW}$ and the fractionation factor of Friedman and O'Neil (1977) was used for the calcite calculations. Mean Annual Temperature (MAT) for the mid-Cretaceous of Utah is estimated as ~ 22.7°C (Ufnar et al., 2002). The relationships between the phosphate $\delta^{18}O$ and phosphate structural carbonate $\delta^{18}O_{sc}$ of Shemesh et al. (1988) and the relationship between phosphate $\delta^{18}O$ and water of Karhu and Epstein (1986) were combined yielding the following equation:

$$\delta^{18}O_w = -2.17\left(\frac{10^6}{T^2}\right) + 0.57\left(\delta^{18}O_{sc}\right) + 6.72 \qquad (3)$$

The calculated $\delta^{18}O$ values of the water that precipitated the calcite and the structural carbonate in the apatite differ by no less than 4.5 ‰ and average ~7‰. We interpret this to mean

the calcite-precipitating waters and the source water for the apatite structural carbonate were different. The fluid responsible for structural carbonate was either from significantly different diagenetic fluids (not related to surrounding calcite) or represents original body water. We believe that the latter is the most likely explanation, as burial processes would produce negative $\delta^{18}O$ values (Lohmann, 1988), while consumption from multiple sources of fluids, including evaporative systems (Sorensen et al., 2002; Ufnar et al., 2008; M. Suarez et al., 2009) and foliage (Koch, 1994), will yield positive co-variant trends. The high variability of isotope values illustrates that environmental or biogenic information from fossil bone carbonate cannot be gleaned from a single sample per bone. Instead, interpretations should be based on full characterization of the sample, both petrographically and geochemically (REE and stable isotopes).

REE Geochemistry

The MREE-depleted patterns seen in Trace 2 and Spots 4-10, specifically the HREE-enrichment, are typical of alkaline solutions in which CO_3^{2-} preferentially complexes the HREE's (Brookins, 1989; Lee and Byrne, 1993; Bau, 1999; LLNL.dat database in Parkhurst and Appelo, 1999). HREE-enriched patterns can also occur if the solution equilibrates with minerals that scavenge LREE and/or MREE. Mn-oxyhydroxides scavenge MREE, which may account for the MREE-depletion (Dubinin, 2004). Competition between apatite and another minerals with greater partition coefficient (K_d) for LREE and MREE will result in a solution that is HREE-enriched (or MREE-depleted) and low in ΣREE concentration (e.g., marine REE patterns) being incorporated into the bone (Koeppenkastrop and De Carlo, 1992; Dubinin, 2004).

Positive Ce anomalies occur throughout the bone and though they are highest in the LREE-enriched portion of the bone, do occur in the MREE-depleted portion of the bone. Under near-surface oxidizing conditions, dissolved Ce^{3+} typically is removed from solution by precipitation of CeO_2 and co-precipitated with Mn and Fe-oxyhydroxides (DeCarlo et al., 1998; Bau, 1999). Dissolution of Mn-Fe oxyhydroxides and associated CeO_2 in saturated sediments, in which organic matter degradation causes Fe and Mn reduction, can lead to positive Ce anomalies in solution (Trueman and Tuross, 2002). The positive Ce anomaly and LREE-enriched portion of the MREE-depleted pattern seen in this portion of the bone suggest that the redox potential was low, and the HREE-enriched portion of the pattern suggests the solution was alkaline with neutral to slightly basic pH, where CO_3^{2-} aqueous complexes dominate.

The LREE-enriched patterns seen in CGDQ-3 Trace 1 and Spots 1-3, 11-16 (Figs. 6 and 7) are typical of REE patterns seen in waters influenced by low redox that dissolve carrier minerals through reductive dissolution (German and Elderfield, 1990; Dubinin, 2004). Similar patterns can be found in acidic waters (Bau, 1999, Bozau, 2004); however, low pH waters are not conducive to fossilization, which occurs at pH of 7.6-8.1 (Berna et al., 2004). Therefore, the positive Ce anomalies, LREE-enriched pattern, and high ∑REE concentration in CGDQ-3 (Spots 1-3 and 11-16) were most likely sourced from reductive dissolution of LREE-bearing mineral phases, such as Fe and Mn oxyhydroxides, suggesting fossilization in a solution with low redox potential (German and Elderfield, 1990; Koeppenkastrop and De Carlo, 1992; Ohta and Kawabe, 2001; Dubinin, 2004; C. Suarez et al., 2007). Additionally, the highest Ce anomalies occur in this portion in the bone, supporting that the LREE-enriched portion of the bone fossilized under reducing conditions.

To test if an Fe or Mn-oxide or oxyhydroxides are a plausible LREE source, simple equilibrium calculations using partition coefficients between REE and apatite, Mn-oxides, and Fe-oxides were used to back-calculate for the REE source. The partition coefficients between REE and apatite (Koeppenkastrop and DeCarlo, 1992) were used to calculate the solution responsible for the LREE-enriched side of the bone (Fig. 9), resulting in the REE pattern seen in Fig 9 (grey diamonds/grey line). The solution REE pattern generated is equilibrated with Mn-oxides (Koeppenkastrop and DeCarlo, 1992; Ohta and Kawabe, 2001) and Fe-oxides (Quinn et al., 2006) resulting in theoretical REE concentration of Mn-oxide (open symbols/black lines) and Fe-oxide (grey symbols/ grey lines) sources. Such LREE-enriched patterns with positive Ce anomalies are documented by German and Elderfield (1990), Koeppenkastrop and De Carlo (1992), Dubinin (2004), and Ohta and Kawabe (2001), suggesting Fe and or Mn-oxides are plausible REE sources for the LREE-enriched side of the bone.

Co-existing REE Patterns

Each REE pattern can be explained independently, but co-existence of both patterns within such a small space is more difficult to explain. Crystal chemical effects, in which the LREE are preferentially sorbed over MREE and HREE (because of their higher partition coefficient for LREE), can result in a shift from LREE to HREE-enrichment from the cortical surface of the bone to the deep cortex (Trueman and Tuross, 2002). However, such a pattern occurs over approximately 60 times greater distance (<1 mm in CGDQ-3 versus ~30 mm in figure 5 of Trueman and Tuross (2002)) and occurs from the cortical surface to the deep cortex. If the two REE patterns in CGDQ-3 were to be explained by crystal chemical effects, it would require directional flow from the LREE side of the bone to the MREE-depleted part of the bone.

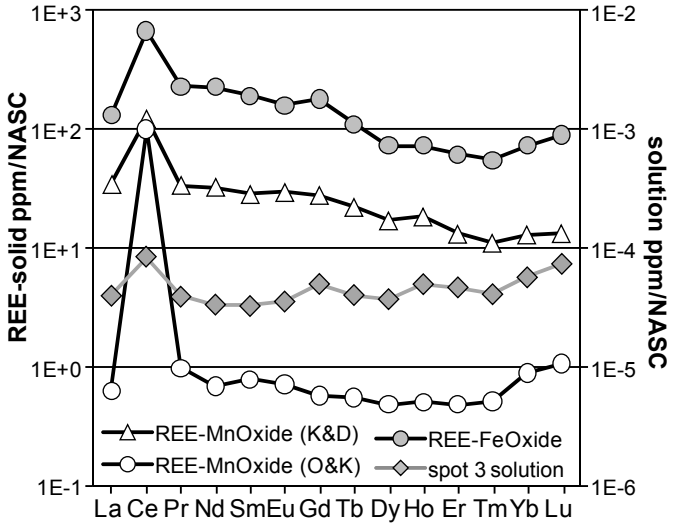

Fig. 9. REE equilibrium patterns. REE patterns from spot 2 are used to calculate solution REE patterns (solid diamonds) using equilibrium partition coefficients from Koeppenkastrop and DeCarlo (1992). The resulting REE solution patterns and REE partition coefficients reported by Quinn et al. (2006) at 5.77 µL of carbonate, Koeppenkastrop and DeCarlo (1992) (labeled "K&D"), and Ohta and Kawabe (2001)(labeled "O&K") are used to calculate the REE-Fe Oxide (grey circles) and REE-Mn oxide (open circles and triangles) patterns.

If this were the case, the steepest concentration gradient profile on the MREE-depleted side of the bone would be greatest on the inner surface of the bone. This is not the case. Additionally, crystal chemical effects could not explain the positive Ce anomaly present in the bone.

Alternatively, a simple mixing calculation between the low concentration MREE-enriched end member (Spot 8) and the high concentration LREE-enriched end member (Spot 3) show that all other patterns fall between these two end members (Fig. 10). Since the bone micromorphology suggests no post-fossilization recrystallization, either fluid mixing during fossilization must have produced the mixing patterns or mixtures of two different generations of authigenic apatite are being sampled during the lasing. Again, since both REE patterns and concentrations change dramatically over a distance of less than 1 mm, fluid mixing seems unlikely. We would expect fluid mixing to produce a more gradual change in geochemistry over longer distances.

An alternative we consider as the most plausible is that the bone was only partially fossilized in a mildly reducing redox environment with a MREE-depleted REE pattern before a fluid with a more reduced redox state and more concentrated LREE-enriched pattern entered the remaining pore spaces, producing apatite with larger positive Ce anomalies and LREE-enriched patterns. Our calculations indicate that no more than 15% of the LREE-enriched end-member is needed to generate the remaining REE patterns on the MREE-depleted side (Fig. 10), indicating ~85% of the MREE-side had already fossilized with a MREE-depleted pattern prior to introduction of a LREE-enriched pattern. The LREE-enriched side of the bone has a lower subset of spots that require only 50-60% of the LREE-enriched apatite and second subset

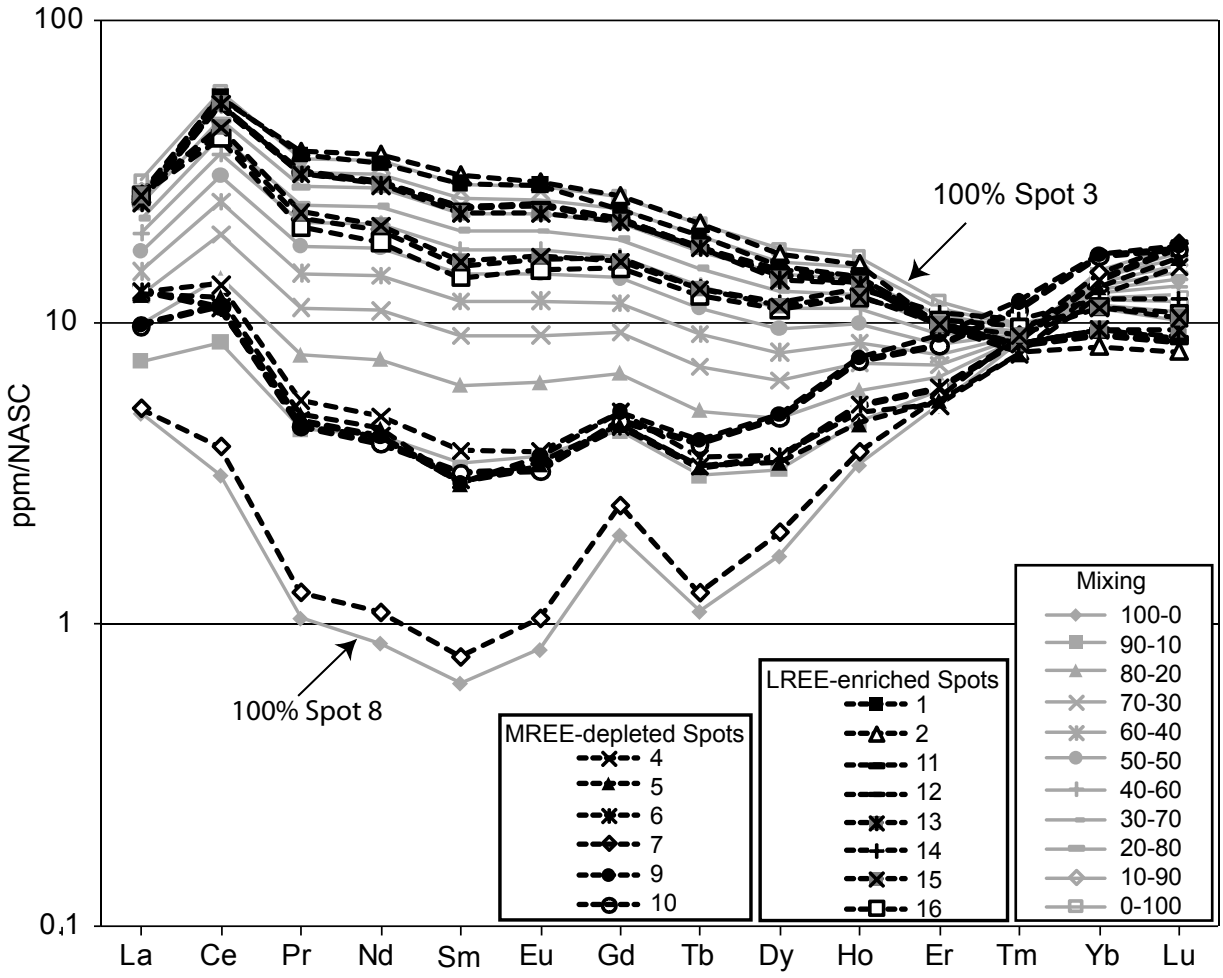

Fig.10. Modeled mixing of REE signatures. The most extreme LREE-enriched pattern (Spot 3) is mixed with the most MREE-depleted pattern (Spot 8). No more than 10-15% of the LREE-enriched pattern is needed to encompass the remaining MREE-depleted patterns. No more than 50% of the MREE-depleted pattern encompasses the LREE-enriched spots, suggesting up to ~50% of the pore space was filled with a MREE-depleted pattern prior to incorporation LREE-enriched apatite.

requiring over 80% of the LREE-enriched end member (Fig. 10), indicating 50-20% of the LREE-enriched portion of the bone partially fossilized with a MREE-enriched pattern prior to introduction of the LREE-enriched pattern. As the lasing techniques samples spots that range from 40 to 60 μm in diameter, the lasing aggregated apatite domains with various proportions of the two main phases of apatite growth and their respective REE patterns. The delicate preservation of bone microstructure and micromorphology suggests that fossilization was carried out by small-scale permineralization, most likely at the sub-micron level (Chinsamy-Turan, 2005).

The sharp differences in REE patterns in the bone examined in this detailed study indicate a complex cementation and fossilization history outlined in Fig 11. Following the precipitation of the Inner Micrite, vadose water produced a pendant micritic calcite on the lower portion of the bone (Outer Micrite) and recrystallized parts of the Inner Micrite to Microsparry Calcite (indicated by the nearly identical isotopic compositions) (Fig. 11, event 3). As these carbonate cements formed, 85-100% of the bone in contact with the vadose water began to fossilize with a MREE-depleted pattern, similar to that of the carbonate phases. As much as 50% to nearly none of the upper portion of the bone (Fig 11, event 3) is fossilized with the MREE-depleted pattern.

After partial fossilization of the bone by MREE-depleted vadose fluids, a further decrease of redox conditions resulted in reductive dissolution and mobilization of Mn, Fe, LREE and Ce from Fe- and Mn-bearing minerals that have a LREE-enriched pattern with a positive Ce anomaly (Fig. 9). Under these lower redox conditions, Fe- and then Mn-rich Sparry Calcites were precipitated (Fig. 11, event 4) from a LREE-enriched fluid (as is evident by the roughly

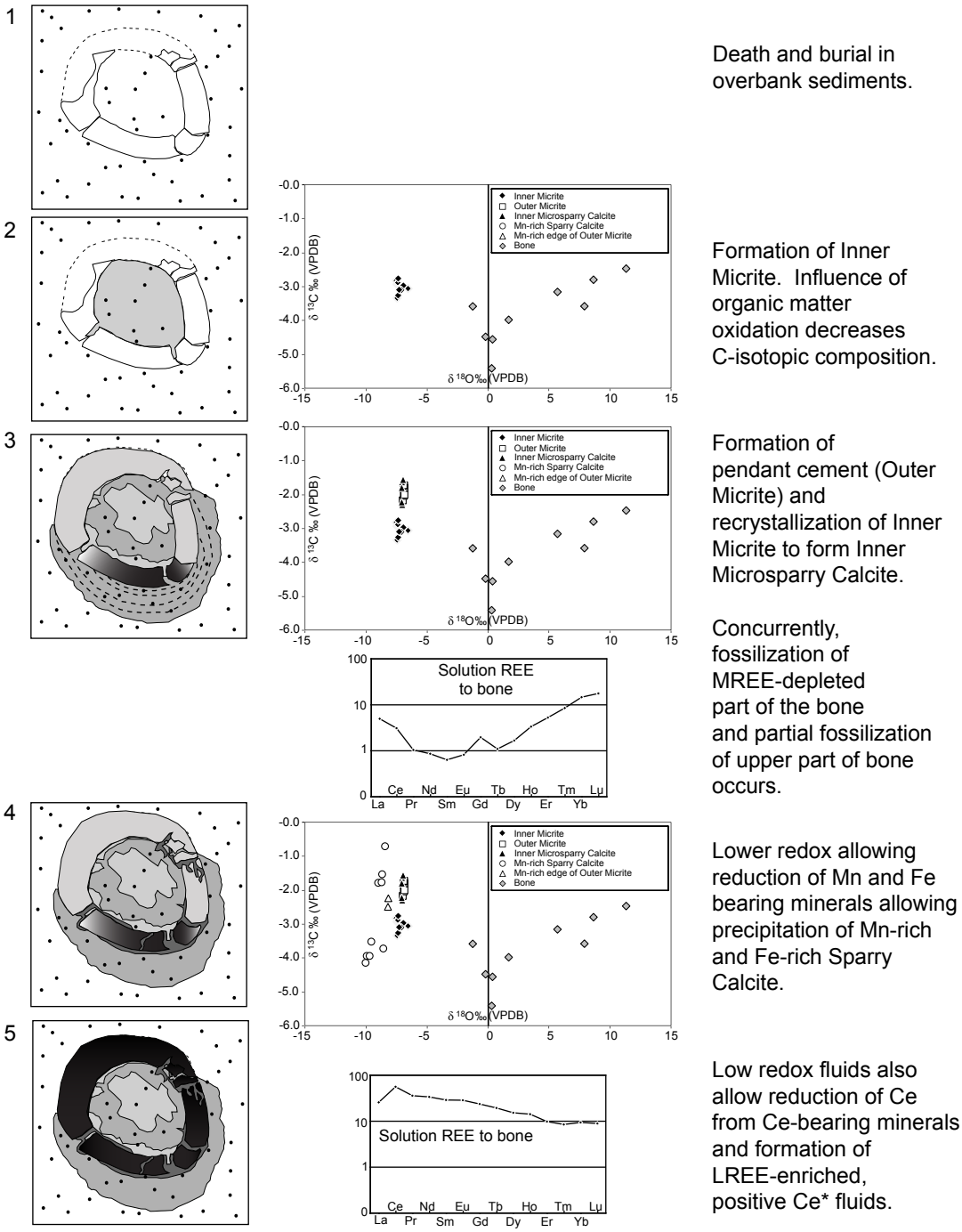

Fig. 11. Interpreted sequence of events 1) Burial of the bone CGDQ-3. 2) Formation of the Inner Micrite 3) Micritic pendant cement (Outer Micrite) formed in the vadose zone which likely started as a thin layer of calcite and grew outward (dashed lines). These infiltrating waters recrystallized the Inner Micrite to Microsparry Calcite resulting in similar isotopic composition to Outer Micrite. As carbonate phases in 2 and 3 formed, vadose water fossilized up to ~90% of the bone (greatest at Spot 8), with the upper ends of this bone segment being less completely fossilized (gradient shading). Up to 50% of the upper part of bone porosity may be filled with a MREE-depleted pattern (grey). 4) More reducing conditions caused reductive dissolution of LREE-enriched Mn and Fe oxides and Mn- and Fe-rich Sparry Calcite precipitated along pre-existing cracks. 5) This lower redox condition completed fossilization of the bone with a LREE-enriched pattern and positive Ce* (black-gradient).

LREE-enriched pattern of the Mn-rich Sparry Calcite (Fig. 9A). At the same time, fossilization with a LREE-enriched, positive Ce anomaly pattern in the remaining upper, "unfossilized" portion of the bone (Fig. 11, event 5) occurred. Finally, a change to oxidizing conditions resulted in the precipitation of Fe oxides in the remaining pore spaces, namely, the osteons, canaliculi and osteocyte lacunae. Analysis of these Fe-oxides should show the effect of depletion of the REE from solution into the apatite and should be HREE-enriched or LREE-depleted. However, the lasing technique, both in spot and trace mode, averages the signal from the target area and material beneath it. Analysis of the Fe-oxide filled osteons, canaliculi, and osteocyte lacunae will include bone apatite, therefore we are unable distinguish REE in the final Fe-oxide stage from the REE in the bone apatite at this time.

Calculated equilibrium rates for both sides of the bone support this scenario. The *t'* curve generated for the low ΣREE, MREE-depleted lower side suggests an equilibrium time of ~5,600 years compared with ~12,300 years for the high ΣREE, LREE-enriched upper side of the bone. Therefore the lower part of the bone may have fossilized over a shorter period than the upper part of the bone.

It is emphasized that the bone does not seem diagenetically altered after fossilization: bone micromorphology is preserved; original apatite alignment is as it was *in-vivo*, and other trace elements that are not redox-sensitive are not different on either side of the bone (e.g., Ba and Sr). REE concentration profiles do not exhibit extreme concentration gradients that would suggest secondary uptake of REE post-fossilization as described by Trueman et al. (2008). Rather, the bone was partially fossilized and acquired two main REE patterns in at least two periods of authigenic apatite growth during the course of fossilization. That the bone managed to

capture these geochemical changes over the course of its fossilization may not be unusual. Other studies have not revealed such heterogeneity, yet most other studies have not analyzed small bones, particularly those fossilized in nodules, by LA-ICP-MS. Therefore, it is difficult to gauge the uniqueness of the heterogeneity of CGDQ-3. The dynamic geochemical environments in this location, possibly associated with springs (Fouke et al., 2000), may contribute to the geochemically heterogeneous pore waters encountered by this bone. The thin nature of the bone that is partially encased in a carbonate nodule allowed it to document these chemically variable pore waters.

Implications

The results of LA-ICP-MS analysis have important implications for both the use of REE geochemistry in taphonomic analyses of bone-bed sites and for understanding the fossilization history of vertebrate material. Previous solution-based REE taphonomic analyses assumed that the REE pattern of a bone sample is representative of the entire bone. If all the bone samples in a bone-bed exhibit the same REE pattern, the bone-bed is interpreted to be autochthonous (e.g., Trueman et al., 2006). Bone-beds with a variety of REE patterns from sample to sample are interpreted as allochthonous deposits (e.g., Trueman and Benton, 1997). Thus, bone samples from an accumulation with a complex fossilization history can produce REE variations within a single bone. These bones, such as CGDQ-3, could erroneously be interpreted as an allochthonous deposit, depending on the portion of the bone sampled. Our results also are important to understanding the taphonomy of bones in pedogenic and/or spring settings, particularly because they have been used as geochemical proxies for terrestrial paleoenvironmental and biogenic data, and because it is common to find bone preserved with or

in association with pedogenic carbonate (Bao et al., 1998; Kohn and Law, 2006). Since most previous taphonomic analyses by both laser and solution analysis are of thicker-walled bone, our results suggest a new criterion for bones that are analyzed, especially if that analysis is to be done by solution ICP-MS. Few criteria have been previously outlined by researchers besides suggesting that samples be of cortical bone that have detailed locality data. We would also suggest that samples of cortical bone be of animals that have cortical bone >1 cm or that thin cortical bone be carefully analyzed by LA-ICP-MS. Springs and carbonate rich soils are not unusual and are actually ideal settings for preservation of bone (Berna et al., 2004). Therefore, their dynamic geochemical environments may commonly be preserved in bones, but few samples preserved in such settings have been analyzed. This study suggests careful LA-ICP-MS analysis of bone preserved in carbonate nodules before taphonomic comparisons to previously analyzed non-encased bone are carried out.

The pedogenic nature of unit 2 and 3 are an example of such settings. Since the REE patterns of unit 2 solution analysis are both LREE-enriched and MREE-depleted, it is likely that intra-bone heterogeneity is common at least in unit 2. Our LA-ICP-MS results shows that Spots 1-3 and 11-16 are similar in REE pattern and concentration to unit 2 LREE-enriched bones analyzed by solution ICP-MS. Spots 4-10 are similar to the three MREE-depleted vertically oriented bones from unit 3 (Fig 12).

A common element between the upright bones of unit 3 and CGDQ-3 is the presence of micritic carbonates infilling the bones and pendant micritic calcite surrounding the bones. This commonality suggests that the MREE-depleted signature in the CGDQ might be a product of processes and chemistry associated with pedogenic, vadose conditions. Moreover, is it likely

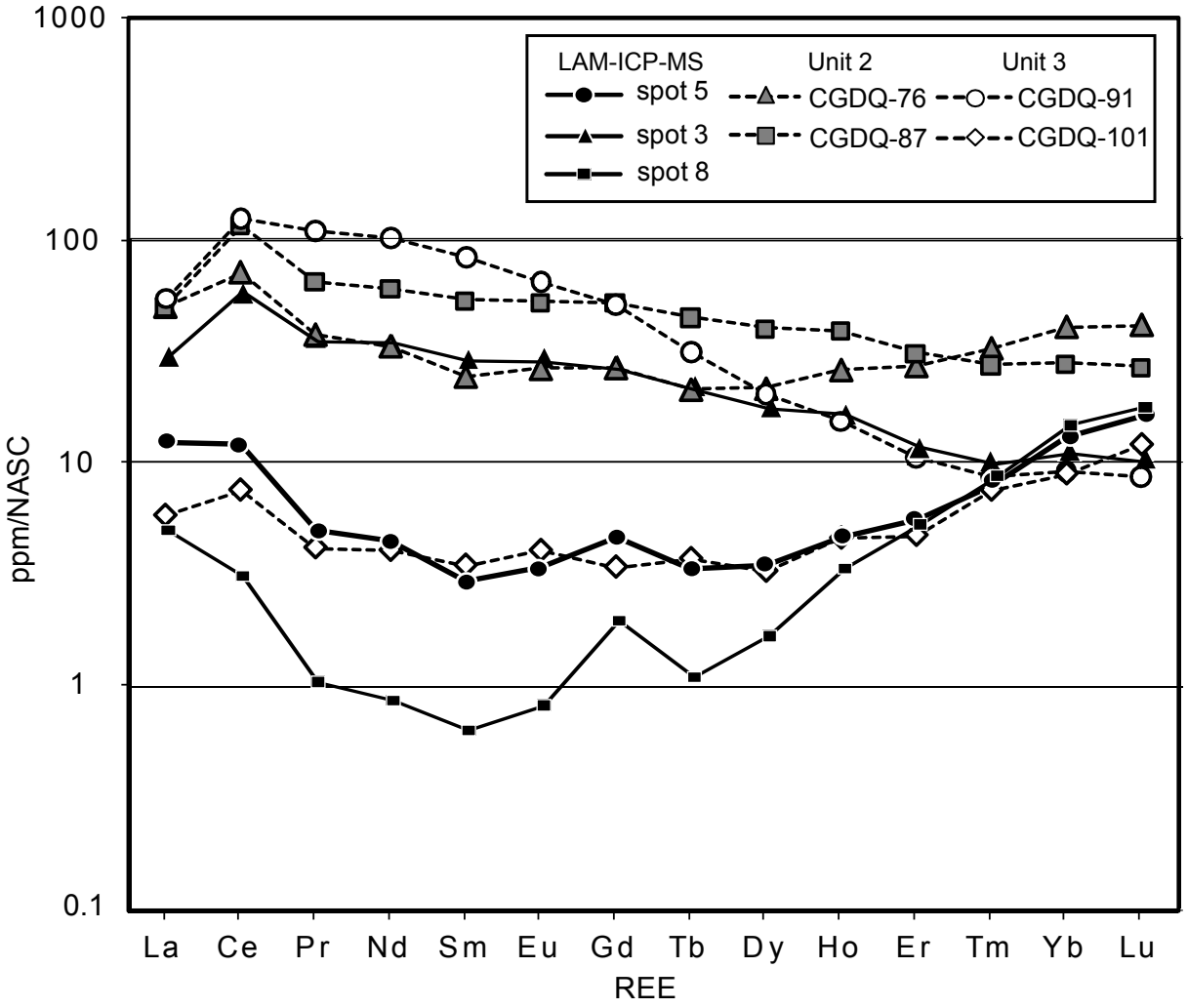

Fig. 12. Comparison of the various REE signatures in Units 2 and 3 from the CGDQ (C. Suarez et al., 2007) with the two main types of REE signatures from LA-ICP-MS analysis. (Spots 3 and 8). Spot 5 represents a mixture of the two end members and compares well with the MREE-depleted, low ∑REE pattern of the three vertically oriented bones from unit 3 (CGDQ-101) that are filled and encrusted by micritic calcite. The LREE-enriched spots are similar to LREE-enriched signatures from unit 2 (Spot 3 and CGDQ-87).

that the reduction in fluid percolation rates through the bones as pendant calcite precipitates on the exterior lowermost portion, allows saturation of the lowermost portion of the bone and hence permineralization in the vadose zone. The low ∑REE concentration, MREE-depleted portions of CGDQ-3, coupled with the patterns of upright carbonate-encased bones in CGDQ unit 3, suggest that REE patterns of bones surrounded by micritic pedogenic or vadose carbonate cements may capture the earliest diagenetic waters effecting fossilization. Incompletely fossilized portions of the bone could be fossilized later under saturated conditions by fluids with different REE concentrations and patterns. This study underscores the need for extensive LA-ICP-MS analysis at multiple localities and on a variety of vertebrate fossils to determine if multistage fossilization as demonstrated in vadose/spring environments is common in other depositional environments.

CONCLUSIONS

The goal of this study was to determine intra-bone REE variability in a single bone, CGDQ-3, using LA-ICP-MS. Our results revealed differences not previously described by other researchers, which may be related to carbonate encrustation and the thin nature of the bone. The data suggest that the homogenization produced by crushing and dissolution of bone for solution ICP-MS analysis may obscure REE variations within individual bones that are important to the interpretation of taphonomic and depositional history of bone accumulations. This may be particularly important in terrestrial environments where geochemical and moisture variability is high. If a site analyzed by solution ICP-MS has significant REE variability from bone to bone, the degree of intra-bone REE variability must be examined if REE geochemistry is to be used as a taphonomic tool. Resolution of this variability is also critical if REE geochemistry is to be

used as a forensic tool to identify illegally removed fossils (Lukens et al., 2009, C. Suarez et al., 2009, Terry et al. 2009). Intra-bone REE variability can easily be resolved with the use of micro-sampling techniques such as LA-ICP-MS analysis (Koenig et al., 2009; this study) or SHRIMP analysis (Trueman et al., 2006).

CGDQ-3 appears to have a relatively complex fossilization history. A pendant carbonate cement reduced fluid flow, allowing rapid fossilization of the lower part of the bone (spots 1-3 and 11-16 and Trace 1) under *relatively* more oxidizing, vadose conditions, and produced low positive Ce anomaly, low ΣREE, MREE-depleted patterns, while the upper portion of the bone was only partially fossilized. Larger positive Ce anomalies, high ΣREE, LREE-enriched patterns (spots 4-10 and Trace 2), and shallower U gradients indicate that the upper part of this bone fossilized over a longer period, possibly in a groundwater environment with conditions sufficiently reducing to promote increased reductive dissolution of Fe and Mn oxides and oxyhydroxides, sources of these elements.

The complexity of the fossilization process here and potentially in other sites makes taphonomic interpretation of REE in bones a more challenging task. Additional research (both field and experimental) is needed to unravel the complexities of fossilization and incorporation of trace elements into bone and teeth, particularly before fossil bones are used for paleoenvironmental, paleoecologic, paleoclimatic, and forensic proxies.

REFERENCES

Anderson, P. E., Benton, M.J., Trueman, C.N., Paterson, B.A., and Cuny, G. (2007) Palaeoenvironments of vertebrates on the southern shore of Tethys: the non-marine Early Cretaceous of Tunisia. *Palaeogeog., Palaeoecol., Palaeoclimatol*. **243**, 118-131.

Armstrong, H. A., Pearson, D.G., and Griselin, M., (2001) Thermal effects on rare earth element and strontium isotope chemistry in single conodont elements. *Geochim. et Cosmochim. Acta* **65**, 435-441.

Bao, M., Koch, P.L., and Hepple, R.P. (1998) Hematite and calcite coatings on fossil vertebrates. *J. of Sed. Res*. **68**, 727-738.

Bau, M. (1999) Scavenging of dissolved yttrium and rare earths by precipitating iron oxyhydroxide: experimental evidence for Ce oxidation, Y-Ho fractionation, and lanthanide tetrad effect. *Geochim. et Cosmochim. Acta* **63**, 67-77.

Berna, F., Matthews, A., and Weirner, S. (2004) Solubilities of bone mineral from archaeological sites: the recrystallization window. *J. Archaeol. Sci*. **31**, 867-882.

Bozau, E. (2004) LREE enrichment in an acid mine lake (Lusatia, Germany). *Appl. Geochem*. **19**, 261-271.

Brookins, D. G. (1989) Aqueous geochemistry of the rare earth elements. *Rev. Mineral. Geochem.* **21**, 201-225.

Chaïrat, C., Oelkers, E. H., Schott, J., and Lartigue, J.-E. (2007) Fluorapatite surface composition in aqueous solution deduced from potentiometric, electrokinetic, and solubility measurements, and spectroscopic observations. *Geochim. et Cosmochim. Acta* **71**, 5888-5900.

Chinsamy-Turan, A. (2005) The Microstructure of Dinosaur Bone. Johns Hopkins University Press, Baltimore. 195p.

De Carlo, E., Wen, X.-Y., and Irving, M. (1998) The Influence of Redox Reactions on the Uptake of Dissolved Ce by Suspended Fe and Mn Oxide Particles. *Aquatic Geochem*. **3**, 357-389.

Dia, A., Gruau, G., Olivie-Lauquet, G., Riou, C., Molenat, J., and Curmi, P. (2000) The distribution of rare earth elements in groundwater: assessing the role of source-rock, redox changes, and colloidal particles. *Geochim. et Cosmochim. Acta* **64**, 4131-4151.

Dubinin, A. V. (2004) Geochemistry of rare earth elements in the ocean. Lithology and Mineral Resources 39, 289-307.

Eggins, S. M., Rudnick, R. L., and McDonough, W. F. (1998) The composition of peridotites and their minerals: a laser ablation ICP-MS study. *Earth and Planet. Sci. Ltrs*. **154**, 53-71.

Elderfield, H. and Pagett, R. (1986) REE in ichthyoliths: variations with redox conditions and depositional environments. *The Science of the Total Environment* **48**, 175-197.

Erel, Y. and Stolper, E.M. (1993) Modeling of rare earth element partitioning between particles and solution in aquatic environments. *Geochim. et Cosmochim. Acta* **57**, 513-518.

Fleet, M. E. and Pan, Y. (1995) Site preference or rare earth elements in fluorapatite. *American Mineralogist* **80**, 329-335.

Fleet, M. E., Liu, X., and Pan, Y. (2000) Rare-earth elements in chlorapatite [$Ca_{10}(PO_4)_6Cl_2$]: Uptake, site preference, and degradation of monoclinic structure. *American Mineralogist* **85**, 1437-1446.

Fouke, B. W., Farmer, J. D., Des Marais, D. J., Pratt, L., Sturchio, N. C., Burns, P. C., and Discipulo, M. K. (2000) Depositional facies and aqueous-solid geochemistry of travertine-depositing hot springs (Angel Terrace, Mammoth Hot Springs, Yellowstone National Park, USA. *J. Sed. Res*. **70**, 565-585.

Friedman, I. and O'Neil, J. R. (1977) Compilation of stable isotope fractionation factors of geochemical interest. In: Fleischer, M. (Ed.), Data of Geochemistry, 6th ed., *Professional Papers U.S. Geological Survey*. 440 KK.

Gates, T.A.. (2005) The Late Jurassic Cleveland-Lloyd Dinosaur Quarry as a drought-induced assemblage. *PALAIOS* **20**, 363-375.

German, C. R. and Elderfield, H. (1990) Application of the Ce anomaly as a paleoredox indicator: the ground rules. *Paleoceanography* **5**, 823-833.

Grandjean-Lecúyer, P., Feist, R., and Albarede, F. (1993) Rare earth elements in old biogenic apatites. *Geochim. et Cosmochim. Acta* **57**, 2507-2514.

Grandstaff, D.E. and Terry, Jr., D.O. (2009). Rare earth element composition of Paleogene vertebrate fossils from Toadstool Geologic Park, Nebraska, USA. *Appl. Geochem*. **24**, 733-745.

Gromet, P. L., Haskin, L. A., Korotex, R. L., and Dymek, R. F. (1984) The "North American shale composite": its compilation, major and trace element characteristics. *Geochim. et Cosmochim. Acta* **48**, 2469-2482.

Gruau, G., Dia, A., Olivie-Lauquet, G., Davranche, M., and Pinay, G. (2004) Controls on the distribution of rare earth elements in shallow groundwaters. *Water Res*. **38**, 3576-3586.

Henderson, P., Marlow, C. A., Molleson, T. I., and Williams, C. T. (1983) Patterns of chemical change during bone fossilization. **Nature** *306*, 358-360.

Günther, D., Horn, L., and Hattendorf, B. (2000) Recent trends and developments in laser ablation-ICP-mass spectrometry. *Fresenius J. Anal. Chem*. **368**, 4-14.

Jackson, S. E. (2001) Ch. 3: The Application of Nd:YAG Lasers in LA-ICP-MS In: Sylvester, P. (Ed.), Laser Ablation ICP-MS in the Earth Sciences, *Mineral. Assoc. of Canada, Short Course Series* **29**, 29-45

Johannesson, K. H. and Zhou, X. (1997) Geochemistry of the rare earth elements in natural terrestrial waters; a review of what is currently known. *Chinese J. of Geochem*. **16**, 20-42.

Johannesson, K. H., Zhou, X., Caixia, G., Stetzenback, K.J., and Hodge, V.F. (2000) Origin of rare earth element signatures in groundwaters of circum-neutral pH from southern Nevada and eastern California, USA. *Chem. Geol*. **164**, 239-257.

Karhu, J. and Epstein, S. (1986) The implications of the oxygen isotope records in coexisting cherts and phosphates. *Geochim. et Cosmochim. Acta* **50**, 1745-1757.

Kirkland, J. I., Zanno, L. E., Sampson, S. D., Clark, J. M., and DeBlieux, D. D. (2005) A primitive therizinosauroid dinosaur from the Early Cretaceous of Utah. *Nature* **435**, 84-87.

Koch, P. L., Fogel, M. L., and Tuross, N. (1994) Ch. 4: Tracing the diets of fossil animals using stable isotopes. In: Lajtha, K. and Michener, R. H. Eds.), Stable isotopes in ecology and environmental science, Wiley-Blackwell, Boston. 63-92.

Koch, P. L., Tuross, N., and Fogel, M. L. (1997) The effects of sample treatment and diagenesis on the isotopic integrity of carbonate in biogenic hydroxylapatite. *J. of Archaeol. Sci*. **24**, 417-420.

Koenig, A.E., Rogers, R.R., and Trueman, C.N. (2009) Visualizing fossilization using laser ablation ICP-MS maps of trace elements in Late Cretaceous bones. *Geology* **37**, 511-514.

Koeppenkastrop, D. and De Carlo, E.H. (1992) Sorption of rare earth elements from seawater onto synthetic mineral particles: and experimental approach. *Chem. Geol*. **95**, 251-263.

Kohn, M. (2008) Models of diffusion-limited uptake of trace elements in fossils and rates of fossilization. *Geochim. et Cosmochim. Acta* **72**, 3758-3770.

Kohn, M. and Law, J.M. (2006)Stable isotope chemistry of fossil bone as a new paleoclimate indicator. *Geochim. Cosmochim. Acta* **70**, 931-946.

Lécuyer, C., Reynard, B., and Grandjean, P. (2004) Rare earth element evolution of Phanerozoic seawater recorded in biogenic apatites. *Chem. Geol*. **204**, 63-102.

Lee, J. H. and Byrne, R.H. (1993) Complexation of trivalent rare earth elements (Ce, Eu, Gd, Tb, Yb) by carbonate ions. *Geochim. et Cosmochim. Acta* **57**, 295-302.

Longerich, H. P., Jackson, S. E., and Gunther, D. (1996) Laser ablation inductively coupled plasma mass spectrometric transient signal data acquisition and analyte concentration calculation. *J. of Anal. At. Spectrom*. **11**, 899-904.

Lohmann, K. C. (1988) Geochemical patterns of meteoric diagenetic systems and their application to studies of paleokarst. In: N. P. James, a. C., P.W. (Ed.), Paleokarst, Springer, New York. 58-80.

Lukens, W. E., Grandstaff, D. E., and Terry Jr., D. O. (2009) Rare earth element signatures in fossil bones: a tool for mitigating fossil poaching on federal lands. In: Foss, S., Cavin, J., Brown, T., Kirkland, J., and Stantucci, V. (Eds.), Proceedings of the 8th Conference on Fossil Resources, May, 19-21, St. George, UT, 10-13.

Lowenstam, H. A. and Weiner, S. (1989) On biomineralization. Oxford University Press, New York, 324p.

MacFadden, B. J., Labs-Hochstein, J., Hulbert, R.C. Jr., and Baskin, J.A. (2007) Revised age of the late Neogene terror bird (Titanis) in North America during the Great American Interchange. *Geology* **35**, 123-126.

Martin, J. E., Patrick, D., Kihm, A. J., Foit, F.F., Jr., and Grandstaff, D.E. (2005) Lithostratigraphy, tephrochronology, and rare earth element geochemistry of fossils at the classical Pleistocene Fossil Lake Area, south central Oregon. *J. of Geol*. **119**, 139-155.

Metzger, C., Terry Jr., D.O., and Grandstaff, D.E. (2004) Effects of paleosol formation on rare earth element signatures in fossil bone. *Geology*. **32**, 497-500.

Millard, A. R. and Hedges, R. E. M. (1995) The role of the burial environment in uranium uptake by buried bone. J*. of Archaeo. Sci.* **22**, 239-250.

Millard, A. R. and Hedges., R.E.M (1996) A diffusion-adsorption model of uranium uptake by archaeological bone. *Geochim. et Cosmochim. Acta* **60**, 2139-2152.

Norman, M. D., Pearson, N. J., Sharma, A., and Griffin, W. L. (1996) Quantitative analysis of trace elements in geological materials by laser ablation ICPMS: instrumental operating conditions and calibration values of NIST glasses. *Geostandards Newsletter* **20**, 247-261.

Ohta, A. and Kawabe, I. (2001) REE (III) adsorption onto Mn dioxide (δ -MnO2) and Fe oxyhydroxide: Ce (III) oxidation by δ-MnO_2. *Geochim. Cosmochim. Acta* **65**, 695-703.

Parkhurst, D.L., and Appelo, C.A.J. (1999) User's guide to PHREEQC (Version 2)--a computer program for speciation, batch-reaction, one-dimensional transport, and inverse geochemical

calculations. *U.S. Geological Survey Water-Resources Investigations Report* **99-4259**, 312 p.

Patrick, D., Martin, J.E., Parris, D.C. and Grandstaff, D.E. (2004) Paleoenvironmental interpretations of rare earth element signatures in mosasaurs (Reptilia) from the Upper Cretaceous Pierre Shale, central South Dakota, USA. *Palaeogeog., Palaeoecol., Palaeoclimatol.* **212**, 277-294.

Patrick, D., Martin, J.E., Parris, D.C., and Grandstaff, D.E., 2007, Rare earth element determination of the stratigraphic position of the holotype of *Mosasaurus missouriensis* (Harlan), the first named fossil reptile from the American West, in Martin, J.E., and Parris, D.C., eds., The Geology and Paleontology of the Late Cretaceous Marine Deposits of the Dakotas: *GSA Special Paper* **427**, p. 155-165.

Picard, S., Lécuyer, C., Barrat, J.A., Garcia, J.P., Dromart, G., and Sheppard, S.M.F. (2002) Rare earth element contents of Jurassic fish and reptile teeth and their potential relation to seawater composition. *Chem. Geol*. **186**, 1-16.

Quinn, K.A., Byrne, R.H., and Schijf, J. (2006) Sorption of yttrium and rare earth elements by amorphous ferric hydroxide: Influence of solution complexation with carbonate. *Geochim. et Cosmochim. Acta*. **70**, 4151-4165.

Sha, L. K. and Chappell, B. W. (1999) Apatite chemical composition, determined by electron microprobe and laser-ablation inductively coupled plasma mass spectrometry, as a probe into granite petrogenesis. *Geochim. et Cosmochim. Acta* **63**, 3861-3881.

Shemesh, A., Kolodny, Y., and Luz, B. (1988) Isotope geochemistry of oxygen and carbon in phosphate and carbonate of phosphorite francolite. *Geochim. et Cosmochim. Acta* **52**, 2565-2572.

Sorensen, A. C., Ludvigson, G.A., González, L.A., Joeckel, R.M., and Kirkland, J.I. (2002) Petrography and diagenesis of palustrine carbonate beds in the Early Cretaceous Cedar Mountain Formation, Eastern Utah: *GSA Abstracts with Programs* **34**, p. 17-18.

Staron, R. M., Grandstaff, B.S., Gallagher, W.B., and Grandstaff, D.E. (2001) REE signatures in vertebrate fossils from Sewell, NJ; implications for location of the K-T boundary. *PALAIOS* **16**, 255-265.

Suarez, C. A., Suarez, M.B., Terry Jr., D.O., and Grandstaff, D.E. (2007) Rare earth element geochemistry and taphonomy of the Early Cretaceous Crystal Geyser Dinosaur Quarry, east-central Utah. *PALAIOS* **22**, 500-512.

Suarez, C. A., Macpherson, G. L., and Grandstaff, D. E. (2009) Rare earth element geochemistry of fossil bone: using geochemical patterns to trace illegally excavated fossils. In: Foss, S., Cavin, J., Brown, T., Kirkland, J., and Stantucci, V. (Eds.), Proceedings of the 8th Conference on Fossil Resources, May 19-21, St. George, UT. 4-6.

Suarez, M. B., Suarez, C.A., Kirkland, J.I., Gonzalez, L.A., Grandstaff, D.E. and Terry Jr., D.O. (2007) Sedimentology, stratigraphy, and depositional environment of the Crystal Geyser Dinosaur Quarry, east-central Utah. *PALAIOS* **22**, 513-527.

Suarez, M.B., Gonzalez, L.A., Ludvigson, G.A., Vega, F.J., and Alvarado-Ortega, J. (2009) Isotopic composition of low-latitude paleoprecipitation during the Early Cretaceous: *GSA Bulletin,* **121**, p. 1584-1595.

Terry Jr., D. O., Grandstaff, D. E., Lukens, W. E., and Beasley, B. A. (2009) The use of rare earth element signatures in vertebrate fossils as a tool to investigate fossil poaching: A cooperative effort between Nebraska Forest and Temple University. In: Foss, S., Cavin, J., Brown, T., Kirkland, J., and Stantucci, V. (Eds.), Proceedings of the 8th Conference on Fossil Resources, May 19-21, St. George, UT. 7-9.

Trueman, C. N. (1999) Rare earth element geochemistry and taphonomy of terrestrial vertebrate assemblages. *PALAIOS* **14**, 555-568.

Trueman, C. N. and Benton, M. J. (1997) A geochemical method to trace the taphonomic history of reworked bones in sedimentary settings. *Geology* **25**, 263-266.

Trueman, C. N. and Tuross, N (2002) Trace elements in recent and fossil apatite. *Rev. Mineral. and Geochem.* **48**, 489-521.

Trueman, C. N., Benton, M.J., and Palmer, M.R. (2003) Geochemical taphonomy and shallow marine vertebrate assemblages. *Palaeogeog., Palaeoecol., Palaeoclimatol*. **197**, 151-169.

Trueman, C. N. G., Reid, J.H., Dortch, J., Charles, B., and Wroe, S. (2005) Prolonged coexistence of humans and megafauna in Pleistocene Australia. *Proceed. of the Nat. Acad. of Sci*. **102**, 8381-8385.

Trueman, C. N., Behrensmeyer, A. K., Potts, R., and Tuross, N. (2006) High-resolution records of location and stratigraphic provenance from the rare earth element composition of fossil bones. *Geochim. Cosmochim. Acta* **70**, 4343-4355.

Trueman, C. N., Palmer, M. R., Field, J., Privat, K., Ludgate, N., Chavagnac, V., Eberth, D. A., Cifelli, R., and Rogers, R. R. (2008) Comparing rates of recrystallisation and the potential

of preservation of biomolecules from the distribution of trace elements in fossil bones. *Comptes Rendus Palevol* **7**, 145-158.

Ufnar, D.F. Gonzalez, L.A., Ludvigson, G.A., Brenner, R.L., Witzke, B.J. (2002) The mid-Cretaceous water bearer: isotope mass balance quantification of the Albian hydrologic cycle: *Palaeogeog., Palaeoclimatol., Palaeoecol*. **188**, 51-71.

Ufnar, D. F., Gröcke, D. R., and Beddows, P. A. (2008) Assessing pedogenic calcite stable-isotope values: Can positive linear covariant trends be used to quantify palaeo-evaporation rates? *Chem. Geol*. **256**, 46-51.

CHAPTER 3. WATER UTILIZATION OF THE CRETACEOUS MUSSENTUCHIT LOCAL FAUNA, CEDAR MOUNTAIN FORMATION, UT, USA: IMPLICATIONS FOR PALEOHYDROLOGY

ABSTRACT

While the oxygen isotopic composition of pedogenic carbonate has successfully been used to address the effects of global climate change on the hydrologic cycle, detailed regional paleohydrologic studies are lacking. Since locally the hydrologic cycle can vary extensively due to regional events such as mountain building, and since pedogenic carbonates (calcite) form in a narrow moisture regime, other proxies, such as vertebrate remains, must be used to decipher local versus regional variations in paleohydrology. In this study, phosphatic remains from a diverse set of vertebrate fossils (fish, turtles, crocodiles, dinosaurs, and micro-mammals) from the Mussentuchit Member (MM) of the Cedar Mountain Formation, UT (late Albian – early Cenomanian) were analyzed for their oxygen isotopic composition ($\delta^{18}O_p$) in order to determine differences among the available water reservoirs and water utilization of each taxa. Calculated changes in water reservoir $\delta^{18}O$ over time are then used to determine the effects of the incursion of the Western Interior Seaway (WIS) and the Sevier Orogeny on paleohydrology during the MM time.

Results suggest turtle $\delta^{18}O_p$ serves as a proxy for river composition during the summer months and are a record of average local precipitation $\delta^{18}O_w$. These values are corroborated by meteoric water values recorded by pedogenic calcites. Pedogenic calcite is slightly biased toward enriched values due to their formation during evaporative conditions. Crocodiles, which live in more evaporatively affected waters relative to turtles yield $\delta^{18}O_w$ values that are similar to

meteoric water calculated from pedogenic carbonate. Fish with *Lepidotes*-like teeth predict temperatures that are consistent with other estimates of mean annual temperature for this latitude and time. The $\delta^{18}O_p$ of Actinopterygian scales and teeth indicates that they ostensibly lived in evaporatively affected water reservoirs, or that they migrated to the enriched estuarine waters of the Western Interior Seaway (WIS). Mammals, herbivorous dinosaurs, and theropods are all evaporative sensitive taxa and primarily drank isotopically depleted river water. Dinosaurs appear to document year-round river water isotopic compositions. Co-existence of aquatic taxa and mammals allows for calculation of humidity. MM mammals suggest humidity averaged ~68% and ranged between ~47% to ~76% relative humidity.

The $\delta^{18}O_w$ estimated from aquatic and semi-aquatic taxa and pedogenic calcite suggest dominance of WIS derived moisture during their growth. Dinosaurs, particularly theropods, indicate that altitude and catchment effects from the Sevier Mountains are seemingly important in the fall through early spring river water. It is suggested that temporal changes in the isotopic composition of the MM fauna are produced by the small-scale regressive-transgressive cycles of the WIS.

INTRODUCTION

Numerous isotopic studies have demonstrated that the mid-Cretaceous global warming caused an intensification of the hydrologic cycle resulting in increased regional rainout in the temperate humid belts, while augmenting evaporation in dry belts (White et al., 2001; Ufnar et al., 2002; Ufnar et al., 2004; M. Suarez 2009). While these studies have explored the hydrologic cycle at hemispheric to global scales, detailed regional isotopic studies are lacking. For example, the relative contribution of local vs. regional water sources to rivers and other water bodies (e.g. lakes and ponds) can vary significantly within a particular region, but this variability is difficult to ascertain. In addition, regional events such as mountain building and transgressions (proximity of moisture source), can significantly alter regional moisture patterns altering the isotopic composition of precipitation. The causes of changing isotopic compositions of precipitation are difficult to constrain using isotopic proxy records that have a narrow moisture window, such as pedogenic carbonates. Because of these limitations, biogenic materials are being used with greater frequency to infer paleohydrology and paleoenvironments (Dettman et al., 2001; Fricke et al., 2008; Billion-Bruyat et al., 2005). It is therefore, imperative that we better understand water utilization behavior of different taxa, and improve the understanding of proxy records than can shed information on the factors that control variability in the isotopic composition for a given site. This is particularly important if we are to use data from deep geologic time, such as the mid-Cretaceous, as analogues for future climate change.

It has been assumed that biogenic or ecologic stable isotope signals are rarely preserved in pre-Cenozoic aged material (Fricke et al., 2008) however the use of isotopic composition of

terrestrial vertebrate fauna is being more frequently used in Mesozoic paleoenvironmental studies (e.g., Billion-Bruyat et al., 2007; Fricke et al., 2007; 2008; Amiot et al., 2009). "Expected" offsets between taxa along physiologic lines are used as indicators of biogenic preservation. While the use of isotopic composition of Mesozoic terrestrial vertebrate fauna is being more frequently used, few paleoecological isotope studies of Mesozoic terrestrial ecosystems have been conducted that elucidate the water sources utilized by a wide variety of co-existing different taxa. In this study, we utilize a diverse late Early Cretaceous vertebrate fauna to investigate water utilization strategies used by different organisms. The Mussentuchit Member (MM) of the Cedar Mountain Formation (CMF) is most amenable for such a study because it preserves a diverse freshwater aquatic, semi-aquatic and terrestrial vertebrate fauna (Cifelli et al., 1999). Furthermore, the vertebrate fauna contains numerous physicochemically resistant elements such as teeth, scales, and scutes that may be used for stable isotopic analysis (Fricke, et al., 2008). Aquatic faunal elements (e.g. fish and turtles) can be used to estimate the isotopic composition of perennial bodies of water (e.g. rivers) while micro vertebrates (i.e. mammals) can be used to constrain precipitation isotopic composition or that of ephemeral water sources. These two end-members provide constraints that permit us to explore water utilization strategies by other vertebrates and to tease out the relative contribution of local vs. regional water sources. Furthermore, the stratigraphic control of available collections allow us to track temporal changes in the isotopic composition of the different water reservoirs available to the MM fauna from the Albian to early Cenomanian. By tracking these changes we can attempt to tease out the impact of the Sevier Orogeny and incursions of the Western Interior Seaway on paleohydrology during Mussentuchit time.

BACKGROUND

There are two main sources of water that continental vertebrates can utilize: 1) regional water affected by local precipitation and 2) distant water drained by larger rivers. While both of these sources are ultimately derived from precipitation, larger river water is influenced by precipitation in the distant portions of the rivers' catchment area. Dutton et al. (2005) provides an extensive review of the differences between river water and local meteoric water isotopic composition. Meteoric water is controlled by water vapor sources (i.e. ocean, or large lakes), distance from the source (continental effect), elevation (altitude effect), temperature, humidity, and evaporative effects. In general, the oxygen isotopic composition of precipitation produced from a given airmass becomes lighter by ~ 2 ‰/1000 km (Rozanski et al., 1993). Similarly, as an airmass moves to higher elevations, the precipitation will become gradually lighter by ~ 2.8 ‰/ km of elevation (Dutton et al., 2005). Temperature effects were among the earliest recognized, with precipitation isotopic composition positively correlated with mean annual temperature (e.g. Dansgaard 1964). Humidity and evaporative effects act in concert to modify the isotopic composition of precipitation with lower humidity resulting in greater evaporation and isotopic enrichment. River water is dominantly controlled by precipitation in its catchment area. As distance and altitude effects result in lighter isotopic compositions, river water sourced at higher elevations tends to be lighter than that of low elevation tributaries and ephemeral streams. In general, river water $\delta^{18}O$ decreases by ~ 4.2 ‰/km of elevation change (Dutton et al., 2005). Thus, precipitation-derived water at a given elevation will be heavier than river waters at the same elevation, but sourced from higher elevations.

By using the stable isotopic composition of the aquatic taxa (e.g. fish), we should be able to fingerprint the isotopic composition of perennial rivers. In the case of terrestrial taxa, water is sourced by a combination of rivers, local precipitation, and food. Herbivorous taxa are influenced not only by their drinking water, but also by processes that influence the composition of their ingested plant water. Plant leaves tend to be enriched over local meteoric water as evaporative enrichment occurs in the leaves (Ehleringer and Dawson, 1992). The lower the humidity, the more enrichment occurs in leaf water isotopes. Therefore, herbivorous taxa will tend to produce isotopically heavier phosphate than carnivorous taxa (Kohn, 1996).

Some modern terrestrial taxa are water dependent and spend most of their time in water (e.g. hippopotamus) and are considered to be insensitive to evaporative conditions, i.e. their isotopic composition is not greatly affected by humidity changes. However, the isotopic compositions of taxa that are drought tolerant (e.g. Dikdik and Grant's Gazelle) are considered to be evaporative sensitive because they are strongly influenced by evaporative conditions as they get their water from evaporatively-influenced sources such as plants and evaporative pools. Levin et al. (2006) utilized the $\delta^{18}O$ of tooth enamel of coexisting terrestrial taxa to calculate the isotopic enrichment (ε) between taxa to determine which taxa were evaporative sensitive (ES) and which were evaporative insensitive (EI). The ε values between ES and EI taxa should be high, while ε between two EI taxa or two similar ES taxa should be low from site to site. The maximum enrichment should be observed between the most EI and ES taxa, and ε is correlated to the degree of aridity (water deficit). In this paper, we compare the changes in ε between ES and EI ($\varepsilon_{ES\text{-}EI}$) taxa at different sites to infer changes in relative aridity during MM time.

Numerous studies have used stable isotopes of continental taxa (aquatic, semi-aquatic, and terrestrial) to determine paleoenvironmental, paleoclimatic, and paleoecologic information (Fricke and O'Neil, 1996; Lee-Thorp and Sponheimer, 2005; Billion-Bruyat et al., 2007; Fricke et al., 2007; Fricke et al., 2008; Amiot et al., 2009). Vertebrate taxa record the isotopic compositions of their water sources in their bones and teeth apatite [$Ca_5(PO_4, CO_3)_3(OH,CO_3)$]. Both the carbonate and phosphate component of bio-apatites have been used for isotopic studies, however, phosphate is diagenetically more resistant than the structural carbonate (Kolodny et al., 1996). Furthermore, enamel apatite and ganoine are more resistant to diagenetic alteration than bone apatite and are considered a more reliable source of biogenic and paleoecologic data (Kolodny et al., 1996; Trueman et al., 2003; Fricke et al., 2008).

The isotopic fractionation between ingested water and bone water is controlled by body temperature at which the bone forms and vital fractionations that occur during the transfer of ingested water to body water (Fricke et al., 2008). For homeothermic mammals, precipitation of bone and teeth occur at a constant temperature of ~37 ± 1°C (Bryant, 1996). Reptiles can control and maintain their temperature through basking and will only grow their shells, teeth, scutes, and bones when their body is at optimal temperature for growth. For crocodiles this temperature ranges from 26 to 36ºC with an average of 29 ± 3ºC (Amiot et al., 2007), and for turtles the range is from 20 to 35ºC with an average of 27 ± 4ºC (Barrick et al., 1999). These organisms often record water isotopic composition of the summer months when they more easily achieve the optimal body temperature. Equations relating ingested water to bio-apatite have been generated for several taxa by previous researchers (Kolodny et al., 1983; Kohn, 1996; Barrick et al., 1999; Amiot et al., 2007).

Until recently, most isotopic studies of fossil vertebrates were restricted to Cenozoic mammals, since their physiology is better known than for extinct archosaurs and because younger material is less likely to have been diagenetically altered. Recent studies of Mesozoic vertebrates, however, have used enamel and ganoine rather than bone and dentine, and examined the presence of expected offsets between 1) taxa that have different life modes (e.g. aquatic versus terrestrial herbivores) and 2) between co-existing pedogenic carbonate and terrestrial taxa, to ensure that biogenic rather than diagenetic signals have been obtained (Billion-Bruyat et al., 2007; Fricke et al., 2007; Fricke et al., 2008; Amiot et al., 2009). These recent studies of Mesozoic ecosystems have successfully demonstrated that carefully selected samples of enamel and ganoine phosphate and structural carbonate can be used to infer paleoecologic information such as diet, water usage, vegetation, paleohydrology, and migration patterns.

Fricke et al. (2008) suggested that for Mesozoic archosaurs such as dinosaurs, one could assume that their bone and tooth oxygen isotopes are primarily controlled by their ingested water and atmospheric oxygen isotopes, and that they also precipitated their bone/teeth at a constant or at least a restricted temperature range. Previous studies suggest that dinosaurs did maintain constant body temperature (Barrick and Showers, 1994, 1995; Barrick et al., 1996; Fricke and Rogers, 2000; Amiot et al., 2006). Therefore, we use the oxygen isotopic composition of enamel and ganoine phosphate from one of the most diverse terrestrial ecosystems documented in the early Cretaceous to infer paleoecology and regional paleoclimatology.

GEOLOGIC SETTING AND MATERIALS

The Cedar Mountain Formation (CMF) was deposited during the Barremian to Cenomanian of Utah and includes, from oldest to youngest, the Buckhorn Conglomerate, Yellow Cat Member, Poison Strip Sandstone, Ruby Ranch Member, and Mussentuchit Member (MM). The focus of this study, the Mussentuchit Member, primarily outcrops on the western side of the San Rafael Swell. Its high smectitic-clay content makes it identifiable by its drab gray popcorn-weathered mudstones that form extensive badlands in the Willow Springs and Short Canyon quadrangles of central-Utah. Several ash layers are present in the MM and give ages that range from 98.3 ± 0.1Ma (Cifelli et al., 1999) to 96.7 ± 0.5Ma (Garrison et al., 2007) suggesting the MM deposition began approximately at the Aptian-Albian boundary and ended in the early Cenomanian. The upper part of the MM, often contains lignitic coal layers, it is commonly interbedded with the overlying Dakota Sandstone, but locally there are erosional unconformities between the MM and Dakota. While carbonate nodules are abundant in the underlying Ruby Ranch Member, they occur less frequently in the MM.

The MM vertebrate fauna was sampled by field crews of the Oklahoma Museum of Natural History in the Mussentuchit Wash and Short Canyon areas (Fig. 1). Representative stratigraphic sections (Fig. 2) illustrate the relative stratigraphic position of seven different sites. Garrison et al. (2007) suggested that these sites were deposited in a lacustrine system in which a perennial lake cyclically transgressed and regressed. Kirkland et al. (1997) suggested that the MM represents fluvial environments with small channels and overbank deposits.

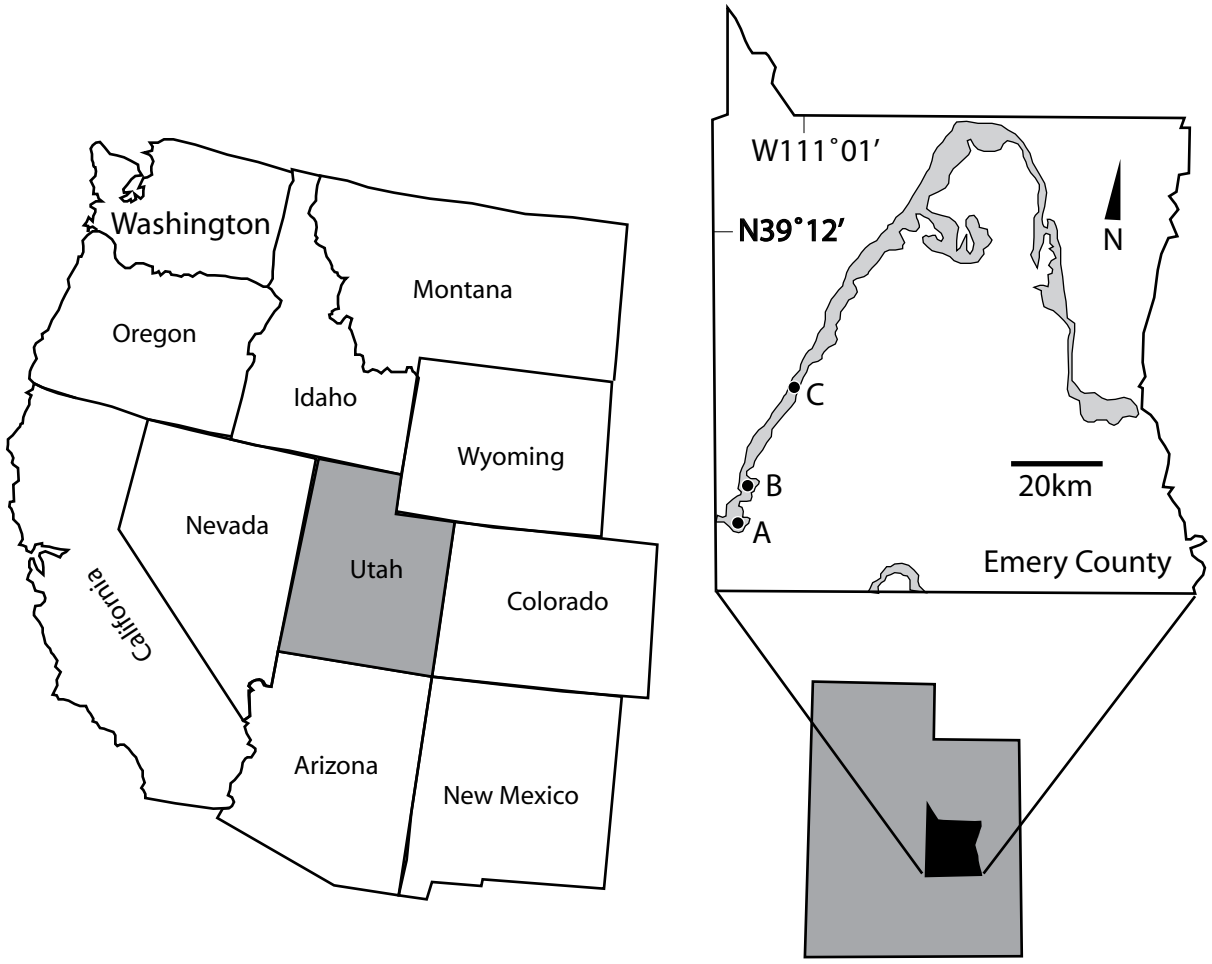

Fig 1. Vertebrate sites from Emery County, Utah. A, B, and C are the location of representative stratigraphic sections in Fig. 2. The grey shaded area within Emery County represents the outcrop belt of the Cedar Mountain Formation.

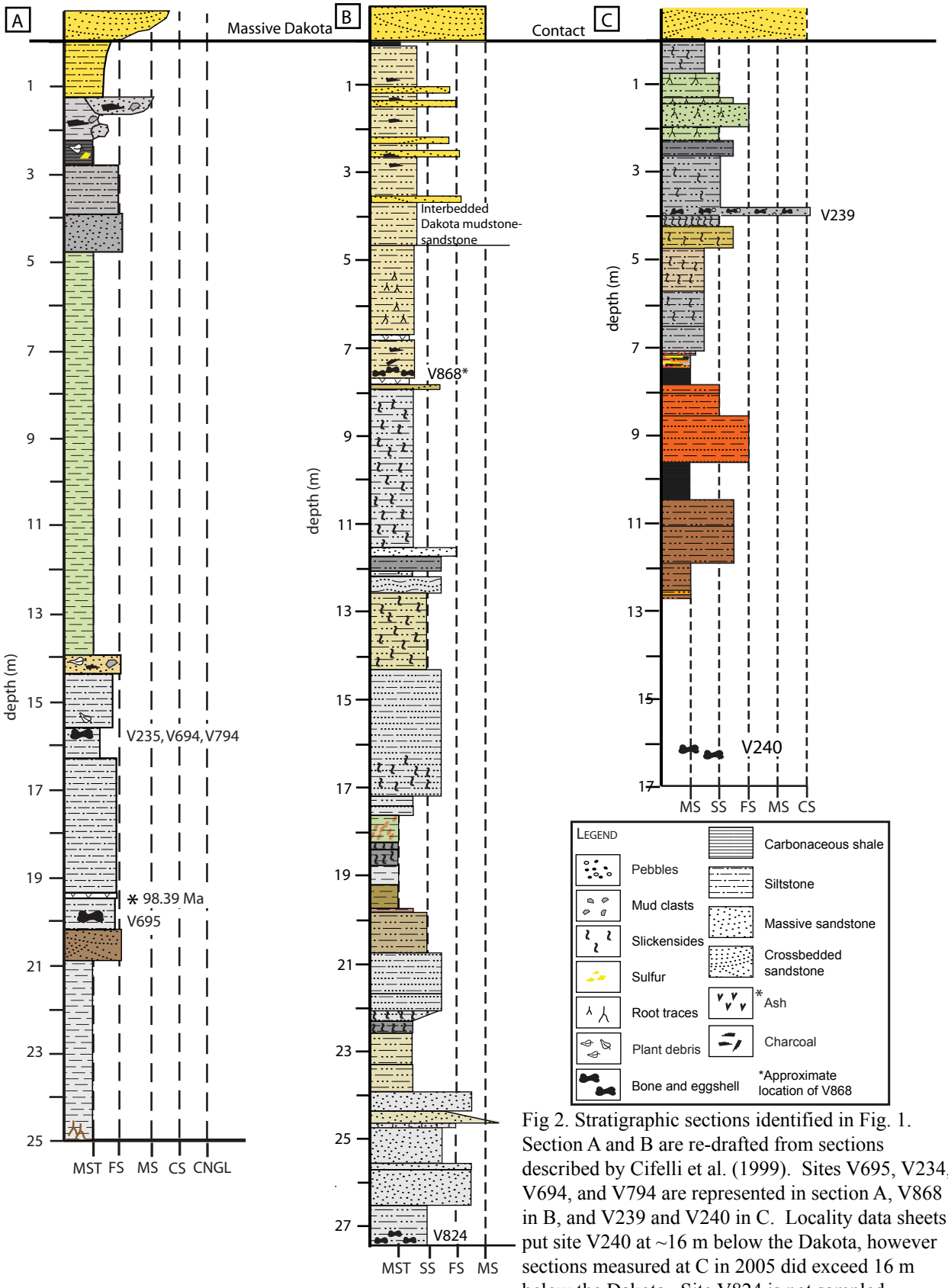

Fig 2. Stratigraphic sections identified in Fig. 1. Section A and B are re-drafted from sections described by Cifelli et al. (1999). Sites V695, V234, V694, and V794 are represented in section A, V868 in B, and V239 and V240 in C. Locality data sheets put site V240 at ~16 m below the Dakota, however sections measured at C in 2005 did exceed 16 m below the Dakota. Site V824 is not sampled.

Mussentuchit Fauna

The MM vertebrate taxa are one of the richest vertebrate faunas described from the early Cretaceous (Cifelli et al., 1999). The fauna appears to be a combination of older European-affiliated taxa such as *Coniophis* (snakes, not analyzed in this study), Pachycephalosauria (Ornithischian), and Hesperornithiformes (birds not analyzed in this study) and a younger Asian-originated fauna such as the carnivorous dinosaurs Troodontidae and Tyrannosauridae, and herbivorous dinosaurs Hadrosauridae and Neoceratopsians (Cifelli et al., 1999).

Fish samples include at least two types of fish teeth as well as fish scales. Scales are only identified to class level as Actinopterygian scales. Teeth include two main forms, pointed teeth and rounded pycnodontid teeth (Cifelli et al., 1999). Some of the rounded teeth can be identified as *Lepidotes*, all rounded pycnodont and *Lepidotes* teeth are referred to as *Lepidotes*-like teeth (Fig. 3A). These rounded teeth probably belong to a durophagous (clam-eating) fish as opposed to the fish whose teeth are smooth and pointed ("Actinopterygian teeth").

Crocodilian teeth and scutes include Goniopholidae, Atoposauridae, and *Bernissartia sp.* teeth. *Bernissartia* has durophagous dentition and has been reported from the early Cretaceous of Europe (Buffetaut and Ford, 1979) and the Aptian-Albian of Texas (Winkler et al., 1990). Like the taxa represented by *Lepidotes*-like teeth, it probably ate mollusks and lived in rivers and streams. Goniopholidae and Atoposauridae are both semi-aquatic mesosuchians (i.e. ancient crocodiles) that span the Upper Jurassic to Lower Cretaceous (Carroll, 1988). Also sampled were several small crocodile osteoderms (scutes) that are not specifically identified (Fig 3B).

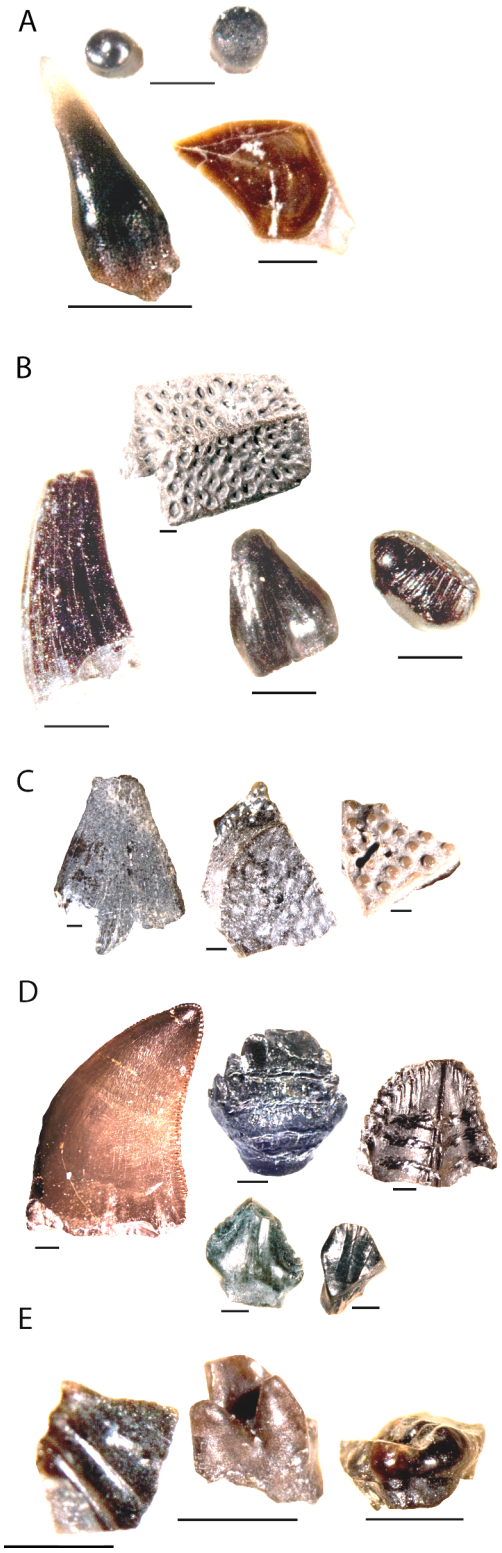

Fig. 3. Examples of tooth, shell, scale, and osteoderm specimens sampled. (A) Representative fish remains. Lepidotes (top left), Lepidotes-like teeth (top right), Actinopterygian teeth (bottom left), and Actinopterygian scales (bottom right). (B) Representative crocodile: from left to right, Goniopholidae, Atopodauridae, Bernissartia sp.and an osteoderm (top) (C) Representative turtle shell fragments from left to right: Trionychidae, Glyptops sp., and Naomichelys sp. (D) Representative dinosaur teeth: dromaeosaurid theropod (top left), polocanthine nodosaur (top center), Eolambia caroljonesa (top right), and two types of unidentified basal ornithopod teeth (bottom). (E) Representative mammalian teeth: two types of generically identified mammalian teeth and Multituberculata (far right). Scale bars = 1 mm.

Most turtle specimens are broadly identified as belonging to the super-order Chelonia, but some samples are more specifically identified as belonging to the family Trionychidae, and few to the species level, i.e. *Glyptops sp.*, and *Naomichelys sp* (Fig. 3C). All taxa are fully aquatic. Trionychidae, or soft-shelled turtles, were freshwater carnivores that lived at the bottom of rivers but also some small ponds (Carroll, 1988; Demar Jr. and Breithaupt, 2006). *Glyptops sp.* is an archaic genus that was a direct ancestor of the family Baenidae that is a clade of the paracryptodirian turtles endemic to North America (Lyson and Joyce, 2009). It is common in both the underlying Morrison Formation and overlying Dakota Formation (Cifelli et al., 1999). Since most Baenids were river-dwelling, it is likely that *Glyptops* was a bottom-dwelling, riverine turtle. *Naomichelys sp.* is a member of the family Solemydidae. It is distinguishable by its pustulate shell ornamentation and has been identified in brackish water deposits near the bottom of the upper Cretaceous Iron Springs Formation (Milner et al., 2006) and in riverine deposits of the Mesaverde Formation (Demar Jr. and Breithaupt, 2006).

Dinosaur teeth from the site are broadly identified as Hadrosauridae, Ornithischia, or Theropoda (Fig. 3D). The Hadrosauridae teeth are from basal (primitive) hadrosaurs, though some have been identified as the advanced iguanodontid, *Eolambia caroljonesa* (Kirkland et al., 1998). Other ornithischian teeth belong to hypsilophodontids such as *Orodromeus*, nodosaurids such as *Animantarx*, and the Marginocephalians: neoceratopsians and pachycephalosaurs. Of the theropod dinosaurs, all teeth are only broadly identified as Theropoda. Most of the teeth represent troodontidae, dromaeosaur, or Tyrannosaurid teeth. Most theropods teeth sampled in this study are dromaeosaur. Tooth morpho-species include cf. *Paronychodon* and cf.

Richardoestesia. Some very small and slender sauropod teeth have also been recovered from the MM, however they are too rare and were not sampled.

Mammalian teeth sampled are broadly identified as "Mammalia" but are sometimes more specifically identified as Multituberculata or Tribosphenida (Fig. 3F). Cifelli et al. (1999) suggest most of the Multituberculata are representatives of the genus *Paracimexomys.* The samples of Tribosphenida were probably from the marsupial-like genus *Kokopellia* (Cifelli, 1993). Both types of sampled mammals are hypothesized to have been omnivorous.

Ecologic and Climatic Setting

The ecologic setting of these animals was affected by two main geologic events that could have impacted local hydrology: 1) mountain building from the Sevier Fold and Thrust Belt (SFTB) and 2) the incursion of the Western Interior Seaway. The SFTB is a segment of the larger Cordilleran retroarc fold-and-thrust belt that formed during the late Mesozoic to early Cenozoic times (DeCelles and Coogan, 2006). The majority of the Cedar Mountain Formation is syndepositional with the SFTB and is made up of sediments shed from the resulting mountains. The Mussentuchit Member was deposited in the foredeep of the foreland-basin system and its deposition is synchronous with the Pavant Thrust event (110 to 86 Ma) (Currie, 1998; DeCelles and Coogan, 2006). The resulting mountains ran from northeast to southwest through central Nevada to western Utah and by the Late Cretaceous, they formed an Andean-style fold-and-thrust belt with a high-elevation, low-relief hinterland plateau. By the end of the Pavant Thrust (and end of MM deposition), paleo-elevation was ~2.2 km in western Utah (DeCelles and Coogan, 2006). Regional paleohydrology was affected by these orogenic events because the rise of the mountains would hinder westward flowing jet stream moisture (Poulsen et al., 2007).

Oboh-Ikuenobe et al. (2008) showed that during the early part of the WIS formation, at least two smaller scale transgression and regressions occurred prior to the major Greenhorn transgression (95-96 Ma) and could have brought sea water sources closer to the MM area. These small-scale transgressions and regressions could have resulted in increased humidity and $\delta^{18}O$ enriched moisture sourced from the seaway.

METHODS

All samples used in this study were obtained from the Oklahoma Museum of Natural History's Sam Noble Museum, and were selected on the basis of the number of taxa per site, close proximity of sites, and distinct stratigraphic location. Analyzed samples include Actinopterygian scales and teeth (OMNH-labeled Lepisosteidae scales and teeth), *Lepidotes*-like palatal teeth (OMNH-labeled Osteichthyes palatal teeth and *Lepidotes sp.*), turtles (Trionychidae, *Glyptops sp.*, and *Naomichelys sp*), crocodiles (Goniopholidae, Atoposauridae, and *Bernissartia sp*), Hadrosauridae teeth, non-hadrosaur Ornithischian dinosaur teeth, theropod teeth, and mammalian teeth (Multituberculata and Tribosphenida) (Table 1). When possible, at least 10 individuals per taxa were analyzed or at least 10 isotopic measurements per specimen were made. For some of the smallest teeth and scales, samples were glued to slides for better control while micro-drilling. Enough enamel or ganoine was milled to yield 200 - 500 µg of powder. Phosphate samples were converted to silver phosphate following the method of O'Neil (1994) as modified by Bassett et al. (2007). Silver phosphate samples were analyzed at the W. M. Keck Paleoenvironmental and Environmental Stable Isotope Laboratory at the University of Kansas, Department of Geology on a Thermo high temperature conversion elemental analyzer (TC/EA)

TABLE 1. Samples Analyzed

SITE	TAXA	$N_{specimen}$	$N_{samples}$
V239 (SC1) Depth:	Actinopterygian scale	9	9
4 m	Lepidotes – like teeth	10	10
	Crocodilia: Atoposauridae + Goniopholidae	8	10
	Turtle: "Chelonia" + *Naomichelys sp.*	2	11
	Ornithischia	5	7
	Theropoda	4	10
	Mammalia	10	10
V868 (WS27)	Actinopterygian scale	10	14
Depth: 8 m	Lepidotes-like teeth	8	9
	Crocodilia: Atoposauridae + Goniopholidae	9	13
	Turtle: "Chelonia"	4	17
	Ornithischia	3	14
	Hadrosauridae	3	21
	Mammalia	10	12
V794 (WS13)	Actinopterygian scale	5	7
Depth: 15 m	Actinopterygian teeth	10	10
	Lepidotes-like teeth	10	11
	Crocodilia: Goniopholidae	5	21
	Turtle: *Naomichelys sp.*	10	10
	Ornithischia	1	10
	Hadrosauridae	2	9
	Theropoda	4	11
	Mammalia: Multituberculata	11	12
V235 (WS4)	Actinopterygian scales	9	9
Depth: 15 m	Actinopterygian teeth	7	8
	Lepidotes-like teeth	5	6
	Crocodilia scutes	4	12
	Crocodilia teeth: Goniopholidae + Atoposauridae	14	15
	Hadrosauridae	3	9
	Theropoda	10	10
	Mammalia: Tribosphenida + Multituberculata	14	14
V694 (WS9)	Actinopterygian scales	10	10
Depth: 15 m	Actinopterygian teeth	10	10
	Lepidotes-like teeth	10	12
	Crocodilia: Goniopholidae + Atoposauridae	11	12
	Mammalia	10	10
V240 (SC2) Depth:	Actinopterygian scales	10	11
16 m	Actinopterygian teeth	10	11
	Lepidotes – like teeth	10	12
	Crocodilia: *Bernissartia* + Goniopholidae + Atoposauridae	13	14
	Turtle: "Chelonia"	1	9
	Hadrosauridae	3	6
	Theropoda	10	12
V695 (WS10)	Actinopterygian scales	10	10
Depth: 19.m	Actinopterygian teeth	10	10
	Lepidotes – like teeth	7	7
	Crocodilia scute	8	12
	Turtle: *Glyptops sp* + Trionychidae + *Naomichelys sp.*	7	20
	Ornithischia	11	11

connected to a ThermoFinnigan MAT 253 continuous flow mass spectrometer. Phosphate $\delta^{18}O$ is reported in parts per thousands (‰) relative to V-SMOW using standard δ-notation. Precision was monitored via analysis of NIST 120c and is better than ± 0.3 ‰ V-SMOW producing an average value of 22.5 ± 0.3 ‰.

Bulk pedogenic and diagenetic carbonate samples from a few MM sections near the vertebrate sites were analyzed for C and O isotopic composition. Approximately 50μg of carbonate was milled and vacuum-roasted at 200°C to remove volatiles. Samples were then analyzed by reaction with 100% H_3PO_4 at 75°C using a Kiel III carbonate reaction device interfaced to the inlet of a ThermoFinnigan MAT 253 Dual Inlet mass spectrometer. Carbonate isotope data are reported relative to V-PDB and converted to V-SMOW for comparison to phosphate isotopic data. Precision was monitored through the daily analysis of NBS-18 and NBS-19 and is better than 0.10 ‰ for both $\delta^{13}C$ and $\delta^{18}O$.

Ingested/living water isotopic composition was calculated from equations presented by Barrick et al. (1999) for turtles, Amiot et al. (2007) for crocodiles and Kohn (1996) for omnivorous mammals. The water compositions derived from turtles were then used to calculate the ambient temperature during ganoine precipitation for fish remains using the Kolodny et al., (1983) equation relating temperature, isotopic composition of water, and isotopic composition of phosphate. Dinosaur ingested water was estimated using biological parameters for birds as presented by Kohn (1996). We modified the Kohn (1996) bird equation to account for a sustained body temperature of 37ºC as suggested by Amiot et al. (2006). Because humidity effects are greater in herbivores than in carnivores we use an intermediate humidity coefficient

between herbivorous birds and carnivorous mammals for the carnivore dinosaur. The following equations are then used to calculate herbivorous dinosaur ingested water:

$$\delta^{18}O_w = 1.41\delta^{18}O_p + 12.11h - 41.59 \quad (1)$$

and carnivorous dinosaur water:

$$\delta^{18}O_w = 1.41\delta^{18}O_p + 7.0h - 41.59 \quad (2)$$

M. Suarez (2009) in modeling water $\delta^{18}O$-paleo-latitudinal gradients as calculated from 2ºS-75ºN using Albian pedogenic carbonates, modeled a humidity of ~ 47% using a zonal mean annual temperature (MAT) estimated from leaf physiognomy for the CMF paleo-latitude at 34ºN. MAT is 23ºC for CMF paleo-latitude (~34-35ºN) based on leaf physiognomy data of Wolfe and Upchurch (1987) and Spicer and Corfield (1992). We use this MAT to calculate the isotopic composition of meteoric water from carbonates.

Epsilon (ε), or isotopic enrichment, was calculated between taxa using the Levin et al., (2006) equation:

$$\varepsilon = \left(\frac{0.001\delta^{18}O_{p1}}{0.001\delta^{18}O_{p2}} - 1 \right) * 1000 \quad (3)$$

Where $\delta^{18}O_{p1}$ represents the average phosphate isotopic composition of one taxa and $\delta^{18}O_{p2}$ represents the average composition of the other taxa.

RESULTS

Of the aquatic taxa, *Lepidotes*-like teeth have the lightest isotopic compositions (average of 15.0 ± 1.6 ‰) and ranges from a minimum of 13.8 ‰ at V239 (-4 m) to a maximum of 15.8 ‰ at V235 (-15 m) (Table 2, Fig. 4). Actinopterygian teeth and scales are not significantly

TABLE 2. Oxygen Isotopic Composition of Phosphate Relative to V-SMOW

SITE	TAXA	*Min*	*Max*	*Avg ± 1σ*
V239 (SC1)	Actinopterygian scale	15.3	16.7	16.0 ± 0.4
Depth: 4 m	*Lepidotes* – like teeth	11.8	14.7	13.8 ± 0.8
	Crocodilia: Atoposauridae + Goniopholidae	15.9	18.5	16.7 ± 0.7
	Turtle: "Chelonia" + *Naomichelys sp.*	14.7	16.4	15.4 ± 0.7
	Ornithischia	15.4	18.6	16.9 ± 1.1
	Theropoda	15.6	20.0	18.3 ± 1.8
	Mammalia	15.1	17.4	16.2 ± 0.7
V868 (WS27)	Actinopterygian scale	15.4	17.8	16.4 ± 0.7
Depth: 8 m	*Lepidotes*-like teeth	13.1	17.7	15.4 ± 1.8
	Crocodilia: Atoposauridae + Goniopholidae	16.4	18.6	17.1 ± 0.5
	Turtle: "Chelonia"	15.0	16.9	16.2 ± 0.6
	Ornithischia	15.5	17.4	16.5 ± 0.6
	Hadrosauridae	14.0	17.5	16.6 ± 0.9
	Mammalia	13.8	17.4	16.3 ± 0.9
V794 (WS13)	Actinopterygian scale	15.1	17.3	15.8 ± 0.7
Depth: 15 m	Actinopterygian teeth	14.6	18.0	15.8 ± 0.9
	Lepidotes-like teeth	12.3	16.7	15.0 ± 1.2
	Crocodilia: Goniopholidae	14.4	18.3	16.3 ± 1.0
	Turtle: *Naomichelys sp.*	14.9	17.1	16.0 ± 0.7
	Ornithischia	14.8	16.1	15.5 ± 0.8
	Hadrosauridae	15.2	17.4	16.2 ± 0.9
	Theropoda	16.4	19.8	18.3 ± 1.0
	Mammalia: Multituberculata	14.8	17.5	16.4 ± 0.9
V235 (WS4)	Actinopterygian scales	14.6	17.1	15.9 ± 0.7
Depth: 15 m	*Lepidotes sp.* teeth	15.0	16.6	15.8 ± 0.6
	Lepidotes-like teeth	15.1	16.8	15.9 ± 0.8
	Crocodilia scutes	15.1	16.6	15.8 ± 0.5
	Crocodilia teeth: Goniopholidae + Atoposauridae	15.8	18.7	17.0 ± 1.0
	Hadrosauridae	15.2	17.9	16.6 ± 1.0
	Theropoda	15.4	18.5	17.0 ± 1.1
	Mammalia: Tribosphenida + Multituberculata	14.4	17.6	16.5 ± 0.8
V694 (WS9)	Actinopterygian scales	14.9	16.5	15.7 ± 0.6
Depth: 15 m	Actinopterygian teeth	14.8	17.9	16.4 ± 1.1
	Lepidotes-like teeth	12.5	16.2	14.4 ± 1.3
	Crocodilia: Goniopholidae + Atoposauridae	14.9	17.6	16.1 ± 0.8
	Mammalia	15.8	17.7	16.7 ± 0.8
V240 (SC2)	Actinopterygian scales	16.0	18.8	17.2 ± 0.7
Depth: 16 m	Actinopterygian teeth	14.6	21.0	17.2 ± 2.2
	Lepidotes – like teeth	13.3	19.7	15.4 ± 2.1
	Crocodilia: *Bernissartia* + Goniopholidae + Atoposauridae	15.5	19.5	17.5 ± 1.3
	Turtle: "Chelonia"	15.5	17.2	15.4 ± 1.6
	Hadrosauridae	14.5	17.1	16.1 ± 0.9
	Theropoda	15.3	18.2	16.5 ± 0.9
V695 (WS10)	Actinopterygian scales	15.5	16.9	16.2 ± 0.5
Depth: 19 m	Actinopterygian teeth	15.0	18.6	16.5 ± 1.0
	Lepidotes – like teeth	12.5	17.1	15.4 ± 1.5
	Crocodilia scute	13.5	16.9	15.5 ± 0.8
	Turtle: *Glyptops sp* + Trionychidae + *Naomichelys sp.*	14.5	16.4	15.7 ± 0.6
	Ornithischia	15.4	18.4	17.3 ±0.9
	Mammalia	14.8	18.0	16.3 ± 1.2

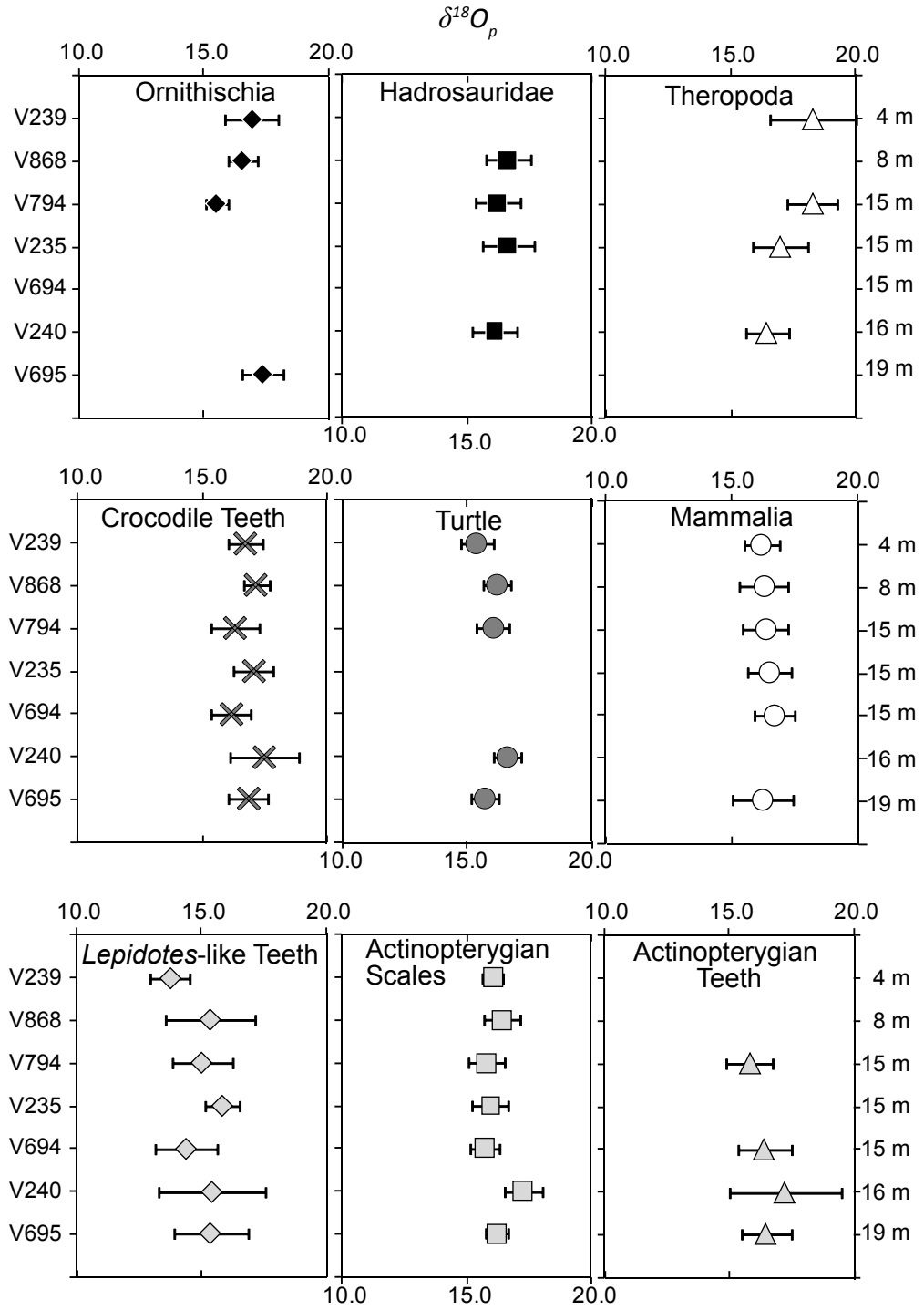

Fig. 4. Average oxygen isotopic compositions of phosphate relative to V-SMOW per site for each taxa sampled. Sites are positioned in relative stratigraphic order. Sites V794, V235, and V694 are at the approximate same stratigraphic level. Error bars represent one standard deviation. Black symbols = herbivorous dinosaurs, white symbols = carnivorous dinosaurs or omnivorous mammals, dark grey symbols = semi-aquatic taxa, light grey symbols = aquatic taxa. Axis on the far right indicates meters below the Dakota Formation.

different from each other. Scales average 16.2 ± 0.8 ‰ and range from a minimum of 15.7 ‰ at V794 and V694 (both at -15 m) to a maximum of 17.2 ‰ at V695 (-19 m).

Of the two semi-aquatic taxa (turtles and crocodiles), turtles consistently have the lightest isotopic compositions and ranges between 15.4 ‰ at V239 (-4 m) to 16.6 ‰ at V240 (-16 m) and have an average composition of 16.0 ± 0.7 ‰. Crocodiles range from a minimum of 16.1 ‰ at site V694 (-15 m) to a maximum of 17.5 ‰ at site V240 (-16 m) with an average composition of 16.6 ± 1.0 ‰. As site V695 lacks crocodile teeth, we estimated crocodilian teeth $\delta^{18}O$ based on the fact that for coexisting teeth and scutes at site V235, scutes tend to be on average 1.3 ‰ lighter than teeth. This phenomenon has been also documented in Jurassic crocodilians from Western Europe (Billon-Bruyat et al., 2005) and in living crocodiles from the Oubangui River, Central Africa (Lécuyer et al., 2003). Therefore, we can estimate the isotopic composition of teeth at V695 to be ~ 16.8 ‰.

Mammal enamel does not significantly vary from site to site but there is a slight trend towards lighter isotopic compositions from site V694 (-15 m) to the top of the MM at site V239 (Fig. 4). Mammal isotopic compositions range from a minimum of 16.3 ‰ at site V695 (-19 m) to a maximum values at V694 (-15 m) of 16.7 ‰. Their average composition is 16.4 ± 0.9 ‰

Theropods tend to have the isotopically heaviest enamel of all the sampled dinosaurs. They average 17.5 ± 1.4 ‰ and ranges between a minimum of a minimum of 16.5‰ at site V240 to a maximum value of 18.3‰ at both sites V239 (-4 m) and V793 (-15 m). Ornithischian enamel averages 16.6 ± 1.0 ‰ and range from 15.5 ‰ at site V794 (-15 m) to 17.3 ‰ at site V695 (-19 m). Hadrosaurs range from 16.1 ‰ at site V240 (-16 m) to 16.6 ‰ at both sites V868 (-8 m) and V235 (-15 m) with an average composition of 16.5 ± 0.9 ‰ (Table 2, Fig. 4).

The average value of carbonate oxygen isotopes (relative to V-SMOW) is 23.3 ± 1.9 ‰ and ranges from 19.9 ‰ for the carbonate cemented sandstone at 15 m below the Dakota Formation to a maximum of 24.3 ‰ at 6 m below the Dakota (Table 3).

Turtles record water compositions (relative to V-SMOW) that average -6.2 ± 0.7 ‰ and range from -6.7 ‰ at site V239 to -5.5 ‰ at site V240 (Table 4). Crocodiles record more enriched water isotopic compositions relative to turtles and average -5.2 ± 0.8‰ with a minimum of -5.9 ‰ at site V694 and a maximum at of -4.8 ‰ at site V240. Mammal ingested water averages -7.0 ±1.4 ‰ and ranges from a minimum of -7.3 ‰ at site V239 to a maximum of-6.5 ‰ at site V694. All of the dinosaur taxa yield water values that are extremely light in isotopic composition. Theropod ingested water ranges from a minimum of-15.2 ‰ at site V240 to a maximum of-12.4 ‰ at sites V239 and average -13.6 ± 2.0 ‰. Ornithischian ingested water averages -12.5 ± 1.4 ‰ and ranges from a minimum of -14.1 ‰ at site V794 to a maximum of-11.5 ‰ at site V695. Hadrosauridae ingested water averages -12.7 ± 1.3 ‰ and ranges from a minimum of -13.2 ‰ at site V240 to a maximum of -12.4 ‰ at site V868 (Table 4, Fig. 5). Carbonate water ranges from -9.1 ‰ for the sandstone at 15 m below the Dakota Sandstone to -4.9 ‰ at 6 m below the Dakota (Table 5). The average oxygen isotopic composition of water that precipitated micritic calcite from MM is -5.8 ± 1.8 ‰.

The temperatures calculated from *Lepidotes*-like teeth remains, using the water composition calculated from turtles, yields temperatures that range from a minimum of 16.6ºC at V235 to a maximum of 23.3ºC and average 20.3 ± 2.5ºC (Table 6). Temperature calculated from Actinopterygian scales are much lower, and range from 13.6ºC at V240 to a maximum of 17.6ºC at V694 and average 15.5 ± 1.7 ºC.

TABLE 3.Oxygen Isotopic Composition of Micritic Calcite Relative to V-SMOW

Depth (m)	sedimentology	$\delta^{18}O_c$-VSMOW
4	Nodule	23.9
6	Mudstone	24.2
6	Mudstone	24.3
15	Sandstone	19.9
26	Mudstone	24.2

TABLE 4. Calculated Oxygen Isotopic Composition of Water from Phosphate

Site	Depth (m)	Turtle	Crocodile	Mammalia	Ornithischia	Hadrosauridae	Theropoda
		$\delta^{18}O_w = 1.01*\delta^{18}O_p - 22.3$ (Barrick et al., 1999)	$\delta^{18}O_w = 0.82*\delta^{18}O_p - 19.13$ (Amiot et al., 2007)	$\delta^{18}O_w = 1.6*\delta^{18}O_p - 35.5 + 6.1h$ (Kohn, 1996)	$\delta^{18}O_w = 1.41\delta^{18}O_p + 12.11h - 41.59$ (modified, Kohn, 1996)		$\delta^{18}O_w = 1.41\delta^{18}O_p + 7.0h - 41.59$ (modified, Kohn, 1996)
V239	4	-6.7 ± 0.7	-5.4 ± 0.6	-7.3 ± 1.1	-12.0 ± 1.5		-12.4 ± 2.4
V868	8	-5.9 ± 0.5	-5.1 ± 0.4	-7.1 ± 1.5	-12.6 ± 0.9	-12.4 ± 1.3	
V794	15	-6.1 ± 0.7	-5.8 ± 0.8	-7.0 ± 1.4	-14.1 ± 0.6	-13.0 ± 1.2	-12.5 ± 1.4
V235	15		-5.2 ± 0.7	-6.8 ± 1.3		-12.5 ± 1.5	-14.2 ± 1.6
V694	15		-5.9 ± 0.6	-6.5 ± 1.2			
V240	16	-5.5 ± 0.6	-4.8 ± 1.2			-13.2 ± 1.4	-15.2 ± 1.2
V695	19	-6.4 ± 0.6	-5.4 ± 0.7	-7.2 ± 1.9	-11.5 ± 1.2		

$h = 0.47$

TABLE 5. Calculated Oxygen Isotopic Composition of Water From Micritic Calcite

Depth (m)	T (K)	$10^3 \ln\alpha$	A	sedimentology	$\delta^{18}O_w$
	295.82	$10^3 \ln\alpha = 2.78(10^6/T^2) - 2.89$			$\delta^{18}O_w = ((\delta^{18}O_c + 10^3)/\alpha) - 10^3$
4		28.878	1.0293	Nodule	-5.3
6				Mudstone	-4.9
6				Mudstone	-4.9
15				Sandstone	-9.1
26				Mudstone	-5.0

TABLE 6. Calculated Temperatures of Fish Scale and Tooth Formation

Site	Depth (m)	Actinopterygian Scales	Actinopterygian teeth	*Lepidotes*-like teeth
		$t°C = 111.4-4.38*(\delta^{18}O_p - \delta^{18}O_w)$ (Kolodny et al., 1983)		
V239	4	14.0 ± 1.5		23.5 ± 3.4
V868	8	15.5 ± 3.1		20.0 ± 7.6
V794	15	17.5 ± 3.1	17.1 ± 4.0	20.5 ± 5.1
V235	15	16.6 ± 3.1*		16.6 ± 3.5*
V694	15	17.7 ± 2.6*	14.9 ± 4.6*	23.3 ± 5.4*
V240	16	13.6 ± 3.2	13.6 ± 9.7	21.4 ± 9.2
V695	19	14.4 ± 2.4	13.0 ± 4.3	17.5 ± 6.5

*no turtles preserved at V235 or V694; used V794 turtles

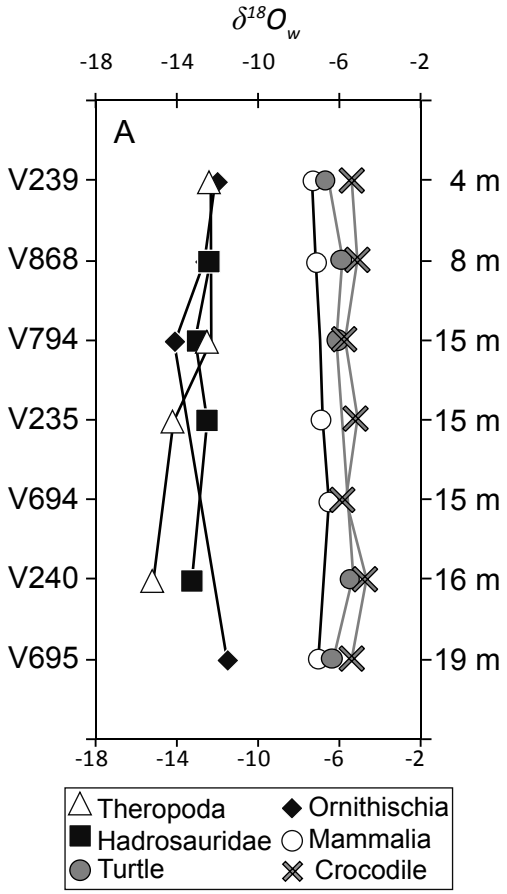

Fig. 5. Average calculated ingested water composition from Table 4. Humidity is held constant at 47% throughout the section and dinosaur body temperature is assumed to be 37ºC (Amiot et al., 2006).

DISCUSSION

Preservation of Biogenic Record

Kolodny et al. (1996) outlines criteria for the selection of vertebrate fossil material for isotopic study of paleoecosystems. First, they suggested that the more diagenetically resistant biominerals, enamel and ganoine, rather than bone or dentine be used. In this study we only use enamel and ganoine. Second, they suggest that if using bone, only materials with micron-scale preservation be used. Although we do not use bone, small scale structures such as growth banding in tooth enamel and in ganoine scales are preserved in most samples. The separation of $\delta^{18}O$ values of vertebrate remains along physiological lines (e.g. aquatic versus terrestrial taxa) has also been used to indicate preservation of original biogenic signals (Fricke et al., 2008; Amiot et al., 2009). Since differences in isotopic composition between taxa of different physiologies (e.g. *Lepidotes*-like teeth versus theropod teeth) are observed in this data set, we interpret that the MM vertebrates do preserve original biogenic isotopic signals.

Ecological Interpretation and Implications

Based on the calculated $\delta^{18}O_w$ for the MM vertebrates and carbonates, we can make reasonable interpretations on the habitats of the different taxa, infer the water reservoirs they lived in or drank from, or estimate the ranges of temperature during which they precipitated phosphate. Water compositions generated from carbonates for the entire member average -5.8 ± 1.8 ‰ and represent local meteoric water. Pedogenic calcite forms under precipitation deficit (Breeker et al., 2009) and therefore its composition is that of precipitation slightly influenced by evaporation. Given that water calculated from aquatic turtles is -6.2 ± 0.7 ‰ we believe their compositions also represent local meteoric water but represent a short time-scale average for

meteoric water while pedogenic calcite represents slightly enriched meteoric water on long-term time scales. As turtles tend to grow their shells in the summer months (Pough et al., 2002; Barrick et al., 1999) it is likely that the $\delta^{18}O_w$ we have calculated is biased toward summer water composition. We cannot ascertain whether turtles inhabited locally recharged streams and rivers or were simply recording base flow composition of regional rivers.

Crocodiles yield water $\delta^{18}O$ values that were heavier (-5.2 ± 0.8 ‰ avg.) than those calculated from turtles but similar to the water calculated from pedogenic calcite. Though the Cretaceous crocodiles (mesosuchians) are extinct taxa, their habitat was probably very similar to that of extant crocodiles (eusuchians). Modern crocodiles spend much of their time as sit-and-wait predators in shallow water near the shore of rivers, lakes, and ponds (Marwick, 1998; Pough, et al., 2002), and they also spend significant amounts of time basking in the sun. The shallow waters inhabited by crocodiles (e.g. lake shorelines, river banks, etc.) are most likely evaporatively enriched relative to the main water body. Thus, our data agrees with the interpreted habitat of crocodiles and indicates that the isotopic compositions are slightly modified (i.e. evaporated) river water. As crocodiles do have a narrow range of temperature under which they precipitate apatite, which is also similar to that of turtles (Amiot et al., 2007), we can infer that these two taxa inhabited similar bodies of water and the behavior of the crocodiles resulted in the slightly enriched $\delta^{18}O_w$.

The average $\delta^{18}O_w$ value of *Bernissartia* is -5.4± 1.1 ‰ at V240. This is slightly lighter than co-existing Atoposauridae (-4.5 ± 0.8‰) and Goniopholidae (-4.3 ± 1.1‰) suggesting *Bernissartia* spent more time in isotopically lighter water than Atoposauridae and Goniopholidae. The durophagous dentition of *Bernissartia sp.* that indicates they fed on clams,

also suggest they must have spent more time in the water grazing the river and stream bottoms for clams, and thus would not be subject to evaporative effects to the same extent as co-existing crocodiles. In addition *Bernissartia sp.* $\delta^{18}O_w$ are indistinguishable from that of co-existing turtles and indicates that they to also preserve a record of river water sourced from local precipitation.

A relative humidity of 47 %, estimated by M. Suarez (2009) for the CMF paleolatitude (34°N), was used to estimate water ingested by the micro-mammals. Their drinking water (-7.0 ± 1.4 ‰) was relatively light compared to crocodiles, and is lighter than the composition of water calculated from turtles (-6.2 ± 0.7 ‰). Modern small mammals show a wide variety of drinking habits that is highly dependent on their habitat (Chew, 1951; McManus, 1974; Smith et al., 2002; Hamilton, 2009). Small mammals from humid or riparian areas tend to get their drinking water from surface water such as streams and lakes (Chew, 1951; Tütken et al., 2006; Hamilton, 2009) whereas small mammals that inhabit dry climates can get almost all of their water from their diet (McManus, 1974; Huertas et al., 1995). Mammals from both habitats do get some portion of water from rain and dew, though the proportions are dependent on rainfall amounts, temperature, and relative humidity (Chew, 1951). Based on the types of MM vertebrate fauna preserved (including frogs and lizards) and sedimentologic evidence (rare carbonate formation) we suggest that humidity was higher than 47 %. Our data (using 47% humidity) suggests that the micro-mammals in the MM ingested water lighter in composition to turtles or crocodiles and was from isotopically depleted river water or isotopically depleted dew. Their water was not solely from food water (Smith et al., 2002; Tütken et al., 2006; Hamilton, 2009) as this would result in relative enrichment over local meteoric water.

Calculated ingested water for dinosaurian taxa is isotopically much lighter than the water calculated from the aquatic/semi-aquatic taxa (as low as -15.2 ‰). This depletion (at least for the dinosaurs) is perplexing at first considering modern terrestrial taxa should be enriched relative to river water due to evaporative enrichment of body water and of their diet (Kohn, 1996; Fricke et al., 2007). The calculated ingested water values depend significantly on the humidity and temperature used in the calculation (eq. 2 and 3). High humidity should result in lower $\delta^{18}O$ of body water and of the precipitated phosphate (Kohn, 1996). Therefore, at the relatively low CMF humidity (47%), the calculated ingested water could result in lighter values than those of the aquatic taxa. As suggested by the sedimentology and fauna preserved in the MM we suggest that humidity was higher during MM time relative to older units of the CMF. Since, small mammals and rodents tend to be greatly affected by humidity (Huertas et al., 1995; Kohn, 1996) we use the isotopic composition of their teeth to constrain humidity for the MM. Rather than calculating mammal drinking water from their isotopic composition of phosphate, we used the equation for omnivorous rodents presented by Kohn (1996) (Table 4) to solve for humidity using water calculated from the potential drinking water reservoirs (calculated from aquatic/semi-aquatic taxa). Depending on which water source is used, the average humidity is as low as ~ 47 % (using turtle-ingested water) to as high as ~ 76 % (using crocodile ingested water). Since mammals ingested water from shallow perennial streams or the enriched end-member of meteoric water, we used water calculated from crocodile phosphate to calculate humidity over the course of the MM (average humidity ~ 68 %). Using calculated variable relative humidity, the calculated isotopic composition of ingested water ranges from -8.6 ‰ for ornithischians at V695 to -12.8 ‰ for theropods at V235 (Table 7). These values are still much lighter than those

of the calculated water from aquatic taxa, suggesting they record isotopically depleted river water. As it has been suggested that dinosaurs are homeothermic (Amiot et al.,

Table 7. Effects of Calculated Humidity on Isotopic Composition of Dinosaur-Ingested Water

Site	***h*** **(turtle)**	Ornithichia	Hadrosauridae	Theropoda	***h*** **(croc.)**	Ornithischia	Hadrosauridae	Theropoda
V239	**0.50**	-11.9		-12.4	**0.74**	-9.0		-10.5
V868	**0.64**	-10.7	-10.6		**0.76**	-9.2	-9.1	
V794	**0.58**	-12.9	-11.9	-11.9	**0.63**	-12.3	-11.3	-11.6
V235	**0.76**		-9.2	-12.2	**0.70**		-9.9	-12.8
V694	**0.47**				**0.53**			
V240								
V695	**0.56**	-10.6			**0.72**	-8.6		

h (turtle) = $0.16* \delta^{18}O_{w\text{-}turtle} - 0.26* \delta^{18}O_{p\text{-}mammalia} + 5.82$; *h (croc)* = $0.16* \delta^{18}O_{w\text{-}croc} - 0.26* \delta^{18}O_{p\text{-}mammalia} + 5.82$

2006), then their apatite synthesis is not limited to the narrow summer window which reptiles and other ectothermic aquatic taxa are constrained to. As dinosaurs drink water year round then they are most likely to record seasonal fluctuations in river water, such as the isotopically depleted melt-water during the late spring as well as the enriched water during the summer. Snow-melt derived water for the higher latitude, Aptian-Albian Kootenai Formation, Montana has been calculated using bivalve shells to be as light as -16.13 ‰ (Glancy et al., 1993). Similar, though perhaps not as light values should be expected to feed large rivers depositing the CMF units. Thus the greater range with a lighter average isotopic composition recorded by dinosaurs relative to the aquatic taxa indicates that dinosaurs are better recorders of regional water values.

The inferred habitats of the fish species *Lepidotes* are wide ranging, from marine to freshwater (Wenz et al., 1994; Kriwet, 2000). Our data suggests *Lepidotes* and *Lepidotes*-like teeth in our samples are fish that were freshwater-inhabitants. The temperature (20.3 ± 2.5ºC) calculated using the isotopic composition of *Lepidotes*-like teeth are consistent with the estimated zonal and latitudinal MAT indicated by M. Suarez (2009). Actinopterygian scales

however, are more enriched than *Lepidotes*-like teeth and therefore calculated temperatures are much lower (~ 15.5 ± 1.7ºC) than for *Lepidotes*-like teeth. If we accept this temperature, then Actinopterygian scales may be formed in colder water during spring melts. However, if we use small theropod calculated $\delta^{18}O_w$ as representing melt water influenced river composition, the calculated temperature for the Actinopterygians is unreasonably and physiological implausible (-10.3°C). The enriched values of Actinopterygian scales must be the result of either inhabiting small evaporative ponds or lakes or, if they exhibit diadromous behavior, it may record isotopically enriched values in estuaries of the WIS encountered during migration.

If we use the $\delta^{18}O_w$ isotopic composition generated from crocodilian phosphate, an enriched river water composition, and assume an apatite synthesis temperature similar to the one obtained for *Lepidotes*-like teeth, then it implies evaporation of at least 10% of the water in which the Actinopterygians resided. If we use $\delta^{18}O_w$ estimated from turtles it would require evaporation of at least 14%. These minimum values do seem reasonable for evaporative ponds, but would require higher proportion of evaporation for higher humidity conditions. It must be noted that if the Actinopterygians migrated toward estuaries of the WIS or tidally influenced mouth of the rivers, they would be exposed to mixed freshwater-seawater. If we use the estimated average isotopic composition of the WIS of ~ -1.2 ‰ (He et al., 2005) and turtle estimated water $\delta^{18}O$ of -6.2 ‰, the Actinopterygian $\delta^{18}O$ values suggest that at a minimum they were exposed to mixed waters with at least 28% seawater. At present, we cannot rule out that migratory behavior of the Actinopterygians led to their enriched compositions. Either diadromous (migration to the estuaries of the WIS) or potamodromous (migration to ephemeral

summer streams) could produce the observed values. Resolution of this issue would require use of other tracers such as strontium isotopes (e.g. Carpenter et al., 2003).

Evaporative sensitivity

Based on habitats of the reptiles we define the aquatic and semi-aquatic taxa (turtles and crocodiles) as EI taxa and the terrestrial taxa (dinosaurs) as ES. The low range in $\varepsilon_{\text{crocodile-turtle}}$ indicates that crocodiles and turtles exhibit the same sensitivity (or lack thereof) to evaporative conditions (Fig. 6A). Likewise, the low range in $\varepsilon_{\text{average herbivorous dinosaur-theropod}}$ indicates similar sensitivity to evaporative conditions for the dinosaurs (Fig. 6B).

We utilize the stratigraphic changes in ε values between ES and EI to infer changes in moisture and the causes of these changes (Fig. 7). Overall trends include a significant decrease in ε from site V695 to V240, followed by a significant increase in ε from site V240 to V235 and an increase in ε between sites V794 to V239 with the exception of $\varepsilon_{\text{theropod-crocodile}}$. These increases in ε are caused by a combination of humidity changes and composition of reservoirs and are discussed below.

Climatic Interpretation and Implications

Based on the isotopic composition of the various taxa and the calculated epsilons, we can interpret climatic changes through the MM. As it is unlikely that the paleo-westerlies delivered significant amounts of moisture to the leeward side of the Sevier Mountains, it follows that moisture was mostly derived from air masses from the WIS. The proximity of the WIS also resulted in the relatively high humidity (~ 68 %) estimated over the course of the MM as calculated from the micro-mammals. Contributions of the Sevier Mountains melt waters are only detected in the isotopically light values of river water recorded by dinosaurs.

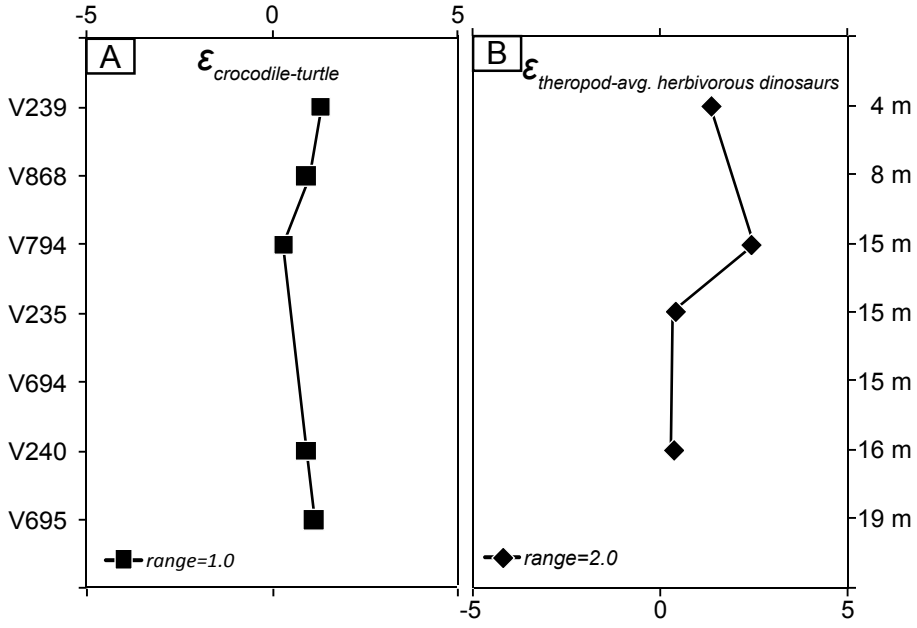

Fig. 6. Calculated epsilon (ε) values between taxa. (A) evaporative insensitive taxa. (B) evaporative sensitive taxa. Ranges are low when compared to $\varepsilon_{ES\text{-}EI}$ in Fig. 7. Low range in epsilon between sites confirms evaporative insensitive and evaporative sensitive taxa since changes in aridity will effect all evaporative sensitive and evaporative insensitive taxa similarly.

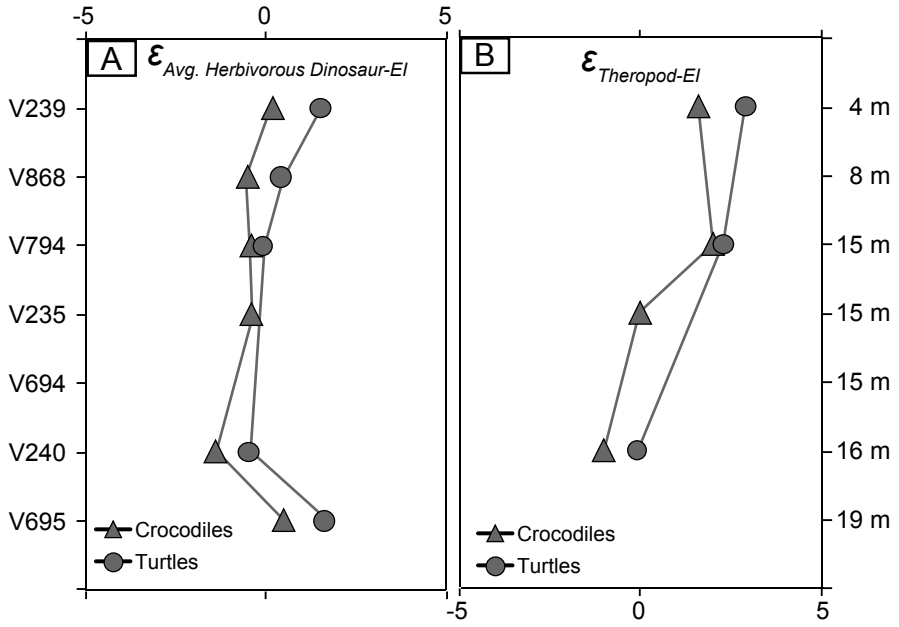

Fig. 7. Epsilon (ε) between evaporative sensitive and evaporative insensitive taxa. (A) Epsilon between theropods and the evaporative insensitive taxa. (B) Epsilon between the average herbivorous dinosaurs and evaporative insensitive taxa

Isotopic compositions of aquatic and semi-aquatic taxa (and their calculated body water) increase dramatically from site V695 (-19 m) to site V240 (-16m) and terrestrial taxa show a dramatic decrease in their $\delta^{18}O_p$. This results in the significant decrease in epsilon between average herbivores and EI taxa (Fig. 7) from V695 to V240 and is interpreted as an increase in humidity. Since only 3 mammal teeth were analyzed for V240, we are not confident in the $\delta^{18}O_p$ of mammals for this site. However, if we do use the average value (15.2 ‰), we obtain an extremely high humidity (> 90%). While this value is most likely too high and an artifact of the small sample size, it does indicate that conditions during deposition at V240 were very humid.

We attribute this increase in humidity to the incursion of the WIS, possibly the sequence 3.1 transgression of Oboh-Ikuenobe et al. (2008) (Fig. 8A,B). The proximity of the sea would have delivered sufficient humidity to allow for relatively isotopically light values in $\delta^{18}O_p$ of terrestrial taxa and abundant precipitation that was isotopically heavy (as recorded by aquatic taxa).

There is a dramatic decrease in relative humidity at site V694 (~53%). Unfortunately, no dinosaur taxa were available for V694, to confirm arid conditions. There is, however, a decrease in the $\delta^{18}O_w$ calculated from the aquatic/semi-aquatic taxa. This change suggests a retreat of the WIS (sequence boundary SB 3.2 of Oboh-Ikuenobe et al. (2008)) and consequently a decrease in isotopically heavier moisture. It is also possible that the changes are caused or magnified by increased contributions of isotopically light melt-water from the Sevier Mountains. possibly resulting from increased elevation of the orogen (Fig. 8C).

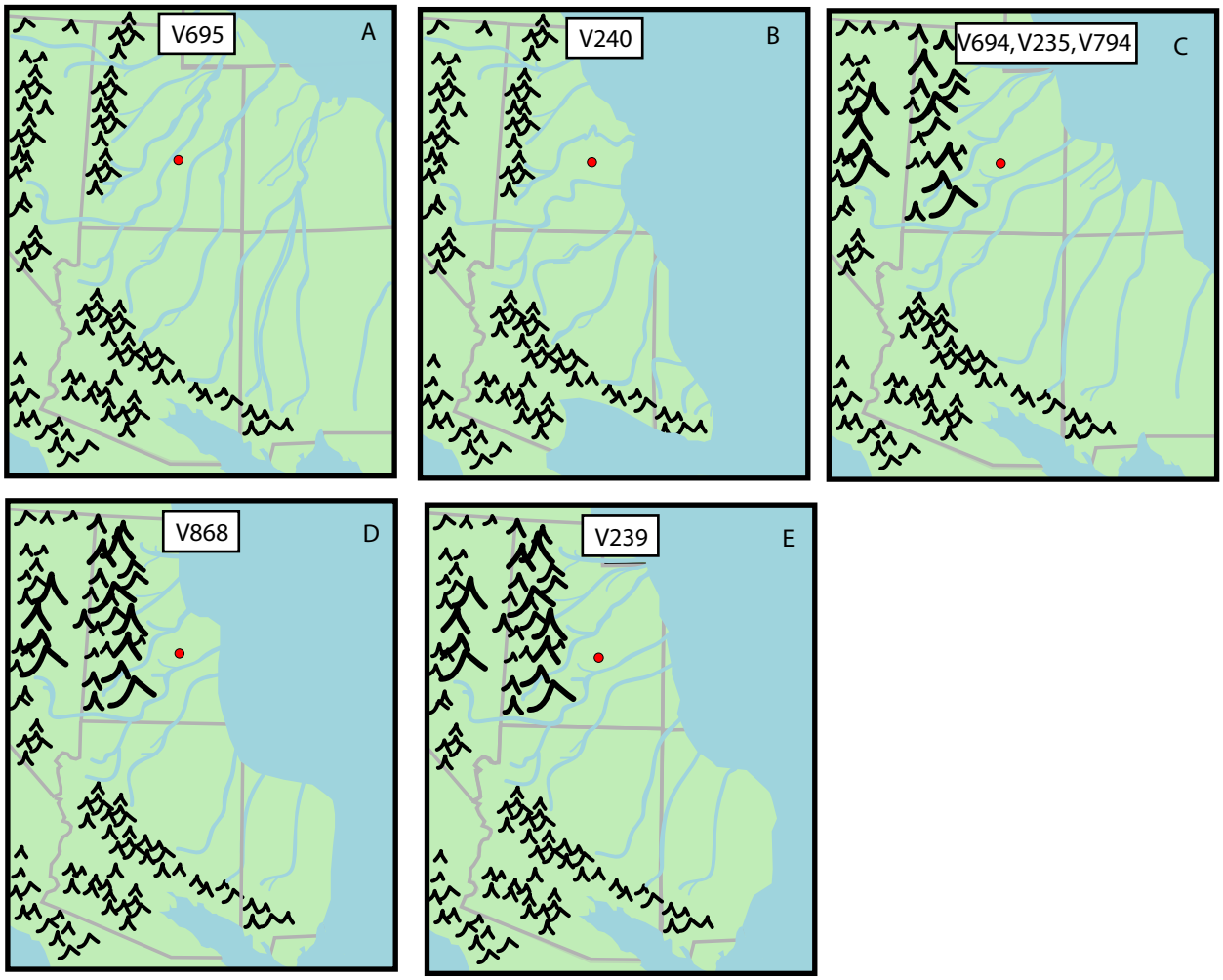

Fig. 8. Hypothetical paleogeographic maps at different times during the Mussentuchit Member deposition. (A) paleogeography at the oldest site (V695). WIS moisture was not as prominent as it was later in the deposition. (B) Incursion of the WIS at site V240 suggested by the negative ε, high δ18Ow values of aquatic taxa and low δ18Ow values of terrestrial taxa. (C) Retreat of the seaway and increased elevation of the Sevier Mountains at sites V694, V235, and V794 as suggested by decreased humidity calculated from mammal data. (D) Incursion of the WIS at the at site V868 as suggested by an increase in humidity, decrease in dinosaur water, and increase in meteoric water determined from turtle. (E) Retreat of the WIS and increased elevation of the Sevier Mountains, as suggested by a decrease in humidity a decrease in aquatic taxa ingested water. Increase in evaporative conditions experienced by dinosaurs off-sets depletion from isotopically depleted river water ingested. (modified from Ron Blakey, NAU Geology)

From the sites 15 m below the Dakota (V694, V235, and V794) to site V868 (8 m below the Dakota), we calculated an increase in average humidity from ~ 62% to ~ 76%. Epsilon between average herbivorous dinosaurs-turtle increases and slightly decreases for average herbivorous dinosaurs-crocodile. Isotopic compositions of water derived from turtles and crocodiles increase relative to sites 15 m below the Dakota to V868 (-8 m), but decrease for dinosaurs. Therefore, from 15 m to 8 m below the Dakota, we suggest that incursion of the WIS increased the input of more isotopically enriched meteoric water (turtles and crocodiles), while increasing humidity and reducing the magnitude of evaporative enrichment of terrestrial taxa (dinosaurs) (Fig. 8D). This may be correlated to the sequence 3.2 transgression documented by Oboh-Ikuenobe et al. (2008).

Finally, there is a significant, and consistent increase in epsilon from site V868 (-8 m) and to site V239 (-4 m). The dramatic increase in epsilon is due to a significant depletion between $\delta^{18}O_p$ of semi-aquatic taxa (though the decrease is greater in turtles than crocodiles) and either a slight enrichment or no change in dinosaurs $\delta^{18}O_p$. Calculated humidity decreases from ~ 77% to ~ 74% when calculated using crocodile-ingested water and decreases from ~ 64% to ~ 50% when using turtle ingested water. Therefore, it is suggested that a significant rise in the elevation of the Sevier Mountains resulted in an increase in the catchment effect on rivers (Dutton et al., 2005), producing the isotopically lighter water of the local river and streams as is recorded by the turtles and crocodiles living in those waters. If river $\delta^{18}O_w$ was influenced by catchment effects, then dinosaurs should also document this decrease in isotopic composition. However, the decrease in humidity would offset the more depleted river water consumed by

dinosaurs because lower humidity results in greater evaporative enrichment of the dinosaurs (as is recorded in the increased epsilon from site V868 to V239). We interpret this data to suggest that the Sevier Mountains were nearing their maximum height, and the WIS retreat caused a decrease in humidity (Fig. 8E), with the retreat possibly correlated to sequence boundary SB4 (Oboh-Ikuenobe et al., 2008).

Recent uses of pedogenic carbonate (calcite and siderite) isotopes suggest that mid-Cretaceous global warming caused an intensified and accelerated hydrologic cycle. Although meteoric water calculated from the isotopic composition of pedogenic carbonates are consistently more enriched relative to meteoric water recorded by turtles (as is expected), meteoric water predicted by turtles are within the range of isotopic compositions of meteoric water predicted for the zonal average at 34°N paleolatitude. Crocodiles record water this is not significantly different from meteoric water predicted by pedogenic carbonates. This suggests that turtles, crocodiles, and pedogenic carbonates are mutually consistent proxies of local meteoric water. The offsets of water recorded by turtles and crocodiles versus water predicted by pedogenic carbonate are explained by the behavior of the animal and so can be used to confirm the intensified hydrologic cycle predicted by other researchers (Ufnar et al., 2004; M. Suarez, 2009). Since dinosaurs seem to record isotopically depleted river water, significant offsets between turtles and dinosaurs and pedogenic carbonate and dinosaurs can be used to identify times when regional river water is affected by catchment effects and snow-melt (dinosaur water) and local precipitation is affected by aridity (pedogenic carbonate and turtles). In the case of the MM, carbonates and turtles yield values that are more enriched than dinosaur water (Tables 4 and 5) and so represent local meteoric water or summer base flow rather than

isotopically light river water recorded by dinosaurs that includes the pulse of isotopically light melt-water contributed over the late spring. Sampling of co-existing pedogenic carbonate, turtles, and dinosaurs are powerful proxies that help unravel regional climate dynamics during the Mesozoic.

CONCLUSIONS

Isotopic compositions of a variety of taxa with differing physiologies for the MM vertebrate fauna reveal differences in environmental water sources, and help identify regional climatic effects produced by the Sevier Orogeny and the incursion/retreat of the Western Interior Seaway. This study indicates that turtles lived in rivers and streams and record average local (lowland) meteoric water, while pedogenic carbonate represents isotopically enriched end-members of local precipitation by ~ 0.4 ‰. Crocodiles record isotopically heavier water values because they live in habitats subject to evaporations, such as the shallow parts of rivers and lakes (i.e. banks and shorelines). These values are similar to meteoric water values calculated from pedogenic carbonate. Fish represented by *Lepidotes*-like teeth grew in rivers during the warm summer months and preserve a summer-biased δ^{18}Ow. The fish represented by Actinopterygian scales either inhabited evaporatively affected streams or ponds, or migrated toward estuaries or to isotopically-enriched ephemeral (seasonal) parts of the rivers.

Documentation of local meteoric water recorded by turtles and crocodiles for the MM, as a whole, confirms the predicted zonal meteoric water predicted by pedogenic carbonates at 34°N paleolatitude (Ufnar et al., 2002, 2004; M. Suarez et al., 2009). This suggests that records of turtle and crocodiles can be used as an additional proxy to determine the global paleohydrology.

Differences from site to site *within* the member can be used to determine small-scale perturbations in regional climate.

Dinosaur $\delta^{18}O_p$ record river $\delta^{18}O_w$ values that are lighter than local meteoric water suggesting they record yearly averages of rivers that includes isotopically depleted snow-melt from higher elevations (catchment effect). The use of aquatic taxa that have a narrow range of temperature for growth, such as the co-existing crocodiles and turtles used in this study, allows mammals to be used as a humidity proxy. The approach used in this study allows for quantitative estimates of humidity in the geologic record, and provide constraints for the boundary conditions used in general circulation models (GCMs), and should translate to improved modeling of ancient climates.

The major control on the small-scale changes in isotopic composition of water recorded by MM fauna from site to site was the incursion of the WIS, with the Sevier Orogeny (Pavant Thrust event) contribution only recorded in larger vertebrates. At least two incursion/retreat cycles are documented by MM fauna (Fig. 8): 1) WIS incursion from site V695 (-19 m) to site V240 (-16 m), followed by a retreat of the seaway from V240 (-16 m) to the sites 15 m below the Dakota (V694, V235, V794) and 2) incursion from 15 m below the Dakota to site V868 (-8 m) followed by a retreat of the seaway at V239 (-4 m). These incursion/retreats are correlated to the transgression/regression cycles documented by Oboh-Ikuenobe et al. (2008)

Analysis of a variety of vertebrate taxa has allowed us to differentiate the range of water compositions for the Cretaceous MM as well as the effects of regional climate change on those water sources. Similar analysis from strata used to interpret global paleoclimate and that may also document regional climate change (due to events such as mountain building) should be

conducted to distinguish between the global and regional climate effects. Specifically, analysis of co-existing aquatic and mammalian taxa can be developed as a proxy for determination of humidity, and dinosaurs can be a proxy for yearly-averages of river water, which are both vital to constructing bounding conditions for global GCM.

REFERENCES

Amiot, R., Lecuyer, C., Buffetaut, E., Escarguel, G., Fluteau, and F. Martineau, F. (2006) Oxygen isotopes from biogenic apatites suggest widespread endothermy in Cretaceous dinosaurs. *Earth Planet. Sci. Lett*. **246**, 41-54.

Amiot, R., Lecuyer, C., Escarguel, G., Billon-Bruyat, J.P., Buffetaut, E., Langlois, C., Martin, S., Martineau, and F. Mazin, J.M. (2007) Oxygen isotope fractionation between crocodilian phosphate and water. *Palaeogeogr. Palaeoclimatol. Palaeoecol*. **243**, 412-420.

Amiot, R., Buffetaut, E., Lecuyer, C., Fernandez, V., Fourel, F., Martineau, F. and Suteethorn, V. 2009. Oxygen isotope composition of continental vertebrate apatites from Mesozoic formations of Thailand; environmental and ecological significance. *Geol. Soc., London. Special Publications* **315**, 271-283.

Barrick, R.E. and Showers, W.J. (1994) Thermophysiology of Tyrannosaurus rex: evidence from oxygen isotopes. *Nature* **265**, 222-224.

Barrick, R.E. and Showers, W.J. (1995) Oxygen isotope variability in juvenile dinosaurs (*Hypacrosaurus*): evidence for thermoregulation. *Paleobiology*. **21**, 552-560.

Barrick, R.E., Showers, W.J. and Fischer, A.G. (1996) Comparison of thermoregulation of four ornithischian dinosaurs and a varanid lizard from the Cretaceous Two Medicine Formation: evidence from oxygen isotopes. *PALAIOS* **11**, 295-305.

Barrick, R.E., Fisher, A.L. and Showers, W.J. (1999) Oxygen isotopes from turtle bone: applications for terrestrial paleoclimates. *PALAIOS* **14**, 186-191.

Bassett, D., MacLeod, K.G., Miller, J.F. and Ethington, R.L. (2006) Oxygen isotopic composition of biogenic phosphate and the temperature of Early Ordovician Seawater. *PALAIOS* **22**, 98-103.

Breecker, D.O., Sharp, Z.D. and McFadden, L.D. (2009) Seasonal bias in the formation and stable isotopic composition of pedogenic carbonate in modern soils from central New Mexico, USA. *GSA Bulletin*. **121**, 630-640.

Billon-Bruyat, J.P., Lecuyer, C., Martineau, F. and Mazin, J.M. (2005) Oxygen isotope compositions of Late Jurassic vertebrate remains from lithographic limestones of western Europe: implications for the ecology of fish, turtles, and crocodilians. *Palaeogeogr. Palaeoclimatol. Palaeoecol.* **216**, 359-375.

Bryant, J.D., Koch, P.L., Froelich, P.N., Showers, W.J. and Bernard, J.G. (1996) Oxygen isotope partitioning between phosphate and carbonate in mammalian apatite. *Geochim. Cosmochim. Acta.* **60**, 5145-5148.

Buffetaut, E. and Ford, R.L.E. (1979) The Crocodilian *Bernissartia* in the Wealden of the Island of Wright. *Palaeontology* **22**, 905-912.

Carpenter, S.J., Erickson, J.M. and Holland Jr., F.D. (2003) Migration of a Late Cretaceous fish. *Nature* **423**, 70-74.

Carroll, R.L. (1988) Vertebrate Paleontology and Evolution. Freeman, pp. 698.

Chew, R.M. (1951) The Water Exchanges of Some Small Mammals. *Ecological Monographs* **21**, 215-225.

Cifelli, R.L. (1993) Early Cretaceous mammal from North America and the evolution of marsupial dental characters. *Proc. Nat. Acad. Sci*. **90**, 9413-9416.

Cifelli, R.L., Nydam, R.L., Gardner, J.D., Weil, A., Eaton, J.G., Kirkland, J.I. and Madsen, S.K., (1999) Medial Cretaceous vertebrates from the Cedar Mountain Formation, Emery County, Utah: The Mussentuchit local fauna. In: Gillette, D., Vertebrate Paleontology in Utah. *Utah Geological Survey, Miscellaneous Publications* **99-1**, 219-242.

Currie, B.S. (1998) Upper Jurassic-Lower cretaceous Morrison and Cedar Mountain Formations, NE Utah-NW Colorado: Relationships between non-marine deposition and early cordilleran forland-basin development. *J. of Sed. Res*. **68**, 632-652.

Dansgaard, W. (1964) Stable isotopes in precipitation. *Tellus* **16**, 436-468.

DeCelles, P.G. and Coogan, J.C. (2006) Regional structure and kinematic history of the Sevier fold-and-thrust belt, central Utah. *GSA Bulletin* **118**, 841-864.

Demar Jr., D.G. and Breithaupt, B.H. (2006) The nonmammalian vertebrate microfossil assemblages of the Mesaverde Formation (Upper Cretaceous, Campanian) of the Wind River and Bighorn Basins, Wyoming. *In*: Lucas, S.G., Sullivan, R.M., Late Cretaceous Vertebrates from the Western Interior. *New Mexico Museum of Natural History and Science, Bulletin* **35**, 33-54.

Dettman, D.L., Kohn, M.J., Quade, J., Ryerson, F.J., Ojha, T.P. and Hamidulla, S. (2001) Seasonal stable isotope evidence for a strong Asian monsoon throughout the past 10.7 m.y. *Geology*. **28**, 31-34.

Dutton, A., Wilkinson, B.H., Welker, J.M., Bowen, G.J. and Lohmann, K.C. (2005) Spatial distribution and seasonal variation in $^{18}O/^{16}O$ of modern precipitation and river water across the conterminous USA. *Hydrol. Process*. **19**, 4121-4146.

Ehleringer, J.R. and Dawson, T.E. (1992) Water uptake by plants: perspectives from stable isotope composition. *Plant, Cell and Environment*. **15**, 1073-1082.

Fricke, H.C. and O'Neil, J.R. (1996) Inter- and Intra-tooth variations in the oxygen isotope composition of mammalian tooth enamel: some implications for paleoclimatological and paleobiological research. *Palaeogeogr. Palaeoclimatol. Palaeoecol*. **126**, 91-99.

Fricke, H.C. and Rogers, R.R. (2000) Multiple taxon-multiple locality approach to providing oxygen isotope evidence for warm-blooded theropod dinosaurs. *Geology* **28**, 799-802.

Fricke, H.C. (2007) Stable isotope geochemistry of bonebed fossils: reconstructing paleoenvironments, paleoecology, and paleobiology. *In*: Rogers, R.R., Eberth, D.A.Fiorillo, A.R., Bonebeds: Genesis, Analysis, and Paleobiological Significance University of Chicago Press, 437-490.

Fricke, H.C., Rogers, R.R., Backlund, R., Dwyer, C.N. and Echt, S. (2008) Preservation of primary stable isotope signals in dinosaur remains, and environmental gradients of the Late Cretaceous of Montana and Alberta. *Palaeogeog. Palaeoclimatol. Palaeoecol*. **266**, 13-27.

Fricke, H.C., Rogers, R.R. and Gates, T.A. (2009) Hadrosaurid migration: inferences based on stable isotope comparisons among Late Cretaceous dinosaur localities. *Paleobiology* **35**, 270-288.

Garrison, J.R., Brinkman, D., Nichols, D.J., Layer, P., Burge, D. and Thayn, D. (2007) A multidisciplinary study of the Lower Cretaceous Cedar Mountain Formation, Mussentuchit Wash, Utah: a determination of the paleoenvironment and paleoecology of the *Eolambia caroljonesa* dinosaur quarry. *Cretaceous Res*. **28**, 461-494.

Glancy, T.J., Arthur, M.A., Barron, E.J. and Kauffman, E.G. (1993) A paleoclimate model for the North American Cretaceous (Cenomanian-Turonian) epicontinental sea. In: Caldwell, W.G.E.Kauffman, E.G., Evolution of the Western Interior Basin. *Geol. Assoc. of Canada, Special paper* **39**, 219-241.

Hamilton, B. T. (2009) Small Mammals in protions of Great Basin National Park Susceptible to Groundwater Withdrawl: Diversity and Stable Isotope Perspectives. Department of Biology. Provo, UT, Brigham Young University. **MS** thesis**:** 69.

He, S., Kyser, T.K., and Caldwell, W.G.E. (2005) Paleoenvironmenta of the Western Interior Seaway inferred from $\delta^{18}O$ and $\delta^{13}C$ of mollusks from the Cretaceous Bearpaw marine cyclothem. *Palaeogeogr. Palaeoclimatol. Palaeoecol*. **217**, 67-85.

Huertas, A.D., Iacumin, P., Stenni, B., Sánchez Chillón, B. and Longinelli, A. (1995) Oxygen isotope variations of phosphate in mammalian bone and tooth enamel. *Geochimica et Cosmochimica Acta*. **59**, 4299-4305.

Kirkland, J.I., Britt, B., Burge, D.L., Carpenter, K., Cifelli, R., DeCourten, F., Eaton, J., Hasiotis, S., and Lawton, T. (1997) Lower to Middle Cretaceous dinosaur faunas of the Central

Colorado Plateau: a key to understanding 35 million years of tectonics, sedimentology, evolution and biogeography. *Brigham Young University Geology Studies*. **42**, 69-104.

Kirkland, J.I., (1998) A new hadrosaurid from the Upper Cretaceous Cedar Mountain Formation (Albian-Cenomanian Cretaceous) if eastern Utah - the oldest known hadrosaurid (Lambeosaurine?). In: Lucas, S.G., Kirkland, J.I.Estep, J.W., Lower and Middle Cretaceous Ecosystems. *New Mexico Museum of Natural History and Sciences Bulletin* **14**, 283-295.

Kohn, M.J. (1996) Predicting animal delta^{18}O: accounting for diet and physiological adaptation. *Geochim. Cosmochim. Acta*. **60**, 4811-4829.

Kolodny, Y., Luz, B. and Navon, O. (1983) Oxygen isotope variation in phosphate of biogenic apatites, I. Fish bone apatite - rechecking the rules of the game. *Earth and Planet. Sci. Lett.* **64**, 398-404.

Kolodny, Y., Luz, B., Sander, M. and Clemens, W.A. (1996) Dinosaur bones: fossils or pseudomorphs? The pitfalls of physiology reconstruction from apatitic fossils. *Palaeogeog. Palaeoclimatol. Palaeoecol*. **126**, 161-171.

Kriwet, J. (2000) The fish fauna from the Guimarota Mine. *In* Martin, T., Krebs, B. (Eds), Guimarota – A Jurassic Ecosystem. Pfeil, München, 41-50.

Lee-Thorp, J.A. and Sponheimer, M. (2005) Opportunities and constraints for reconstructing palaeoenvironments from stable light isotope ratios in fossils. *In*: Sponheimer, M., Polish Geological Institute : Warsaw, Poland, **49**, 195-204.

Levin, N.E., Cerling, T.E., Passey, B.H., Harris, J.M. and Ehleringer, J.R. (2006) A stable isotope aridity index for terrestrial environments. *Proc. Nat. Acad. Sci*. **103**, 11201-11205.

Lyson, T.R. and Joyce, W.G. (2009) A revision of Plesiobaena (Testudines: Baenidae) and an assesment of baenid ecology across the K/T boundary. *J. of Paleontol*. **83**, 833-853.

McManus, J.J. (1974) Bioenergetics and Water Requirements of the Redback Vole, Clethrionomys gapperi. *J. of Mammal.* **55**, 30-44.

Milner, A.R.C., Vice, G.S., Harris, J.D. and Lockley, M.G. (2006) Dinosaur tracks from the Upper Cretaceous Iron Springs Formation, Iron County, Utah. In: Lucas, S.G., Sullivan, R.M., Late Cretaceous Vertebrates from the Western Interior. New Mexico *Museum of Natural History and Science Bulletin* **35**, 105-114.

Oboh-Ikuenobe, F.E., Holbrook, J.M., Scott, R.W., Akins, S.L., Evetts, M.J., Benson, D.G. and Pratt, L.M. (2008) Anatomy of epicontinental flooding: late Albian-early Cenomanian of the southern U.S. Western Interior Basin. *Geol. Assoc. of Canada. Special Paper* **48**, 1-27.

O'Neil, J.R., Roe, R.R., Reinhard, E. and Blake, R.E. (1994) A rapid and precise method of oxygen isotope analysis of biogenic phosphate. *Isreal J. of Earth-Sci*. **43**, 203-212.

Pough, F.H., Janis, C.M. and Heiser, J.B. (2002) Vertebrate life, sixth ed. Prentice Hall, Upper Saddle River.

Poulsen, C., David, P. and White, T.S. (2007) General circulation model simulation of the $\delta^{18}O$ content of continental precipitation in the middle Cretaceous: a model-proxy comparison. *Geology* **35**, 199-202.

Rozanski, K., Araguas-Araguas, L. and Gonfiantini, R. (1993) Isotopic patterns in modern global precipitation. In: Swart, P.K., Lohmann, K.C., McKenzie, J.Savin, S., Climate Change in Continental Isotopic Records. *American Geophysical Union Geophysical Monograph* **78**, 1-36.

Sharp, Z.D., Atudorei, V. and Furrer, H. (2000) The effect of diagenesis on oxygen isotope ratios of biogenic phosphates. *Amer. J. of Sci*. **300**, 222-237.

Smith, K.F., Sharp, Z.D. and Brown, J.H. (2002) Isotopic composition of carbon and oxygen in desert fauna: investigations into the effects of diet, physiology, and seasonality. *J. of Arid Environ.* **52**, 419-430.

Spicer, R.A. and Corfield, R.M. (1992) A review of terrestrial and marine climates in the Cretaceous with implications for modeling the "Greenhouse Earth". *Geol. Mag.* **2**, 169-180.

Suarez, M.B., Gonzalez, L.A., Ludvigson, G.A., Vega, F.J., and Alvarado-Ortega, J. (2009) Isotopic composition of low-latitude paleoprecipitation during the Early Cretaceous: *GSA Bulletin*, **121**, 1584-1595.

Suarez, M.B. (2009), Global Hydrologic Perspectives on the mid-Cretaceous Greenhouse Climate (Aptian-Albian). Department of Geology, Lawrence, KS, University of Kansas. **PhD** dissertation: 179.

Trueman, C., Chenery, C., Eberth, D.A. and Spiro, B. (2003) Diagenetic effects on the oxygen isotope composition of bones of dinosaurs and other vertebrates recovered from terrestrial and marine sediments. J. *of the Geol. Soc. London* **160**, 895-901.

Tütken, T., Vennemann, T.W., Janz, H. and Heizmann, E.P.J. (2006) Palaeoenvironment and palaeoclimate of the Middle Miocene lake in the Steinheim basin, SW Germany: A reconstruction from C, O, and Sr isotopes of fossil remains. *Palaeogeog., Palaeoclimatol., Palaeoecol*. **241**, 457-491.

Ufnar, D.F., Gonzalez, L., Ludvigson, G., Brenner, R.L. and Witzke, B.J. (2002) The mid-Cretaceous water bearer: isotope mass balance quantification of the Albian hydrologic cycle. *Palaeogeog. Palaeoclimatol. Palaeoecol*. **188**, 51-71.

Ufnar, D.F., Gonzalez, L.A., Ludvigson, G.A., Brenner, R.L. and Witzke, B.J. (2004) Evidence for increased latent heat transport during the Cretaceous (Albian) greenhouse warming. *Geology* **32**, 1049-1052.

Wenz, S., Bernier, P., Barale, G., Bourseau, J.-P., Buffetaut, E., Gaillard, C., and Gall, J.-C. (1994) L'ichthyofaune des calcaires lithographiques du Kimméridgien supérieur de Cerin (Ain, France). *Géobios, Mém. Spéc*. **16**, 16-70.

White, T., Gonzalez, L., Ludvigson, G. and Poulsen, C. (2001) Middle Cretaceous greenhouse hydrologic cycle of North America. *Geology* **29**, 363-366.

Winkler, D.A., Murry, P.A. and Jacobs, L.L. (1990) Early Cretaceous (Comanchean) vertebrates of central Texas. *J. of Vertebr. Paleontol*. **10**, 95-116.

Wolfe, J.A. and Upchurch, G. (1987) North American nonmarine climates and vegetation during the Late Cretaceous. *Palaeogeog. Palaeoclimatol. Palaeoecol*. **61**, 33-77.

CHAPTER 4. MULTI PROXY INVESTIGATION OF THE PALEOHYDROLOGY IN ANCIENT TERRESTRIAL ECOSYSTEMS; THE EARLY CRETACEOUS CEDAR MOUNTAIN FORMATION OF EASTERN UTAH

ABSTRACT

Stable isotopic analyses of phosphate from continental fauna of the early Cretaceous (Barremian – early Cenomanian) Cedar Mountain Formation (CMF), UT, USA were conducted to constrain differences in water utilization among taxa and determine the regional climate during the deposition of the CMF. We analyzed a robust data set of aquatic (Actinopterygian scales), semi-aquatic (turtles and crocodiles), and terrestrial (iguanodontid, ornithopod, theropods, and sauropod dinosaurs) taxa and compared them to pedogenic carbonates analyzed by previous researchers. Vertebrate fossils were grouped together into four main faunas from distinct stratigraphic units (lower Yellow Cat Member, upper Yellow Cat Member, Ruby Ranch Member, and Mussentuchit Member). Based on differences in isotopic composition along physiologic lines, the data does preserve records of biogenic isotopic compositions. When taken as a whole for the formation, turtles and crocodiles document water compositions that are within the range of the zonal average for meteoric water at 34°N paleolatitude documented by pedogenic carbonates. Consistency between these multiple meteoric water proxies gives credence to the use of pedogenic carbonates for global paleohydrologic studies. When teasing out small-scale differences between taxa and between sites, turtles record surface average meteoric waters that are on average lighter than pedogenic calcites, which are slightly biased toward enriched local meteoric waters due to their formation under evaporative conditions. Crocodiles are isotopically more enriched than turtles, probably because they lived in

evaporative bodies of water and were more affected by evaporative enrichment of body water. Sauropods appear to have been sensitive to aridity because of their reliance on food-water as a major source of their water intake. Adult sauropod water intake seems to have been solely from food-water (leaves), whereas juvenile water intake seems to have been from both surface water and plants. Ornithopods and smaller theropods may have acquired much of their living water from rivers, and may have been more obligate drinkers than sauropods, while large carnosaurs such as Acrocanthosaurid dinosaurs may have obtained their water from a combination of river water and food water (namely sauropods). The dominant control on climate in the Cedar Mountain Formation is the uplift of the Sevier Mountains to the west. We isotopically confirm the presence of a rainshadow caused by the Sevier Orogeny. This rainshadow caused significant aridity during the deposition of the upper Yellow Cat Member, and reached high enough elevations by the end of the deposition of the Ruby Ranch Member to allow at least seasonal snow accumulation. The rainshadow attenuated influences of Pacific moisture on the foreland basin. By Mussentuchit Member time, the incursion of the Western Interior Seaway dominated climate patterns by providing moisture to the region, inhibiting significant aridity despite the continued rise of the Sevier Mountains.

INTRODUCTION

The Cedar Mountain Formation preserves some of the oldest terrestrial Cretaceous sediments in North America (Currie, 2002; DeCelles and Coogan, 2006; Kirkland and Madsen, 2007) and preserves a terrestrial fauna that is at the nexus of evolutionary radiation that would eventually result in the diverse North American fauna of the late Cretaceous (Kirkland and Madsen, 2007). Since a major influence on evolution is climate-induced habitat change, it is important to decipher past climate changes and its causes to improve effects of future climate change.

One way to do this is to examine the paleohydrology of ancient ecosystems. Since climate and hydrology are explicitly linked, and oxygen isotopes are a useful measure of hydrologic change, oxygen isotopic analyses of ancient ecosystems are a valuable way of understanding past hydrology and climate. Successful uses of oxygen isotopic analyses of fossil invertebrates, vertebrates, and authigenic minerals have been used to decipher past ocean compositions and temperatures, precipitation rates and compositions, paleoaltimetry, paleo-migrations, and global temperatures and climates (Huber et al., 1995; Ufnar et al., 2004; M. Suarez, 2009; Kohn and Dettman, 2007; Fricke et al.; 2008; 2009).

Here, we determine the effects of changing tectonics, sea-level, and climate on the regional water reservoirs and the hydrologic cycle of the Cedar Mountain Formation (CMF) ecosystem. To do this, we analyzed the isotopic composition of ingested/living water recorded in representative vertebrate fauna (fish, turtles, crocodiles, and dinosaurs) from each member of the CMF. These faunas include a lower Yellow Cat Member fauna, an upper Yellow Cat Member fauna, a Ruby Ranch Member fauna, and a Mussentuchit Member fauna. In doing so,

we have determined the effects of the rise of the Sevier Mountains and the incursion of the Western Interior Seaway on local climate during the deposition of the CMF. The successful use of multiple paleohydrology proxies (carbonates and vertebrate remains) is promising for paleontologists, paleoclimatologists, and climate modelers intending to decipher climate changes on millennial time scales.

GEOLOGIC SETTING AND MATERIALS

Stratigraphy and Paleontology

The Cedar Mountain Formation has been a recognized unit for over 50 years (Stokes, 1949). The unit was originally described by Stokes as the drab mudstone above the Jurassic Morrison Formation and below the Dakota Formation (Fig. 1). Currently, the Cedar Mountain Formation (CMF) is informally recognized by 5 members: the Buckhorn Conglomerate, Yellow Cat Member, Poison Strip Sandstone, Ruby Ranch Member, and Mussentuchit Member and likely spans the Barremian through early Cenomanian (Kirkland and Madsen, 2007).

The Buckhorn Conglomerate represents a northeast flowing river that cuts into the Morrison Formation and is made of up of fossiliferous Paleozoic marine carbonates reworked from uplifted mountains (Sevier Mountains) in Arizona and Nevada (Currie 2002; DeCelles and Coogan, 2006; Kirkland and Madsen, 2007). It is overlain by the Yellow Cat Member in some places, and in others, further to the west, is overlain by either the Ruby Ranch Member or Mussentuchit Member. Though it has been suggested to be Jurassic in age (Aubrey, 1998), it is assigned an early Cretaceous age here based on the presence of an isolated ankylosaur skeleton,

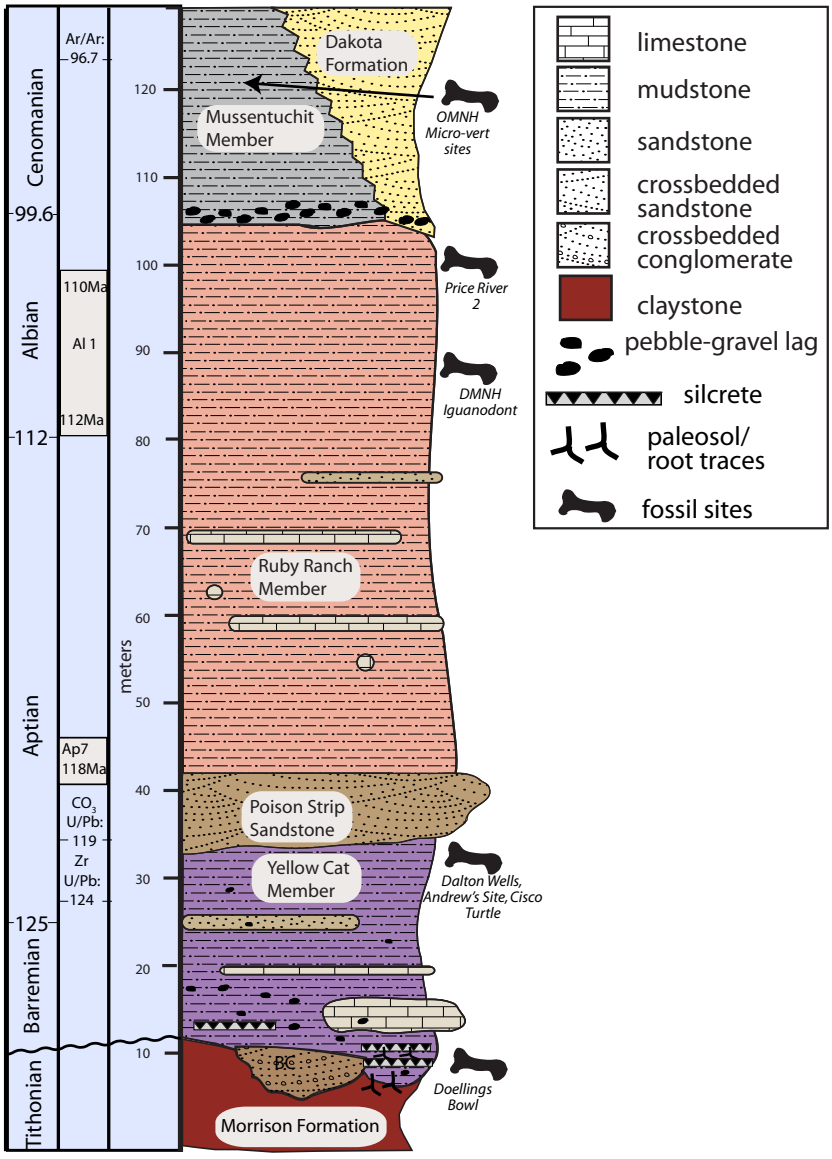

Fig. 1. Relative Stratigraphy. Combined stratigraphy and relative location of sites within the Cedar Mountain Formation. Far left-left hand column represents the Cretaceous stages and age boundaries to those stages, middle column presents published dates from either U/Pb or Ar/Ar, dating of detrital zircons, bentonites, or pedogenic carbonate. Grey bars in the column represent published carbon-isotopic excursions identified by Ludvigson et al. (in revision), and right hand column represents relative meters about the Morrison starting at the Buckhorn Conglomerate (BC)-Morrison boundary.

which is a prominent taxa of the early Cretaceous (Kirkland and Madsen, 2007). No samples were analyzed from the Buckhorn Conglomerate.

Until recently, the Yellow Cat Member was defined as the unit of poorly-sorted drab green and purple, carbonate rich pebbly-siltstone between either the Buckhorn Conglomerate and Poison Strip Sandstone, or Morrison Formation and Poison Strip Sandstone. It has been suggested that a carbonate rich paleosol (calcrete) that overlies and pedogenically alters the Buckhorn Conglomerate and/or Morrison represents a major unconformity between the Jurassic and Cretaceous and marks the lower contact of the Yellow Cat Member (Kirkland and Madsen, Greenhalgh, 2007). However, recent finds of Cretaceous-aged dinosaurs below this contact suggests that yet older Cretaceous sediments are preserved in the CMF outcrop of Utah (Kirkland and Madsen, 2007). Therefore, we informally split the Yellow Cat Member into a lower Yellow Cat Member represented by green pebble-siltstone and mudstone with abundant silicified rootlets, tree stumps, and silcretes that is well exposed in the Doelling's Bowl area (Kirkland and Madsen, 2007) (Fig. 2). This location preserves the lower Yellow Cat Member fauna analyzed in this study. We sampled several terrestrial faunal elements: Brachiosaurid teeth, Acrocanthosaurid teeth, smaller theropod teeth, several iguanodontid teeth and jaw-bones, and semi-aquatic fauna represented by several crocodile teeth. Calcitic carbonate nodules are not common in the lower Yellow Cat Member, and so no co-existing pedogenic or diagenetic carbonate was sampled. The age of the lower Yellow Cat Member is not well constrained. It likely represents sedimentation that occurred sometime between ~149 to 124 Ma, as the youngest recorded date for the Morrison Formation is a U/Pb zircon date from a Morrison bentonite of

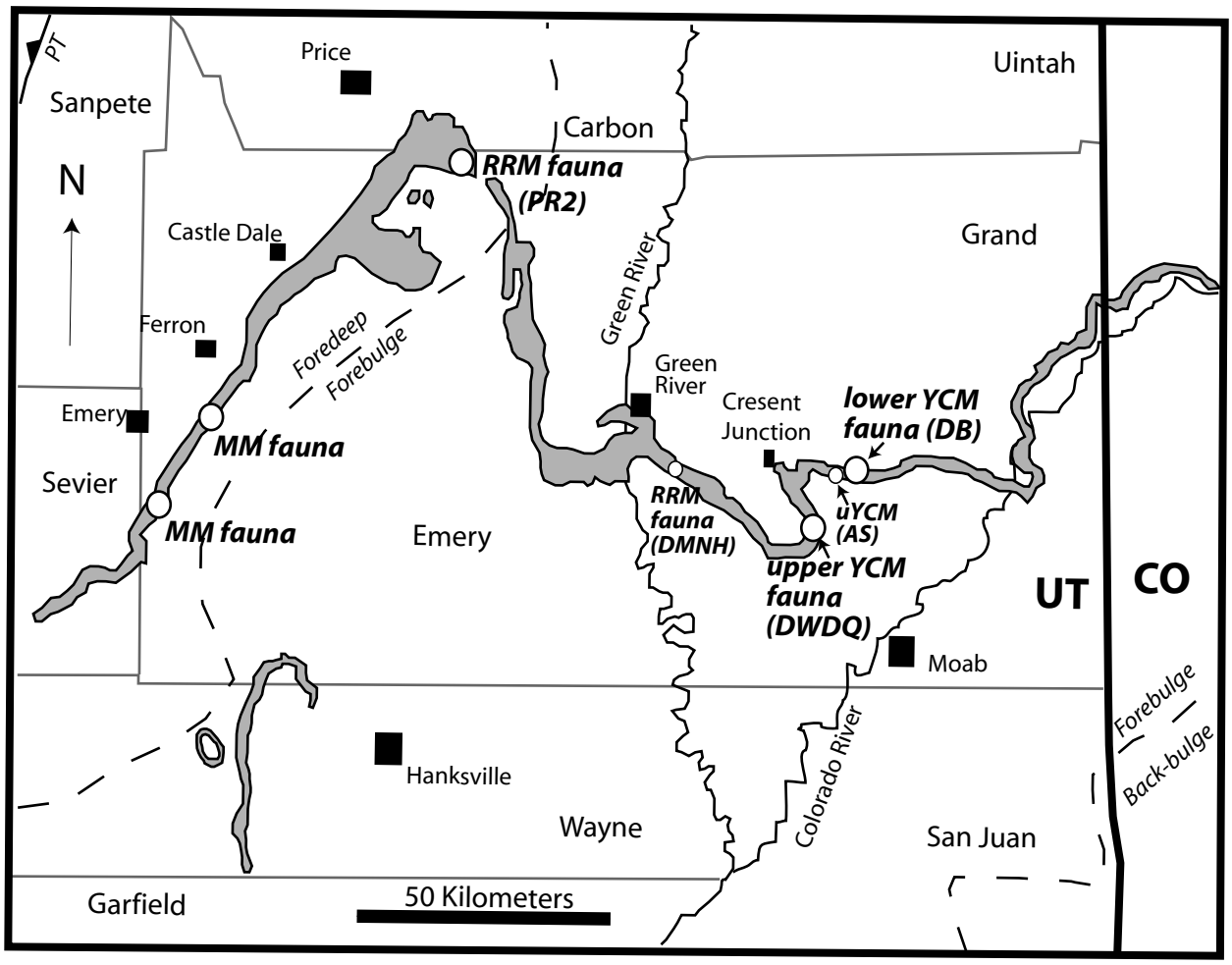

Fig. 2. Map of Cedar Mountain Formation outcrop (grey shaded area). County boundaries are in grey. Dashed lines represent boundaries between the paleo-foredeep, forebulge, and backbulge during Albian time (Currie, 2002). The location of the Pavant Thrust front (PVT) is located in the far northwest. Fossil localities are in bold-italics. Members: lYCM = lower Yellow Cat Member, uYCM = upper YCM, RRM = Ruby Ranch Member, MM = Mussentuchit Member. Sites: DB = Doelling's Bowl, DWDQ = Dalton Wells Dinosaur Quarry, PR2 = Price River 2, AS = Andrew's Site, DMNH = location of iguanodontid jaw from the Denver Museum of Nature and Science.

~149 Ma (Kowallis et al., 2007) and a detrital zircon date of ~124 Ma (Britt et al., 2007) is reported for the upper Yellow Cat Member near Moab, UT.

The upper Yellow Cat Member is defined as a poorly sorted pebble-siltstone with abundant pedogenic carbonates, spring-carbonates, and palustrine carbonates with interbedded small-channel sandstones. The upper Yellow Cat Member has produced a number of significant vertebrate fossils of both European and Asian affinity including brachiosaurid and basal titanosaurid sauropods (e.g. *Cedarsaurus weiskophae*), nodosaur ankylosaurs (*Gastonia burgei*), large iguanodontids (*Iguanodon ottingeria*), a small coelosaur *Nedcolbertia justinhoffmanii*, a large dromaeosaur, *Utahraptor sp,*. and the basal therizinosaur *Falcarius utahensis* (Tidwell et al., 1999; Britt et al., 1997; Kirkland, 1998a; Kirkland et al., 1993; 2005). The majority of the upper Yellow Cat Member fauna sampled are from the Dalton Wells Dinosaur Quarry (DWDQ) (Eberth et al., 2006; Britt et al., 2009). The site is ~6-10 m below the Poison Strip Sandstone in a poorly-sorted carbonate rich pebbly-siltstone. All taxa sampled from the DWDQ are terrestrial in nature and include *Utahraptor* teeth, sauropod (brachiosaurid or camarasaurid) teeth, and teeth and bone from a very large iguanodontid dinosaur. To supplement this terrestrial data set with semi-aquatic and aquatic taxa, several samples from turtle shell fragments near Cisco and Actinopterygian scales from a lacustrine carbonate-rich sandstone along Yellow Cat Road were also sampled. Both samples are within 10 m of the overlying Poison Strip Sandstone. A large crocodile scute from a site (Andrew's Site) just off Yellow Cat Road, south of Crescent Junction, UT was also sampled to complete a data set that includes terrestrial, aquatic, and semi-aquatic taxa for the upper Yellow Cat Member fauna.

The Poison Strip Sandstone is a thick, ledge-forming fluvial sandstone that is medium to coarse-grained. It is light tan to white in color and contains cross-bedded to planar bedded sandstone sourced from the highlands to the west. Few vertebrate remains are found in the Poison Strip Sandstone, though dinosaur, bird, and pterosaur tracks are locally abundant in the units north of Arches National Park. Vertebrate fossils included a large nodosaurid dinosaur (Bodily, 1969; Carpenter et al., 1999; Kirkland and Madsen, 2007), an iguanodontid dinosaur *Planicoxa venenica* (DiCroce and Carpenter, 2001), and a titanosaurimorph *Venenosaurus dicrocei* (Tidwell et al., 2001). Ludvigson et al. (in revision) radiometrically dated a palustrine carbonate from the base of the Poison Strip Sandstone resulting in an age of ~119 Ma. This age is consistent given the detrital zircon age of the upper Yellow Cat Member of 124 Ma reported by Britt et al. (2007). Insufficient vertebrate teeth are available from the Poison Strip Sandstone and so no Poison Strip Sandstone fauna was sampled.

The Ruby Ranch Member is a complex of reddish and grey mudstones and carbonate-nodule bearing mudstones. Irregularly-shaped carbonate nodules can be up to tens of centimeters in dimension. In places, carbonate nodules form thick carbonate horizons of intergrown spheroidal to cylindroidal carbonate layers or calcrete (Al-Suwaidi, 2007; Ludvigson et al., in revision). The calcretes show diagnostic features that indicate they are in some cases, palustrine to lacustrine in origin (Shapiro et al., 2009) while in other cases are the result of vadose processes (Al-Suwaidi, 2007). In many cases both palustrine/lacustrine and vadose characteristics are preserved indicating complex carbonate growth, dissolution, and recrystallization. Recently, a carbon isotope chemostratigraphic study by Ludvigson et al. (in revision) identified several distinct carbon-isotope excursions that constrain the age the Ruby

Ranch Member. Carbon isotope feature Ap7 (Herrle et al., 2004) is preserved at the base of the Ruby Ranch Member while the upper part of the member preserves the Al1 C-isotope feature, bracketing the age of the Ruby Ranch Member from the early-mid Aptian (~118Ma) to the end of the Albian (~105Ma). Dinosaurs from the Ruby Ranch Member are rare in the lower to middle part of the unit, presumably because the area was too arid at the time of deposition to sustain significant dinosaurian fauna. However, significant dinosaur finds from the middle to upper part of the member are preserved. These include the ankylosaurid *Cedarpelta bilbyhallorum* (Carpenter et al., 2001), a large ornithopod, *Tenontosaurus*, slender-toothed brachiosaurid dinosaurs, small dromaeosaurids, and the derived allosaurid *Acrocanthosaurus* (Kirkland and Madsen, 2007). The fauna sampled for this study is from the top of a very thick section of Ruby Ranch Member. The Price River 2 (PR2) site has been excavated by the College of Eastern Utah, and has produced a diverse faunal assemblage. Samples include several teeth from a "slender-toothed" brachiosaurid, *Acrocanthosaurus* teeth, small dromaeosaurid teeth, crocodile teeth, and turtle shell fragments from an un-identified turtle, and from *Naomichelys sp*. In order to compare the iguanodontids from the lower and upper Yellow Cat Member, a juvenile iguanodontid jaw and teeth from the middle of the Ruby Ranch Member southeast of Green River was provided by the Denver Museum of Nature and Science.

The Mussentuchit Member primarily outcrops on the western limb of the San Rafael anticline. The unit's high smectitic-clay content makes it identifiable by its drab gray popcorn-weathered mudstone that forms extensive badlands in the Willow Springs and Short Canyon quadrangles of central-Utah (Fig. 2). Several ash layers are present in the Mussentuchit Member and give ages that range from 98.3 ± 0.07 Ma (Cifelli et al., 1999) to 96.7 ± 0.5 Ma (Garrison et

al., 2007) and palynologic studies of correlative strata (Oboh-Ikuenobe et al., 2007) suggest the Mussentuchit Member deposition began approximately at the end of the Albian and ended in the mid-Cenomanian, with both inter-bedding and truncation of the Mussentuchit by the Dakota Formation. The majority of the Mussentuchit Member is composed of inter-bedded grey smectitic mudstones, siltstones, and occasional fine-grained sandstones. The upper part of the Member is interbedded with the overlying Dakota Formation and often contains lignitic coal layers. Carbonate nodules are less common compared to the extensive carbonate nodule layers found in the underlying Ruby Ranch Member. The majority of vertebrate remains are micro-vertebrates sampled using screen-washing techniques by field crews of the Oklahoma Museum of Natural History. The vertebrate taxa represent one of the richest vertebrate faunas described from the early Cretaceous (Cifelli et al., 1999). The fauna appears to be a combination of older European-affiliated taxa such as *Coniophis* (snakes, not analyzed in this study), Pachycephalosauria, and Hesperornithiformes (birds not analyzed in this study) and a younger Asian-originated fauna such as Troodontidae, Tyrannosauridae, Hadrosauridae, and some Neoceratopsians (Cifelli et al., 1999). Other taxa preserved from the Mussentuchit Member included mammalians (including the marsupial-like *Kokopellia judii*), lizards, and frogs. Samples used for this study were originally analyzed for an isotopic study of the Mussentuchit Member fauna and paleohydrology (Chapter 3) and were averaged from 7 sites spanning ~15 m. Taxa include dromaeosaurid teeth, teeth from the advanced iguanodontid *Eolambia caroljonesa* (Kirkland et al., 1998), polocanthine ankylosaur teeth, an un-described species of basal ornithopod, turtle shell fragments (including *Naomichelys sp.*, *Glyptops sp.*, and Trionychlidae),

crocodiles (including Goniopholidae, Atoposaruidae, and *Bernissartia sp.*), and Actinopterygian scales.

Tectonic and Climatic Setting

The CMF sediments were sourced from highlands to the west, which were eroded from the Sevier Fold and Thrust Belt (SFTB). The SFTB is a segment of the larger Cordilleran retroarc fold-and-thrust belt which formed during the late Mesozoic to early Cenozoic times (DeCelles and Coogan, 2006). The CMF is synchronous with two of the four thrust events that make up the SFTB. The Yellow Cat Member and Ruby Ranch Member sediments were deposited during the Canyon Range Thrust (145 – 110 Ma) event in the resulting foredeep to back-bulge. The Canyon Range thrust front was located in far northwest Utah and eastern Nevada, creating mountains in eastern Nevada and Western Utah. By the end of the Canyon Range thrust events, maximum elevation increased by 1.57 km (DeCelles and Coogan. 2006). Upper Ruby Ranch Member through Mussentuchit Member were deposited in the foredeep to forebulge of the Pavant Thrust event (110 – 86Ma) (Currie, 1998; DeCelles and Coogan, 2006). By the end of the Pavant thrust (and end of Mussentuchit Member deposition), the change paleo-elevation was ~ 2.8 km in western Utah (DeCelles and Coogan, 2006) resulting in mountains >3 km in elevation. The SFTB forebulge migrated to the east over time so that in the earliest Cretaceous (Yellow Cat Member), sediments were deposited between the distal foredeep and proximal backbulge. The Ruby Ranch Member was deposited in the distal foredeep to forebulge area, and the Mussentuchit Member was deposited in the foredeep. By the Late Cretaceous, the SFTB formed an Andean-style fold-and-thrust belt with a high-elevation, low-relief hinterland plateau (Currie, 2002; DeCelles and Coogan, 2006). Regional paleohydrology was likely

affected by these orogenic events because the rise of the mountains likely hindered moisture transported to the east by the paleo-westerlies (Poulsen et al., 2007). One of the goals of this study is to determine the extent to which the Sevier Orogeny affected paleohydrology, by analyzing the isotopic compositions of vertebrate phosphates.

Climatically, the mid-Cretaceous (here defined as Aptian to Albian) was a time of global warming prior to the thermal maximum in the Cenomanian-Turonian. Isotopic studies of pedogenic carbonates (White et al., 2001; Ufnar et al., 2002, 2004; M. Suarez et al. 2009) suggest that this increased temperature led to an acceleration of the global hydrologic cycle. An accelerated hydrologic cycle resulting in an increase in the intensity of isotopic rainout, has been used to explain significantly greater isotopic depletion of meteoric groundwaters seen along the eastern margin of the WIS (White et al., 2001), in the British Wealden (Robinson et al., 2010), and from the equator to poles (M. Suarez, 2009). Poulsen et al. (2007) however suggested that the cause of extreme depletion of pedogenic carbonates at high latitudes was due to very local orogenic effects. Though orogenic effects have not been used to explain meteoric water composition in the CMF, this study will illustrate the dynamics of the hydrologic cycle in a tectonically active setting. Results of this study can then be compared to high-latitude sites under contention.

METHODS

A detailed listing of samples and their museum identifications can be found in the supplementary data appendix A. Samples were provided by the Oklahoma Museum of Natural History (OMNH), Utah Museum of Natural History, (UMNH), College of Eastern Utah Museum

(CEUM), Denver Museum of Nature and Science (DMNH), and Brigham Young University Museum of Paleontology (BYUVP). The numbers of specimens and samples analyzed are found in Table 1. When possible, at least 10 individuals per taxa or at least 10 isotopic measurements per taxa per site were analyzed. Samples were micro-milled for enamel or ganoine producing 200 - 500 μg of powder. Significant care was taken to avoid sampling of dentine since it is more prone to diagenetic exchange of oxygen isotopes than ganoine and enamel (Kolodny et al., 1996). Phosphate samples were converted to silver phosphate following the method of O'Neil, (1994) and Basset et al. (2007). Silver phosphate samples were analyzed at the W. M. Keck Paleoenvironmental and Environmental Stable Isotope Laboratory at the University of Kansas, Department of Geology on a high temperature conversion elemental analyzer (TC/EA) connected to a ThermoFinnigan MAT 253 continuous flow mass spectrometer. Phosphate oxygen ($\delta^{18}O_p$) is reported in parts per thousands (‰) relative to V-SMOW using standard δ-notation. Precision was monitored via analysis of NIST 120c and is ± 0.3‰ V-SMOW with an average value of 22.5‰.

Ingested/living ($\delta^{18}O_w$) water isotopic compositions were calculated from equations presented by Barrick et al. (1999) for turtles and Amiot et al. (2007) for crocodiles. The temperature (t°C) at which fish precipitate their scales was determined by using the isotopic composition of water derived from turtles ($\delta^{18}O_w$) and using the relationship between water, fish phosphate ($\delta^{18}O_p$), and temperature presented by Kolodny et al., (1983).

$$t^oC=111.4 + 4.3(\delta^{18}O_p - \delta^{18}O_w) \quad (1)$$

By using the equation for birds presented in Kohn (1996) and adjusting the humidity coefficient to express the isotopic enrichment of terrestrial herbivores over carnivores and an

TABLE 1. Specimen and Sample List

Fauna	TAXA	$N_{specimen}$	$N_{samples}$
Mussentuchit	19-4m below Dakota		
	Actinopterygian scale	63	70
	Crocodilia	59	103
	Turtle.	24	67
	Ornithischia	42	86
	Theropoda	28	42
Ruby Ranch	55 m below Dakota (25m above Poison Strip SS)		
	Crocodilia	2	5
	Turtle	3	18
	Iguanodontid	6	13
	Acrocanthosaurid	4	25
	Small Theropod	4	5
	Sauropoda	2	25
Upper Yellow Cat	3-15m below Poison Strip SS		
	Actinopterygian scale	11	8
	Crocodilia scute	1	12
	Turtle	1	5
	Iguanodontid	3	6
	Theropoda: *Utahraptor*	4	19
	Sauropoda	4	22
Lower Yellow Cat	30 m below Poison Strip SS (8 m above Morrison)		
	Crocodilia	2	9
	Iguanodontid	8	33
	Acrocanthosaurid	1	29
	Small theropod	3	22
	Sauropoda	3	44

average body temperature of 37ºC (Amiot et al., 2006), the following equations were then used to estimate herbivorous dinosaur ingested water ($\delta^{18}O_w$):

$$\delta^{18}O_w = 1.41\delta^{18}O_p + 12.11h - 41.59 \quad (2)$$

and carnivorous dinosaur water:

$$\delta^{18}O_w = 1.41\delta^{18}O_p + 7.0h - 41.59 \quad (3)$$

where $\delta^{18}O_p$ = the isotopic composition of phosphate oxygen and h = relative humidity.

Epsilon (ε), or ^{18}O isotopic enrichment, was calculated between evaporative sensitive and evaporative insensitive taxa to determine the extent of relative aridity (Levin et al., 2006; Chapter 3). The greater the ^{18}O enrichment of evaporative sensitive taxa over evaporative insensitive taxa results in higher epsilon values. Therefore, we calculated ε between evaporative sensitive taxa and evaporative insensitive taxa and compared the ε between sites using the following equation:

$$\varepsilon = \left(\frac{0.001\delta^{18}O_{ES}}{0.001\delta^{18}O_{EI}} - 1 \right) * 1000 \qquad (4)$$

Where $\delta^{18}O_{ES}$ represents the average isotopic composition of evaporative sensitive (ES) taxa and $\delta^{18}O_{EI}$ represents the average composition of evaporative insensitive (EI) taxa from a given stratigraphic level and taxon-pair.

RESULTS

The isotopic compositions of enamel for taxa from the lower Yellow Cat Member fauna ranges from 16.9 ± 1.8‰ for small theropods to 21.9 ± 2.8 ‰ for sauropods (Table 2, Fig. 3). Iguanodontids average 17.7 ± 2.3 ‰, Acrocanthosaurids average 19.1± 1.7 ‰, and crocodiles average 19.2 ± 0.5 ‰. The isotopic composition of vertebrate phosphate from upper Yellow Cat Member fauna ranges from a minimum of 14.1 ± 0.4 ‰ for turtles to a maximum of 21.9 ± 3.0 ‰ for sauropods. Crocodile scutes average 13.7 ± 0.6 ‰, Actinopterygian scales average 17.2 ± 0.7 ‰, *Utahraptor* teeth average 18.1 ± 0.9 ‰, and iguanodontid teeth average 21.7 ± 0.6 ‰. The average oxygen isotopic composition of carbonate (converted to V-SMOW) is 22.0 ± 1.2‰. The Ruby Ranch Member fauna ranges from a minimum isotopic composition of 14.9 ± 0.8 ‰

TABLE 2. Oxygen Analysis of Phosphate relative to V-SMOW

Fauna	TAXA	*Min*	*Max*	*Avg±1σ*
Mussentuchit : 19-4m below Dakota				
	Actinopterygian scale	14.6	18.8	16.2 ± 0.8
	Crocodilia	14.4	19.5	16.8 ± 0.9
	Turtle.	14.3	17.2	15.7 ± 2.0
	Avg. Herbivores	14.0	18.6	16.6 ± 0.9
	Theropoda	15.3	20.0	17.5 ± 1.4
Ruby Ranch: 55 m below Dakota (25 m above Poison Strip SS)				
	Crocodilia	16.7	17.7	17.2 ± 0.4
	Turtle	13.4	16.1	14.9 ± 0.8
	Iguanodontid	14.4	15.8	15.1 ± 0.4
	Acrocanthosaurid	15.2	24.9	20.3 ± 2.5
	Small Theropod	16.7	21.4	18.2 ± 1.9
	Sauropoda	16.6	22.2	19.7 ± 1.6
Upper Yellow Cat: 3-15 m below Poison Strip SS				
	Actinopterygian scale	16.2	18.6	17.2 ± 0.7
	Crocodilia scute	12.5	14.3	13.7 ± 0.6
	Turtle	13.5	14.5	14.1 ± 0.4
	Iguanodontid	20.5	22.2	21.7 ± 0.6
	Theropoda: *Utahraptor*	15.6	19.1	18.1 ± 0.9
	Sauropoda	16.8	26.1	21.9 ± 3.0
Lower Yellow Cat: 30 m below Poison Strip SS (8 m abv Morrison)				
	Crocodilia	18.5	19.9	19.2 ± 0.5
	Iguanodontid	13.8	21.3	17.7 ± 2.3
	Acrocanthosaurid	17.7	20.3	19.1 ± 1.7
	Small theropod	14.7	20.2	16.9 ± 1.8
	Sauropoda	17.0	24.4	21.9 ± 2.8

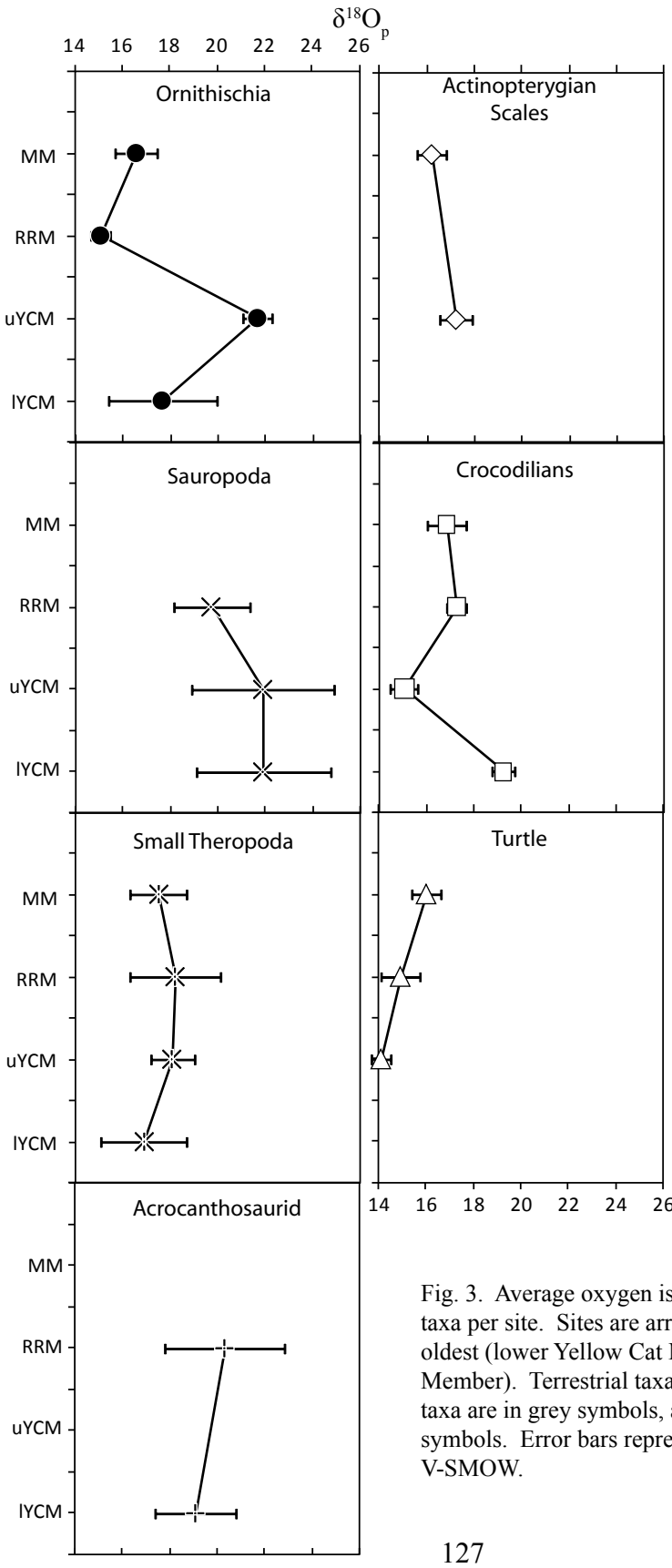

Fig. 3. Average oxygen isotopic composition of phosphate per taxa per site. Sites are arranged in stratigraphic position from oldest (lower Yellow Cat Member) to youngest (Mussentuchit Member). Terrestrial taxa are in black symbols, semi-aquatic taxa are in grey symbols, and aquatic taxa are in white symbols. Error bars represent 1σ. All data relative to V-SMOW.

for turtle shells and a maximum composition of 20.3 ± 2.5 ‰ for Acrocanthosaurids. Isotopic compositions of iguanodontid teeth average 15.1 ± 0.4 ‰, 17.2 ± 0.4 ‰ for crocodiles, 18.2 ± 1.9 ‰ for small theropods, and 19.7 ± 1.6 ‰ for sauropods. The average oxygen isotopic composition of carbonates (from above and below PR2) is 23.5 ± 0.6‰ (Al-Suwaidi, 2007; Ludvigson et al., in revision). The isotopic compositions of Mussentuchit Member fauna ranges from a minimum of 15.7 ± 2.0 ‰ for turtle shell to a maximum of 17.5 ± 1.4 ‰ for theropods. Actinopterygian scales have an isotopic composition of 16.2 ± 0.8 ‰, herbivorous dinosaurs (includes iguanodontids, ornithopods, and nodosaurs) have an average tooth enamel isotopic composition of 16.6 ± 0.9 ‰, and crocodile enamel averages 16.8 ± 0.9 ‰. Carbonates from the Mussentuchit Member have an average oxygen isotopic composition of 23.3 ± 1.9 ‰ (Chapter 3).

Calculated ingested/living water ($\delta^{18}O_w$) from the lower Yellow Cat Member ranges from a minimum of -14.7 ± 2.5 ‰ ingested by small theropods to a maximum isotopic composition of -3.4 ± 1.9 ‰ ingested by crocodiles (Table 3, Fig. 4). Acrocanthosaurid-ingested water is calculated as -11.5 ± 1.0 ‰, iguanodontid-ingested water (labeled "Ornithischia" in Table 3) is calculated as -11.1 ± 3.3 ‰, and sauropod-ingested water is -5.2 ± 3.9 ‰ (Table 3, Fig. 4).

Meteoric water estimated by pedogenic carbonate from the upper Yellow Cat Member averages -7.1 ± 1.2 ‰. Ingested water composition ranges from a minimum of -12.9 ± 1.3 ‰ estimated from small theropods to a maximum of -5.1 ± 4.3 ‰ estimated from sauropods. Isotopic compositions of environmental water derived from turtles are -8.1 ± 0.4 ‰. For the upper Yellow Cat Member crocodile, only one crocodile scute was available, rather than tooth enamel. Since the drinking/living water-phosphate relationship established by Amiot et al.

TABLE 3. Calculate Ingested/ Living Water Composition

Site	carbonate	Turtle	Crocodile	Ornithischia	Sauropoda	Acrocanthosaurid	Small Theropod
	$\delta^{18}O_w = ((\delta^{18}O_c + 10^3)/\alpha) - 10^3$	$\delta^{18}O_w = 1.01*\delta^{18}O_p - 22.3$ (Barrick, 1999)	$\delta^{18}O_w = 0.82*\delta^{18}O_p - 19.13$(Amiot et al., 2007)	$\delta^{18}O_w = 1.41\delta^{18}O_p + 12.11h - 53.6 +0.32T_b$ºC(modified, Kohn, 1996)		$\delta^{18}O_w = 1.41\delta^{18}O_p + 7.0h - 53.6+0.32T_b$ºC (modified, Kohn, 1996)	
MM	-5.8 ± 1.8	-6.2 ± 0.7	-5.2 ± 0.8	-10.1 ± 1.4			-12.1 ± 2.0
RRM	-5.6 ± 0.6	-7.3 ± 0.8	-5.0 ± 0.3	-14.9 ± 0.6	-8.3 ± 2.3	-9.6 ± 3.3	-12.9 ± 2.6
uYCM	-7.1 ± 1.2	-8.1 ± 0.4	-6.9 ± 0.5	-5.5 ± 0.9	-5.1 ± 4.3		-12.9 ± 1.3
lYCM			-3.4 ± 0.4	-11.1 ± 3.3	-5.2 ± 3.9	-11.5 ± 1.0	-14.7 ± 2.5

α = 1.0293; h = 0.47 for YCM and RRM; h = 0.68 for MM; Dinosaur t_b = 37ºC; uYCM = upper Yellow Cat Member, lYCM = lower Yellow Cat Member, RRM = Ruby Ranch Member, MM = Mussentuchit Member

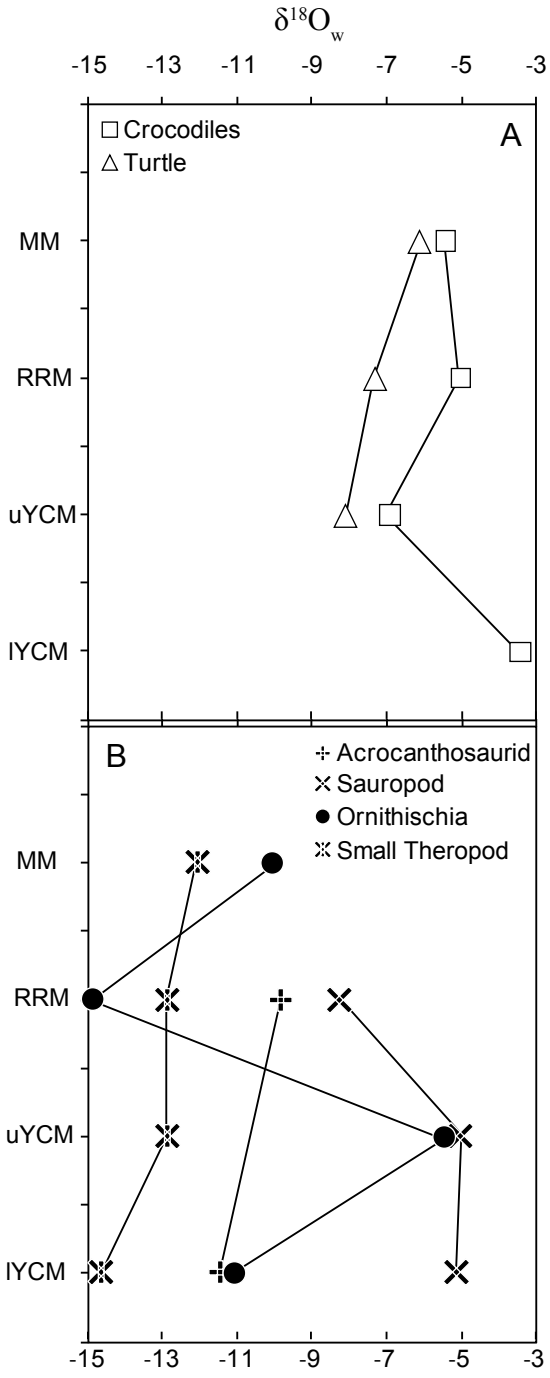

Fig. 4. Calculated average ingested/living water for each taxon. Calculations are determined from equations presented in table 3. A) Aquatic and semi-aquatic taxa. B) Terrestrial taxa. All data is relative to V-SMOW.

(2007) is for tooth phosphate, enamel values were estimated by adding 1.3‰ to each sample analyzed. Several studies have previously shown that crocodilian scutes are depleted between 1.1 – 1.5 ‰ relative to tooth enamel from the same individual (Lecúyer et al., 2003; Billion-Bruyat et al., 2005; Chapter 3). Based on the calculated tooth values, crocodile living/ingested water was calculated as -6.9 ±0.5 ‰. Iguanodontid (labeled "Ornithischia" in Table 3) ingested water is estimated at -5.5 ± 0.9 ‰. Ruby Ranch Member meteoric water composition (from carbonates) is -5.6 ± 0.6 ‰, while the isotopic composition of ingested-water determined by phosphate ranges from a minimum of -14.9 ± 0.6 ‰ estimated from iguanodontids to a maximum of -5.0 ± 0.3 ‰ for crocodiles. Small theropod-ingested water averaged -12.9 ± 2.6 ‰, turtle shell formed from living-water with an oxygen isotopic composition of -7.3 ± 0.8 ‰, and sauropod-ingested water averages -8.3 ± 2.3 ‰. Mussentuchit Member carbonates formed from water with an isotopic composition of -5.8 ± 1.8 ‰. Mussentuchit Member fauna record ingested-water compositions that range between -12.1 ± 2.0 ‰ for small theropods to -5.4 ± 0.8 ‰ for crocodiles. Ornithischians precipitated their teeth from ingested-water with a composition of -10.1 ± 1.4 ‰ and turtles precipitated their shell from environmental-water with an average isotopic composition of -6.2 ± 0.7 ‰

The temperature of formation (water temperature) derived from fish scales that lived in water with an isotopic composition derived from the Cisco turtles for the upper Yellow Cat Member average 2.4 ± 3.1ºC. Fish scales that formed in water with an isotopic composition derived from Mussentuchit Member turtles average 15.5 ± 3.0ºC.

DISCUSSION

Primary vs. Diagenetic Biogenic Isotope Signals

The successful use of isotopic proxies in paleoecology and paleoclimatology studies require that biogenic signals are preserved in fossils on the order of millions to hundreds of millions years old (Sharp et al., 2000; Fricke et al., 2008; Amiot et al., 2009). Kolodny et al. (1996) suggested some criteria for selection of material for isotopic analysis of paleoecosystems. We suggest our data set meets most of these requirements, and those requirements suggested by other researchers. First, we use the more diagenetically resistant form of bioapatite, enamel and ganoine, rather than bone or dentine. Enamel and ganoine are more resistant to diagenesis because of their larger crystal sizes (up to two orders of magnitude greater than bone at 350Å x 350Å x 25Å) and because the organic content in both tissues is low. Decomposition of high organic content coupled with the small crystallite sizes of bone and dentine result in high surface areas for bone and dentine crystallites that can react with diagenetic pore waters. Larger crystallite sizes and lower organic content reduces isotopic exchange with the surrounding pore water due to a decrease in diagenetic reactivity because of lowered surface area to volume ratio.

Kolodny et al. (1996) suggested that if using bone, micron-scale structural preservation should be observed. We do not use bone, however, small scale structures such as growth banding in tooth enamel and in ganoine scales were observed during micro-drilling. Levels of heavy trace elements such as high REE concentrations and shallow concentration gradients have been used to suggest diagenetic alteration. Trueman et al. (2008) analyzed Cedar Mountain Formation bone from the Mussentuchit Member and suggested that they likely do not preserve original biogenic signals. However, they did not analyze enamel or ganoine. Bones from Dalton

Wells and Doelling's Bowl have been analyzed and total REE concentrations range between 500 to 3,400 ppm for Dalton Wells and 1,200 to 3,300 ppm for Doelling's Bowl (C. Suarez, 2006). These are relatively low to moderate REE concentrations for fossil bone, which typically range from 1 to 10^5 ppm. Since we only analyzed enamel and ganoine that are typically 2-3 orders of magnitude lower in REE concentration, we suggest that this data set preserves original biogenic signals.

Vertebrate remains that are isotopically distinguished along physiological lines (e.g. aquatic versus terrestrial taxa) have also been used to suggest that original biogenic signals are preserved (e.g. Fricke et al., 2008; Amiot et al., 2009). Since differences in isotopic compositions between taxa of different physiologies (e.g. co-existing turtles versus sauropods at all sites) are observed in this data set, it is suggest that the CMF faunas do preserve original biogenic isotopic signals.

Comparisons to Zonal Averages

The latitudinal effect on paleohydrology has been documented by previous researchers for the late Aptian – early Cenomanian (Ufnar et al., 2002, 2004; M. Suarez et al., 2009) using a global record of pedogenic carbonates (calcite and siderite). The latitudinal effect is the documented depletion of meteoric water due to increased rainout and fractionation at progressively lower temperatures at higher latitudes. When compared to the zonal average for 34°N paleolatitude (-6.6 to -4.8 ‰), there is remarkable consistency in the carbonate, turtle, and crocodile data documented in this study. The carbonate data documented here includes carbonate samples from the early Aptian (upper Yellow Cat Member), and so increases the lower range in meteoric water documented from carbonates to a minimum of -7.1 ± 1.2 ‰. Turtles are

within this range, though their minimum (also at the upper Yellow Cat Member) are ~1 ‰ depleted relative to carbonate (8.1 ± 0.4 ‰. This depletion relative to carbonate can be explained by the formation of calcite under evaporative conditions (Breeker et al., 2009) and the preferential habitat and growth period during the summer months by turtles. All crocodile data are within the range of carbonate data with the exception of the lower Yellow Cat Member data, which does not preserve carbonate or turtles remains to compare. The mutual consistency of multiple local meteoric water proxies strongly supports the use of pedogenic carbonate records for global-scale paleohydrology reconstruction.

Ecologic Partitioning

On a global-scale, the semi-aquatic taxa record local meteoric water similar to that documented by pedogenic calcite. By looking at this data at a smaller-scale, from proxy to proxy (i.e. carbonate versus turtles) and site to site (e.g. upper Yellow Cat versus lower Yellow Cat Members), subtle differences can be attributed to behaviors and biology of the animal and biases in mineral formation. Environmental water derived from turtle shells tend to be lighter than meteoric water derived from pedogenic calcite by 0.4 to 1.7 ‰. Since pedogenic calcite forms under evaporative conditions, they tend to be slightly biased toward isotopically enriched meteoric water (Breeker et al., 2009). Therefore, turtles seem to accurately represent average meteoric water (Barrick et al., 1999; Chapter 3) and can be used when a record of pedogenic carbonate does not exist. Since the CMF turtles analyzed in this study are inferred to live in freshwater streams and ponds, they likely record the isotopic composition of streams and ponds influenced by local meteoric water. Turtles mostly grow during the summer months, therefore, the water calculated from turtles are also biased toward summer water compositions, and are

probably slightly enriched relative to base flow isotopic compositions of rivers (Barrick et al., 1999; Pough et al., 2002).

Crocodile ingested-water on the other hand, are consistently more enriched than both turtle-ingested water (i.e. average meteoric water) and meteoric water derived from pedogenic calcite, suggesting that they lived in shallow ponds and lakes affected by evaporative enrichment. This is consistent with the inferred behavior of extinct crocodiles, which are thought to be similar to modern crocodiles. Modern crocodiles not only spend more time out of the water than turtles and are therefore more affected by evaporative conditions, but as sit-and-wait predators, they also inhabit shallower parts of water-bodies that tend to be evaporatively enriched relative to deeper water inhabited by turtles (Pough et al., 2002).

Terrestrial taxa are not restricted to bodies of water as turtles and crocodiles are, and so document a variety of water reservoirs. Sauropods have the most evaporatively enriched water source of all the terrestrial taxa. A major component of herbivore ingested-water is a diet of isotopically-enriched leaf water (Kohn, 1996). Based on their extreme isotopic enrichment relative to the other terrestrial, sauropods likely acquired a large proportion of their water from leaves, and thus were not obligate drinkers. An interesting relationship documented in this data is the increased $\delta^{18}O_p$ values of sauropod teeth associated with increased size of the tooth crown (Fig. 5). Tooth size (length of tooth crown) and isotopic composition of $\delta^{18}O_p$ is positively correlated for all sites, and for all the data combined. This is opposite to the relationship between body size and isotopic composition of bioapatites documented in mammals. Bryant and Froelich (1995) showed that larger mammals increased their intake of surface water and decreased their intake of plant water as their size increased, resulting in a negative correlation

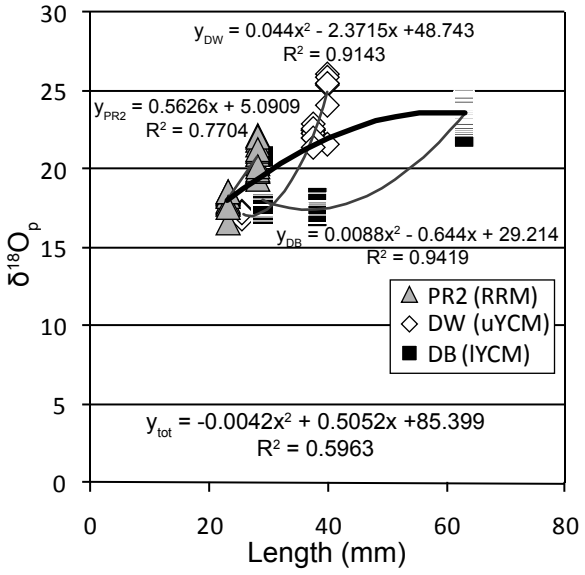

Fig. 5. Isotopic composition of sauropod enamel relative to the length of the tooth crown. Isotopic composition is positively correlated to tooth length. Equations presented on the graph are polynomial regressions for sauropods at each site (DB, DW, and PR2) and have R^2 from 0.7704 to 0.9419. When aggregating all teeth (tot = total), the $R^2 = 0.5963$. This positive correlation suggests either a behavioral or physiological change in sauropods from juveniles to adults.

between body size and $\delta^{18}O_{body\ water}$. This relationship does not seem to be the case in sauropods. We hypothesize that this isotopic enrichment may be the result of changing proportions of water sources as sauropods age; an opposite relationship to that of large mammals. Based on this data, it can be hypothesized that juvenile sauropods obtained their water from a combination of surface water (pools, rivers, lakes, etc) and plants, but older sauropods increased their proportion of plant-intake and therefore increased consumption of isotopically enriched water. This could also be explained by a significant decrease in body temperature as sauropods age (which is not likely, as calculated changes in temperature would have to be greater than 15°C) or greater magnitude of evaporative enrichment as the sauropod ages.

Ingested-water consumed by ornithischians (iguanodontids, ornithopods, hadrosaurs, and nodosaurs) is lighter than that of crocodiles, sauropods, and turtles (except in the upper Yellow Cat Member where they are more enriched than crocodiles and turtles). Their ingested-water is more enriched relative to all carnivores, with the exception of the Ruby Ranch Member, in which ornithischians record the most depleted isotopic composition of water. Based on this data, ornithischians drank water from isotopically depleted water sources such as rivers sourced from high-altitude melt water, but are enriched relative to carnivores that also drank similar water because ornithischians consumed evaporatively enriched plant water. Since ornithischians consumed water that is more depleted than sauropods, it is suggested that ornithischians were obligate drinkers, more so than sauropods. Since dinosaurs probably drank water year round, they likely preserved the yearly isotopic composition of river water. This value should be lighter in isotopic composition relative to turtles, since yearly river water includes melt-water from

high-altitude sources. This interpretation could be investigated by growth series sampling of larger ornithischian teeth (i.e. sampling every mm along the growth trajectory of the tooth).

Acrocanthosaurid $\delta^{18}O_w$ is enriched when compared to the small theropods and ornithischians (with the exception of the lower Yellow Cat Member) and more depleted than turtles, crocodiles, and sauropods. This suggests that the isotopic composition of their ingested water was heavier than the river water ingested by small theropods and ornithischians, but lighter than the meteoric water recorded by turtles and crocodiles. Acrocanthosaurid intermediate water compositions suggest they obtained their water from a mixture of water sources such as river water and evaporative food sources (flesh and blood of their prey). The heavy isotopic composition of sauropod body water, and the likelihood that the only predator that could have preyed upon such large animals was Acrocanthosaurids, suggests that Acrocanthosaurid prey was predominantly sauropods.

As is typical for carnivores in a terrestrial setting (Kohn, 1996), small theropods have lighter calculated ingested water than co-existing herbivores, with the exception of the iguanodontid from the Ruby Ranch Member fauna. This suggests that their water was sourced from rivers that are isotopically depleted relative to local meteoric water (Dutton et al., 2005). They are more depleted than co-existing ornithischians, likely because of the ornithischians' diet of isotopically-enriched plants. Therefore, we suggest that ornithischians and small theropods probably drank water from the same isotopically light river water.

Water temperatures for Actinopterygian scales, assuming the meteoric water $\delta^{18}O_w$ composition derived from turtles is unreasonably cold (2.4ºC for the upper Yellow Cat Member and 15.5ºC for the Mussentuchit Member) for the warm Cretaceous climate. The cold

temperatures calculated are the result of relatively enriched ganoine composition. Such cold waters are not likely the same waters that turtles inhabited. The enriched composition can result from two other possibilities: 1) habitat in an enriched water source (e.g. evaporative lakes) or 2) diadromous (migration between freshwater and marine or estuarine waters) migration to relatively enriched seawater. When using isotopically enriched meteoric water documented by pedogenic calcite, temperature increases to 6.9ºC for the upper Yellow Cat Member and 16.8ºC for the Mussentuchit Member, which is still unreasonably cold. If Actinopterygian scales formed under evaporative conditions, those conditions would have to be significantly more enriched relative to meteoric water. We can estimate the water composition under more reasonable temperatures using calculated temperatures documented from other proxies. Co-existing *Lepidotes* tooth $\delta^{18}O_p$ values from the Mussentuchit Member result in a more reasonable water temperature for the CMF of 20.9ºC (Chapter 3) and an estimated zonal MAT from Wolfe and Upchurch (1987) and Spicer and Corfield (1992) is 22.7ºC. Using these water values and the $\delta^{18}O_p$ of Actinopterygian scales, we can get a target $\delta^{18}O_w$ value of -3.4 ‰ for the upper Yellow Cat Member and -4.8 ‰ for the Mussentuchit Member. Using simple Rayleigh fractionation and a starting water composition recorded by turtles (-8.1 ‰ for the upper Yellow Cat Member and -6.2 ‰ for the Mussentuchit Member) at least 10% (for the Mussentuchit Member) and 40% (for the upper Yellow Cat Member) of water must be evaporated to get the targeted evaporatively-enriched water values. This is not an unreasonable amount for the Mussentuchit Member. For the upper Yellow Cat Member, evaporative enrichment would have been more extreme, however sauropod ingested water and epsilon values (discussed below) suggest the time represented by the upper Yellow Cat Member was a time of extreme aridity.

Migration (diadromous behavior) to isotopically-enriched seawater may also result in enriched fish-scale phosphate. As was calculated in chapter 3, at least 28% seawater must be mixed with freshwater to get such isotopically enriched phosphate which is reasonable for mixed estuary waters. However, during deposition of the upper Yellow Cat Member, the WIS was far from the depositional basin, and therefore upper Yellow Cat Member fish would have to have migrated much farther to the northern Boreal sea or the southern Tethyan sea, and would also have to grow in waters with at least a 68% component of seawater (assuming a seawater composition of -1.2 ‰). Modern fishes (such as the King Salmon) can migrate distances as much as several hundreds to thousands of kilometers, live in seawater, and only migrate upstream to spawn (anadromous). Therefore, this may not be unreasonable. Based on the data presented, however, we cannot make an accurate assessment as to the living water of these fish unless additional data (such as strontium isotopes) are collected.

Orogenic and Small-Scale Regional Climatic Impacts

The lack of significant carbonate accumulation in the lower Yellow Cat Member suggests that climate during that time was rarely in moisture deficit. Rather, regional climate during the lower Yellow Cat Member may have been relatively humid. Only one proxy for meteoric water was sampled (crocodiles), however, and suggests the enriched end-member of local meteoric water was relatively high (-3.5‰) suggesting more arid conditions. When compared to the terrestrial taxa, however, sauropod-ingested water was more depleted than the water values calculated from crocodiles, suggesting relatively high local humidity or consumption of isotopically depleted water. Calculated isotopic enrichment (ε) for the lower Yellow Cat Member fauna is relatively low, also suggesting higher humidity (Fig. 6). The low ε might be

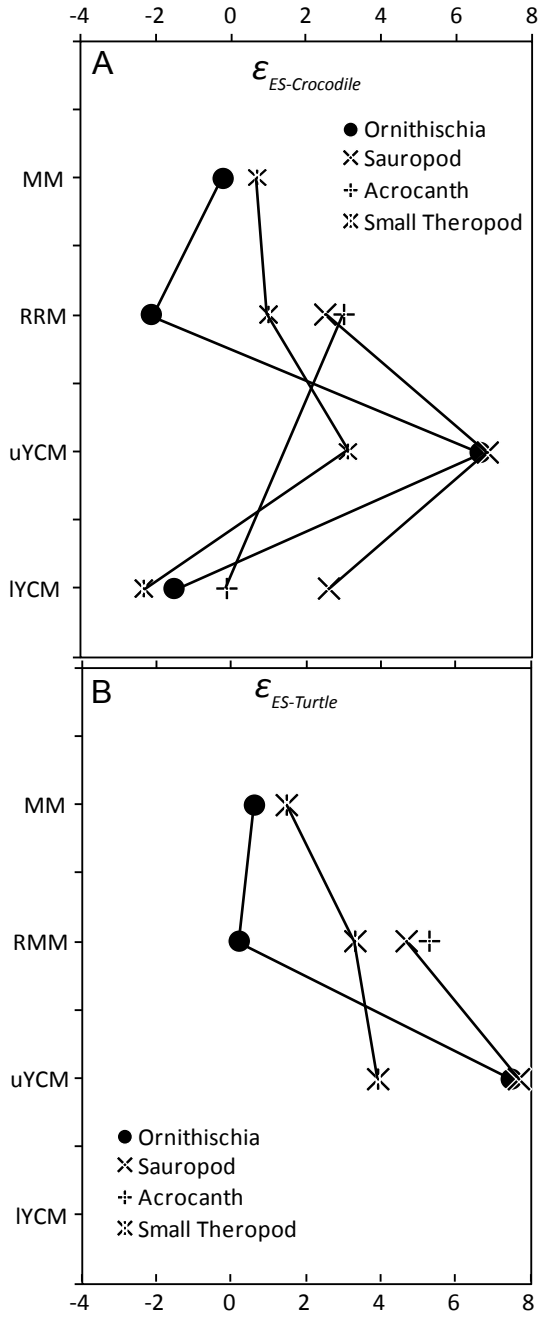

Fig. 6. Isotopic enrichment (ε) calculated between evaporative sensitive (ES) and evaporative insensitive (EI) taxa. A) ε between all ES taxa and crocodiles. B) ε between all ES taxa and turtles. For all εES-EI the upper Yellow Cat Member is the most enriched (had the highest water deficit) suggesting the most arid conditions. For all εES-EI (except εornithischians-crocodiles) the Ruby Ranch Member is the least enriched. Though the lowest ε (at the Ruby Ranch Member) typically would represent the wettest time, lithologic data does not support this. Depleted snow-melt may obscure aridity signals (see text for details).

due to isotopically depleted river water consumed by dinosaurs. Interpretation of the climate at this time is difficult without another (carbonate or turtle) proxies to estimate meteoric water. However, based on the current data, the lower Yellow Cat Member fauna likely represents a fluvial setting in which rainfall supply and precipitation-evaporation balance was sufficient to suppress precipitation of significant amounts of pedogenic calcite. Isotopically depleted precipitation due to continental rainout was drained into rivers with a large catchment basin that was sourced from distant northeast-flowing rivers whose catchment basins also included orographically depleted run-off from the Sevier Mountains (Fig. 7A), resulting in depleted river water. Evaporative enrichment must have taken place in order for crocodiles to become so enriched, and for the evaporative sensitive taxa (sauropods) to become enriched relative to the other dinosaurs. Therefore, the lower Yellow Cat Member may represent a semi-humid climate with rainfall that was sufficient enough to inhibit pedogenic calcite from forming, but arid enough to enrich local meteoric water and plant leaves.

The upper Yellow Cat Member fauna represents a dramatic change in the regional climatic setting. Estimated ages for the upper Yellow Cat Member suggest it was between 124-119 Ma, indicating it was deposited during the latter part of the Canyon Range Thrust event. Therefore, highlands to the west were well established which may have dominated the local climate as evidenced by the isotopic composition of the sampled upper Yellow Cat Member fauna.

Meteoric water $\delta^{18}O$ values calculated from pedogenic calcite and turtle shell phosphate were -7.1 ‰ and, -8.1 ‰ respectively. Terrestrial taxa are extremely enriched relative to meteoric water values (Table 3). Sauropod and iguanodontid isotopic compositions suggest that

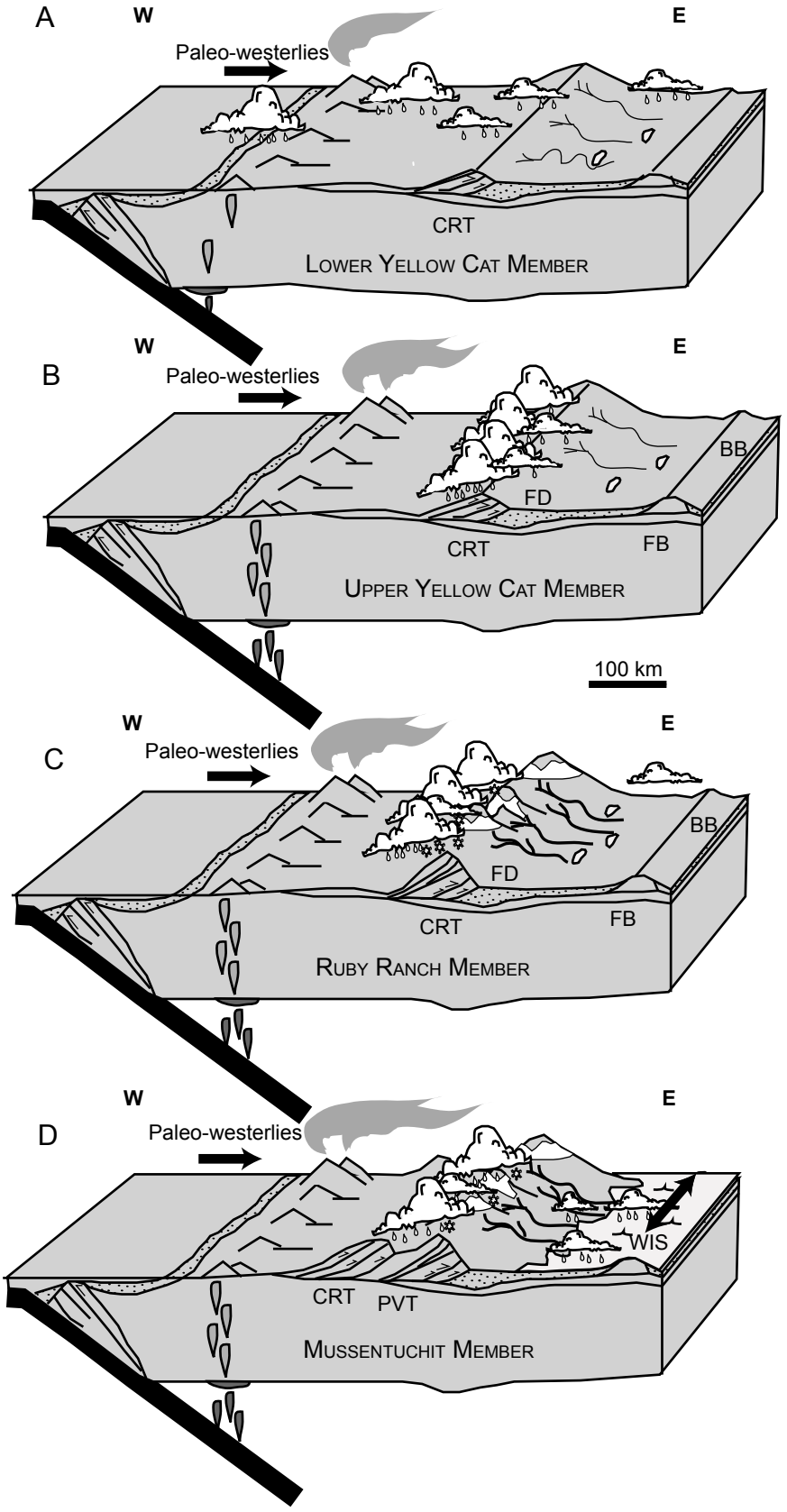

Fig. 7. Block diagrams of interpreted paleoclimatic and paleogeographic settings represented by the isotopic composition of each fauna. A) At the lower Yellow Cat Member the Canyon Range Thrust event initiated uplifted highlands (Sevier Mountains). Climate was semi-humid and moisture sourced from paleo-westerlies became enrichment due to evaporative enrichment. Rivers were isotopically depleted as recorded by the obligate drinkers. B) By the upper Yellow Cat Member time, the Sevier Mountains increased in height resulting in significant rainout on the western and crest of the mountains. The little rain (meteoric water) that does make it over the mountains is depleted. The rainshadow created extremely arid conditions on the leeward side of the mountains. C) The Canyon Range thrust was completed by the Ruby Ranch Member time and paleo-elevations reach their maximum for the Canyon Range thrust causing a rainshadow and slight enrichment of meteoric water. Elevations were high enough for significant snowfall and accumulation in the mountains to occur causing extremely depleted river water to be discharged to the foreland basin. Moisture from the northern Boreal Sea and southern Tethys Sea began to make its way inland providing humidity, but not significant rainfall. D) Initiation of the Pavant Thrust event began, increasing elevation; however, incursion of the Western Interior Seaway (WIS) provided significantly enriched moisture to the region. FD = foredeep; FB = forebulge; BB = backbulge (modified from Elliot et al., 2007.

their water intake was as much as 3.0 ‰ more enriched than the local meteoric water recorded by turtles. The highest epsilon values (isotopic enrichment) between ES and EI taxa are consistently found at the upper Yellow Cat Member for all ES taxa (Fig. 6). This indicates that climate during the upper Yellow Cat Member deposition was more arid. This is in agreement with the high amounts of pedogenic carbonates, and high amounts of intermittent to ephemeral alluvial systems described by Elliot et al. (2007) from the foreland basin system. Since dinosaurs seemed to record yearly river water composition, and since the calculated isotopic composition of ingested water is so much heavier than the rest of the CMF, it is suggested that a lack of isotopically-depleted snow-melt river water (i.e. the Sevier Mountains have not reached adequate height to reduce air temperature to freeze precipitation) and high aridity resulted in increased isotopic composition of precipitated dinosaur tooth phosphate. Arid conditions would be conducive to high degrees of erosion of denuded landforms and therefore instability of those landforms as is indicated by very poorly sorted sediments (Elliot et al., 2007; Eberth et al., 2006. Aridity during this time period is interpreted to be the result of orogenic effects (rainshadow) from the Canyon Range thrust event of the Sevier Orogeny (Fig. 7B).

For all meteoric water proxies in the Ruby Ranch Member (crocodiles, turtles, and pedogenic carbonate), isotopic composition of water increases from the upper Yellow Cat Member to the Ruby Ranch Member. The significant amounts of pedogenic carbonate specifically in the Ruby Ranch Member have been suggested to be the result of aridity caused by Sevier Orogeny rainshadow effects during the Albian (Elliot et al., 2007). However, for terrestrial taxa, isotopic composition of ingested-water dramatically decreases by as much as 9.4‰ for iguanodontids and 3.3‰ for sauropods. This suggests a lack of evaporative

enrichment effects (high humidity) on the terrestrial taxa and a relatively depleted water source. This is apparently conflicting with the isotopically higher $\delta^{18}O_w$ values from the aquatic taxa and pedogenic carbonate. Ludvigson et al. (in revision) suggests that the approximate age of the PR2 quarry is ~110-109 Ma, which correlates with the end of the Canyon Range thrust event and the initiation of the Pavant thrust event, and likely the maximum elevation during the Ruby Ranch Member deposition. The decrease in isotopic composition of terrestrial taxa, therefore, may suggest they were drinking water from isotopically depleted, snow-melt influenced river waters rather than an increase in humidity. Whereas in the upper Yellow Cat Member, one potential cause of the lower isotopic compositions of meteoric water was the lack of moisture making it over the Sevier Mountains, the height of the Sevier Mountains during the Ruby Ranch Member does not allow for moisture to make it over the mountains, resulting in an increase in the isotopic composition of local meteoric water due to evaporative enrichment. The only evidence of isotopically depleted orographic effects is from snow-melt influenced river water (documented by dinosaur-ingested water). Seasonal snowfall in the Himalayas can occur at an elevation as low as 1500 km (Singh and Kumar, 1997; Kaur et al., 2009). At 23ºN latitude, where modern MAT is ~23ºC (the average MAT for the early Cretaceous at 34ºN) seasonal snow fall in the Mexican Sierra Madres occurs at elevations of ~ 3000 km (Palacios and Vasquez-Selem, 1996) suggesting seasonal snowfall was possible during the time of Ruby Ranch Member deposition. If we use the river water as recorded by small theropods and a gradient of ~ -4.2‰/km of elevation for river water, paleo-elevation would have been at least ~ 2.1 km. The Canyon Range thrust increased pre-thrusting paleo-elevations by ~ 1.57 km (DeCelles and Coogan, 2006). Since the upper Jurassic Morrison in Utah consists entirely of terrestrial sediments and since the Buckhorn

Conglomerate suggests pre-thrust elevations were well above sea-level, it is reasonable to suggest that paleo-elevation by the end of the Canyon Range thrust was well over 2 km. Since these dinosaurs are not likely to be living at the peaks of the mountains, the estimate of 2.1 km is lower than the maximum elevation of the mountains. River water had to have been exceptionally light to off-set evaporative enrichment of terrestrial taxa, or humidity must have been high enough to reduce the evaporative effects caused by any rainshadow-induced aridity. Meridional moisture patterns as the northern Boreal Sea and southern Tethyan Sea moved further inland may have also resulted in increased humidity during the Ruby Ranch Member (Fig. 7C).

The Mussentuchit Member fauna increase in isotopic composition for all fauna (except crocodiles) and carbonate sampled. As reported in Chapter 3, the Mussentuchit Member is effected by a combination of orographic effects in the form of isotopically depleted river water (documented by dinosaurs), but predominantly by progressive incursion of the WIS and associated moisture delivery (represented by isotopically heavier pedogenic carbonate, turtle-derived water, and crocodile-derived water). Sampled mammalian taxa suggest average humidity ranged between ~50 to 75% humidity and averaged about 68% (Chapter 3). The sedimentology (lesser abundance of carbonate nodules) agrees with these calculated humidity values. Therefore, the relative increase in carbonate, turtles, and terrestrial taxa $\delta^{18}O$-ingested water suggests the Mussentuchit Member was influenced climatically by the WIS and more positive $\delta^{18}O$ water vapor (Fig. 7D).

Implications

This data shows successful utilization of isotopic proxies for continental paleoecologic and paleoclimatic studies of ecosystems as old as the Mesozoic. Combinations of terrestrial,

aquatic and semi-aquatic taxa, and pedogenic carbonates yield useful data to decipher climatic effects of orogeny and marine transgressions. We also, for the first time, isotopically validate the presence of a rainshadow suggested by Elliot et al. (2007), for the "Nevadaplano" paleotopography suggested by DeCelles and Coogan (2006). The rise of the Sevier Mountains significantly affected climate by ~124 Ma (upper Yellow Cat Member fauna) and by ~110-105 Ma inhibited Pacific moisture from entering the foreland basin east of the highlands (Fig. 7). Incursions of the WIS dominated weather patterns by 98-96 Ma, resulting in diminished orographic effects during the Pavant thrust event (Fig. 7). Carbonate, turtle, and crocodile data does estimate meteoric water, but without co-existing terrestrial (dinosaurian) taxa, we could not accurately identify the rainshadow effects of the SFTB on regional climate. The successful use of this data set suggests that a similar data set may be used to differentiate orographic effects versus rainout effects for high latitude settings, as has been under contention in the mid-Cretaceous (White et al., 2001; Ufnar et al 2002, 2004, M. Suarez, 2009; Poulsen et al., 2007).

CONCLUSIONS

The isotopic composition of local meteoric water predicted by turtles and crocodiles are consistent with estimate of zonal precipitation on a global scale for the late Aptian – early Cenomanian, as documented by global records of pedogenic carbonate. These multiple independent lines of evidence support the use of pedogenic carbonates for global-scale documentation of paleohydrology. The addition of turtle and crocodile data provides a robust record of local meteoric water at 34°N paleolatitude. Variability in the data set between taxa at each site and between proxies can be attributed to the unique processes of formation for those

proxies (i.e. calcite versus vertebrate phosphate) and the living habits of these proxies (i.e. turtles versus crocodiles). Variability between data from site to site can be explained by changing record of water reservoirs caused by small-scale regional climate change.

The two main driving forces behind this regional climatic change were the formation of the Sevier Mountains and the incursion of the Western Interior Seaway. The Canyon Range Thrust (145-110 Ma) event significantly impacted regional climate starting in the upper Yellow Cat Member through the Ruby Ranch Member. By the initiation of the Pavant Thrust event (110-86 Ma), climate was dominated by the moisture patterns moving north-south along the Western Interior Seaway.

Pedogenic calcites record more isotopically-enriched values of meteoric water due to their formation under evaporative conditions, while turtles record average isotopic composition of local rainfall. Crocodiles lived in the shallows of rivers and ponds, and therefore represent isotopically-enriched river and pond water that is similar to the enriched end-member of local meteoric water recorded by pedogenic calcite. Terrestrial taxa such as sauropod, ornithischian, and theropod dinosaurs represent evaporative sensitive taxa. More specifically, sauropods were extremely affected by evaporative enrichment and may represent a useful proxy for aridity. Ornithischians are affected by aridity, but were more obligate-drinkers than sauropods. Smaller theropod dinosaurs such as *Utahraptor* primarily ingested river water and may represent a proxy for river water. Large theropods such as *Acrocanthosaurus* have a wide range of isotopic composition of phosphate, and likely got their water from a combination of river water and food (sauropod flesh and blood).

Data also suggests behavioral or physiological changes during the ontogenetic growth of sauropods. Larger adult sauropods have isotopically enriched tooth enamel relative to smaller juvenile sauropods. This may represent a transition of water resources from a combination of river/meteoric water and plant water to an increased proportion of plant water as the animal transitioned from a juvenile to an adult. This trend seems to hold no matter which CMF member is in question, suggesting that this was a long-standing behavioral trend in sauropods, however further analysis of a series of teeth at different ontogenetic growth stages needs to be carried out to confirm this trend.

The combined analysis of terrestrial taxa of different physiologies with analysis of pedogenic carbonates can potentially elucidate small scale (1-10 millennia) climate change due to forcings such as orogenic effects and marine regression and transgression. Additional analyses of fossil material, such as freshwater clams may further constrain water reservoirs and changes to those reservoirs over time. Studies similar to this one at other geologic times and locations can be used to decipher between regional orogeny-induced climate change and global climate change.

REFERENCES

Al-Suwaidi, A. H. (2007) A ped's story, Dept. of Geology, Lawrence, University of Kansas, MS thesis, 135p.

Amiot, R., Buffetaut, E., Lecuyer, C., Fernandez, V., Fourel, F., Martineau, F., and Suteethorn, V. (2009) Oxygen isotope composition of continental vertebrate apatites from Mesozoic

formations of Thailand; environmental and ecological significance. *Geol. Soc., London* **Special Publications 315**, 271-283.

Amiot, R., Lecuyer, C., Buffetaut, E., Escarguel, G., Fluteau, F., and Martineau, F. (2006) Oxygen isotopes from biogenic apatites suggest widespread endothermy in Cretaceous dinosaurs. *Earth & Planet. Sci. Ltrs.* **246**, 41-54.

Amiot, R., Lecuyer, C., Escarguel, G., Billon-Bruyat, J. P., Buffetaut, E., Langlois, C., Martin, S., Martineau, F., and Mazin, J. M. (2007) Oxygen isotope fractionation between crocodilian phosphate and water. *Palaeogeog., Palaeoclimat., Palaeoecol.* **243**, 412-420.

Aubrey, W. M. (1998) A newly discovered, widespread fluvial facies and unconformity marking the Upper Jurassic/Lower Cretaceous boundary, Colorado Plateau. In: Carpenter, K., Chure, D., and Kirkland, J. I. Eds.), *The Upper Jurassic Morrison Formation - An Interdisciplinary Study, Part 1: Modern Geology*, **22**. 209-233

Barrick, R. E., Fisher, A. L., and Showers, W. J. (1999) Oxygen isotopes from turtle bone: applications for terrestrial paleoclimates. *PALAIOS* **14**, 186-191.

Bassett, D., MacLeod, K. G., Miller, J. F., and Ethington, R. L. (2006) Oxygen isotopic composition of biogenic phosphate and the temperature of Early Ordovician Seawater. *PALAIOS* **22**, 98-103.

Billon-Bruyat, J.P., Lecuyer, C., Martineau, F. and Mazin, J.M. (2005) Oxygen isotope compositions of Late Jurassic vertebrate remains from lithographic limestones of western Europe: implications for the ecology of fish, turtles, and crocodilians. *Palaeogeogr. Palaeoclimatol. Palaeoecol.* **216**, 359-375.

Bodily, N. M. (1969) An armoured dinosaur from the Lower Cretaceous of Utah. *Brigham Young University Studies* **16**, 35-60.

Breecker, D. O., Sharp, Z. D., and McFadden, L. D. (2009) Seasonal bias in the formation and stable isotopic composition of pedogenic carbonate in modern soils from central New Mexico, USA. *GSA Bulletin* **121**, 630-640.

Britt, B. B., Stadtman, K. L., and Scheetz, R. D. (1997) The Early Cretaceous Dalton WElls dinosaur fauna and the earliest North American titanosaurid sauropod. *J. of Vert. Paleo.* **16**, 24A.

Britt, B. B., Burton, D., Greenhalgh, B. W., Christiansen, E., and Chure, D. (2007) Detrital zircon ages for the basal Cedar Mountain Formation (Early Cretaceous) near Moab, and Dinosaur National Monument, Utah. *GSA Abstracts with Programs* **39**, 16.

Britt, B. B., Eberth, D. A., Scheetz, R., Greenhalgh, B. W., and Stadtman, K. L. (2009) Taphonomy of debris-flow dinosaur bonebeds at Dalton Wells, Utah (Lower Cretaceous, Cedar Mountain Formation, USA. *Palaeogeog., Palaeoclimat., Palaeoecol.* **280**, 1-22.

Bryant, J. D. and Froelich, P. N. (1995) A model of oxygen isotope fractionation in body water of large mammals. *Geochim, et Cosmochim, Acta* **59**, 4523-4537.

Carpenter, K., Kirkland, J. I., Burge, D., and Bird, J. (1999) Ankylosaurs (Dinosauria: Ornithischia) of the Cedar Mountain Formation, Utah, and their stratigraphic distributions. In: Gillette, D. (Ed.), *Vertebrate Paleontology in Utah*, **Miscellaneous Publication 99-1**, Utah Geological Survey, Salt Lake City, UT. 243-251

Carpenter, K., Kirkland, J. I., Burge, D., and Bird, J. (2001) Disarticulated skull of a primative ankylosaur from the Lower Cretaceous of eastern Utah. In: Carpenter, K. (Ed.), *The Armoured Dinosaurs*, Indiana University Press, Bloomington. 211-238

Cifelli, R. L., Nydam, R. L., Gardner, J. D., Weil, A., Eaton, J. G., Kirkland, J. I., and Madsen, S. K. (1999) Medial Cretaceous Vertebrates from the Cedar Mountain Formation, Emery County, Utah: The Mussentuchit Local Fauna. In: Gillette, D. D. (Ed.), *Vertebrate Paleontology in Utah*, **Misc. Publications 99-1**, Utah Geological Survey, Salt Lake City. 219-242

Currie, B. S. (1998) Upper Jurassic-Lower cretaceous Morrison and Cedar Mountain Formations, NE Utah-NW Colorado: Relationships between non-marine deposition and early cordilleran forland-basin development. *J. of Sed. Res.* **68**, 632-652.

Currie, B.S. (2002) Structural configuration of the Early Cretaceous cordilleran foreland-basin system Sevier Thrust Belt, Utah and Colorado. *J. of Geol*. **110**, 697-718.

DeCelles, P. G. and Coogan, J. C. (2006) Regional structure and kinematic history of the Sevier fold-and-thrust belt, central Utah. *GSA Bulletin* **118**, 841-864.

DiCroce, T. and Carpenter, K. (2001) New ornithopod from the Cedar Mountain Formation (Lower Cretaceous) of eastern Utah. In: Tanke, D. H. and Carpenter, K. Eds.), *Mesozoic Vertebrate Life*, Indiana University Press, Bloomington. 183-196.

Dutton, A., Wilkinson, B.H., Welker, J.M., Bowen, G.J. and Lohmann, K.C. (2005) Spatial distribution and seasonal variation in $^{18}O/^{16}O$ of modern precipitation and river water across the conterminous USA. *Hydrol. Process*. **19**, 4121-4146.

Eberth, D. A., Britt, B. B., Scheetz, R., Stadtman, K. L., and Brinkman, D. B. (2006) Dalton Wells - geology and signiciant of a debris-flow-hosted dinosaur bonebed in the Cedar Mountain Formation (Lower Cretaceous) of eastern Utah, USA. *Palaeogeog., Palaeoclimat., Palaeoecol.* **236**, 217-245.

Elliott, W. S., Suttner, L. J., and Pratt, L. M. (2007) Tectonically induced climate and its control on the distribution of depositional systems in a continental foreland basin, Cloverly and Lakota Formations (Lower Cretaceous) of Wyoming, USA. *Sed. Geol.* **202**, 730-753.

Fricke, H. C., Rogers, R. R., Backlund, R., Dwyer, C. N., and Echt, S. (2008) Preservation of primary stable isotope signals in dinosaur remains, and environmental gradients of the Late Cretaceous of Montana and Alberta. *Palaeogeog., Palaeoclimat., Palaeoecol.* **266**, 13-27.

Fricke, H. C., Rogers, R. R., and Gates, T. A. (2009) Hadrosaurid migration: inferences based on stable isotope comparisons among Late Cretaceous dinosaur localities. *Paleobiology* **35**, 270-288.

Garrison Jr., J. R., Brinkman, D. B., Nichols, D. J., Layer, P., Burge, D., and Thayn, D. (2007) A multidisciplinary study of the Lower Cretaceous Cedar Mountain Formation, Mussentuchit Wash, Utah: a determination of the paleoenvironment and paleoecology of the *Eolambia caroljonesa* dinosaur quarry. *Cret. Res.* **28**, 461-494.

Greenhalgh, B. W. (2007) A stratigraphic and geochronologic analysis of the Morrison Formation/Cedar Mountain Formation boundary, Dept. of Geology, Provo, Brigham Young University, MS thesis, 61p.

Herrle, J.O., Koßler, P., Erleneuser, H. and Hemleben, C. (2004) High-resolution carbon isotope records of the Aptian to Lower Albian from SE France and the Mazagan Plateau (DSDP Site 545): a stratigraphic tool for paleoceanographic and paleobiologic reconstruction. *Earth and Planet. Sci. Ltrs*. **218**, 149-161.

Huber, B. T., Hodell, D. A., and Hamilton, C. P. (1995) Middle-Late Cretaceous climate of the southern high latitudes: stable isotopic evidence for minimal equator-to-pole thermal gradients. *GSA Bulletin* **107**, 1164-1191.

Kaur, R., Saikumar, D., Kulkarni, A.V. and Chaudhary, B.S. (2009) Variation in snow cover and snowline altitude in Baspa Basin. *Current Science*. **96**, 1255-1258.

Kirkland, J. I., Burge, D., and Gaston, R. (1993) A large dromaeosaurid (Theropoda) from the Lower Cretaceous of Eastern Utah. *Hunteria* **2**, 1-16.

Kirkland, J. I. (1998a) A new hadrosaurid from the Upper Cretaceous Cedar Mountain Formation (Albian-Cenomanian Cretaceous) if eastern Utah - the oldest known hadrosaurid (Lambeosaurine?). In: Lucas, S. G., Kirkland, J. I., and Estep, J. W. Eds.), *Lower and Middle Cretaceous Ecosystems*, **Bulletin 14**, New Mexico Museum of Natural History and Sciences. 283-295

Kirkland, J. I. (1998b) *A polocanthine ankylosaur from the Early Cretaceous of eastern Utah*. New Mexico Museum of Natural History and Science Bulletin.

Kirkland, J. I., Zanno, L. E., Sampson, S. D., Clark, J. M., and DeBlieux, D. D. (2005) A primative therizinosaurid dinosaur from the Early Cretaceous of Utah. *Nature* **435**, 84-87.

Kirkland, J. I. and Madsen, S. K. (2007) The Lower Cretaceous Cedar Mountain Formation, Eastern Utah: the view up an always interesting learning curve (Field tripe guide for the

2007 Geological Society of America)*GSA Rocky Mountain Section Annual Meeting*. Utah Geological Association Publications, 35, St. George, Utah.

Kohn, M. J. (1996) Predicting animal delta^{18}O: accounting for diet and physiological adaptation. *Geochim, et Cosmochim. Acta* **60**, 4811-4829.

Kohn, M. J. and Dettman, D. L. (2007) Paleoaltimetry from Stable Isotope Compositions of Fossils. *Rev. in Mineral. and Geochem.* **66**, 119-154.

Kolodny, Y., Luz, B., and Navon, O. (1983) Oxygen isotope variation in phosphate of biogenic apatites, I. Fish bone apatite - rechecking the rules of the game. *Earth and Planet. Sci. Ltrs.* **64**, 398-404.

Kolodny, Y., Luz, B., Sander, M., and Clemens, W. A. (1996) Dinosaur bones: fossils or pseudomorphs? The pitfalls of physiology reconstruction from apatitic fossils. *Palaeogeog., Palaeoclimat., Palaeoecol.* **126**, 161-171.

Kowallis, B. J., Britt, B. B., Greenhalgh, B. W., and Sprinkel, D. A. (2007) A new U-Pb zircon ages from an ash bed in the Brushy Basin Member of the Morrison Formation near Hanksville, UT. *GSA Abstracts with Programs* **39**, 9.

Levin, N. E., Cerling, T. E., Passey, B. H., Harris, J. M., and Ehleringer, J. R. (2006) A stable isotope aridity index for terrestrial environments. *Proc. of the Nat. Acad. of Sci.* **103**, 11201-11205.

Ludvigson, G. A., Joeckel, R. M., Gonzalez, L. A., Gulbranson, E. L., Rasbury, E. T., Hunt, G. J., Kirkland, J. I., and Madsen, S. K. (in revision) Correlation of Aptian-Albian carbon isotope excursions in continental strata of the Cretaceous foreland basin of eastern Utah. *J. of Sed. Res*.

O'Neil, J. R., Roe, R. R., Reinhard, E., and Blake, R. E. (1994) A rapid and precise method of oxygen isotope analysis of biogenic phosphate. *Isreal J. of Earth-Sci.* **43**, 203-212.

Oboh-Ikuenobe, F. E., Benson, D. G., Scott, R. W., Holbrook, J. M., Evetts, M. J., and Erbacher, J. (2007) Re-evaluation of the Albian-Cenomanian boundary in the U.S. Western Interior based on dinoflagellate cysts. *Rev. of Palaeobot. and Palynol.* **144**, 77-97.

Palacios, D. and Vasquez-Selem, L. (1996) Effects of the retreat of Jampa Glacier, Pico de Orizaba Volcano (Mexico). *Physical Geography*. **78**, 19-34.

Pough, F. H., Janis, C. M., and Heiser, J. B. (2002) *Vertebrate life*. 6th ed., Prentice Hall, Upper Saddle River, N.J. 699.

Poulsen, C., David, P., and White, T. S. (2007) General circulation model simulation of the d^{18} O content of continental precipitation in the middle Cretaceous: a model-proxy comparison. *Geology* **35**, 199-202.

Robinson, S.A., Scotchman, J.I., White, T.S. and Atkinson, T.C. (2010) Contraints on palaeoenvironments in the Lower Cretaceous Wealden of southern England, from the geochemistry of sphaerosiderites. *J. of the Geol. Soc., London*. **167**, 303-311.

Shapiro, R. S., Fricke, H. C., and Fox, K. (2009) Dinosaur-bearing oncoids from ephemeral lakes of the Lower Cretaceous Cedar Mountain Formation, Utah. *PALAIOS* **24**, 51-58.

Sharp, Z. D., Atudorei, V., and Furrer, H. (2000) The effect of diagenesis on oxygen isotope ratios of biogenic phosphates. *Amer. J. of Sci.* **300**, 222-237.

Singh, P. and Kumar, N. (1997) Effect of orography on precipitation in the western Himalayan region. *J. of Hydrol*. **199**, 183-206.

Spicer, R.A. and Corfield, R.M. (1992) A review of terrestrial and marine climates in the Cretaceous with implications for modeling the "Greenhouse Earth". *Geol. Mag.* **2**, 169-180.

Stokes, W. L. (1949) Morrison and related deposits in and adjacent to the Colorado Plateau. *GSA Bulletin* **55**, 951-992.

Suarez, C. A., Macpherson, G. L., Gonzalez, L. A., Kirkland, J., and Grandstaff, D. E. (2006) Preliminary geochemical taphonomy of bone bed sites in the Yellow Cat Member of the Cedar Mountain Formation, Utah. *GSA Abstracts with Programs* **38**, 395.

Suarez, M. (2009) Global Hydrologic Perspectives on the mid-Cretaceous Greenhouse Climate, Dept. of Geology, Lawrence, University of Kansas, PhD dissertation, 179p.

Suarez, M. B., Gonzalez, L., Ludvigson, G., Vega, F. J., and Alvarado-Ortega, J. (2009) Isotopic composition of low-latitude paleprecipitation during the Early Cretaceous. *GSA Bulletin* **121**, 1584-1595.

Tidwell, V. C., Carpenter, K., and Brooks, W. (1999) New sauropod from the Lower Cretaceous of Utah, USA. *Oryctos* **2**, 21-37.

Tidwell, V. C., Carpenter, K., and Meyer, S. (2001) New titanosauriform (Sauropoda_ from the Poison Strip Member of the Cedar Mountain Formation (Lower Cretaceous), Utah. In: Tanke, D. H. and Carpenter, K. Eds.), *Mesozoic Vertebrate Life*, Indiana University Press, Bloomington. 139-165

Trueman, C. N., Palmer, M. R., Field, J., Privat, K., Ludgate, N., Chavagnac, V., Eberth, D. A., Cifelli, R., and Rogers, R. R. (2008) Comparing rates of recrystallisation and the

potential of preservation of biomolecules from the distribution of trace elements in fossil bones. *Comptes Rendus Palevol* **7**, 145 - 158.

Ufnar, D. F., Gonzalez, L., Ludvigson, G., Brenner, R. L., and Witzke, B. J. (2002) The mid-Cretaceous water bearer: isotope mass balance quantification of the Albian hydrologic cycle. *Palaeogeog., Palaeoclimat., Palaeoecol.* **188**, 51-71.

Ufnar, D. F., Gonzalez, L. A., Ludvigson, G. A., Brenner, R. L., and Witzke, B. J. (2004) Evidence for increased latent heat transport during the Cretaceous (Albian) greenhouse warming. *Geology* **32**, 1049-1052.

White, T., Gonzalez, L., Ludvigson, G., and Poulsen, C. (2001) Middle Cretaceous greenhouse hydrologic cycle of North America. *Geology* **29**, 363-a-366.

Wolfe, J.A. and Upchurch, G. (1987) North American nonmarine climates and vegetation during the Late Cretaceous. *Palaeogeog. Palaeoclimatol. Palaeoecol*. **61**, 33-77.

CHAPTER 5. CONCLUSIONS

In the preceding chapters I have shown the utility of geochemical analysis of fossil bone for paleontological and geological investigations. In chapter 2, I addressed the diagenesis and fossilization history of fossil bone using REE geochemistry. In chapters 3 and 4 the oxygen isotopic composition of teeth and scales was used to infer life habits and paleoecology of animals, as well as infer regional paleohydrology and paleoclimatology.

I investigated REE variability within a thin-walled bone fragment using laser ablation inductively coupled plasma mass spectrometry. LA-ICP-MS reveal that differences in REE patterns within a fossil record changes in geochemical conditions during fossilization. These changes were caused by encasement of the bone by materials that reduced permeability, i.e. micritic vadose calcite. A MREE-depleted pattern in the lower portion of the analyzed bone and in the pendant micritic calcite cements suggests that portion fossilized contemporaneously with cement precipitation in the vadose zone. In the saturated zone (i.e., below the water table) lower redox conditions caused reductive dissolution of minerals (such as hydrous ferric oxides and manganese oxides) that resulted LREE-enrichment and a positive Ce anomaly. This LREE-enriched pattern was incorporated during the fossilization of the upper part of the bone. The thinness of the bone and presence of a pendant cement helped facilitate partial fossilization of the bone in the vadose zone, preserving the REE signature of an earlier fluid. These results have important implications for the selection of samples for REE analysis and suggest thin-walled bone preserved in vadose conditions carefully be analyzed by LA-ICP-MS before use in taphonomic, forensic, or geochronologic studies.

The oxygen isotopic composition of the phosphatic ($\delta^{18}O_p$) remains from a diverse set of vertebrate fossils (fish, turtles, crocodiles, dinosaurs, and micro-mammals) from the Mussentuchit Member of the Cedar Mountain Formation (CMF), UT, USA (late Albian – early Cenomanian) preserve important information on the water utilization habits of each taxa and allow for estimation of the isotopic composition of various water reservoirs. Results suggest turtle and crocodile $\delta^{18}O_p$ are mutually consistent on a global scale with that of zonal meteoric waters predicted from records of pedogenic carbonate. Slight variations between local meteoric water predicted by turtles and that predicted from crocodiles and calcite can be attributed to slightly evaporative conditions in which carbonates form and crocodiles lived in relative to turtles. Variability in the turtle, crocodile, and carbonate data from site to site can be explained by small-scale regional climate change.. Turtle derived $\delta^{18}O_w$ is used to estimate growth temperature of fish with *Lepidotes*-like teeth, which appear to grow at temperatures that are consistent with estimated mean annual temperature for this latitude and time. The $\delta^{18}O_p$ of Actinopterygian scales and teeth indicates that they lived in evaporatively affected water reservoirs or that they migrated to the enriched estuarine waters of the Western Interior Seaway (WIS). Mammals, herbivorous dinosaurs, and theropods are all evaporative sensitive taxa and primarily drank river water during much of the year and thus capture an isotopically depleted $\delta^{18}O_w$. Dinosaurs appear to document year-round river water isotopic compositions most isotopically depleted $\delta^{18}O_w$ due to snow-melt. Co-existence of aquatic taxa and mammals allows for calculation of relative humidity. Mussentuchit Member mammals suggest humidity averaged ~68% and ranged between ~47% to ~76% relative humidity.

These results are significant since, locally, the hydrologic cycle varies due to regional events such as mountain building, and because pedogenic carbonates (calcite), traditionally used for global paleoclimatic studies, form in a narrow moisture regime. Other climate proxies, such as vertebrate remains, can be used to decipher local versus regional variations in paleohydrology. In this study, the $\delta^{18}O_w$ estimated from aquatic, semi-aquatic, and pedogenic calcite indicate that during the periods of mineralization, WIS derived moisture is the dominant source of water . Dinosaurs, particularly theropods, record catchment effects from the Sevier Mountains that are more important in the fall through early spring. Based on the stratigraphic changes in the presented data, I conclude that temporal changes in the isotopic composition of the Mussentuchit Member fauna were produced by the small-scale sea level oscillations of the WIS.

The analytical strategy applied to the Mussentuchit Member is expanded to the underlying CMF members to determine the water utilization habits of fauna in the older portions of the CMF (Barremian – early Cenomanian), and substantiates the identified water habits of taxa analyzed from the Mussentuchit Member. Turtles and crocodiles again corroborate predictions of isotopic composition of zonal meteoric water derived from global records of pedogenic carbonates. The expanded data set includes larger dinosaurs such as sauropods and larger theropods such as *Acrocanthosaurus*. Oxygen isotopic composition of their phosphate suggests that sauropods are extremely evaporative sensitive and may be used as a proxy for aridity. Adult sauropod water-intake seems to be dominated by food (leaves) whereas juvenile water-intake is from both surface water and plants. Ornithischians and smaller theropods tend to get much of their living water from rivers and are more obligate drinkers than sauropods, while Acrocanthosaurid dinosaurs obtain their water from a combination of rivers and food (namely

sauropods). Based on the isotopic composition of the different water reservoirs preserved by the $\delta^{18}O_p$ of the different animals, I conclude that the dominant control on climate in the CMF is the rise of the Sevier Mountains. Isotopic evidence confirms the presence of a rain shadow caused by the Sevier Orogeny. This rain shadow caused significant aridity during the upper Yellow Cat Member. By the end of the Ruby Ranch Member deposition, the Sevier Mountains reached a height that prohibited Pacific moisture from reaching the foreland basin. By Mussentuchit Member time, the incursion of the WIS dominated climate patterns, as its proximity provide moisture to the region and decreased the impact of the rising Sevier Mountains.

The application of geochemical analyses to fossil bone, such as those presented in this research, is a promising avenue for future studies. As techniques and instrumentation improve, results are providing more detailed information while being less destructive to these valuable resources. The future for utilizing REE composition of bone is encouraging. Laser ablation techniques are now allowing researchers to make detailed maps of REE distribution within bone (Koenig et al., 2008). These maps will allow for more accurate interpretations of bone fossilization history. Once that history is clear, we can begin to use REE for a number of scientific and practical applications, such as a means for directly dating fossil material and as a forensic tool used to identify stolen fossil resources. The relationships between REE uptake in bone and stable isotopic composition of bone are intriguing. We contend that biogenic signals are retained in the enamel and ganoine we analyze. REE concentrations are typically low in these biominerals, leading researchers to suggest that high amounts of REE in bioapatite is an indicator of diagenetic exchange of isotopes within the phosphatic and carbonate components. However, these are all qualitative suggestions. What is the quantitative relationship between

REE uptake and preservation of biogenic isotopes? Is there a concentration at which the REE suggest complete diagenetic exchange? High resolution analysis using laser ablation of bone and co-existing stable isotopes may allow us to determine the relationship between REE concentration and stable isotopic composition of bioapatites (bone, enamel, ganoine, dentine, acrodine). An understanding of these relationships can then allow us to use REE in bioapatites as an indicator of biogenic preservation of stable isotopes.

Stable isotopes have been and will continue to be an important proxy of ecological and climatic interactions. Further detailed analysis of not only vertebrate, but also invertebrate fossils using traditional isotopes will be invaluable to understand past climates and ecosystems. Incorporation of less traditional isotopes such as Ca isotopes may be a new avenue of geochemical analysis that provides researchers a glimpse into the paleo-dietary habits of vertebrates. Ca-isotopes become depleted by ~ 1.3 ‰ relative to an animals' diet. This relationship has been used for both modern and paleo-ecosystem food-web studies, but has not been used for ecosystems older than 15 Ma (Clementz et al., 2003; DePaolo, 2004). Can Ca isotopes be used for older ecosystems? What is the relationship of Ca-isotopes to REE given that REE tend to replace Ca in the apatite crystal structure? Extensive research needs to be conducted to answer these questions, but there is potential for some exciting research endeavors using non-traditional isotopes. Finally, use of other analytical techniques such as Fourier transform infrared spectroscopy (FTIR), raman spectroscopy, and matrix assisted laser desorption ionization (MALDI) spectrometry of bone can be coupled with REE analysis and stable isotopic analysis to understand issue of diagenesis and biomolecule preservation.

Integration and optimization of these methods will allow paleontologists, geologists, and climatologists to use the fossil record as a means to understand the past and predict future impacts of climate change on the biosphere.

REFERENCES

Clementz, M.T., Holden, P., and Koch, P.L. (2003) Are calcium isotopes a reliable monitor of trophic level in marine settings? *Inter. J. of Osteoarch*. **13**, p. 29 – 36.

DePaolo, D.J. (2004) Calcium isotopic variations produced by biological, kinetic, radiogenic, and nucleosynthetic processes. *Rev. in Mineral. and Geochem*. **55**, p. 255 – 288.

Koenig, A. E., Rogers, R. R., and Trueman, C. N. (2009) Visualizing fossilization using laser ablation inductively coupled mass spectrometry of trace elements in Late Cretaceous bones. *Geology* **37**, 511-514.

APPENDIX A. MUSEUM SAMPLE LIST AND ISOTOPIC COMPOSITION

sample	site	taxa	$\delta^{18}O_p$	$\delta^{18}O_{p\text{-}r}$	±1σ	comment
SAM NOBLE OKLAHOMA MUSEUM OF NATURAL HISTORY						
OMNH 26251-a1	V239	Ornithischia	17		0.1	Enamel base
a2			17.2		0.1	rest of enamel
b1			17.5		0.1	base
b2			18.6		0.1	rest of enamel
b3			*16.6*		*0.2*	*dentine, soft dull material @ base of tooth*
c1			*15*		*0.1*	*dentine,tip*
c2			*15.3*		*0.1*	*dentine*
d			*15.7*		*0.2*	*dentine; upper dull layer but dull*
e			15.6		0.2	enamel; shinny
f			15.5		0.2	enamel @ base
g1			15.5		0.2	soft material abv 'enamel'
g2			17		0.2	enamel @ base
i			*14.3*		*0.2*	*dentine; upper layer dull*
OMNH 26195-a4	V239	Theropoda	15.6		0.2	enamel
b1			19.8		0.1	large tooth
b2			20		0.1	
b3			19.9		0.1	
b4			19.4		0.1	enamel
b4_dup			18.9		0.2	duplicate
b5			19.7		0.2	abt same level as b3
c1			16.5		0.1	tip
c2			16		0.1	
d			17.5		0.1	small theropod tooth; got some dentine
OMNH 27198-1	V239	Chelonia	15.3	14.9	0.1/0.1	large carapace fragment; top surface
2			14.3	15.5	0.1/0.1	top surface
3			16.6		0.1	bottom surface
4			16.1		0.6	bottom surface
6			15.3		0.1	top surface
7			14.7		0.1	top surface
8			16.2		0.1	bottom surface
9			16.4		0.1	bottom surface

sample	site	taxa	$\delta^{18}O_p$	$\delta^{18}O_{p\text{-}r}$	±1σ	comment
10			16.2		0.1	bottom surface
OMNH 28278-a	V239	*Naomichelys?*	15.1		0.1	mis-id'd as fish teeth? Naomichelys shell ornamentation
b			14.9		0.1	mis-id'd as fish teeth? Naomichelys shell, very dark powder
c			14.7		0.1	mis-id'd as fish teeth? Naomichelys shell, dark powder
OMNH 28268-a1	V239	Goniopholidae	16.5		0.1	large tooth; base of ridges
a2			15.9		0.1	
a3			16.2		0.6	
b1			16.5		0.1	smaller
c1			16.2		0.1	smaller
OMNH 28265-a1	V239	Atoposauridae	16.9		0.1	
b1			18.5		0.1	
c1			16.9		0.1	
d1			16.8		0.1	base; larger and pointer
d2			16.6		0.1	tip; larger and pointer
OMNH 25768-a	V239	Mammalia	15.8		0.1	triple cusps, in-line; molar?
b			16.2		0.1	flat w/ ridges
c			15.6		0.1	4-6 cusp, molar?
d			*16.7*		*0.1*	*4 cusps; some dentine & glue*
e			15.9		0.1	triple cusps, staggered
f			16		0.2	pointy, crushed whole tooth
g			16.3		0.2	
h1			*15.7*		*0.2*	*dentine; molar*
h2			15.1		0.2	enamel; molar
i			17.2		0.2	enamel; molar
j			17.4		0.2	enamel; molar
OMNH 63051-a	V239	Lepisosteideae scale	16.5		0.1	
b		"Actinopterygian Scales"	16.1		0.1	got some dentine
c			15.8		0.1	got some dentine
d2			*15.3*		*0.1*	*dentine*

sample	site	taxa	$\delta^{18}O_p$	$\delta^{18}O_{p\text{-}r}$	±1σ	comment
e1			16.7		0.1	ganoine; crushed into small flakes
f1			16.1	16.1	0.1/0.1	ganoine
f2			*16.6*		*0.4*	*dentine; harder than d and e*
g			16.1		0.1	whole crushed
h			15.3		0.1	whole crushed
i			15.9		0.1	whole crushed
j			15.8		0.1	whole crushed
OMNH 28278-a	V239	Osteichthyes palatal teeth	13.9		0.09	got some dentine
b		"*Lepidotes*-like teeth"	11.8		0.11	crushed; dentine weathered out; brown
c1			13.3		0.09	ganoine
d			13.6	13.8	0.1/0.1	whole crushed + dentine
e			14.7		0.1	crushed ganoinel dentine weathered out
f			14.1		0.4	enamel only; drilled out dentine
g1			14.4		0.1	enamel
g2			*14.1*		0.1	*dentine only*
h1			13.8		0.4	enamel
h2			*14.8*		*0.4*	*dentine soft*
i			14.1		0.1	enamel and some dentine; small tooth
j			13.7		0.1	enamel
OMNH 33404a	V868	Ornithischia	16.2		0.2	base; dentine?
a2			16.8		0.2	dentine
a3			16.1		0.3	dentine + enamel
a4			17.2		0.2	mostly enamel
a5			16.2		0.3	mostly enamel
a6			16.4		0.2	mostly enamel
a7			15.9		0.3	enamel + dentine
a8			16.2		0.3	enamel only
a9			16.1		0.3	enamel only
b1			17.4		0.5	enamel + dentine
b3			17.3		0.5	enamel
b5			17		0.3	enamel only
b6			17.3		0.3	enamel and a crushed denticle

sample	site	taxa	$\delta^{18}O_p$	$\delta^{18}O_{p\text{-}r}$	±1σ	comment
c			15.5		0.3	enamel and a crushed denticle
OMNH-32104a	V868	Hadrosauridae	17.5		0.5	well formed occlusal surface; enamel?
2			17.4		0.5	enamel? Base of tooth
3			16.9		0.5	enamel? Base of tooth
4			14		0.5	??
5			17.5		0.5	enamel
6			16.8		0.5	
7			17.3		0.5	
OMNH-32104b			16.0	16.8	0.5	poorly preserved occlusal surface; 16.80; base..much softer
2			16.6		0.5	base much softer
3			16.7		0.5	base much softer
4			16.6		0.5	much harder than base
5			16.9		0.5	much harder than base
6			16.6		0.5	much harder than base
7			16.5		0.5	much harder than base
8			17.2		0.5	much harder than base
OMNH 32104-c1			17		0.5	weird occlusal surface; soft
2			17.2		0.5	soft
3			17		0.5	harder
4			14.5		0.5	??
5			17.2		0.5	
6			15.9		0.5	
OMNH 60901-a1	V868	Chelonia	16.6		0.3	soft; surface; shell
a2			16.5		0.3	shell
a3			15.6		0.2	shell
a4			16.2		0.2	bone
a5			16.3		0.3	bone
a6			16.8		0.3	shell
a7			16.9		0.3	shell
b1			*10.6*		*0.3*	*not spongy, very hard, recrystallized?*
b2			*11.1*		*0.3*	
b3			*10.9*		*0.3*	
b4			*10.5*		*0.3*	

sample	site	taxa	$\delta^{18}O_p$	$\delta^{18}O_{p\text{-}r}$	±1σ	comment
b5			*10.5*		*0.3*	
b6			*9.9*		*0.3*	
c1			16.5		0.3	spongy w/lots of calcite; underside
c2			16.7		0.3	
c3			16.7		0.3	
c4			16.6		0.3	
d1			15		0.2	spongy w/ lots of calcite; upper surface
d2			15.8		0.3	
d3			16.1		0.3	
d4			15.4		0.2	
d5			15.5		0.2	
e2			16.3		0.2	
OMNH 22092-a3	V868	Goniopholidae	17.3		0.9	
a4			16.9		0.9	
a5			17.2		0.9	
a6			17.6		0.9	
abulk			18.6		2.2	
b3			16.9		0.9	
b4			16.5		0.9	
b6			17.4		0.9	
c3			17.4		0.9	
c4			17.1		0.9	
c5			17		0.9	
d1			16.8		0.7	
d2			16.4	16.7	0.9/0.7	
OMNH 22090-a1	V868	Atoposauridae	16.9		0.9	?? Labeled as 22092
a2			17.7		0.9	
OMNH 22090-b2			17.1		0.9	
c3			16.4		0.9	+ dentine
d2			16.8		0.9	
e2			17.2		0.9	
OMNH 32963 a2	V868	Mammalia	16.90		0.9	enamel + dentine
b			13.80		0.9	enamel + a little dentine
d2			17.10		0.9	dentine + enamel
e			15.50		0.9	mostly enamel

sample	site	taxa	$\delta^{18}O_p$	$\delta^{18}O_{p\text{-}r}$	±1σ	comment
h			16.80		0.9	whole crushed
i			16.20		0.9	whole crushed
j			17.40		0.3	whole crushed
k			16.90		0.4	bicuspid; enamel mostly drilled & some crushed
l			16.00		0.3	enamel; drilled out dentine and crushed enamel
l_dentine			16.20		0.4	dentine from l
m			16.50		0.3	enamel; drilled out dentine and crushed enamel
n			16.30		0.3	
OMNH 61018-a1	V868	Lepisosteidae scale	15.6		0.9	center
a-2		"Actinopterygian scale"	16.9		0.9	outer
b			15.4		0.3	bulk
c			15.6		0.3	+ dentine
d			16.1		0.7	ganoine only
e			16		0.7	ganoine only
f1			17.8		0.7	dentine
f2			16.6		0.7	ganoine only + some glue
g1			17.3		0.7	dentine
g2			17		0.3	ganoine
h1			16.3		0.3	dentine
h2			15.6		0.3	ganoine
i			16.8		0.3	ganoine
j			16.5		0.3	ganoine
OMNH 22078-a	V868	Osteichthyes palatal teeth	13.1		0.9	drilled
b		"*Lepidotes*-like teeth"	13.8		0.9	drilled
c			17		0.9	drilled
d1			17.2		0.9	dentine
d2			17.7		0.9	enamel
g			13.8		0.3	enamel; drilled out dentine crushed enamel
h			16.5		0.3	crushed; drilled out dentine?

sample	site	taxa	$\delta^{18}O_p$	$\delta^{18}O_{p\text{-}r}$	±1σ	comment
i			13.9		0.3	a bit of sediment in center; crushed; drilled out dentine?
j			15.2		0.4	a bit softer than g-i
OMNH-28880-1	V794	Theropoda	19		0.3	blade thickness = 3.17mm; highly recurved; lots of dentine
2			18.7		0.3	enamel + dentine
4			18.3		0.3	between 1&2; all enamel
OMNH-61560a-1			17.3		0.4	blade thickness = 2.19mm; highly recurved; 0.5mm wide line
a2			16.4		0.4	1 mm wide line
a3			17.5		0.4	1.5 mm wide line
b2			19.1		0.4	1 mm wide line
b3			17.8		0.0	enamel+dentine; 3mm wide line @ base
c1			19.1		0.5	blade thickness = 1.42; 1 mm wide line
c2			18.2		0.5	2 mm wide line
c3			19.8		0.4	all enamel; a bit of dentine
OMNH 28302 -1	V794	Ornithischia	15.7		0.3	strangely weathered; bacterially dissolution? Pitted
2			15.8		0.3	
4			15.7		0.3	
5			16.1		0.3	
6			15.4		0.0	between 1&2; enamel only; pitted
7			15.6		0.0	between 2&3; enamel only; pitted
8			14.8		0.0	between 3&4; enamel only; pitted
9			*14.8*		0.0	*mostly dentine*
10			15.2		0	enamel only; rest of enamel @ base
OMNH-27852-a1	V794	Hadrosauridae	17.4		0.5	low mass
a2			16.2		0.4	
a3			17.3		0.4	

sample	site	taxa	$\delta^{18}O_p$	$\delta^{18}O_{p\text{-}r}$	±1σ	comment
a4			17.2		0.4	
a5			*16.3*		*0.0*	*soft "upper layer" at base*
a6			*16.6*		*0.0*	*soft "upper layer" at base*
a7			*16.7*		*0.0*	*below soft upper layer; hard black layer; white powder*
OMNH-27852-b1			*15.9*		*0.4*	*dentine only?*
b3			15.5		0.4	
b4			15.4		0.4	
b5			16.2		0.4	below # 1
b6			15.5		0.0	same level as #1; light soft "upper layer" soft pwdr; dull
b7			15.2		0.0	same level as #3; light soft "upper layer" soft pwdr; dull
OMNH 27852-c1			*14.4*		*0.4*	*not enamel?*
c2			*14.3*		*0.4*	
c3			*14.4*		*0.5*	*low mass*
c4			*13.5*		*0.0*	*"dark layer" below soft upper layer; hard; dentine? Abv #1*
c5			*13.3*		*0.0*	*"dark layer" below soft upper layer; hard; dentine?; below #1*
OMNH-28036-1	V794	*Naomichelys sp.*	15.9		0.5	surface bumpe broken into hole
2			16.4		0.3	on side of shell
3			16.3		0.3	bump
4			17.1		0.3	between bumps
5			14.9		0.3	smooth part of underside
6			15.4		0.3	bump on underside
8			15.7		0.6	between bumps
9			15.7		0.6	side
10			16.2		0.3	between bumps
11			16.8		0.4	between bumps
OMNH 28887-a2	V794	Goniopholidae	16.3		0.2	
a3			17.3		0.2	
a4			16.6		0.2	

sample	site	taxa	$\delta^{18}O_p$	$\delta^{18}O_{p\text{-}r}$	±1σ	comment
a5			17.1		0.2	
a6			14.4		0.2	
a7			17		0.2	
a8			15.5		0.5	
a10			16.2		0.5	
OMNH 28887-b1			14.7		0.2	broken, base of tooth is missing
b3			16		0.2	
b4			17.4		0.2	
b5			18.3		0.2	
b6			17.4		0.2	
OMNH 28887-c1			16.6		0.4	glued to slide
c4			14.9		0.4	
c5			15.8		0.4	
c6			15.8		0.4	
OMNH 28887-d3			16.2		0.4	
d4			16.3		0.4	
OMNH 28887-e1			15.9		0.4	glued to slide
e3			16.6		0.4	
OMNH 30477-a	V794	Multituberculata	17		0.4	incisor; whole crushed
b			16.5		0.4	fragment; fragment w/ enamel only?
c			15.5		0.4	fragment; fragment w/ enamel only?
d			14.8		0.0	some enamel drilled; crushed some w/dentine too
e			15.3		0.0	mostly enamel; drilled out dentine
f1			17.3		0.0	enamel only; drilled out dentine; flat w/ridges
f1_dup			17.3		0.0	duplicate (extra powder)
f2			16.4		0	dentine only
OMNH 33973-a1		Mammalia	15.6		0.1	enamel; drilled and crushed
c1			17.5		0.1	enamel; drilled out dentine
c2			16.9	16.8	0.1	dentine only
e			16.3		0.1	enamel; drilled out most of dentine

sample	site	taxa	$\delta^{18}O_p$	$\delta^{18}O_{p\text{-}r}$	±1σ	comment
OMNH 33642-a1	V794	Lepisosteidae scale	15.6		0.6	drilled ganoid scale center
a2		"Actinopterygian scales"	15.7		0.6	+1mm outside
a3			15.7		0.6	+1mm outside
b1			15.2		0.6	ganoine
c			15.7		0.6	tip broken; ganoine
d			15.1		0.5	enamel
e			17.3		0.5	enamel
OMNH 33652-a	V794	Lepisosteidea tooth	15.4		0.6	entire tooth w/ inner dentine
b		"Actinopterygian tooth"	15.6		0.6	enamel broken off w/ dentine scrapped out
c			14.6		0.6	crushed tip only
d			15.8		0.0	combined enamel only from 2 teeth
e			14.9		0.0	mostly enamel whole crushed
f			15.8		0.3	mostly enamel whole crushed
g			15.6		0.3	mostly enamel whole crushed
i			16.5		0.3	picked out dentine; mostly enamel; whole crushed
j			18		0.3	picked out dentine; mostly enamel; whole crushed
k			16.1		0.3	enamel + dentine; hard to pick out dentine
OMNH 28016-b	V794	Osteichthyes palatal tooth	15.7		0.6	enamel only
c1		"*Lepidotes*-like tooth"	12.3		0.6	enamel
c2			*13.3*		*0.6*	*dentine*
e			14.5		0.4	entire palatal tooth fragment w/ mostly enamel
f			13.9		0.4	entire palatal tooth fragment w/ mostly enamel; orange rather than black
g			16.7		0.4	entire palatal tooth fragment w/ mostly enamel

sample	site	taxa	$\delta^{18}O_p$	$\delta^{18}O_{p\text{-}r}$	±1σ	comment
h			14.8		0.3	orange; drilled out dentine; enamel only
i			14.8		0.3	orange; drilled out dentine; enamel only
j			16		0.3	drilled and picked out dentine; enamel only
k1			15.5		0.3	light colored enamel
k1_dup			15.5		0.3	duplicate of k1
k2			*15.5*		*0.3*	*dark dentine*
l			15.8		0.3	enamel only; drilled out dentine; soft dentine
OMNH 32073-a1	V235	Hadrosauridae	15.4		0.5	dentine? Kind of shinny, but soft; measured from occlusal surface
a2			15.6	15.1	0.7/0.5	
b2			17.2		0.6	both hard and soft
b3			17.6		0.6	both hard and soft
b4			15.2		0	2mm below b1 (base of tooth); (might be C) enamel; soft; cracked
c1			16.1		0.6	enamel? Hard and soft layers
c2			16.4		0.7	"
c3			16		0.6	"
c4			17.8		0	got remaining enamel at base of tooth; lighter pwdr; harder (might be b)
OMNH 34374 a	V235	Theropoda	15.4		0.6	crushed; w/ dentine
b			17.2		0.6	enamel only
c			17.5		0.6	broke; crushed denticles and dentine
d			17.6		0	
e			15.5		0	enamel; tip of tooth; drilled and crushed
f			15.4		0	enamel and denticles of a larger tooth
g			17.8		0	slightly thinner enamel
h			18.2		0	enamel
i			18.5		0	tip of small tooth; crushed whole thing;

sample	site	taxa	$\delta^{18}O_p$	$\delta^{18}O_{p\text{-}r}$	±1σ	comment
						dentine + enamel
j			17		0	tip of small tooth; crushed whole thing; dentine + enamel
j_dup			17.4		0.3	duplicate of j
OMNH 25544 a1	V235	Crocodylia scute	15.1		0.5	top surface
a2			15.3		0.5	bottom surface
a3			15.8		0.5	middle layer
a4			16		0	large croc scute frag; a (I think)
b1			15.5	15.6	0.5/0.6	top layer
b2			15.8		0.5	bottom surface
b3			15.7		0.5	center of scute
c1			15.4		0.5	top surface
c2			15.6		0.5	bottom surface
c3			16.1		0.5	middle layer
OMNH 25543-S-a		Crocodylia scute	16.6		0	baby croc scute
b			16.6		0	another baby croc scute
OMNH 30054-a1	V235	Goniopholidae tooth	17.3		0.5	enamel?
a2			17.7		0.5	below a1
b1			18		0.5	looks almost recent; tan gray, not black
d			16.6		0	1 line around circum of tooth
e			17.6		0	1 line around circum of tooth
f			18.7		0	1 line around circum of tooth
OMNH 28270 a	V235	Atoposauridae	16.4		0.5	drilled whole tooth enamel
b			17.7		0.5	drilled whole tooth enamel
c			16.9		0.5	?
d			17		0	most of enamel on tooth
e			16.1		0	looks like Bernissaritta sp.; most enamel on tooth
f			16.4		0	most of enamel on tooth
OMNH 25543-T-a	V235	Crocodylia	16.6		0	thinner enamel; looks like Goniopholidae

sample	site	taxa	$\delta^{18}O_p$	$\delta^{18}O_{p\text{-}r}$	±1σ	comment
b			16.5		0	thinner enamel; looks like Goniopholidae
b_dup			15.8		0	duplicate of b
OMNH 25606-a	V235	Tribosphenida	17.1		0.5	whole tooth crushed
b			16.4		0.5	whole tooth crushed; below min voltage (-500mv
c			17.6		0.3	mostly enamel; some dentine; hard to drill out dentine
d			16		0	more dentine than c included; dentine also hard
OMNH 29743-a	V235	Mammalia	15.8	16.3	0.5/0.5	whole tooth crushed; dentine weathered out
b					0.5	whole tooth crushed; dentine weathered out; below min voltage (-979mv)
c			16.3		0.5	whole tooth crushed; dentine weathered out
d			16.5		0.5	mostly enamel
e			16.7	16.5	0.5 /0.6	crushed frags…broke off slide
f1			*18.4*		*0.3*	*dentine; soft white powder*
f2			17		0	crushed enamel
g			14.4		0	enamel; flat w/ ridges; lighter brown dentinel soft white enamel
h			17.1		0	enamel; dentine is light colored and drilled out
OMNH 25585-a	V235	Multituberculata	15.9		0.5	whole tooth crushed
b			17.3		0.5	drilled (have a crushed duplicate w/ 96micrograms
c			16.4		0.5	whole tooth crushed (+ dentine)
d			17.5		0.0	drilled out most dentine; dentine is hard
e			16.1		0.0	drilled out most dentine; dentine is hard
f			16.6		0.0	drilled out most dentine; mostly enamel + a bit of dentine

sample	site	taxa	$\delta^{18}O_p$	$\delta^{18}O_{p-r}$	±1σ	comment
OMNH 28715-1	V235	Lepisosteidae scale	16.1		0.6	bulk crushed
3		"Actinopterygian scale"	15.8		0.0	ganoine
4			17.1		0.0	ganoine
e			14.6		0.0	ganoine; dentine is hard and difficult to differentiate between ganoine; no growth rings
f			15.2		0.0	ganoine; dentine is hard but not as hard as e
g			*16.7*		*0.0*	*dentine is hard; not as hard as e; no growth rings; hard to differntiate ganoine from dentine*
h1			16.1		0.3	ganoine; softer dentine; no growth rings
h2			*16.6*		*0.3*	*dentine; dark and soft*
i			15.8		0.0	ganoine; dentine is softer; can see poorly developed growth rings
j1			16.3		0.0	ganoine; most dentine pulled off by gluing dentine down
j2			*20.90*		*0.3*	*dentine; hard*
OMNH 34395-a1	*V235*	*Osteichthyes palatal tooth*	*15.7*		*0.7*	*dentine;*
c		"*Lepidotes*-like tooth"	15.3		0.0	enamel; looks like Lepidotes
d			15.2		0.0	enamel; looks like Lepidotes
e			16.7		0.0	enamel + dentine; looks like Lepidotes
OMNH 34395-1a			*14.30*		*0.0*	*dentine*
1b			16.8		0.0	enamel
1b_dup			16.6		0.0	enamel; duplicate
2			15.1		0.0	enamel; salt xtls formed?
OMNH 25564-b2	V235	*Lepidotes sp*	15.4		0.2	enamel; light colored or cream colored

sample	site	taxa	$\delta^{18}O_p$	$\delta^{18}O_{p\text{-}r}$	±1σ	comment
b2			15.2		0.0	whole crushed
b3			16.4		0.4	salt xtals produced? Whole crushed
b4			15.3		0.0	no comments
c			15.8		0.0	enamel
c_dup			16.3		0.0	duplicate of c
d			15		0.0	enamel
e			16.6		0.0	enamel; (still a bit of dentine left)
OMNH 29953-a3	V694	Goniopholidae	14.9		0.9	
b1			16		0.2	dark banded growth line
c1			15.2		0.6	enamel only?
c2			15.7		0.2	below c1
d			16.6		0.9	enamel only; total tooth drilled
e			15.9		0.9	enamel only; total tooth drilled
f			17.2		0.9	enamel only; lower half only
OMNH 29952 -a	V694	Atoposauridae	16.1		0.6	enamel; whole tooth drilled; fat tooth
c			16.7		0.7	messy
d			15.8		0.9	drilled all enamel on tooth; use 1/2 solns (except bleach)
e			15.8		0.9	got some dentine; use 1/2 solns (except bleach)
f			17.6		0.9	enamel only
OMNH 29716-a	V694	Mammalia	15.8		0.6	got some dentine
b			17.1		0.7	
c			15.9		0.7	
f			16.3		0.9	crushed whole; 3 pointy cusps
g			16.5		0.9	crushed whole; flat w/ ridges
h			17.3		0.3	drilled out most dentine; enamel + some dentine
i			17.7		0.9	molar? Enamel + some dentine
j			17.7		0.3	tricuspid; molar; pointy mostly enamel

sample	site	taxa	$\delta^{18}O_p$	$\delta^{18}O_{p\text{-}r}$	±1σ	comment
k			16.1		0.3	frag of tricuspid; enamel + some dentine
OMNH 30033-a	V694	Lepisosteidae scale	15.2			dentine + enamel
b		"Actinopterygian scale"	15.8		1.2	some dentine; mostly enamel
c			14.9		0.7	some dentine; mostly enamel
d1			16.5		0.7	a little less dentine
e1			16.1		0.3	ganoine only; broken in vial
e2			*16*		*0.9*	*dentine only*
f1			15.4		0.9	crushed ganoine into flakes in vial w/ glass pestel
f2			*14.1*		*0.9*	*dentine only; soft dark*
g			15.5		0.9	ganoine only; broken in vial
h			16.4		0.9	ganoine only; broken in vial
i1			14.9		0.9	ganoine only; broken in vial
i2			*15.2*		*0.9*	*dentine drilled*
j			16.2		0.9	crushed in vial
OMNH 29949-a	V694	Lepisosteidae tooth	17.9		1.2	dentine weathered out; enamel only; whole crushed
c		"Actinopterygian tooth"	17.2		0.7	a bit of dentine
d			14.8		1.2	some dentine
e			17.6		0.0	crushed in vial; most dentine picked out
f			16.2		0.0	
g			15.1		0.0	weird whitish on inside
h			16.8		0.0	
i			16.6		0.0	white opaque in color; not dark dentine
j			15.1		0.0	
k			16.2		0.0	
OMNH 29945-a	V694	Osteichthyes palatal tooth	16.2		1.2	whole crushed; enamel only, dentine weathered out; repeat

sample	site	taxa	$\delta^{18}O_p$	$\delta^{18}O_{p\text{-}r}$	±1σ	comment
						below min voltage - 57mV
b1		*"Lepidotes*-like teeth"	14.6		1.2	dentine
b2			14.2		1.2	enamel; repeat run as small sample
c1			14.7		1.2	dentine
c2			13		1.2	enamel?
d2			13.9		1.2	enamel; light brownish-orange
e			15.8		0.0	extra frags in vial
f			16		0.0	soft dark dentine
g			13.4		0.3	soft dark dentine
h			15.2		0.0	dentine harder than e-g
i			12.5		0.0	dentine lighter & harder than e-h; white-bluish pwdr
j			13		0.0	very soft & drk dentine ; drk enamel too
OMNH 26285-a	V240	Theropoda	16.5		0.3	enamel + dentine; whole tooth drilled
b			16.6		0.3	mostly enamel; but some dentine
d			16.4		0.2	crushed small tooth; tip and base missing
e			18.2		0.3	denticles; mostly enamel; drilled out dentine; use 1/2 soln
f			15.3		0.2	crused denticles (enamel + dentine)
f_dup			16.1		0.3	duplicate; run as small samples
g1			16.8		0.2	denticles; mostly enamel; drilled out dentine; mush larger tooth
g2			*16.9*		*0.3*	*dentine*
h			16.8		0.3	denticles; drilled out most of dentine
i1			15.6		0.2	enamel; denticels + enamel on adjacent; larger tooth
i2			15.3		0.2	denticles only; mostly enamel; use 1/2 solns; lots of white xtls while rinse

sample	site	taxa	$\delta^{18}O_p$	$\delta^{18}O_{p\text{-}r}$	±1σ	comment
j			17.5		0.2	
OMNH 32701-a1	V240	Hadrosauridae	15.3		0.3	enamel
a3			14.5		0.2	pitted + some dentine
b1			*17*		*0.3*	*dentine; "harder" than a's dentine*
b2			*16.4*		*0.3*	*"*
b3			17.1		0.3	
b4			16.7		0.3	striated enamel + dentine
c1			16.7		0.3	rest of enamel from one surface; half solns; lots of white xtals during rinse
c2			16.4		0.3	enamel frm another surface; use 1/2 solns
c3			*15.1*		*0.2*	*dentine next to c2*
c4			*15.7*		*0.2*	*dentine next to c1*
OMNH 26277-a1	V240	Chelonia costal frag	16.8		0.3	soft, dark pwder, midline upper surface
a2			16.4		0.3	edge top surface
a3			15.5		0.3	bottom; midline along bone
a4			17.2		0.3	shell; top
a5			16.6		0.2	shell; top
a6			17.2		0.2	shell; top
a7			16.2		0.2	across bone; bottom
a8			16.4		0.2	across bone; bottom
a9			17.1		0.2	shell; bone
b1			*13.2*		*0.3*	*top midline; harder than a; recrystallized?*
b2			*13.7*		*0.3*	*top edge*
b4			*13.6*		*0.2*	*dark powder; top surface*
b6			*13.3*		*0.2*	*dark powder; top surface*
b8			*13.8*		*0.2*	*bottom surface; shell*
b9			*14*		*0.2*	*shell; bottom*
OMNH 28785-a	V240	*Bernissartia sp*	19		0.3	hard enamel; crustacean crusher?
b			17.1		0.3	got some dentine
d			16.1		0.2	all enamel drilled

sample	site	taxa	$\delta^{18}O_p$	$\delta^{18}O_{p\text{-}r}$	±1σ	comment
e			15.5		0.2	tried to drill out dentine but hard; crushed whole
e_dup			15.8		0.2	duplicate
OMNH 28783-b		Atoposauridae	18.5		0.3	got some dentine
d			16.8		0.2	all enamel
OMNH 32782-a	V240	Goniopholidae	16.1		0.2	got some dentine; enamel is very thin
b			19.5		0.2	"
d			18.4		0.2	drilled all enamel
OMNH 26291-a	V240	Crocodylia	17.7		0.09	got a bit of dentine; enamel is hard and thick
b			17.1		0.2	drilled several vertical lines; enamel
c			19.3		0.2	drilled 2 lines around circumference; enamel
OMNH 28795-a	V240	Lepisosteidae scale	18.8		0.09	ganoine only
b		"Actinopterygian scale"	17.9		1.2	
c			17.3		1.2	
d			16.8		1.2	
e			17.6		0.2	ganoine flakes
f			17.6		0.2	ganoine; calcite and pyrite within canal in scale dentine
f_dup			17.1		0.2	ganoine
g1			17		0.2	ganoine; lots of white xtals while rinse
g2			*15.5*		*0.2*	*dentine*
h			16		0.2	ganoine
i			16.9		0.2	ganoine
j			16.7		0.2	ganoine
OMNH 26297-L-a	V240	Lepisosteidae tooth	15.1		0.1	whole crushed
a duplicate		"Actinopterygian tooth"	14.7		0.1	
b			16.5		0.3	lighter colored pwder; whole crushed; cleaner?
c			20.1		0.3	picked out dark pieces w/ dentine
d			14.6		0.3	picked out dentine

sample	site	taxa	$\delta^{18}O_p$	$\delta^{18}O_{p\text{-}r}$	±1σ	comment
e			19.1		0.9	picked and drilled out most dentine; mostly enamel
f			16.4		0.9	repacement tooth on inside? Crushed all; dark powder
g			21		0.9	dentine weather out; mostly enamel
h			15.6		0.9	mostly enamel; picked out most dentine
i			17.8		0.9	mostly enamel; picked out most dentine; used 1/2 soln (expt bleach)
j			18.8		0.3	mostly enamel; picked out most dentine; used 1/2 soln (expt bleach)
OMNH 26297-O-a1	V240	*Osteichthyes palatal tooth*	*16.3*		*1.2*	*dentine*
a2		"*Lepidotes*-like tooth"	14.7		0.7	enamel
b2			19.7		1.2	enamel
c1			*14.9*		*1.2*	*dentine*
c2			15.5		1.2	enamel
d1			14		1.2	enamel
d2			*14.9*		*1.2*	*dentine*
e			13.3		0.2	enamel
e_dup			13.6		0.2	enamel
f1			14.8		0.2	enamel
f1_dup			14.4		0.2	enamel
f2			*16.4*		*0.9*	*dentine*
g			18.4		0.9	enamel
h			15.3		0.9	enamel
i			18.1		0.3	enamel; use 1/2 solns (except bleach)
j			13.3		0.9	enamel
OMNH 26496-b1	V695	Ornithischia	17.6		0.7	pointed
d			18		0.5	anky?
e			18.4		0.2	
c*			17.1		0.2	accidently labeled 'c' (didn't notice I already had a c); dark colored pwdr; initially white; base of tooth; enamel

sample	site	taxa	$\delta^{18}O_p$	$\delta^{18}O_{p\text{-}r}$	±1σ	comment
d*			17.3		0.5	enamel; middle of tooth; 1.5mm thick line
e1*			17.4		0.5	enamel; 1mm thick line @ base
f			16.9		0.2	pointy
g			15.4		0.2	rest of enamel @ tip
h1			17.5		0.2	crushed enamel (drilled out dentine)
h2			*16.90*		*0.2*	*dentine only*
i			18.4		0.2	enamel; very small tooth; crushed
j			16.6		0.5	enamel; very small tooth; crushed
OMNH 27954-a1	V695	*Glyptops sp?*	15.3		0.6	large frag
a2			15.4		0.6	
a3			14.5	15.1	0.1/0.1	
b1			15.6		0.11	top surface; medium sized
b2			16.4		0.6	bottom surface
b3			15.9		0.6	bottom surface
c1			15.8		0.6	small frag
OMNH 28830-a1	V695	Trionyclidae	16.4		0.6	top surface
a2			16.2		0.6	crushed lateral spike
a3			14.7		0.6	bottom surface
a4			16.2		0.6	top surface
OMNH 27958-a1	V695	*Naomichelys sp*	15.9		0.6	bump; soft
a2			16.2		0.6	btwn bumps; soft
a3			15.6		0.6	broken bump; a little harder
a4			15.6		0.6	btwn and broken bump
b1			16.1		0.6	thinner shell; younger; bump
b2			16		0.6	btwn and w/ bumps
b3			16.3		0.6	bottom surface
c1			16.0	15.5	0.1/0.1	top surface (lighter in color)
c2			14.5		0.6	sampled from side; below top surface; darker and harder
OMNH 34571croc-2	V695	Crocodylia scute	15.6		0.6	miss ID'd as fish scale; white grey pwder

sample	site	taxa	$\delta^{18}O_p$	$\delta^{18}O_{p\text{-}r}$	±1σ	comment
croc-3			13.5		0.6	miss ID'd as fish scale; black-brown powder;
croc-4			15.9		0.0	upper surface; light colored pwdr
OMNH 27956-a1			15.3		0.6	juvenile or baby; top surface
a2			15.2		0.6	top surface midline
a3			15.3		0.6	bottom surface just off midline
a4			15.1		0.0	upper surface; light colored pwder
b1			15.2		0.6	bottom surface
b2			15.3		0.6	top surface
c1			15.9		0.6	top; harder than a and b; whiter powder
c2			16.9		0.6	bottom; harder than a and b; whiter powder
OMNH 26585-a	V695	Mammalia	18			semi-flat w/ ridges
b			17.4		0.5	double cusp
c			14.8		0.2	single pointy cusp
d			17		0.2	most dentine eroded out; light brown-yellow, translucent
e			14.8		0.2	inscisor; moslty enamel + some dentine
f			16.4		0.2	enamel; double cusp
g			18		0.2	enamel; molar? Partial
h			16		0.2	enamel; molar? Partial
i			14.9		0.2	enamel; bicuspid
j			15.5		0.2	enamel; molar partial
k			16.4		0.2	molar
OMNH 34571-a	V695	Lepisosteidae scale	15.9		0.7	still clear
b		"Actinopterygian scale"	16.9		0.2	darker
c			15.7		0.6	still clear
d1			16.5		0.2	ganoine + a bit of dentine; poorly developed growth rings for d-j
d2			*16.0*		*0.5*	*dentine; hard; white pwdr*
e			15.5		0.2	ganoine; dentine is a little softer than d

sample	site	taxa	$\delta^{18}O_p$	$\delta^{18}O_{p\text{-}r}$	±1σ	comment
f1			16.5		0.2	ganoine; darker pwder
f2			*16.4*		*0.5*	*dentine; softer than d and e*
g			16.5		0.2	ganoine; similar to d and e
h			16.4		0.2	ganoine; softer; kind of like f
i			16.1		0.2	ganoine; softer; kind of like f
j			15.7		0.2	ganoine
OMNH 28537-a	V695	Lepisosteidae tooth	18.6		0.1	whole crushed
b		"Actinopterygian tooth"	16.6		0.1	whole crushed
c			16.7		0.1	whole crushed
d			15.4		0.1	whole crushed
e			16		0.0	enamel; most dentine weathered out; crushed in vial
f			17.4		0.3	enamel; more dentine than e; crushed in vial; run no He dil
g			16.6		0.0	a bit more dentine than f; crushed in vial
h			16.1		0.0	mostly enamel
i			16.3		0.0	mostly enamel
j			15		0.2	crushed whole; dentine looks well mineralized
OMNH 28539 a	V695	Osteichthyes palatal tooth	16.7		0.7	
b		"*Lepidotes*-like tooth"	15.4		0.6	
c			15.5		0.6	
d			12.5		0.2	small tooth; still some dentine; hard to drill out too small
e			17.1		0.2	crush in vial; still some dentine; hard to drill out; too small
f			15.7		0.2	ligher in color; crushed in vial; enamel + dentine
g			14.8		0.2	crushed in vial; enamel + dentine; looks like Lepidotes

sample	site	taxa	$\delta^{18}O_p$	$\delta^{18}O_{p-r}$	±1σ	comment
			COLLEGE OF EASTERN UTAH			
CEUM 31234-1	Price River2	Brachiosaur	17.9		0.6	
2			18		0.6	
3			18.5		0.6	
4			18.4		0.6	
5			18.3		0.6	
6			18.6		0.6	
7			17.8		0.6	
8			18.6		0.6	
a			16.6		UM	
b			17.6		UM	
CEUM 31948-1			19.4		0.6	
2			20.4		0.6	
3			19.9		0.6	
4			20.2		0.6	
5			20		0.6	
6			20.4		0.6	
7			21.9		0.6	
8			21.6		0.6	
9			21		0.3	
10			22.2		0.3	
11			21.2		0.3	
12			22.1		0.3	
13			21.3		0.4	
14			20.2		0.4	
CEUM12500-1	Price River2	Acrocanthosaur	18.2		0.6	
2			18		0.6	
3			17.9		0.6	
4			18.5		0.6	
5			17.8		0.6	
6			18.5		0.6	
7			18.1		0.6	
8			18.3		0.6	
CEUM23266-1			20.6		0.4	
2			20.4		0.4	
3			20.7		0.4	
4			21.5		0.4	

sample	site	taxa	$\delta^{18}O_p$	$\delta^{18}O_{p\text{-}r}$	±1σ	comment
5			21.7		0.4	
6			22.1		0.4	
7			23.5		0.4	
8			23		0.4	
CEUM 35842 - 1			19.7		0	
2			20.2		0	
3			18.7		0	
4			18.3		0	
6			15.2		0	
CEUM 31232-1			24.9		0	
2			23.7	23.9	0/0	
3			24.7		0	
4			23.1		0	
CEUM 38739-1	Price River2	small theropod	17.4		0	
-2			16.7		0	
CEUM 31946			17.6		0	
CEUM 12760			17.7		0	
CEUM 26312			21.4		0	
CEUM 11736 a	Price River2	turtle scute	14		UM	
b			13.4		UM	
c			15.9		0.6	
d			14.8		0.6	
e			16.1		0.6	
f			15.8		0.4	
g			15.7		0.4	
h			15.6		0.4	
CEUM 12843 - 1	Price River2	*Naomichelys sp*	14.5		0	
-2			14.8		0	
-3			15.5		0	
-4			14.8		0	
-5			14.7		0	
-6			14.8		0	
NoID turtle - 1		turtle	13.7		0	
-2			14.3		0	
-3			14.7		0	
-4			14.9		0	

sample	site	taxa	$\delta^{18}O_p$	$\delta^{18}O_{p\text{-}r}$	±1σ	comment
CEUM 35798 - 1		crocodile tooth	17		0	
-2			17.7		0	
-3			17.5		0	
-4			17		0	
CEUM 10882			16.7		0	
BRIGHAM YOUNG UNIVERSITY MUSEUM OF PALEONTOLOGY						
BYUVP11532-1	Dalton Wells	sauropod	25.2	25.8	0.1/1	
2			26.1	25.7	0.1/0.1	
3			25.8	24.9	0.1/2	
4			25.8	25.2	0.1/0.2	
5			21.6		0.1	
6			24.3	23.9	0.1/01	
7			26.3	25.9	0.1/0.2	
BYUVP 18156-1			22.3		0.2	Camarasaurid? Lingual side; 37.6mm x 28.1mm
2			22		0.2	lingual side
3			22.5		0.2	lingual side
4			22.4	22.7	0.1/0.1	lingual side
5			22.5		0.1	labial side
BYUVP-18171-1			22.3		0.1	labial side; 37.6mm x 24.7mm
2			22.9		0.1	labial side
3			22.6		0.1	labial side
4			22		0.1	labial side
5			21.4		0.1	labial side
BYUVP 18185-1			17.3		0.1	labial side; 25.5mm x 18.9mm
2			16.8		0.1	labial side
3			17.1		0.1	labial side
4			17.2		0.1	labial side
5			17.2		0.1	labial side
BYUVP14173-1	Dalton Wells	*Utahraptor*	18		0.2	
2			18.7		0.2	
3			19.1		0.2	
4			18.5		0.2	
BYUVP 18104-1			15.6		0.1	got some dentine
2			16.8		0.1	got a bit of dentine

sample	site	taxa	$\delta^{18}O_p$	$\delta^{18}O_{p\text{-}r}$	±1σ	comment
3			16.7		0.1	some dentine
4			18.3		0.1	a bit of dentine
5			18.6		0.1	mostly enamel
BYUVP 14452-1			17.7		0.1	2lines; got dentine
2			17.7		0.1	got a little less dentine 1
3			18		0.1	mostly enamel
4			19.1		0.5	mostly enamel
5			18.7		0.1	mostly enamel
BYUVP 18099-1			17.8		0.5	lots of root stains: tried to avoid; some dentine
2			17.9		0.5	some dentine
3			19		0.5	some dentine
4			18.8		0.1	mostly enamel
5			19		0.1	mostly enamel
BYUVP11340-1	Dalton Wells	Iguanodontid	22.3		0.2	
2			22		0.2	
3			20.9		0.2	
4			22.2		0.2	
5			21.6		0.2	
6			22.2		0.2	
BYUM-CISGO-TS014-1	Cisco, UT	Chelonia	14.2		0.4	small frag; no vinac; approx same level as dalton wells
2			14.3		0.3	small frag; no vinac
3			13.5		0.3	small frag; no vinac
4			14		0.3	large frag w vinac
5			14.5		0.3	large frag w vinac
UTAH GEOLOGICAL SURVEY						
DB-Brach-1	Doelling's Bowl	Brachiosaur	24		0.2	63mm x 31mm
2			23.7		0.2	
3			23.7		0.2	
4			23.6		0.2	
5			22.8		0.2	
6			23.2		0.2	
7			22.8		0.2	

sample	site	taxa	$\delta^{18}O_p$	$\delta^{18}O_{p\text{-}r}$	±1σ	comment
8			23.1		0.1	
10			23.3		0.1	
11			24.2		0.1	
12			24.1		0.1	
13			23.5		0.1	
14			24.1		0.1	
15			24.3		0.1	
16			24.1		0.1	
17			24		0.1	
18			24		0.1	
19			23.8		0.1	
20			23.4		0.1	
21			23.5		0.1	
22			23.8		0.1	
23			23.9		0.1	
24			24.4		0.1	
25			24.4		0.1	
26			23.7		0.1	
27			23.2		0.1	
28			23.4		0.1	
29			23.7		0.1	
30			22.9		0.1	
31			23.1		0.1	
32			22.1		0.1	
DB-Brach2-1			18.2		0.2	18.7mm wide
2			17		0.2	
3			17.3		0.2	
4			17.8		0.2	
5			17.3		0.2	
6			17.2		0.2	
DB-Brach3-1			17.8		0.2	14.2mm wide
2			17.7		0.2	
3			17.1		0.2	
4			20.8		0.2	
5			17.8		0.2	
6			17.4		0.2	
7			17.1		0.2	
DB-Acro-1	Doelling's Bowl	Acrocanthosaur	19.8		0.2	50mm x 31mm

sample	site	taxa	$\delta^{18}O_p$	$\delta^{18}O_{p\text{-}r}$	±1σ	comment
2			20		0.2	
3			20.3		0.2	
4			19.7		0.2	
5			20		0.2	
6			19.7		0.2	
7			20.1		0.2	
9			18.4		0.2	
10			18.8		0.2	
11			19.1		0.2	
12			19.1		0.2	
13			19.2		0.2	
14			18.8		0.2	
15			18.5		0.2	
16			19.3		0.2	
17			19.1		0.2	
18			17.8		0.2	
19			18.5		0.2	
20			19.5		0.2	
21			19.7		0.2	
22			19.6		0.2	
23			18.9		0.2	
24			19.2		0.2	
25			19.6		0.2	
26			19.3		0.2	
27			18.8		0.2	
28			18.2		0.2	
29			18		0.2	
30			17.7		0.2	
DB-Theropod1-1	Doelling's Bowl	small theropod	15.2		0.2	
2			15.5		0.2	
3			15.9		0.2	
4			15.9		0.2	
5			15.5		0.2	
6			15.5		0.2	
7			15.8		0.2	
8			14.7		0.2	
9			15.1		0.2	
10			15.2		0.2	

sample	site	taxa	$\delta^{18}O_p$	$\delta^{18}O_{p\text{-}r}$	±1σ	comment
11			15.2		0.2	
DBDP-57-4			17.5		0.2	
5			15.9		0.2	
6			16.9		0.2	
1			17.8		0.2	
2			17.8		0.2	
3			20.2		0.2	
DB-Theropod2-1			20.2		0.1	
2			18.8		0.1	
3			18.7		0.1	
4			19		0.1	
5			18.6		0.1	
DB-Iguano1-1	Doelling's Bowl	Iguanodontid	15.6		0.2	
2			14.9		0.2	
3			15.3		0.2	
4			14.7		0.2	
5			14.8		0.2	
6			14.5		0.2	
7			13.8		0.2	
DB-Iguano2-1			14.9		0.2	
2			15		0.2	
3			15.4		0.2	
DBDP-28-1			19.6		0.2	
2			19.9		0.2	
3			18.6		0.2	
4			17.6		0.2	
5			18		0.2	
DBDP-107a-1			16.7		0.1	
2			17		0.1	
DBDP-58-1			21.3		0.1	
2			18		0.1	
3			18.2		0.1	
4			19.5		0.1	
5			18.1		0.1	
DBSP-3-1a			16.8	16.81	0.1/0.2	
2a			16.2	16.21	0.1/0.2	
2b			16.7	16.74	0.1/02	
DBDP-15-1			18.6		0.2	

sample	site	taxa	$\delta^{18}O_p$	$\delta^{18}O_{p\text{-}r}$	±1σ	comment
2			20.8	20.3	0.2/0.2	
3			20.9	21.5	0.2/0.2	
4			20.8	20.8	0.2/0.2	
5			20.9	20.9	0.2/0.2	
DB-Iguano3-1			20.1		0.2	
2			20.3		0.2	
3			20.6		0.2	
4			18.8		0.2	
DB-Croc1-1	Doelling's Bowl	Crocodile	18.9		0.2	
2			19.4		0.2	
3			19.6		0.2	
5			18.8		0.2	
4			18.6		0.2	
DB-Croc2-1			19		0.1	
2			19.9		0.2	
3			18.5		0.2	
4			19.7		0.2	
uYCM-a-e	upper YCM lake	Actinopterygian scales	17.1		0	ganoine only; combined a-e, but not d; cleaned in acetone
g-h			17.4		0	ganoine only; cleaned in acetone; combined g-h
g-h dup			17.4		0	
i-j			16.2		0	cleaned in acetone; ganoine only
d&f			16.7		0	combined d and f; ganoine only
-3			18.6		0.4	ganoine only (chips); small xtals formed
-9			17.7		0	mostly ganoine
-10			16.8		0	mostly ganoine
UTAH MUSEUM OF NATURAL HISTORY						
UMNH 16867-1	Andrew's Site	crocodilian scute	13.3		0.1	scute
2			13.3		0.1	scute
3			12.5		0.1	scute
4			14.1		0.1	scute
5			13.7		0.1	scute

sample	site	taxa	$\delta^{18}O_p$	$\delta^{18}O_{p\text{-}r}$	±1σ	comment
6			14.1		0.1	scute
7			13.3		0.1	cross bone
8			14.1		0.1	cross bone
9			13		0.1	cross bone
10			14		0.1	cross bone
11			14.1		0.1	cross bone
12			14.3		0.1	cross bone
DENVER MUSEUM OF NATURAL AND SCIENCE						
DMNH-55492-a4			15.3		0	tooth A
a5			14.9		0.9	
a6			15.8		0.9	
a7			15.4		0.9	
b1			15.3		0	tooth B
b2			14.4		0	"
b3			15.3		0	"
c1			15.1		0	tooth C
c2			15.6		0.4	"
d1			14.5		0	tooth D
d2			14.6		0	"
e			14.9		0	tooth E
f1			14.6		0	tooth F

UM = University of Missouri Analyzed; Grey italics = dentine not included in analysis; $\delta^{18}O_{p\text{-}r}$ = repeat

APPENDIX B. OXYGEN ISOTOPIC COMPOSITION OF CARBONATES

sample	member	$\delta^{18}O$ - V-SMOW	± 1σ
MI-I-50cm dwn	upper Yellow Cat	22.65	0.01
MI-I-100cm dwn		22.62	0.01
MI-I-150cm dwn		22.71	0.02
MI-I-170cm dwn		22.79	0.01
MI-I-210cm dwn		22.62	0.03
MI-II-40cm up		22.37	0.01
MI-II-80cm up		21.47	0.04
MI-II-120cm up		21.02	0.02
MI-II-160cm up		21.39	0.02
MI-II-180cm up_mudst		22.61	0.02
MI-II-180cm up_carb nod		21.69	0.01
MI-II-70cm dwnfrmtop		21.65	0.03
MI-II-top of unit		21.59	0.03
MI-III-bottom of bed		21.84	0.02
MI-III-50cm upfrmbase		19.62	0.02
MI-III-100cm upfrmbase		22.89	0.02
MI-III-220cm upfrmbase		22.79	0.02
MI-III-340cm dwn		22.70	0.01
MI-III-220cm dwnfrmtop		22.93	0.02
MI-III-180cm dwnfrmtop		23.75	0.01
MI-III-120cm dwnfrmtop		23.01	0.01
MI-III-20cm dwnfrmtop		22.22	0.01
MI-III-top of bed		17.97	0.01
ET-2005-1-011	Mussentuchit	24.19	0.02
ET-2005-1-005ss		19.91	0.02
ET-2005-4-015		24.21	0.01
ET-2005-4-016		24.27	0.03
ET-2005-Eggshell carbnods		23.89	0.01

APPENDIX C. DETAILED STRATIGRAPHIC SECTIONS

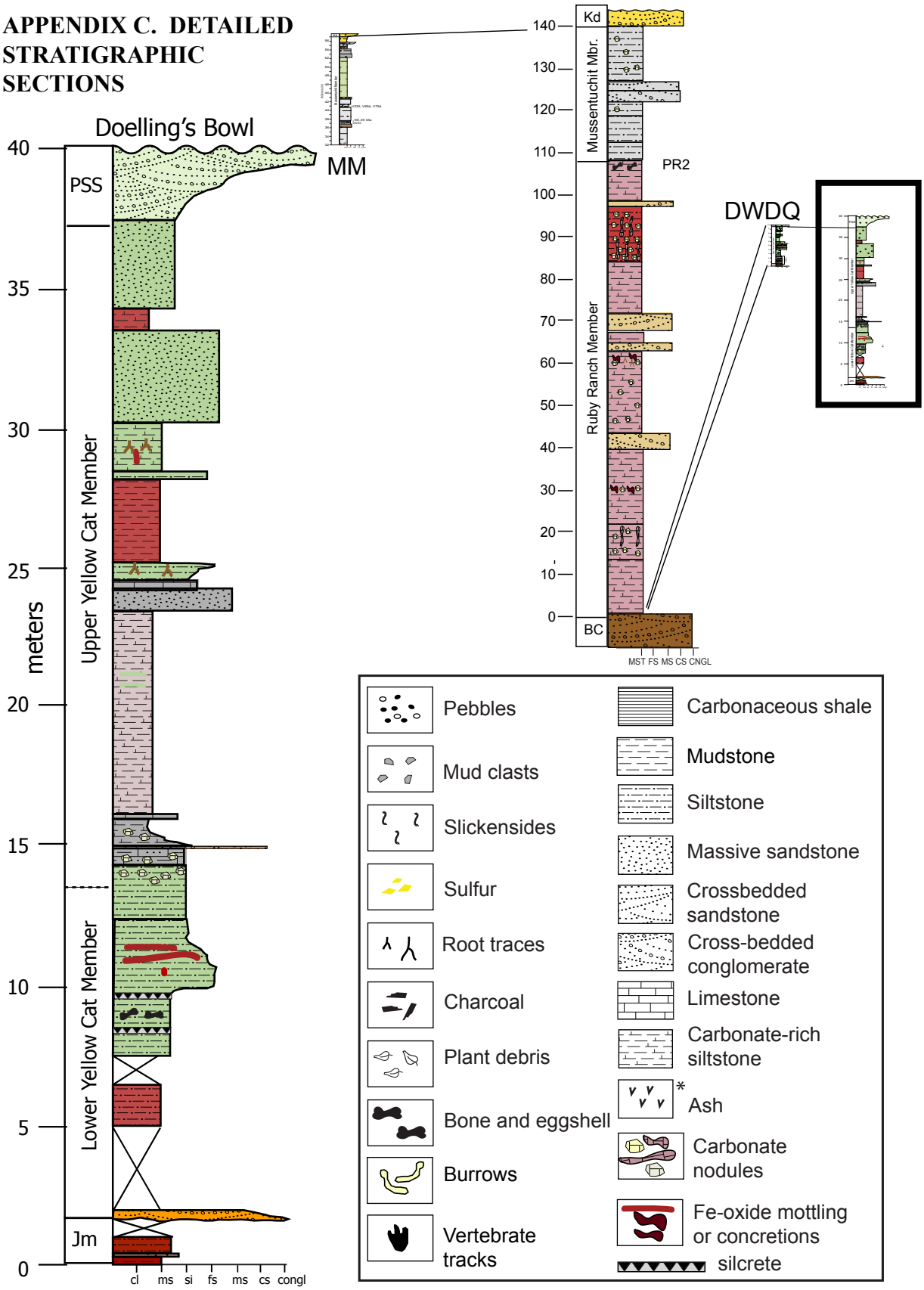

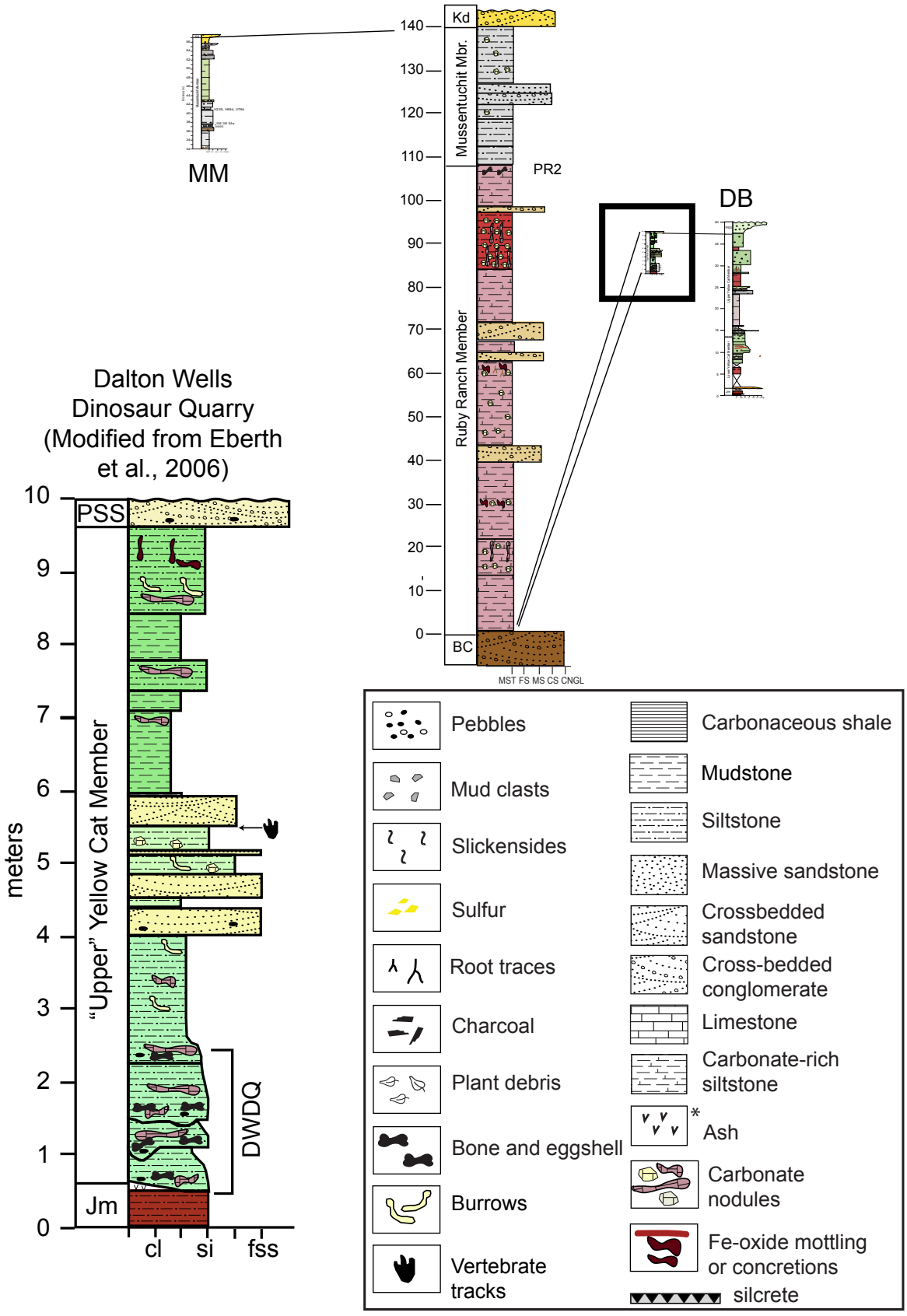
MM
Kd
Mussentuchit Mbr.
Ruby Ranch Member
BC
PR2
DB
140
130
120
110
100
90
80
70
60
50
40
30
20
10
0
MST FS MS CS CNGL
Dalton Wells
Dinosaur Quarry
(Modified from Eberth
et al., 2006)
meters
10
9
8
7
6
5
4
3
2
1
0
PSS
"Upper" Yellow Cat Member
Jm
DWDQ
cl
si
fss
Pebbles
Mud clasts
Slickensides
Sulfur
Root traces
Charcoal
Plant debris
Bone and eggshell
Burrows
Vertebrate tracks
Carbonaceous shale
Mudstone
Siltstone
Massive sandstone
Crossbedded sandstone
Cross-bedded conglomerate
Limestone
Carbonate-rich siltstone
* Ash
Carbonate nodules
Fe-oxide mottling or concretions
silcrete

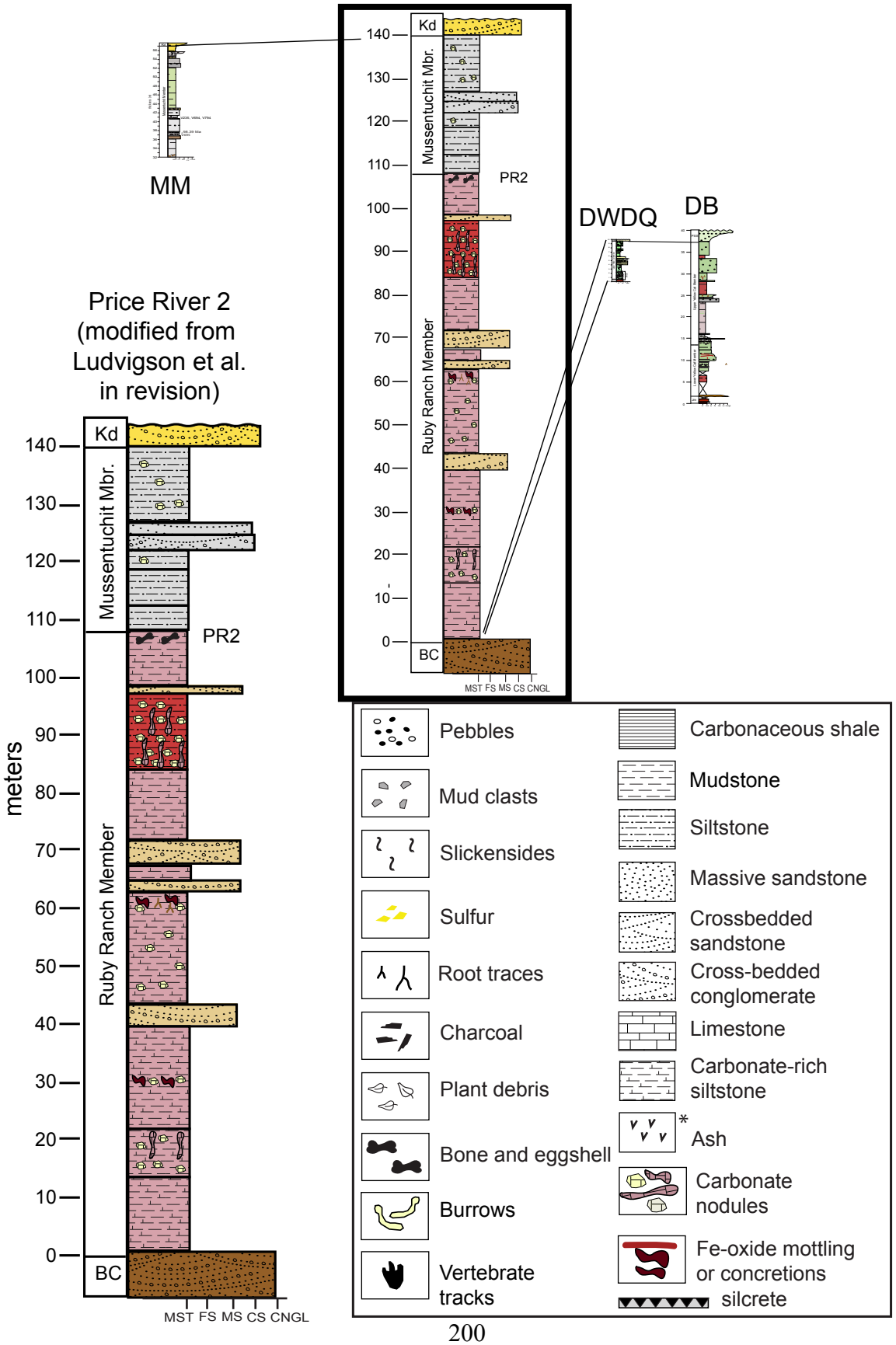
MM
DWDQ
DB
Price River 2
(modified from
Ludvigson et al.
in revision)
meters
Kd
Mussentuchit Mbr.
Ruby Ranch Member
PR2
BC
MST FS MS CS CNGL
Pebbles
Mud clasts
Slickensides
Sulfur
Root traces
Charcoal
Plant debris
Bone and eggshell
Burrows
Vertebrate tracks
Carbonaceous shale
Mudstone
Siltstone
Massive sandstone
Crossbedded sandstone
Cross-bedded conglomerate
Limestone
Carbonate-rich siltstone
Ash
Carbonate nodules
Fe-oxide mottling or concretions
silcrete

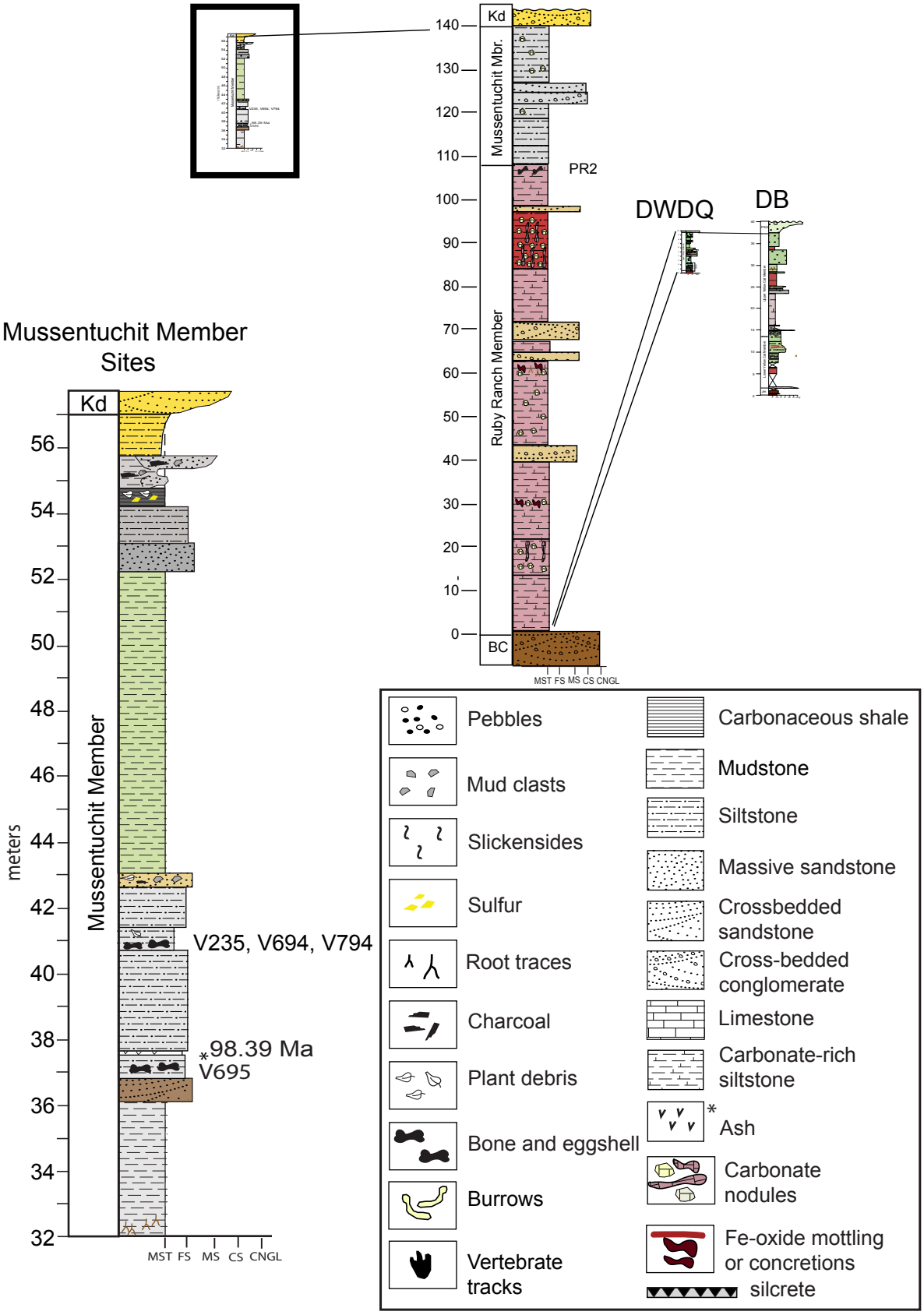
Mussentuchit Member Sites
Kd
Mussentuchit Member
meters
56
54
52
50
48
46
44
42
40
38
36
34
32
V235, V694, V794
*98.39 Ma
V695
MST FS MS CS CNGL
Kd
Mussentuchit Mbr.
Ruby Ranch Member
BC
140
130
120
110
100
90
80
70
60
50
40
30
20
10
0
PR2
DWDQ
DB
MST FS MS CS CNGL
Pebbles
Mud clasts
Slickensides
Sulfur
Root traces
Charcoal
Plant debris
Bone and eggshell
Burrows
Vertebrate tracks
Carbonaceous shale
Mudstone
Siltstone
Massive sandstone
Crossbedded sandstone
Cross-bedded conglomerate
Limestone
Carbonate-rich siltstone
* Ash
Carbonate nodules
Fe-oxide mottling or concretions
silcrete

APPENDIX D. STATISTICAL TESTS

Table 1. Statistical Comparison of Sites Stratigraphically

Variable (site) 1	Variable (site) 2	t-test	P value	Significance (Y/N)
V695 (-19 m): turtle	V240 (-16 m): turtle	Equal variance	P<<0.05	Y
V240 (-16 m): turtle	V794 (-15 m): turtle	Equal variance	P=0.059	N
V794 (-15 m): turtle	V868 (-8 m): turtle	Equal variance	P=0.451	N
V868 (-8 m): turtle	V239 (-4 m): turtle	Equal variance	P=0.002	Y
V695 (-19 m): crocodile	V240 (-16 m): crocodile	Unequal variance	P=0.100	N
V240 (-16 m): crocodile	V694 (-15 m): crocodile	Unequal variance	P=0.007	Y
V240 (-16 m): crocodile	V235 (-15 m): crocodile	Unequal variance	P=0.315	N
V240 (-16 m): crocodile	V794 (-15 m): crocodile	Equal variance	P=0.006	Y
V235 (-15 m): crocodile	V694 (-15 m): crocodile	Equal variance	P=0.006	Y
V235 (-15 m): crocodile	V794 (-15 m): crocodile	Equal variance	P=0.021	Y
V694 (-15 m): crocodile	V794 (-15 m): crocodile	Equal variance	P=0.573	N
V235 (-15 m): crocodile	V868 (-8 m): crocodile	Unequal variance	P=0.711	N
V694 (-15 m): crocodile	V868 (-8 m): crocodile	Equal variance	P<<0.05	Y
V794 (-15 m): crocodile	V868 (-8 m): crocodile	Unequal variance	P=0.002	Y
V868 (-8 m): crocodile	V239 (-4 m): crocodile	Equal variance	P=0.074	N
V695 (-19 m): ornithischian	V794 (-15 m) ornithischian	Unequal variance	P<<0.05	Y
V794 (-15 m): ornithischian	V868 (-8 m): ornithischian	Equal variance	P<<0.05	Y
V868 (-8 m): ornithischian	V239 (-4 m): ornithischian	Equal variance	P=0.586	N
V235 (-15 m): hadrosaur	V794 (-15 m): hadrosaur	Equal variance	P=0.041	Y
V794 (-15 m): hadrosaur	V868 (-8 m): hadrosaur	Equal variance	P<<0.05	Y
V235 (-15 m): theropod	V794 (-15 m): theropod	Equal variance	P=0.061	N
V794 (-15 m): theropod	V239 (-4 m): theropod	Unequal variance	P=0.347	N

Table 2. Statistical Comparison of humidity calculated from mammal phosphate and crocodile-ingested water

Variable (site) 1	Variable (site) 2	t-test	P value	Significance (Y/N)
V695 (-19 m)	V694 (-15 m)	Equal variance	P=0.127	N
V695 (-19 m)	V235 (-15 m)	Equal variance	P=0.873	N
V695 (-19 m)	V794 (-15 m)	Equal variance	P=0.462	N

V694 (-15 m)	V235 (-15 m)	Equal variance	P=0.095	N
V694 (-15 m)	V794 (-15 m)	Equal variance	P=0.296	N
V794 (-15 m)	V235 (-15 m)	Equal variance	P=0.482	N
V694 (-15 m)	V868 (-8 m)	Equal variance	P=0.027	Y
V235 (-15 m)	V868 (-8 m)	Equal variance	P=0.500	N
V794 (-15 m)	V868 (-8m)	Equal variance	P=0.178	N
V868 (-8 m)	V239 (-4 m)	Equal variance	P=0.780	N

Table 3. More statistical comparisons

Variable (site) 1	Variable (site) 2	t-test	P value	Significance (Y/N)
MM: calcite	MM: turtle	Unequal variance	P=0.711	N
MM: crocodile	MM: turtle	Equal variance	P<<0.05	Y
V240: *Bernissartia sp.*	V240: Atoposauridae + Goniopholodae	Equal variance	P=0.090	N
MM: mammalia	MM: turtles	Unequal variance	P<<0.05	Y
MM: dinosaurs	MM: aquatic/semi-aquatic	Unequal variance	P<<0.05	Y

Table 4. Statistical Comparison of CMF Sites Stratigraphically

Variable (site) 1	Variable (site) 2	t-test	P value	Significance (Y/N)
uYCM: Carbonate	RRM Carbonate	Unequal variance	P<<0.05	Y
RRM: Carbonate	MM: Carbonate	Unequal variance	P=0.794	N
uYCM: Turtles	RRM: Turtles	Equal variance	P=0.040	Y
RRM: Turtles	MM: Turtles	Equal variance	P<<0.05	Y
lYCM: Crocodiles	uYCM: Crocodiles	Equal variance	P<<0.05	Y
uYCM: Crocodiles	RRM: Crocodiles	Equal variance	P<<0.05	Y
RRM: Crocodiles	MM: Crocodiles	Unequal variance	P=0.338	N
lYCM: Ornithischians	uYCM: Ornithischians	Unequal variance	P<<0.05	Y
uYCM: Ornithischians	RRM: Ornithischians	Equal variance	P<<0.05	Y
RRM: Ornithischians	MM: Ornithischians	Unequal variance	P<<0.05	Y
lYCM: Sauropods	uYCM: Sauropods	Equal variance	P=0.922	N
uYCM: Sauropods	RRM: Sauropods	Unequal variance	P=0.004	Y
lYCM: Small Theropods	uYCM: Small Theropods	Unequal variance	P=0.007	Y
uYCM: Small Theropods	RRM: Small Theropods	Unequal variance	P=0.948	N
RRM: Small Theropods	MM: Small Theropods	Equal variance	P=0.443	N

Table 5. Statistical Comparison of CMF taxa by site

Variable (site) 1	Variable (site) 2	t-test	P value	Significance (Y/N)
uYCM: crocodile	uYCM: turtle	Equal variance	P<<0.05	Y
uYCM: crocodile	uYCM: calcite	Unequal variance	P=0.538	N
RRM: crocodile	RRM:turtle	Unequal variance	P<<0.05	Y
RRM: crocodile	RRM: calcite	Equal variance	P=0.058	N
MM: crocodile	MM:turtle	Equal variance	P<<0.05	Y
MM: crocodile	MM: calcite	Unequal variance	P=0.487	N
lYCM: sauropods	lYCM: ornithischians	Equal variance	P<<0.05	Y
lYCM: sauropods	lYCM: acrocanthosaurs	Unequal variance	P<<0.05	Y
lYCM: sauropods	lYCM: small theropods	Unequal variance	P<<0.05	Y
uYCM: sauropods	uYCM: ornithischians	Unequal variance	P=0.727	N
uYCM: sauropods	uYCM: small theropods	Unequal variance	P<<0.05	Y
RRM: sauropods	RRM: ornithischians	Unequal variance	P<<0.05	Y
RRM: sauropods	RRM: acrocanthosaurs	Unequal variance	P=0.082	N
RRM: sauropods	RRM: small theropods	Equal variance	P<<0.05	Y
lYCM: ornithischians	lYCM: crocodiles	Unequal variance	P<<0.05	Y
uYCM: ornithischians	uYCM: turtles	Equal variance	P<<0.05	Y
uYCM: ornithischians	uYCM: crocodiles	Unequal variance	P=0.012	Y
RRM: ornithischians	RRM: turtles	Equal variance	P<<0.05	Y
RRM: ornithischians	RRM: crocodiles	Equal variance	P<<0.05	Y
MM: ornithischians	MM: turtles	Unequal variance	P<<0.05	Y
MM: ornithischians	MM: crocodiles	Unequal variance	P<<0.05	Y
lYCM: acrocanthosaurs	lYCM: crocodiles	Unequal variance	P<<0.05	Y
lYCM: acrocanthosaurs	lYCM: small theropods	Unequal variance	P<<0.05	Y
RRM: acrocanthosaurs	RRM: turtles	Unequal variance	P=0.003	Y
RRM: acrocanthosaurs	RRM: crocodiles	Unequal variance	P<<0.05	Y
RRM:	RRM: small	Unequal	P=0.047	Y

acrocanthosaurs	theropods	variance		
uYCM: sauropods	uYCM: turtle	Unequal variance	P=0.004	Y
uYCM: sauropods	uYCM: calcite	Unequal variance	P=0.054	N